

**Institut für Nutzpflanzenwissenschaften und Ressourcenschutz (INRES)**

**Fachbereich Pflanzenzüchtung**

---

**Breeding progress for drought tolerance and  
nitrogen use efficiency in winter wheat  
(*Triticum aestivum* L.)**

**Dissertation**

**zur Erlangung des Grades**

**Doktor der Agrarwissenschaften (Dr. agr.)**

**der Landwirtschaftlichen Fakultät**

**der Rheinischen Friedrich-Wilhelms-Universität Bonn**

**vorgelegt von**

**Ahossi Patrice Koua**

**aus**

**Angbanou, Côte d'Ivoire**

**Bonn 2022**

Referent:

Prof. Dr. Jens Léon

Koreferent:

Prof. Dr. Uwe Rascher

Tag der mündlichen Prüfung:

21. September 2021

Angefertigt mit Genehmigung der Landwirtschaftlichen Fakultät der Universität Bonn

**Summary (English)**

Drought is the major abiotic stress factor limiting agricultural production in arid, semi-arid as well as in temperate regions around the world, whereas nitrogen (N) is one of the most important nutrients for crop production. With the current threat of climate change, drought-prone land is predicted to increase in the four corners of the planet. The development of drought-tolerant genotypes is seen as the most efficient and economical approach to curb the problem of drought and increase crop productivity. In this study, we employed a forward genetic approach to understanding the genetic basis of traits related to drought tolerance and nitrogen use efficiency, with the ultimate goal to find genetic variants that can be used to improve drought tolerance and N use efficiency in wheat.

A number of 200 winter wheat genotypes released from 1946 to 2013 were used to screen the genotypic variation in agronomic, photosynthetic-related and grain quality traits under different water regimes. The evaluated genetic variation was used to identify traits with higher contribution to grain yield (GY) and highlighted the role played by breeding to enhance drought tolerance, photosynthesis efficiency and GY in the last seven decades. Results indicated significant effects of genotype, water regime, and their interactions for agronomic and photosynthesis-related traits. Kernels number per square meter was the yield-component with highest contribution to GY. Breeding has increased GY over years through improving the kernels number per area and the harvest index, which were due to improvement in the photosynthesis efficiency in modern cultivars. Genome wide association study (GWAS) and haplotypes effects analysis confirm that major haplotypes favorable for higher GY, and higher photosynthesis efficiency, especially under drought conditions were selected through breeding.

The effect of drought on plant nitrogen uptake and use efficiency was examined to uncover genomic regions that simultaneously contributed to drought tolerance and N use efficiency. The results indicated a total of 27 potential QTL with main effects on evaluated traits, while 10 QTL regions were interacting with N availability. The transcript abundance analysis showed that the cold shock protein gene in the vicinity of a pleiotropic QTL region was highly expressed under drought stress conditions. Our result from the experiment conducted to assess the effect of fungicide and nitrogen supply on wheat grain productivity revealed a synergistic effect of nitrogen and fungicide on GY. Forty-six high-yielding cultivars showed different stability levels under three cropping systems (CS) including low N, high N and high N plus fungicide, suggesting that resource use efficiency can be improved via cultivar selection for targeted CS. The breeding progress in the wheat panel for most traits including GY was consistent across all three CS.

The present study demonstrated that breeding has improved genotypes performance not only under optimum conditions but also under various stress conditions such as drought and N deprivation. This improvement could be explained by the increment of favorable alleles for photosynthesis efficiency. Upon validation of the genomic regions harboring the favorable alleles highlighted in this study, they can be exploited to improve drought tolerance and N use efficiency in wheat.

**Kurzfassung (Deutsch)**

Trockenheit ist der wichtigste abiotische Stressfaktor, der die landwirtschaftliche Produktion in ariden, semiariden sowie in gemäßigten Regionen der Welt begrenzt, während Stickstoff (N) einer der wichtigsten Nährstoffe für die Pflanzenproduktion ist. Angesichts des drohenden Klimawandels wird prognostiziert, dass die Zahl der dürregefährdeten Flächen in vielen Gebieten der Erde zunehmen wird. Die Entwicklung von trockenheitstoleranten Genotypen wird als der effizienteste und wirtschaftlichste Ansatz angesehen, um das Problem der Trockenheit einzudämmen und die Produktivität der Pflanzen zu erhöhen. In dieser Studie verwendeten wir einen als forward-genetics gerichteten Ansatz, um die genetische Grundlage von Merkmalen im Zusammenhang mit Trockenheitstoleranz und Stickstoffnutzungseffizienz zu verstehen, mit dem Ziel, genetische Varianten zu finden, die zur Verbesserung der Trockenheitstoleranz und N-Nutzungseffizienz in Weizen verwendet werden können. Zweihundert zwischen 1946 und 2013 zugelassene Winterweizen-Genotypen wurden verwendet, um die genotypische Variation in agronomischen, photosynthetischen und Getreidequalitätsmerkmalen unter verschiedenen Wasserregimen zu untersuchen, um Merkmale mit einem höheren Beitrag zum Getreideertrag (GY) zu identifizieren, sowie die Rolle der Züchtung zur Verbesserung der Trockenheitstoleranz, Photosyntheseeffizienz und GY in den letzten sieben Jahrzehnten zu bewerten. Die Ergebnisse zeigten signifikante Auswirkungen des Genotyps, des Wasserhaushalts und ihrer Interaktionen auf diese Merkmale. Die Anzahl der Körner pro Quadratmeter war die Ertragskomponente mit dem höchsten Beitrag zum GY. Genomweite Assoziationsstudie (GWAS) und Haplotyp-Effektanalyse bestätigten, dass durch Züchtung Haupthaplotypen ausgewählt wurden, die für einen höheren GY und eine höhere Photosyntheseeffizienz, insbesondere unter Dürrebedingungen, günstig sind. Der Einfluss von Trockenheit auf die Stickstoffaufnahme und Nutzungseffizienz der Pflanzen wurde untersucht und die Ergebnisse zeigten insgesamt 27 potenzielle QTL mit Haupteffekten auf diese Merkmale, während 10 QTL-Regionen mit der N-Verfügbarkeit interagierten. Die Transkriptabundanzanalyse zeigte, dass das Kälteschockprotein-Gen in der Nähe einer pleiotropen QTL-Region unter Trockenstressbedingungen stark exprimiert wurde. Unser Ergebnis aus dem Experiment, das durchgeführt wurde, um die Wirkung von Fungizid und Stickstoffzufuhr auf die Weizenkornproduktivität zu bewerten, zeigte eine synergistische Wirkung von Stickstoff und Fungizid auf den GY. Die Genotypleistung von 46 ertragreichen Sorten zeigte unter drei verschiedenen Anbausystemen (CS) unterschiedliche Stabilitätsniveaus, was darauf hindeutet, dass die Effizienz der Ressourcennutzung durch die Sortenauswahl für gezielte CS verbessert werden kann. Der Zuchtfortschritt im Weizenpanel war bei den meisten Merkmalen, einschließlich GY, über alle drei CS hinweg konsistent. Die vorliegende Studie zeigte, dass die Züchtung dazu beigetragen hat, die Leistung der Genotypen nicht nur unter optimalen Bedingungen, sondern auch unter verschiedenen Stressszenarien zu verbessern. Dies könnte durch die Zunahme günstiger Allele für die Photosyntheseeffizienz erklärt werden. Nach Validierung der genomischen Regionen, können diese zur Verbesserung der Trockenstresstoleranz und der N-Nutzungseffizienz bei Weizengenutzt werden.

## **Table of Contents**

Summary (English).....	i
Kurzfassung (Deutsch) .....	ii
Table of Contents .....	iii
List of Abbreviations .....	v
List of Figures .....	vii
List of Tables .....	ix
List of Supplementary Figures .....	x
List of Supplementary Tables .....	xii
List of Supplementary Excel Tables.....	xiii
Chapter 1.....	1
1.1.    General Introduction .....	1
1.1.    Plant water and nutrients demands.....	1
1.2.    Drought stress, N deficiency and plant response under stress conditions .....	2
1.3.    Breeding for drought tolerance and nitrogen use efficiency.....	13
1.4.    Breeding progress and dissection of the genetic basis of traits of interest .....	25
1.5.    Research hypothesis and objectives .....	28
Chapter 2.....	30
2.1.    Abstract .....	31
2.2.    Introduction .....	32
2.3.    Materials and Methods .....	35
2.4.    Results .....	39
2.5.    Discussion.....	55
2.6.    Conclusion.....	60
Chapter 3.....	61
3.1.    Abstract: .....	62
3.2.    Introduction .....	63
3.3.    Materials and Methods .....	65
3.4.    Results .....	71

3.5.	Discussion.....	92
3.6.	Conclusion.....	96
Chapter 4.....		97
4.1.	Abstract .....	98
4.2.	Introduction .....	99
4.3.	Materials and methods.....	101
4.4.	Results .....	105
4.5.	Discussion.....	121
4.6.	Conclusion.....	124
Chapter 5.....		125
5.1.	Abstract .....	126
5.2.	Introduction .....	127
5.3.	Materials and Methods .....	129
5.4.	Results .....	134
5.5.	Discussion.....	144
5.6.	Conclusion.....	149
Chapter 6.....		150
General Discussion.....		150
6.1.	Drought stress has reduced plant agronomic performance by reducing photosynthesis efficiency 150	
6.2.	Breeding has increased yield through improving photosynthesis performance over years .....	151
6.3.	Population structure and linkage disequilibrium pattern .....	151
6.4.	Genome wide association scan analysis .....	152
6.5.	Candidate gene in the region of associated polymorphisms .....	153
References.....		155
Supplementary Figures .....		180
Supplementary Tables .....		217
List of Publications.....		264
Acknowledgements .....		265

## **List of Abbreviations**

A	CO <sub>2</sub> assimilation rate
AATs	Amino acid transporters
ABA	Abscisic acid
ABC	ATP-binding cassette (ABC) transporters
ABI	Abscisic acid insensitive ABRE abscisic acid-responsive elements
ANOVA	Analysis of Variance
BBCH	Biologische Bundesanstalt für Land- und Forstwirtschaft, Bundessortenamt und Chemische Industrie
BRISONr.	BRIWECS Sortennummer
BRIWECS	Breeding Innovation in Wheat for Resilient Cropping System
bZIP	basic-domain leucine zipper
C <sub>i</sub>	intracellular CO <sub>2</sub> concentration
DEG	differentially expressed gene
DRE	dehydration responsive elements
DREB	dehydration responsive element binding factors
E	transpiration rate
FBPase	Fructose-1,6-bisphosphatase
FDR	False discovery rate
g <sub>s</sub>	stomatal conductance
GWAS	Genome-wide association study
HI	Harves Index
HNO <sub>2</sub>	Nitrous acid
HNO <sub>3</sub>	Nitric acid
(NH) <sub>2</sub> SO <sub>4</sub>	Ammoniumsulfat
MAF	Minor allele frequency
MDA	Malondialdehyde
N	Nitrogen
n.PC	Number of principal components
N <sub>2</sub> O	Nitrous oxide
NAB	N absorption by aerial parts of the plants
NAC	derived from the initials of three genes no apical meristem, Arabidopsis NAC domain-containing protein and cup-shaped cotyledon which possess conserved NAC domain

NADP-ME	NADP-malic enzyme
NDVI	normalized difference vegetation index
NH <sub>3</sub>	Ammoniac
NHI	Nitrogen Harvest Index
NIR	Near infra-red region of the electromagnetic spectrum (from 780 nm to 2500 nm).
NIRS	Near infra-red spectrometry
NO <sub>3</sub> -	Nitrat
NR	Nitratreductase
NRE	Nitrogen Remobilization Efficiency
NRT	Nitrattransporter
NUE	Nitrogen Use Efficiency
NU <sub>p</sub> E	Nitrogen Uptake Efficiency
NU <sub>t</sub> E	Nitrogen Utilization Efficiency
PCA	Principal Component Analysis
PEPCase	Phosphoenolpyruvatcarboxylase
PPDK	Pyruvat-Phosphat-Dikinase
QTL	Quantitativen trait loci
ROS	Reactive Oxygen Species
RSA	Root System Architecture
Rubisco	Ribulose-1,5-bisphosphat-carboxylase/ oxygenase
SNP	Single Nucleotide Polymorphism
SPAD	Soil Plant Analysis Development
TASSEL	Trait Analysis by aSSociation, Evolution and Linkage
VI	Vegetationsindizes
Y(II)	effective quantum yield of photosystem II at steady-state photosynthesis under ambient light conditions

## List of Figures

<b>FIGURE 1.1.</b> The most important spatial pattern (top) of the monthly Palmer Drought Severity Index (PDSI) for 1900 to 2002. ....	4
<b>FIGURE 1.2.</b> Plant responses at molecular, cellular, and organ to the whole plant level under drought. ...	5
<b>FIGURE 1.3.</b> Photosynthesis under drought stress. ....	6
<b>FIGURE 1.4.</b> Description of possible mechanisms of growth reduction under drought stress.....	9
<b>FIGURE 1.5.</b> Physiological changes in tolerant and susceptible wheat and barley genotypes in response to drought stress. ....	9
<b>FIGURE 1.6.</b> The nitrogen cycle from soil to plant product.....	12
<b>FIGURE 1.7.</b> Hypothetical nitrogen stocks and flows of two contrasting cropping systems. ....	12
<b>FIGURE 1.8.</b> (A) Global cereal production has risen from 877Mt in 1961 to 2351 Mt in 2007 (blue). (B) World map showing countries according to their average wheat production (tonnes).....	14
<b>FIGURE 1.9.</b> Root and stomatal traits that define drought tolerant and susceptible wheat plant ideotypes. ....	16
<b>FIGURE 1.10.</b> Overview of photosynthesis reactions.....	20
<b>FIGURE 1.11.</b> Genome to phenome and back: identification of photosynthetic traits for integration into breeding programs or gene technologies. ....	23
<b>FIGURE 1.12.</b> Scheme of contrast of GWAS and candidate-gene association mapping.....	27
<b>FIGURE 2.1.</b> Comparison of breeding progress in agronomic and grain quality traits between two contrasting years of release groups under rainfed (control) and drought stress conditions. ....	45
<b>FIGURE 2.2.</b> Regression plots showing breeding progress in agronomic traits on Blues values for two growing seasons. ....	45
<b>FIGURE 2.3.</b> Representation of the studied cultivars based on SWP. ....	46
<b>FIGURE 2.4.</b> Association mapping for year of release. ....	49
<b>FIGURE 2.5.</b> Principal component analysis (PCA) plot using a PCA matrix (Tassel 5.2) ....	50
<b>FIGURE 2.6.</b> Allele <i>AX-158576764</i> effect on GSC and The trend in the allele frequency of the haplotype block including the markers <i>AX-158576764</i> and <i>AX-111076088</i> over years of release.....	52
<b>FIGURE 2.7.</b> Genes annotation and ontological classifications of the associated DNA sequences underlying breeding progress and the traits of interest. ....	54
<b>FIGURE 3.1.</b> NADH-ubiquinone oxidoreductase genes <i>TraesCS3A02G287600</i> . ....	70
<b>FIGURE 3.2.</b> Drought stress effect on the photosynthesis related traits across growth stages. ....	72
<b>FIGURE 3.3.</b> Relationship between photosynthesis rate vs (A) stomatal conductance; (B) and transpiration rate after anthesis growth stage in 2018 growing season. ....	74

<b>FIGURE 3.4.</b> Relationship among evaluated traits. ....	76
<b>FIGURE 3.5.</b> Illustration of breeding progress of evaluated traits. ....	78
<b>FIGURE 3.6.</b> Presentation of GWAS results for YII and SPAD. ....	80
<b>FIGURE 3.7.</b> Circular plot showing the epistatic interactions SNPs with the corresponding positions on the genetic map of wheat. ....	82
<b>FIGURE 3.8.</b> Representation of most pleiotropic SNPs detected under drought. ....	85
<b>FIGURE 3.9.</b> Allelic effect of AX-158576783 on YII and GY. ....	86
<b>FIGURE 3. 10.</b> Representation of forty contrasting cultivars. ....	87
<b>FIGURE 3. 11.</b> DNA alignment displaying positions of allelic variation in the promoter region of two groups of contrasting cultivars. ....	90
<b>FIGURE 3.12.</b> Dendrogram displaying similarities among the four cultivars. ....	91
<b>FIGURE 4.1.</b> Overview of experimental setup and phenotyping tools. ....	102
<b>FIGURE 4.2.</b> Comparison of means between both N treatments under rainfed and drought. ....	108
<b>FIGURE 4.3.</b> Pearson correlation matrix for phenotypic traits of 200 different wheat genotypes grown under 4 treatments. ....	109
<b>FIGURE 4.4.</b> Bar graphs of the root and shoot mass. ....	112
<b>FIGURE 4.5.</b> Phenotypic correlations of 30 different wheat genotypes. ....	113
<b>FIGURE 4.6.</b> Allelic effects of the haplotype <i>Hap1B</i> and <i>Hap5A</i> . ....	116
<b>FIGURE 4.7.</b> Gene Ontology classification group of 2653 genes retrieved from 27 QTL regions. ....	118
<b>FIGURE 4.8.</b> Transcript abundance of 24 candidate genes under different biological conditions. ....	120
<b>FIGURE 5.1.</b> Differences between the three cropping systems. ....	135
<b>FIGURE 5.2.</b> Contribution of nitrogen and fungicide to grain yield ( $\text{Mg}\cdot\text{ha}^{-1}$ ) production. ....	136
<b>FIGURE 5.3.</b> (A) Nitrogen use efficiency; (B) Agronomy efficiency of Nitrogen. ....	137
<b>FIGURE 5.5.</b> Correlations between GY and yield components traits under each CS. ....	140
<b>FIGURE 5.4.</b> Relationship between GY and evaluated traits. ....	140
<b>FIGURE 5.6.</b> Graphical representation of CS performance index. ....	142
<b>FIGURE 5.7.</b> Temporal trends observed in traits of interest. ....	143

**List of Tables**

**TABLE 2.1.** ANOVA and descriptive statistics on agronomic, grain quality traits of 200 wheat genotypes (G) evaluated in two water regimes (T) across 2017 and 2018 years (Y). ..... 41

**TABLE 4.1.** ANOVA and descriptive statistics on agronomic, grain quality traits of 200 wheat genotypes (G) evaluated under two water regimes (T) in 2017 and 2018. .... 106

**TABLE 4.2.** Descriptive statistics of evaluated traits in the field experiment from 2018 under drought and N stress. .... 107

**TABLE 4.3.** Anova table for the root and shoot traits of the pot experiment 2019..... 111

**TABLE 4.4.** Descriptive statistics for the root and shoot traits of the pot experiment 2019..... 111

## List of Supplementary Figures

**Figure 2.S1.** Above ground and underground weather data.

**Figure 2.S2.** Pearson correlation coefficients between evaluated traits in both growing seasons.

**Figure 2.S3.** The principal component analysis of evaluated traits visualized in the first two principal components.

**Figure 2.S4.** Linear regression of GY on yield components traits showing the proportion of the variance in GY explained by the variation in each component trait ( $R^2$ ).

**Figure 2.S5.** Regression plots showing breeding progress in agronomic traits and grain quality on Blues values for two growing seasons.

**Figure 2.S6.** Comparison of breeding progress in agronomic and grain quality traits between two contrasting years of release groups under control and drought stress conditions.

**Figure 2.S7.** Barplot of total detected MTAs across chromosomes.

**Figure 2.S8.** Circular Manhattan plots displaying association mapping for GSC.

**Figure 2.S9.** Effect of *AX-158576764* haplotype bloc of chromosome 3A on (A) GSC and (B) GY under drought stress conditions; (C) GSC and (D) GY under control conditions.

**Figure 3.S1.** Genetic diversity of 200 winter wheat cultivars including the core set of 20 cultivars.

**Figure 3.S2.** Pearson correlation coefficients between evaluated photosynthesis-related traits.

**Figure 3.S3.** Principal component analysis biplot using 11 photosynthesis and transpiration-related traits.

**Figure 3.S4.** SNP density across genomes of the studied winter wheat genotypes.

**Figure 3.S5.** Sliding windows showing the rate of linkage disequilibrium decay among the 200 cultivars of the diversity set across A, B, D genomes.

**Figure 3.S6.** (A) Classification of pairwise relative kinship into 3 classes; (B) Distribution of pairwise relative kinship estimates among 200 wheat genotypes.

**Figure 3.S7.** Representation of the wheat panel population structure.

**Figure 3.S8.** Manhattan plot for SPAD under control including significant MTAs in (A) 2017 and (B) 2018.

**Figure 3.S9.** Illustration of marker by treatment interactions on photosynthesis related traits.

**Figure 3.S10.** Allelic effect of *Excalibur\_rep\_c76510\_255* on YII and GY.

**Figure 4.S1.** Distribution of MTAs number across chromosomes.

**Figure 4.S2.** Allelic effects of the haplotype Hap5A on NUEGr under (A) rainfed high N and (B) drought high nitrogen. Comparison of year of release of cultivars caring the two haplotypes forms of (C) Hap5A and (D) Hap1B.

**Figure 4.S3.** (A) Hierarchical clustering tree summarizing the correlation among significant pathways listed in the Enrichment tab showing the biological process of 2653 genes retrieved from 27 QTL regions. Pathways with many shared genes are clustered together. Bigger dots indicate more P-values that are significant.

**Figure 4.S3.** (B) Hierarchical clustering tree summarizing the correlation among significant pathways listed in the Enrichment tab showing the molecular function of 2653 genes retrieved from 27 QTL regions. Pathways with many shared genes are clustered together. Bigger dots indicate more P-values that are significant.

**Figure 4.S4.** Differential genes expression (DEG) pattern estimated in TPM (transcripts per kilobase million) of 24 candidate genes.

**Figure 5.S1.** Weather conditions, rainfall and temperature data from the experimental site.

**Figure 5.S2.** Significant differences among the three cropping systems (CS) for evaluated traits with LN-NF in gray, HN-NF in green, and HN-WF in red color.

**Figure 5.S3.** Agronomy efficiency use of nitrogen supplied.

**Figure 5.S4.** (A) Grain harvested N yield (GNY) under three CS (HN-NF in green color, HN-WF in red color, LN-NF in blue color) across the three years; (B) Resilience to YR infestation of GY contrasting cultivars; (C) Chlorophyll content (SPAD) of GY contrasting cultivars.

**Figure 5.S5.** Pearson correlation coefficients and associated probability among evaluated traits based on of the cultivar mean from the three tested cropping systems in three years of trials.

**Figure 5.S6.** Relationship between GY and traits of interest.

**Figure 5.S7.** Temporal trends observed in evaluated traits in relation to year of registration among 209 cultivars under three CS, HN-WF in green, HN-NF in red and LN- NF in blue color.

**Figure 5.S8.** Graphical representation of selected cultivars based on performance index.

**Figure 5.S9.** Biplot of the Coefficient of variation (Y-axis) plotted against mean yield (X-Axis) of GY of 46 winter wheat cultivars under HN-NF.

## **List of Supplementary Tables**

**Table 1.S1.** QTL and association mapping of drought tolerance traits in wheat.

**Table 1.S2.** Identification of candidate genes for drought tolerance through transcriptome and proteome profiling, and genetic manipulation.

**Table 1.S3.** Examples of transcriptional activators involved in modulation of drought response.

**Table 2.S1A.** Complete description and abbreviation of evaluated traits in the study.

**Table 2.S1B.** Duration of developmental growth stages and trial management relating information.

**Table 2.S2.** ANOVA and descriptive statistics developmental (Dev) traits of 200 wheat genotypes evaluated under drought stress across 2017 and 2018 growing seasons.

**Table 2.S3.** Multiple linear regression of evaluated traits under rain fed and drought stress conditions during 2017 and 2018. Note that PBW and HI were not included in the regression because PBW is the sum of SDW and GY, and not an independent component. HI is the ratio of GY to PBW weight.

**Table 2.S4.** Summary statistics of breeding progress (absolute and relative) of GY related traits and grain quality for 2017 and 2018 growing seasons together (Lsmeans) and the type of dynamic in the ABP.

**Table 2.S5.** Pairwise comparison of regressions coefficients (intercepts and slopes) of model GY vs yield components, and traits of interest vs year of release under both water regimes.

**Table 2.S6.** Drought-tolerant and Drought-sensitive genotypes identified based on the SWP values of agronomic, developmental and grain quality traits.

**Table 2.S7.** Summary of SNP markers significantly associated with evaluated traits under both water regimes.

**Table 3.S1.** List of measured leaf chlorophyll a fluorescence parameters.

**Table 3.S2.** Complete description and abbreviation of evaluated traits in the study.

**Table 3.S3.** Chlorophyll content and fluorescence ratio parameters across growth stages in 2017 and 2018 growing seasons.

**Table 3.S4.** Dark and light adapted chlorophyll fluorescence ratio parameters measured at anthesis growth stage

**Table 3.S5.** Stomatal conductance (gsw) dynamic across growth stage in 2018.

**Table 3.S6.** Photosynthesis related parameters measured with the Licor 6800 at anthesis growth stage.

**Table 4.S1.** List of the thirty winter wheat cultivars grown in pot experiment in 2019.

**Table 4.S2.** Traits description for field trials in 2017 and 2018 and pot experiment in 2019.

**Table 4.S3.** SNP loci showing multiple and interacting effects on the evaluated traits and the corresponding underlying genes.

**Table 5.S1.** Year wise soil information of the experimental site.

**Table 5.S2.** Fertilizer application, amount and the developmental stage of crop.

**Table 5.S3.** Application of fungicides/pesticides on different developmental stages of the wheat.

**Table 5.S4.** Description of the measured variable in the experiments.

**Table 5.S5.** Summary of analysis of variance of agronomic and grain quality traits of 220 genotypes tested in 3 different environments.

**Table 5.S6.** Arithmetic mean and treatments effect of agronomic and grain quality traits of 220 genotypes tested in 3 different CS over three growing seasons.

**Table 5.S7.** GY (dt.ha<sup>-1</sup>) statistics for the applied cropping systems and the years of experiments.

**Table 5.S8.** Detailed analysis of variance of GY of winter wheat genotypes in cropping systems (CS) by year (Y).

**Table 5.S9.** Three ways ANOVA of GY of winter wheat genotypes (G) in three cropping systems (CS) across three years (Y).

**Table 5.S10.** N flow related analysis of variance and statistics.

**Table 5.S11.** Pairwise comparison of GYs and its components correlation coefficients among cropping systems.

**Table 5.S12.** Pairwise comparison of coefficients (intercepts and slopes) of regressions model GY vs traits of interest under three CS.

**Table 5.S13.** Full regression (A) and path models (B) with direct and indirect effects of 13 independent variables on GY of 220 cultivars tested in 3 different CS over three growing seasons.

**Table 5.S14.** Summary of winning genotypes in the three environments and their year of release.

**Table 5.S15.** Pairwise comparison of coefficients (intercepts and slopes) of regressions model traits of interest vs years of release under three CS.

The following Excell tables are available at Zenodo Digital Repository:  
<https://doi.org/10.5281/zenodo.5196777>

### **List of Supplementary Excel Tables**

**Table 2.Sxl1.** Full description of MTAs including 85 MTAs and 266 significant at P<10<sup>-4</sup> and P<10<sup>-3</sup>, respectively.

**Table 2.Sxl2.** Full description of MTAs (P<10<sup>-4</sup>) underlying evaluated traits across both water regimes.

**Table 2.Sxl3.** Chromosomal LD and information on the SNP density across genomes.

**Table 2.Sxl4.** SNP cluster or QTLs regions associated with evaluated traits.

**Table 2.Sxl5.** Candidate genes in the regions of MTAs–clusters associated to a trait.

**Table 2.Sxl6.** Information on MTAs—clusters interacting with water regimes, and the majors and minor alleles average values.

**Table 2.Sxl7.** Candidate genes in the regions of MTAs—clusters interacting with water regimes.

**Table 2.Sxl8.** Pleiotropic SNP for GSC under both water regimes across two growing seasons.

**Table 2.Sxl9.** Phenotypic data (BLUEs values) under two water regimes.

**Table 3.Sxl1.** Description of SNP number per chromosome and chromosomal LD.

**Table 3.Sxl2.** Full description of detected significant MTAs (10-4) from GWAS under both water regimes in 2017, 2018 and with the means values of both years.

**Table 3.Sxl3.** Summary of significant SNPs QTL detected in the marker\*treatment interaction GWAS.

**Table 3.Sxl4.** Table of QTL regions in the marker\*treatment interaction GWAS and alleles combination effect.

**Table 3.Sxl5.** GWAS results from four physiological traits and three final aboveground biomass traits highlighting SNPs with stable and pleiotropic effects.

**Table 3.Sxl6.** Candidate genes in the QTLs regions with stable and pleiotropic effects.

**Table 3.Sxl7.** Candidate genes in the QTLs with high significant marker\*treatment interactions effects.

**Table 3.Sxl8.** Table of significant SNPs in the genome wide SNP-SNP epistatic interaction.

**Table 3.Sxl9.** Candidate genes in the QTLs regions harboring SNPs with epistatic effects.

**Table 3.Sxl10.** Mean of alleles effect of *AX-158576783* on YII and GY.

**Table 3.Sxl11.** Transcription factors binding sites in the promoter region of NADH-ubiquinone oxidoreductase, 20 Kd subunit genes *TraesCS3A02G287600* that co-segregated with *AX-158576783*.

**Table 4.Sxl1.** Description of 443 MTAs under four treatments (DMN, DHN, RMN, RHN).

**Table 4.Sxl2.** Description of 27 QTL regions showing number of significant SNPs by QTL.

**Table 4.Sxl3.** List 372 SNP involved in main GWAS and their pleiotropic level.

**Table 4.Sxl4.** List 524 SNP involved in SNP\*N treatment interaction GWAS.

**Table 4.Sxl5.** List of candidate genes from QTL regions of main GWAS.

**Table 4.Sxl6.** Gene ontology classification grouping genes of same GO category.

**Table 4.Sxl7.** Gene ontology classification relating biological process.

**Table 4.Sxl8.** Gene ontology classification relating molecular functions.

**Table 4.Sxl9.** List of candidate genes from QTL regions of QTL with pleiotropic effect and QTL regions interacting with N treatments.

## Chapter 1

### 1.1. General Introduction

#### 1.1. Plant water and nutrients demands

The agricultural community has the challenge of increasing food production up to more than 70% to meet the demand from the global population predicted to increase to 9 billion by 2050 (Friedrich, 2015; FAO, 2020). Sustainable crop production involves the efficient and successful use of available resources that are of paramount importance in agriculture such as water (Barnabás et al., 2008; Mohammadi, 2018) and nitrogen (Hawkesford, 2017). It aims to meet human food needs, while protecting the environment through less carbon, nitrous emission, and increasing biological resources (Allahyari et al., 2019).

##### 1.1.1. Importance of water in crop production

Water input is essential for crops, and its deficit is the most prominent abiotic stress factor limiting agricultural production (McElrone et al., 2013a; Nezhadahmadi et al., 2013). Globally, agriculture account for 80-90% of existing fresh water used by humans (Morison et al., 2008b; D'Odorico et al., 2020). Water is important for plant's growth, development and reproduction, and consequently for its yield and quality. Water profoundly influences photosynthesis, respiration, absorption, translocation and utilization of mineral nutrients, and cell division besides some other processes production (McElrone et al., 2013). Water acts as base material for all metabolic activities in plant systems and helps to transport metabolites from source to sink.

Considering the importance of water in plants, the increase in crop production would undoubtedly imply increasing water use. Globally, around  $2.7 \times 10^3 \text{ km}^3$  of water were used in agriculture in the year 2000 (Morison et al., 2008). A production of 1 kg of wheat requires  $1 \text{ m}^3$  of water and 1 kg of rice requires at least  $1.2 \text{ m}^3$  of water (Pimentel et al., 2004). In temperate zones and in arid regions, an amount of  $0.7\text{--}2 \text{ m}^3$  and  $3\text{--}5 \text{ m}^3$ , respectively, is required for 1 kg of grain yield (Gregory, 2004; Morison et al., 2008). Water's importance for crop production stems from its central role in plant nutrition as it is the solution through which other production inputs such as minerals are absorbed from soil (Kaggwa, 2013).

##### 1.1.2. Importance of nitrogen in crop production

Nitrogen is the most important nutrient that impacts crop production (Perchlik and Tegeder, 2017) and its absorption mostly depends on environmental conditions, particularly on the soil moisture content (Abreu et al., 1993) Ladha et al., 2016). This nutrient plays a key role in the plant life cycle and it is needed for chlorophyll production and for the synthesis of other plant cell components (proteins, nucleic acids,

amino acids). Moreover, nitrogen contributes to the production of chemical components that protect against parasites and plant diseases. The amount of nitrogen supply plays a key role in the cropping systems and nitrogen is part of various enzymatic proteins that catalyze and regulate plant-growth processes (Gregory, 2011; Muñoz-Huerta et al., 2013; Barraclough et al., 2014). For instance, nitrogen is required in large quantities to constitute the plant proteins that convert solar radiation into carbohydrates through photosynthesis (Ladha et al., 2016).

In cereals, N fertilizer applications have facilitated the increase in grain yields and grain protein contents (Garnett et al., 2009). Nitrogen application greatly affects gluten and protein content, protein composition, starch composition and grain quality of wheat (Wang et al., 2004). A wheat crop requires about 168-336 kg ha<sup>-1</sup> of fertilizer N for optimum yields, and contains 15-17 kg of N per 454 kg of grain whose protein content ranges from 12-14% (Ottman and Thompson, 2006; Kaggwa, 2013).

## **1.2. Drought stress, N deficiency and plant response under stress conditions**

### **1.2.1. Causes of drought stress and his effect on crop production**

Drought is defined as a period of weeks to years when precipitation is below the normal condition, resulting in a water shortage (Mitra, 2001; Dai, 2011). Droughts are categorized according to how they develop and what types of impact they have. They are three major categories of drought, namely, meteorological drought, hydrological drought, and agricultural drought (Shrestha, 2020). The category affecting crop production is agricultural drought, which refers to the period during a cropping season when the rainfall and soil moisture cannot meet the evapotranspiration demand of the crops (Dai, 2011). Droughts are caused by a combination of factors and can occur naturally or by human activity, such as deforestation, land degradation and inappropriate water use and management. Although, most causes of droughts over recent years seem to be natural in terms of where and when they occur (Hoerling et al., 2010), the anthropogenic factor of climate change, generating extra heat from global warming, is expected to increase the intensity and severity of drought (Trenberth et al., 2014).

Approximately 82% of the world's cultivated areas are devoted to rainfed agriculture, whereas, drought stress on plants accounts for approximately 70% of potential yield loss worldwide (Kang et al., 2009; Huang et al., 2013). Compared to other abiotic stress, drought has the largest spatial extent with nearly 80% of the total cultivated area worldwide and also has the longest duration (Sheffield and Wood, 2012). Drought is expected to increase due to the current effect of climate change (**Figure 1.1**). The anomaly of global land (60° S to 75° N) precipitation times series, revealed very high variation in rainfall across years between 1950 and 2010 (Trenberth et al., 2014). These data highlight the importance of rainfall for crop production, and how much its irregularity due to drought can threaten the food security worldwide. Drought stress effect on plants combines several types of abiotic stress, such as high

temperatures, high irradiance, and nutrient toxicities or deficiencies (Mohammadi, 2018). Drought affects the plant–water relations at all scales, from molecular, cellular, and organ to the whole plant levels (Oyiga et al., 2020). Following drought, stomata close progressively with a parallel decline in net photosynthesis which is the key physiological process for crop production (**Figure 1.2**). The immediate consequence is the production of smaller organs, and hampered flower production and grain filling (Farooq et al., 2014). The impact of drought on yield production varies with the developmental stage when it occurs, the crop and cultivars, and the occurrence of other abiotic stress factors such as high temperature and nutrient toxicities. Reports indicated that yield loss could reach 90% when a prolonged stress occurs from anthesis to maturity (Dhanda and Sethi, 2002a; Mohammadi, 2018). These reductions in yield mainly stem from the negative effect of drought stress on photosynthesis efficiency.

During photosynthesis, drought causes stomatal restriction (Carmo-Silva et al., 2010), which lowers the intercellular CO<sub>2</sub> concentration. Drought might also lead to a non-stomatal restriction defined as the inhibition of the ribulose-1,5-bisphosphate carboxylase/oxygenase (RuBisCo) or changes in photosynthetic pigments, reducing the activity of enzymes involved in Calvin cycle reaction. Both stomata activities hampered crop photosynthesis and yield production (Anjum et al., 2003; Friso et al., 2004; Zhao et al., 2020). Severe drought conditions limit photosynthesis through a decrease in the activities of RuBisCo, phosphoenolpyruvate carboxylase (PEPCase), NADP-malic enzyme (NADP-ME), fructose-1,6-bisphosphatase (FBPase) and pyruvate orthophosphate dikinase (PPDK). Reduced contents of tissue water also increase the activity of RuBisCo-binding inhibitors. Due to the reduction of NADPH produced, non-cyclic electron transport is downregulated, and thus reduces ATP synthesis (Farooq et al., 2009).

Another important effect of drought that reduces plant growth and photosynthetic abilities is the loss of balance between the production of reactive oxygen species (ROS) and the antioxidant defense (Reddy et al., 2004). Consequently, ROS is accumulated, inducing oxidative stress in proteins, membrane lipids and other cellular components. Some important components of photosynthesis affected by drought are shown in **Figure 1.3**. The primary sites where ROS are produced in plants are chloroplasts, mitochondria, and peroxisomes (Mittler et al., 2004; Asada, 2006). These important organs and especially the cellular membranes, enzymes and DNA are very sensitive to ROS and are damaged under the high accumulation triggered by drought stress. The deciphering of mechanisms of drought tolerance requires a deep understanding of plant physiology. Drought-adapted species control stomatal function to allow carbon fixation under stress, therefore improving water use efficiency (Lawlor and Cornic, 2002).

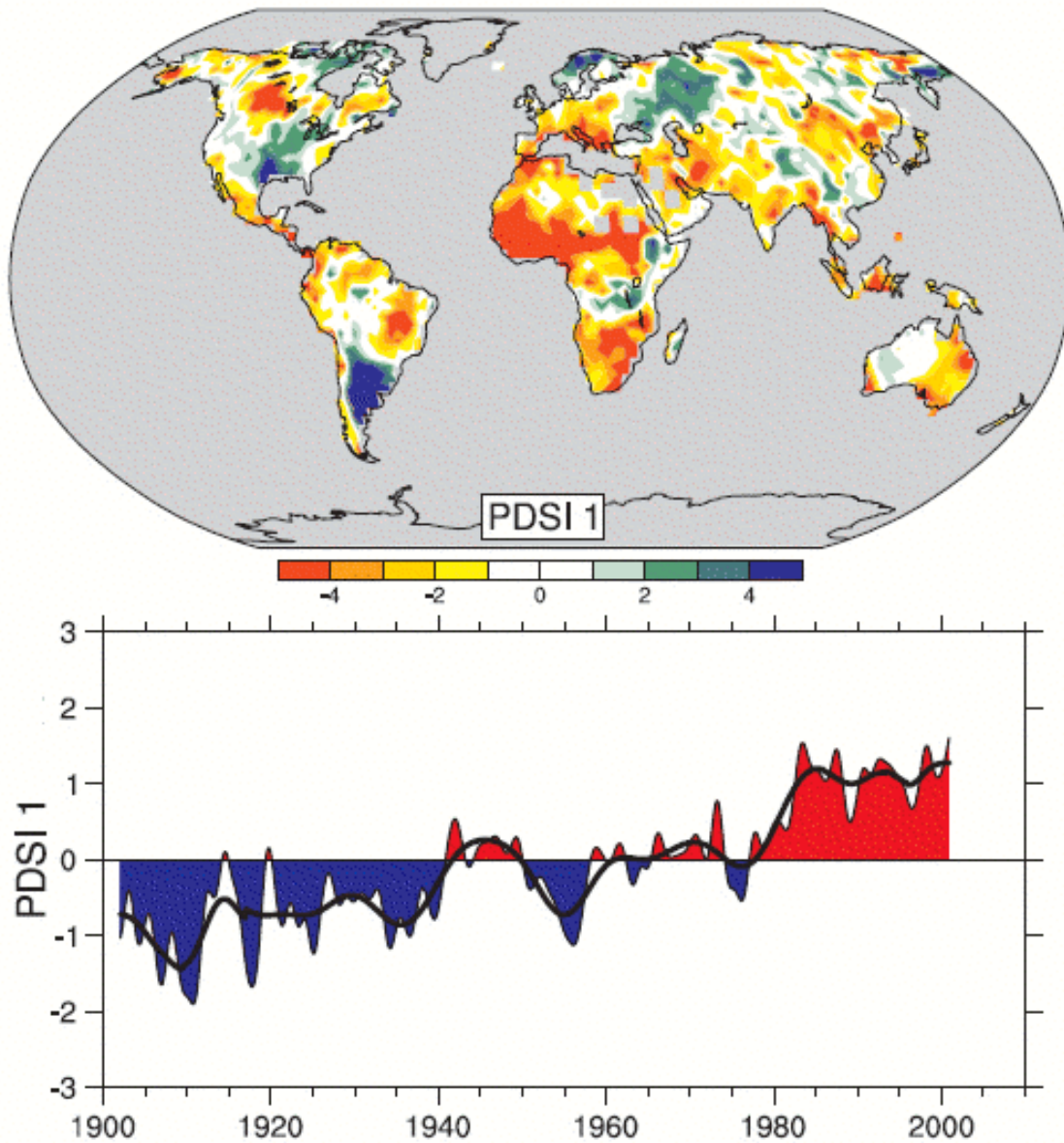


**FIGURE 1.1** | The most important spatial pattern (top) of the monthly Palmer Drought Severity Index (PDSI) for 1900 to 2002. The PDSI is a prominent index of drought and measures the cumulative deficit (relative to local mean conditions) in surface land moisture by incorporating previous precipitation and estimates of moisture drawn into the atmosphere (based on atmospheric temperatures) into a hydrological accounting system. The lower panel shows how the sign and strength of this pattern has changed since 1900. Red and orange areas are drier than average and blue and green areas are wetter than average when the values shown in the lower plot are positive. The smooth black curve shows decadal variations. The time series approximately corresponds to a trend, and this pattern and its variations account for 67% of the linear trend of PDSI from 1900 to 2002 over the global land area. It therefore features widespread increasing African drought, especially in the Sahel, for instance. Note also the wetter areas, especially in eastern North and South America and northern Eurasia. Source: (Solomon et al., 2007).

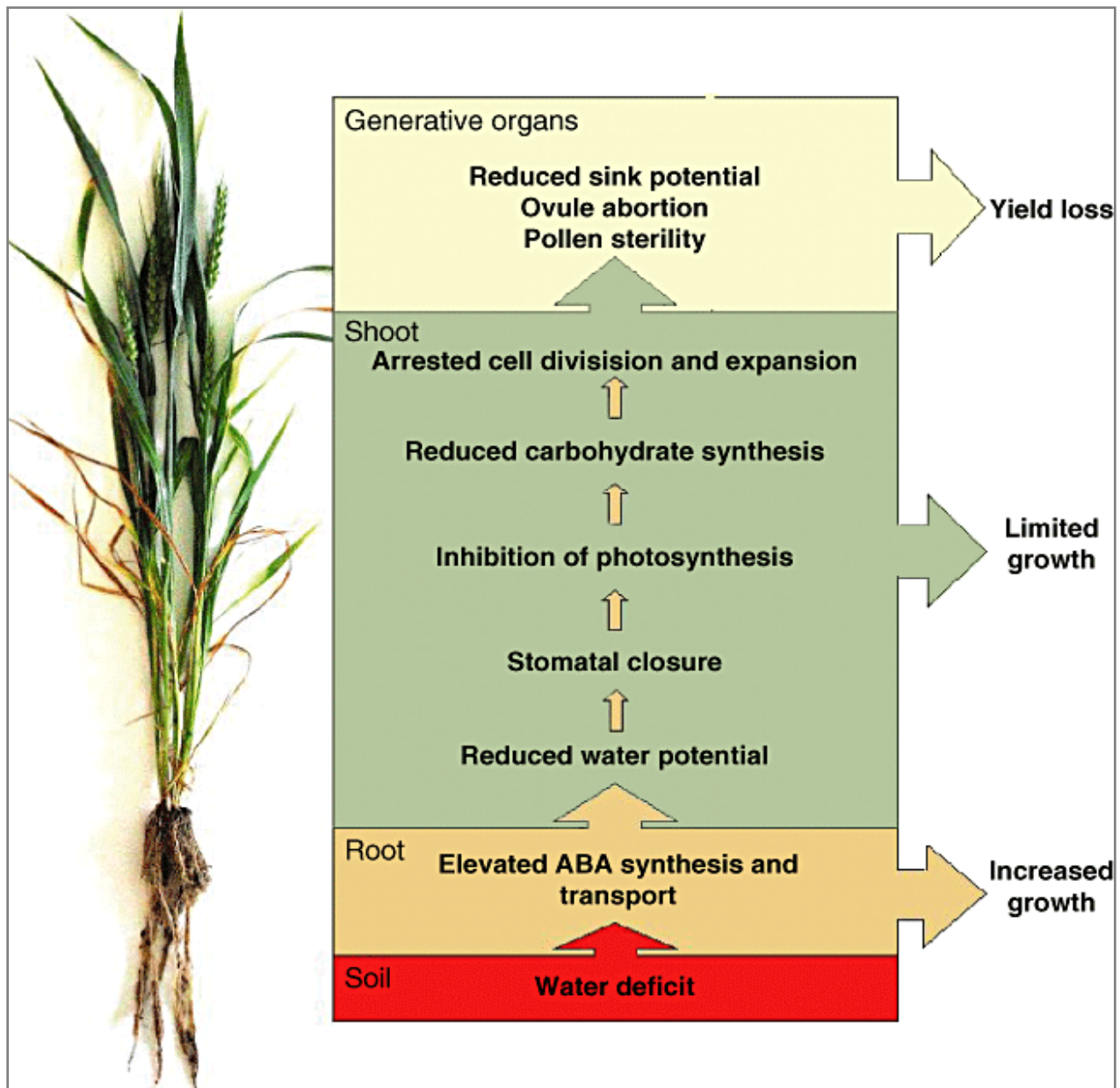


**FIGURE 1.2** | Plant responses at molecular, cellular, and organ to the whole plant level under drought. Source: Barnabás et al. (2008).

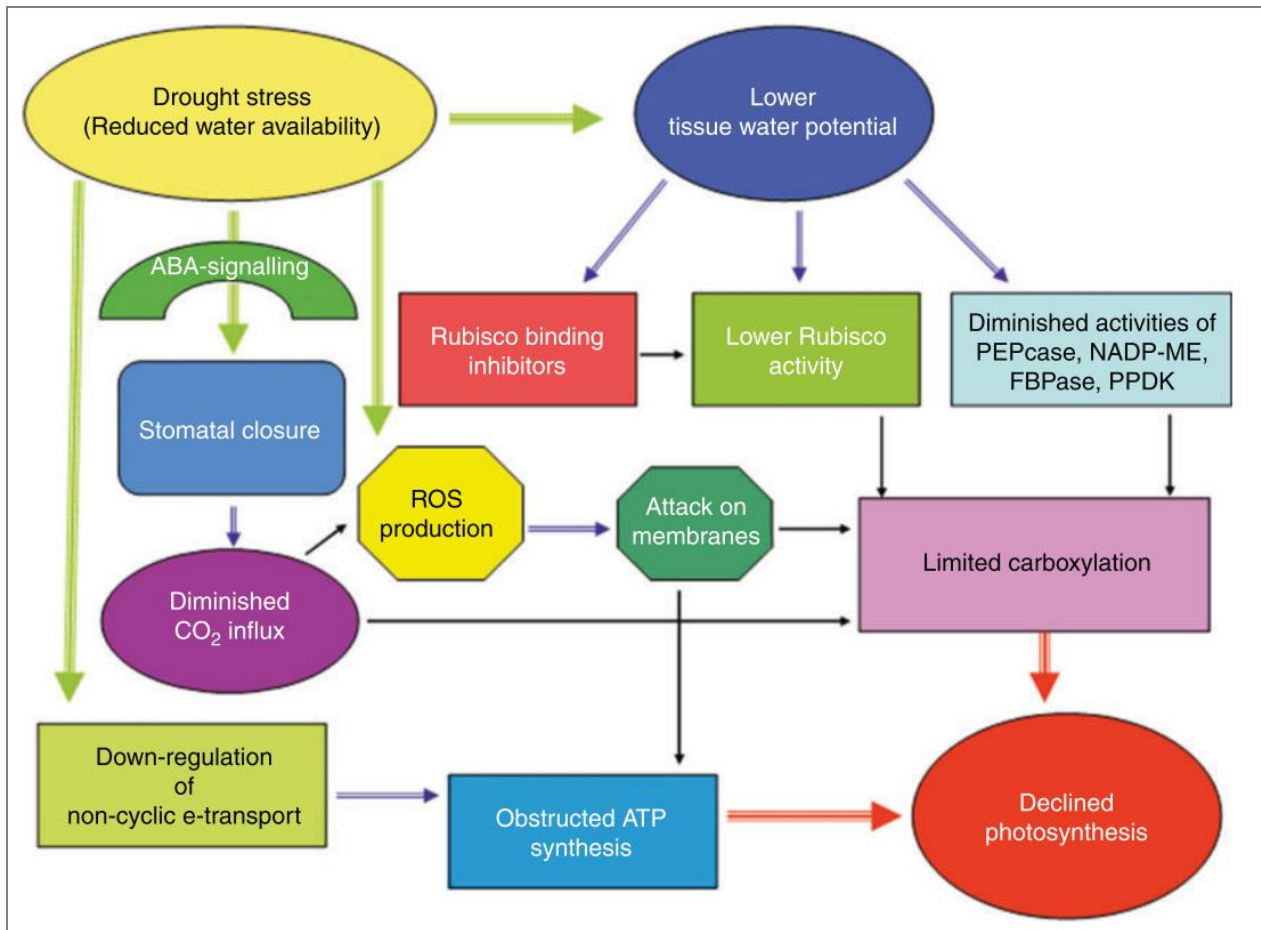


**FIGURE 1.3** | Photosynthesis under drought stress. Possible mechanisms by which photosynthesis is reduced under drought stress conditions. Source: Farooq et al. (2009)

### 1.2.2. Crop plant response to drought stress

Plants, as sessile organisms have developed various mechanism to cope with temporary water limitations that prevent their growth and productivity (**Figure 1.4**) (Barnabás et al., 2008; Fang and Xiong, 2015). Depending on the drought stress level, plants integrate diverse responses and adaptive mechanisms at the morphological, physiological, and molecular levels, to overcome water-deficit (**Figure 1.4**). These adaptations leading to plant resistance to drought can be genotypes and/or species-specific, (Fang and Xiong, 2015) and involve four mechanisms: drought avoidance (DA) (or ‘‘shoot dehydration avoidance’’), drought tolerance (DT), drought escape (DE), and drought recovery (Fang and Xiong, 2015). DA and DT are the two major mechanisms employed by plants to tolerate mild, moderate, and severe drought (Yue et al., 2006). DE is a natural or artificial adaptation of the plant life cycle to avoid encountering local seasonal or climatic drought, by accelerating reproductive growth (Mitra, 2001; Shavrukov et al., 2017). Drought recovery, as indicated by the name, refers to the capacity of the plant to resume growth after severe drought stress that results in a loss of turgor pressure and leaf dehydration.

DA refers to morphological and physiological changes occurring at leaf or root level to respond to drought stress. The changes at leaf level involve leaf rolling and increasing wax accumulation to prevent water loss. The leaf rolling is caused by loss of turgor pressure, resulting in reduction of water loss and increase of photosynthesis activity, as found on rice (Zou et al., 2011), wheat (Omarova et al., 1995), and maize (Prechamandra et al., 1992). Delay of leaf rolling under water stress can be achieved through osmotic adjustment (Fang and Xiong, 2015). Besides leaf rolling traits, epidermal hairs, cuticular wax, along with leaf water potential, relative water content, water loss rate, and importantly canopy temperature, are also used as criteria for appraisal of DA (Hu and Xiong, 2014). Another leaf trait is stomata closure, which reduces water loss from transpiration (Tardieu, 2013). Several molecular mechanisms are underlying leaves stomata closure, among which abscisic acid (ABA) is the positive regulator during drought stress and plays an important role in  $\text{Ca}^{2+}$  influx and  $\text{K}^{+}$  efflux across the guard cells (Daszkowska-Golec and Szarejko, 2013). The endogenous phytohormone ABA is synthesized and transported to leaves cells to trigger the stomatal closure after drought stress is detected by roots cells.

Besides leaf adaptation to overcome drought stress, plants generally mine water from underground through root system under early water-stress. Development of plant root system architecture plays an important role in response to water deficit (Ashraf et al., 2019). After the onset of drought, water is often found in deeper soil layers (Trachsel et al., 2011). Drought-adaptive traits related to root physiology and morphology have been identified in maize (*Zea mays*), sorghum

(*Sorghum bicolor*), rice (*Oryza sativa*) and wheat (Richard et al., 2015). Wheat cultivars with narrower lateral root distribution and higher proportion of roots at depth can access more soil moisture deep in the soil profile (Richard et al., 2015). Furthermore, DA can refer to phenological changes resulting in the reduction or extension of the vegetative stage to respond to drought stress.

DT is the capability of plants to maintain physiological activities through the regulation of genes to reduce or repair damages from drought stress (Yue et al., 2006; Luo, 2010). The mechanisms associated with DT involve cell osmotic adjustment, production of antioxidants, phytohormones and increase in the chlorophyll content (Fang and Xiong, 2015). Osmotic adjustment, via production and accumulation of organic and inorganic substances such as sugars, amino acids polyols (proline, glycine), alkaloids and inorganic ions, allows cells to manage their dehydration and membrane structural integrity to give tolerance against drought and cellular dehydration (Loutfy et al., 2012). For instance, under severe drought stress wheat genotypes accumulate more soluble sugars that become an essential replacement for water (Farshadfar et al., 2008; Hussain et al., 2018; Sallam et al., 2019). The detoxification of reactive oxygen species (ROS) through antioxidants defense is one of the drought tolerance mechanisms. The accumulation of ROS, such as singlet oxygen  $^1\text{O}_2$ , hydrogen peroxide ( $\text{H}_2\text{O}_2$ ), superoxide radicals ( $\text{O}_2^-$ ), and hydroxyl radical (OH) increase under drought stress and may lead to cell death, chlorophyll destruction, metabolism perturbations, and severe injury (Cruz de Carvalho, 2008; Gill and Tuteja, 2010). To detoxify cells from excessively accumulated ROS, plants produce protective enzymatic and non-enzymatic antioxidants to maintain the equilibrium of the intracellular redox state. Among the enzymatic type are catalase (CAT), superoxide dismutase (SOD), peroxidase (POD), ascorbate peroxidase (APX), monodehydroascorbate reductase (MDHAR). On the other hand, non-enzymatic antioxidants include ascorbic acid (AsA), glutathione (GSH), carotenoids (CAR),  $\alpha$ -tocopherol (vitamin E), and anthocyanins.

As discussed above, the processes coordinating the response to drought stress involve a network of stress-responsive genes (Osakabe et al., 2014). Succinctly, at least three principal pathways are used by genes networks to convey drought tolerance, two ABA-dependent and one ABA-independent pathways (Abrahám et al., 2003; Nakashima et al., 2009). Several candidate genes with kinase domain, such as calcium-dependent protein kinases (CDPKs), CBL (calcineurin B-like) interacting protein kinase (CIPK), mitogen-activated protein kinases (MAPKs), and sucrose non-fermenting protein (SNF1)-related kinase 2 (SnRK2), have been reported to participate in drought response. Genes encoding many transcription factor (TFs) family members have been identified as involved in drought tolerance e.g., DREB, NAC, WRKY, MYB, bZIP, TZF, APETALA2/Ethylene-responsive element binding protein (AP2/EREBP), and zinc finger (Joshi and Nayak, 2010; Samarah, 2016). The

major physiological changes that occur in tolerant and susceptible wheat and barley genotypes are illustrated in **Figure 1.5**.

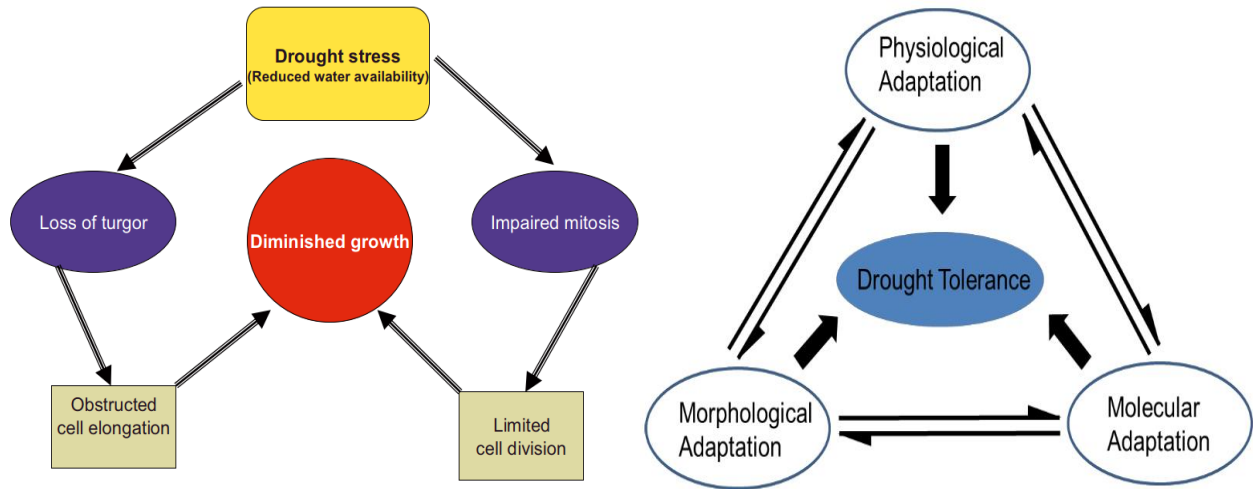


**FIGURE 1.5** | Description of possible mechanisms of growth reduction under drought stress (left panel) and the representation of the three adaptive mechanisms (physiological, morphological and molecular) and their connection in drought tolerance (right panel). The double arrows represent the interaction among the different adaptive mechanisms. Source: left panel; (Farooq et al., 2009); right panel (Reinert, 2017).

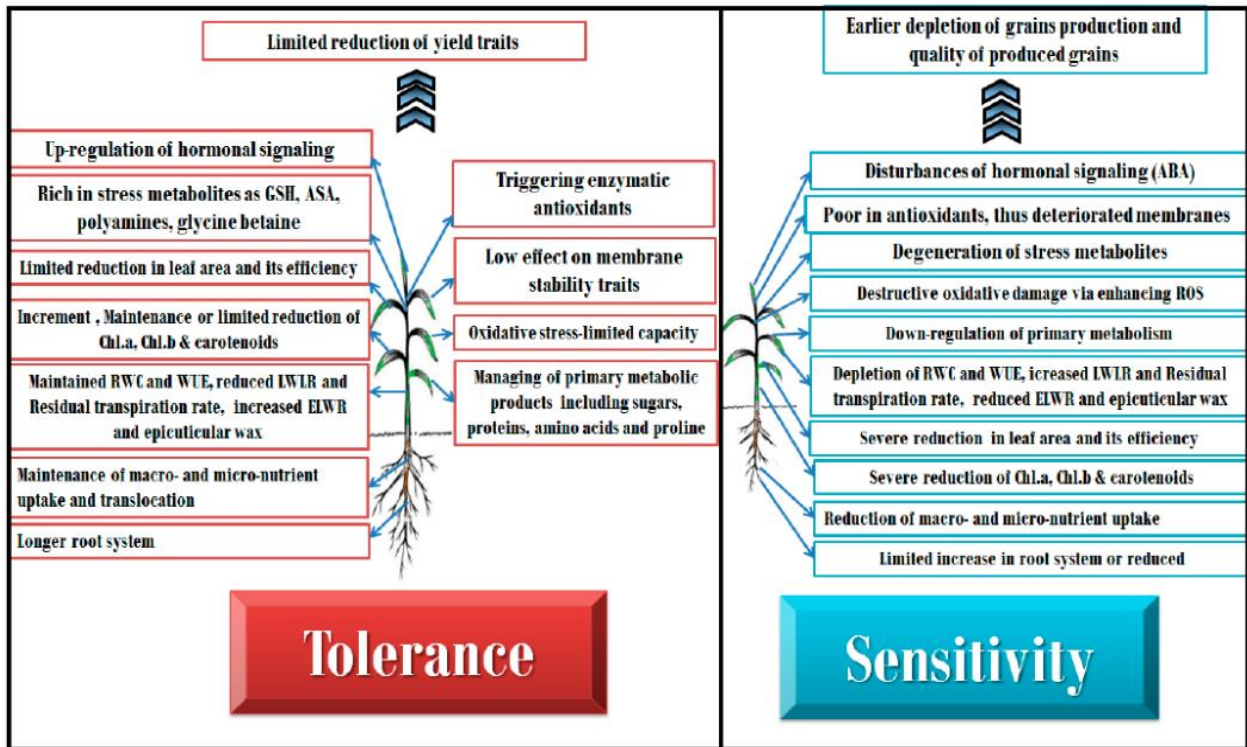


**FIGURE 1.5** | Physiological changes in tolerant and susceptible wheat and barley genotypes in response to drought stress. Source: Sallam et al., 2019.

### 1.2.3. Nitrogen uptake and use efficiency, particularly under drought conditions

Nitrogen has a strong effect on plant metabolism and biological processes that regulate plant growth, development and yield (Gregory, 2011; Barraclough et al., 2014). Plants absorb nitrogen as a mineral nutrient mainly from soil solution, in the form of ammonium ( $\text{NH}_4^+$ ) and nitrate ( $\text{NO}_3^-$ ), with  $\text{NH}_4^+$  being ~10% of the  $\text{NO}_3^-$  concentration (Marschner et al., 2011; Garnett et al., 2015). Nitrogen transformation process closely depend on water and its mobility in the soil (Gonzalez-Dugo et al., 2010). Nitrogen absorption by plants is related to three major steps, including uptake, assimilation, and re-mobilization (**Figure 1.6**) (Han et al., 2016). The nitrogen use efficiency (NUE) is the product of N uptake efficiency (NUpE) and N utilization efficiency (NUtE) (Good et al., 2004). NUE can be calculated in many ways (Fageria and Baligar, 2005), but it is widely accepted that NUE is the ratio of output (economic yield) to N fertilizers input (Moll et al., 1982). Increased NUE usually positively correlates with the crops aboveground biomass, seed production, grain protein, and yield (Masclaux-Daubresse et al., 2010), an indication that selection based on high NUE can improve crop productivity (Garnett et al., 2015).

Considering the importance of nitrogen (N) in ensuring higher crop yield and productivity, farmers tend to overuse it (Good and Beatty, 2011) but paying little attention on important aspects on plant nitrogen absorption and use efficiency. Rather than increasing yield, higher N supply can also decrease the nitrogen use efficiency, causing low yields due to over-stimulation of tillering and plant vegetation (i.e. haying-off) and high N loss (Van Herwaarden et al., 1998; Vitousek et al., 2009). Worldwide, only a third of nitrogen inputs to cereal crops are recovered in grain for consumption. The remaining part could stay in the agro-system or be lost through N leaching, erosion, and runoff, and have negative impacts on the environment (Hawkesford, 2017; SHEN et al., 2017) such as salinization and eutrophication (Cai et al., 2011). That could accelerate the global warming due to Nitrous oxide ( $\text{N}_2\text{O}$ ) emission (Thompson et al., 2019) (**Figure 1.7**). In Europe, between 2004 and 2011, most of the soils were characterized by N surpluses of around 40 to 80 kg N/ha (Buckwell and Nadeu, 2016). In the context of political and environmental constraints on agrochemical supply and climatic changes, reduction of agricultural inputs will contribute to lessen negative impacts of agriculture on the environment (Gregory, 2011).

Soil water content is an important factor affecting the availability of N and thus plants NUE (Kaggwa, 2013). There is a reduction of N availability, uptake, translocation and assimilation under drought stress condition (Gregersen, 2011). Besides being the medium for N in soil, water convey nutrients from soil to plants via mass flow and diffusion (Marschner et al., 2011) (Under water stress, nitrate flow is reduced by 50% to 0.2 mm/day due to the reduction of the transpiration rate due to low

water uptake (Farooq et al., 2009). Therefore, increasing the water uptake under drought conditions will improve nitrogen uptake and use efficiency.

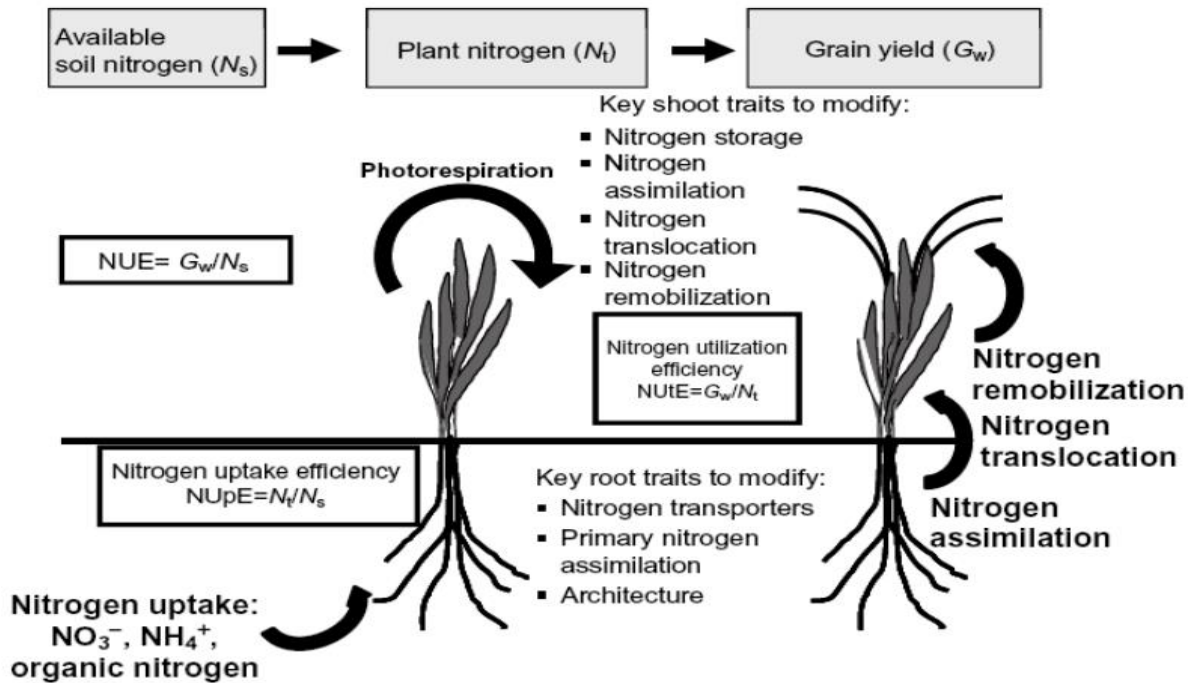


**FIGURE 1.7** | The nitrogen cycle from soil to plant product. Nitrogen use efficiency (NUE) is determined by uptake efficiency (NUpE) which is the amount of nitrogen taken up by the plant and by N utilization efficiency (NUE).  $\text{NUpE} = N_t$  (total plant nitrogen)/ $N_s$  (total available soil nitrogen).  $G_w$  is grain yield or weight.  $\text{NUE} = G_w/N_t$  key components (traits) that have been modified and should be evaluated in more detail are shown. Source: (Good and Beatty, 2011).

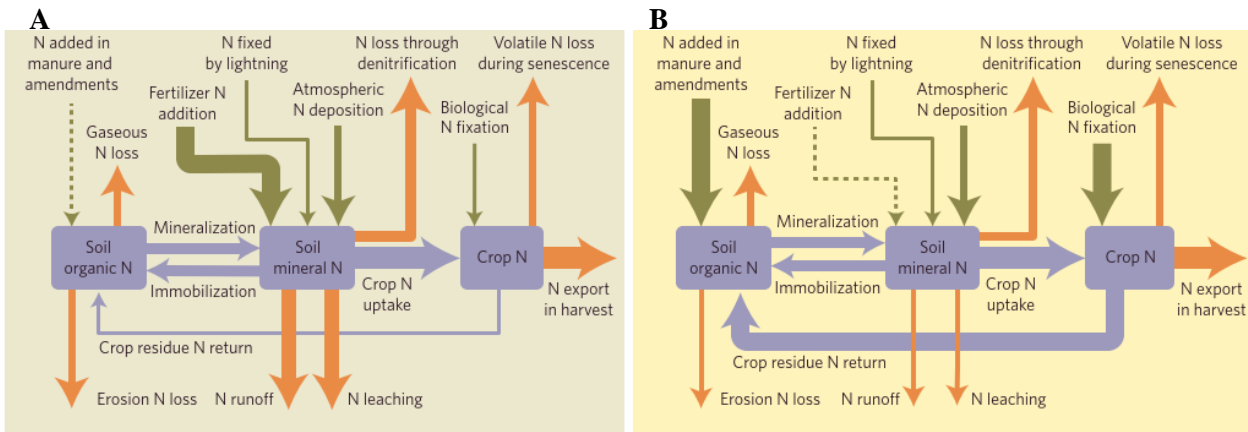


**FIGURE 1.7** | Hypothetical nitrogen stocks and flows of two contrasting cropping systems. Cropping systems relying mainly on mineral nitrogen inputs (**A**) have relatively higher nitrogen losses to air and water than cropping systems with emphasis on biological N fixation, manure and other organic matter amendments, cover crops and perennial crops, and low reliance on mineral N fertilizer, such as organic and integrated systems (**B**). The width of the arrows is relative to the size of the nitrogen flux; boxes representing nitrogen stocks are not scaled to the pool size. Arrows represent nitrogen inputs (green), losses (orange) and transformations (blue). Source:(Reganold and Wachter, 2016).

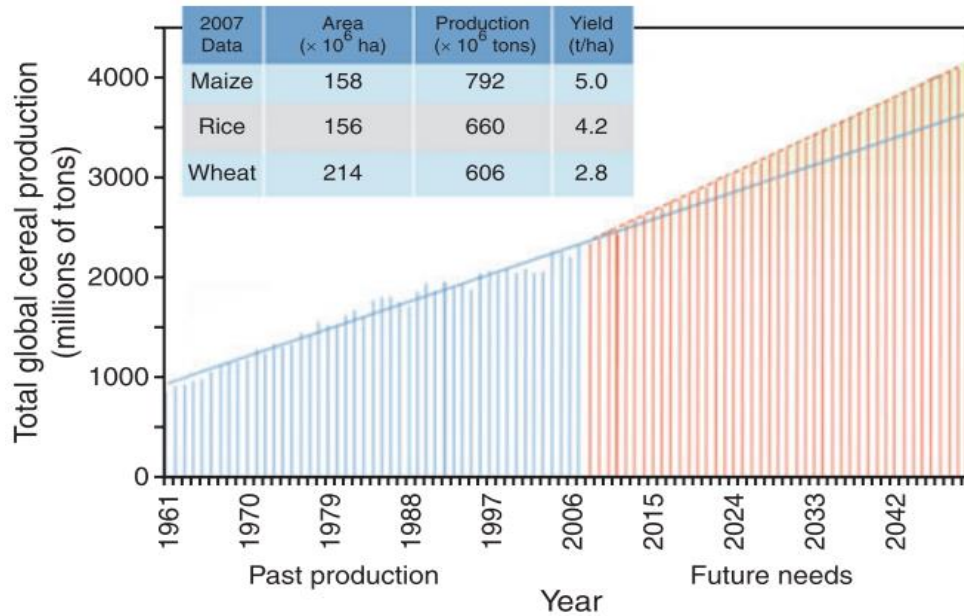
### 1.3. Breeding for drought tolerance and nitrogen use efficiency

Wheat (*Triticum aestivum* L.) is an allohexaploid (6x) with a genome of 21 pairs of chromosomes ( $2n = 6x = 42$ ) sub-divided into 3 closely related (homologous) groups of chromosomes, the A, B and D sub-genomes. Each sub-genome has 7 pairs of chromosomes. The estimated size of wheat genome is 17 Gbp (Shi and Ling, 2018), which is larger than the one of barley (~5.3 Gbp in 7 chromosomes) and rice (~430 Mb in 12 chromosomes) due to high content of repeated sequences. Recent technology developments have enabled the identification of high numbers of DNA-markers but also the production of the whole genome sequence draft of wheat (Shi and Ling, 2018).

Wheat is one of the most important cereals with an annual yield of 760.1 million tones (FAO, 2020). It provides ~20% of human daily calories and ~21% protein requirements (Braun et al., 2010; Hawkesford et al., 2013; Kulkarni et al., 2017), thus plays a major role in global food security (Oyiga et al., 2019). However, wheat production is challenged by various abiotic stress factors, among which drought accounts for approximately 70% loss of potential yield worldwide (Huang et al., 2013). Besides, inefficient cropping management practices such as inappropriate higher nitrogen fertilization rates, growing cultivars with low N use efficiency level are factors that decrease wheat yield and associate with a number of environmental problems (Thompson et al., 2019). Despite these challenges of drought stress and regulations for reducing N supply, the global wheat production needs an annual increase of 44 Mt to meet demand by 2050 (**Figure 1.8**) (Semenov et al., 2014; Mohammadi, 2018).

Optimizing wheat productivity in rainfed agricultural systems and under drought prone environment, while reducing the amount of N input, require the development of drought tolerant and nitrogen use efficient cultivars. Breeding to increase nitrogen use efficiency has become an object of intense research to reduce economical costs and ensure sustainability (Hawkesford et al., 2013; Muñoz-Huerta et al., 2013). Currently, research involving phenotyping, genetics, and breeding for tolerance against drought is receiving attention worldwide. However, many challenges reside in the complex nature of traits associated with improved performance of wheat under water limitation, as each of these traits is controlled by many genes with small effect (Richards et al., 2007; Yang et al., 2007). Fortunately, significant genetic variation for traits associated with drought tolerance seems to be available in wheat germplasm and can be used to develop drought tolerant cultivars (Reynolds et al., 1994; Joshi et al., 2007; Gupta et al., 2012, 2017). The understanding of the shoot-root system and the genetic basis of drought tolerance and NUE in crop plants is of paramount importance for developing superior genotypes (Fleury et al., 2010; Monneveux et al., 2012).

A



B

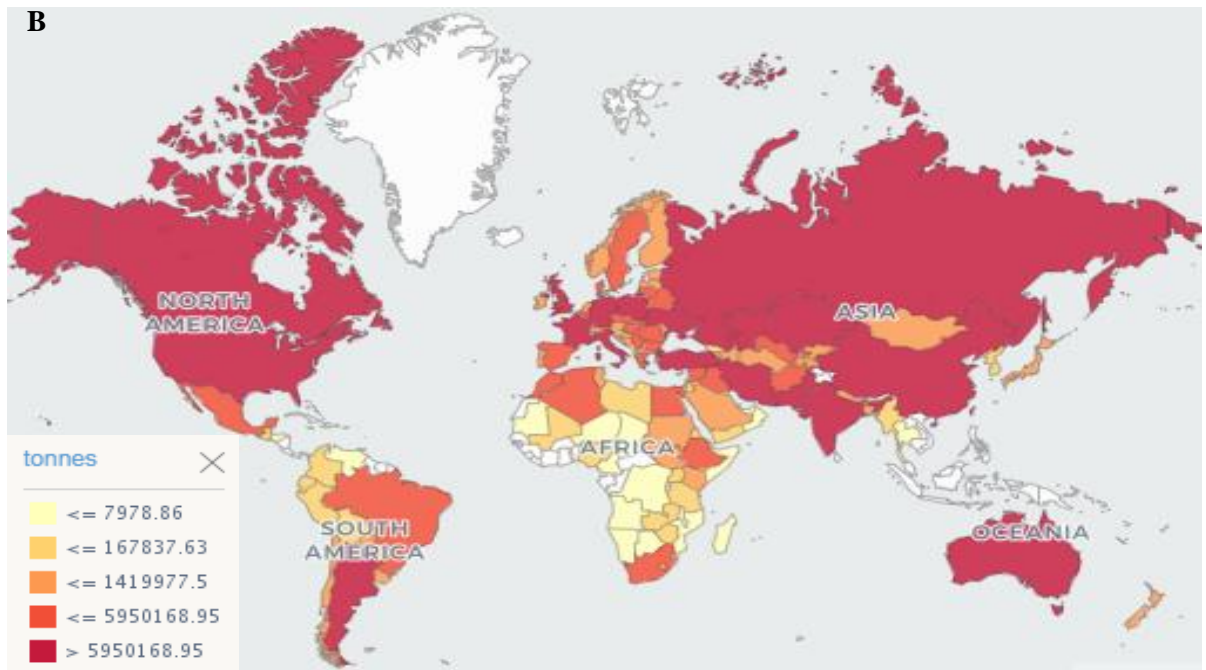


**FIGURE 1.8** | (A) Global cereal production has risen from 877Mt in 1961 to 2351 Mt in 2007 (blue). To meet predicted demands, production will need to rise to > 4000Mt by 2050 (red). The rate of yield increase must move from the blue trend line (32 Mt year<sup>-1</sup>) to the red dotted line (44 Mt year<sup>-1</sup>) to meet this demand, an increase of 37% is required. The inset table shows 2007 data for the three major cereals. Source: Mohammadi 2018. (B) World map showing countries according to their average wheat production (tonnes) from 1961 to 2019 based on data from the Food and Agriculture Organization Corporate Statistical Database. Source: [www.fao.org/faostat/](http://www.fao.org/faostat/).

### 1.3.1. Improving root system architecture

The future gains in productivity, especially under low input conditions, can be achieved through optimization of root system architecture (RSA) (Zhu et al., 2011; Xie et al., 2017). The root system provides the plant anchorage, competitiveness and adaptation to stress. Roots also have significant roles in soil exploration, stand establishment, adaptation to drought, belowground carbon sequestration, soil structure improvement and maintenance of soil fertility by driving microbial processes (Kaggwa, 2013a; Richard et al., 2015; Siddiqui et al., 2020).

Despite the importance of roots, direct selection for optimal RSA characteristics in the field has not been routine because of the complex interactions between roots system and rhizosphere. Different approaches and methods have been used to study these interactions, but most methods failed to represent the system plant-soil and environment as it is in the field where roots and shoots are exposed to very different environmental conditions, especially temperature, which is an important regulator of root development (Ruta et al., 2010). For these reasons, breeding efforts have typically focused on improving above-ground traits with an obvious emphasis on yield (Zhu et al., 2011). In order to improve plant performance for higher yield under stress conditions, breeders need to select genotypes with root system architecture adapted to low input conditions such as nitrogen fertilizer and water deficit (Trachsel et al., 2011; Kaggwa, 2013).

Cultivars with narrow development of lateral roots and suberized roots have better performance plants under drought conditions (Schreiber, 2010). Higher root biomass and deeper rooting (**Figure 1.9**) could increase water and N uptake, and contribute to reductions in N fertilizer wastes and losses associated with wheat production systems (Kaggwa, 2013a; Kulkarni et al., 2017). Higher genotypic variations were found on RSA traits of wheat seedlings (Richard et al., 2015). RSA traits such as seminal root number and total root length were highly correlated with grains  $m^{-2}$ , grains per spike, above-ground biomass  $m^{-2}$  and grain yield. More seminal roots and longer total root length were also associated with delayed maturity and extended grain filling, which is likely to be a consequence of more grains being produced before anthesis (Xie et al., 2017). Similarly, maximum width of RSA displayed positive associations with yield related traits. The higher phenotypic correlations between wheat RSA and yields were confirmed at genetic level with detection of common QTL regions underlying roots traits and grain yield and thousand grain weight (Cao et al., 2014; Maccaferri et al., 2016). The **Table 1.S1-1.S2-1.S3** provide a review of some genomic regions harboring important genes (Dro1, ERECTA) and transcription regulators (AP2/ERF, ZFPs, WRKY, and MYB) that are associated with drought tolerance through enhanced root development.

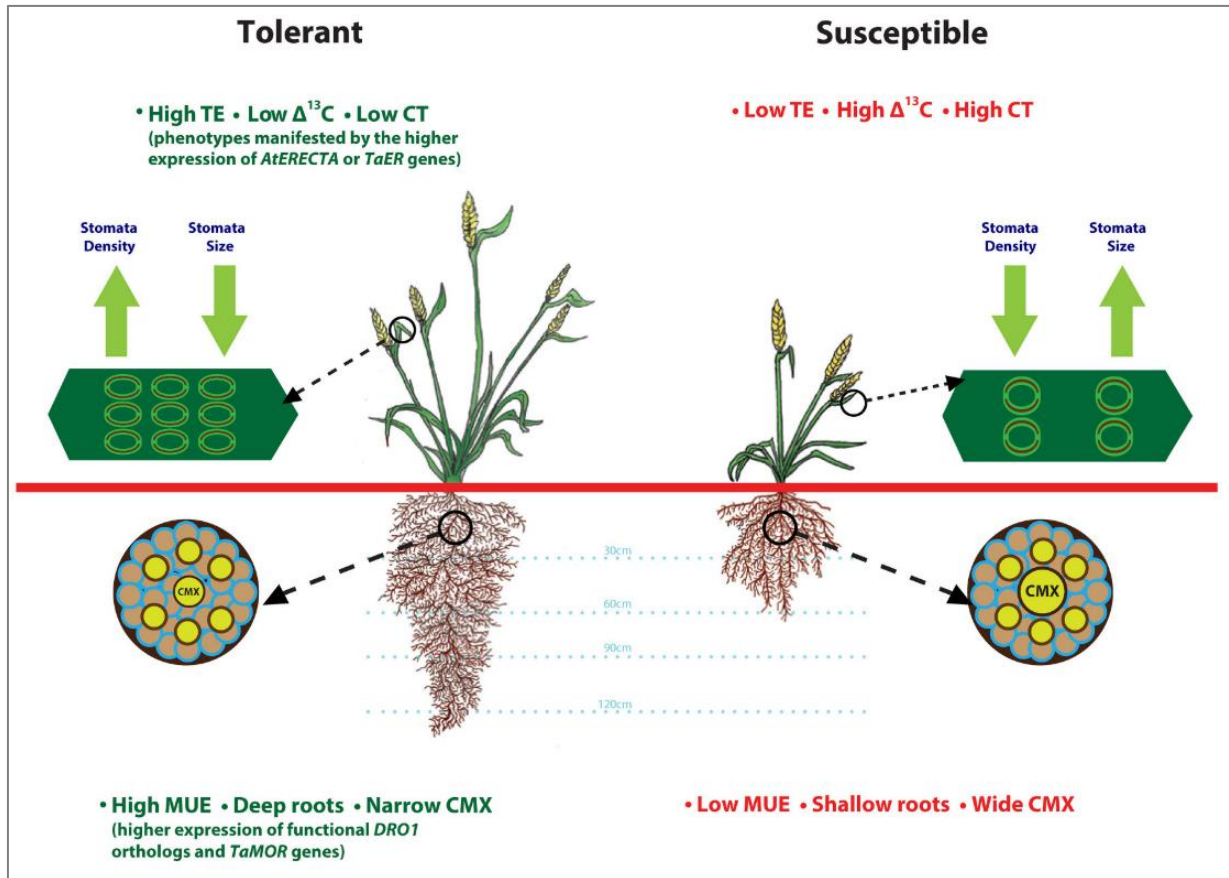


**FIGURE 1.9** | Root and stomatal traits that define drought tolerant and susceptible wheat plant ideotypes. This illustration is prepared based on the findings from various articles cited throughout the manuscript. Plant tolerance to drought stress relies on favorable root anatomical features such as, deeper roots and smaller central metaxylem (CMX) that contribute to improved moisture uptake-efficiency (MUE), and stomatal features such as high density and smaller size that contribute to lower canopy temperature (CT) and reduced carbon isotope discrimination. Source: (Kulkarni et al., 2017).

### 1.3.2. Morphological and physiological traits linked to drought tolerance and NUE

#### *Photosynthesis activity*

Drought stress is associated with other several abiotic stress, such as heat stress, which negatively impact agricultural production (Lobell et al., 2011; IPCC, 2014). Therefore, development of crop varieties with improved water use efficiency (WUE) could help maintaining higher yield under predicted future environmental constraints. WUE can be estimated at an agronomic level as the ratio of water used in crop production versus biomass or yield, while at the physiological view it is the amount of CO<sub>2</sub> fixed in photosynthesis (A) relative to the amount of water vapor lost in the atmosphere (E) (Condon et al., 2004; Medrano et al., 2015). Leaf structural traits, such as the cuticle and cuticular waxes, leaf “Stay Green” are playing important role in WUE under drought stress (Bi et al., 2017; Zeisler-Diehl et al., 2018). Leaf “Stay Green” habit, which is related to its chlorophyll content is linked to the grain filling duration. Furthermore, leaf rolling, leaf membrane thermostability are playing important role in maintaining photosynthesis activity under drought stress. Differences in photosynthesis among genotypes under heat and drought stress have been shown to be associated with a loss of chlorophyll and a change in the chlorophyll a/ b ratio due to premature leaf senescence (Gupta et al., 2012; Reynolds et al., 1994). Plant canopy temperature measured by infrared thermometry has been used to identify water stress in wheat. Canopy temperatures were negatively correlated with cultivars water uptake and photosynthesis activity under drought stress condition (Reynolds et al., 2000a; Lopes and Reynolds, 2010; Sarieva et al., 2010).

Genes controlling those physiological changes are very important sources for geneticists and breeders to genetically improve drought tolerance through a breeding program. The positive regulations of genes expression both at transcriptional and post-transcriptional level has a pivotal role in plant adaptation to drought stress (López-Maury et al., 2008; Kulkarni et al., 2017). In addition, transcription factors such as AP2/ERF consisting of four sub-families in wheat DREB, ERF, AP2, and RAV are mediating these mechanisms underlying stress tolerance (Licausi et al., 2013; Kulkarni et al., 2017).

#### *Photosynthesis mechanism*

Photosynthesis is the physicochemical process by which green plants and certain other organisms convert light energy into chemical energy (Singer et al., 2020; Yang et al., 2020). During photosynthesis in green plants, light energy is captured and used to convert water, carbon dioxide into oxygen and energy-rich organic compounds through the equation 1. This chemical energy-rich compound is stored in carbohydrate molecules, such as sugars (Baker, 2008).



Photosynthesis consist of two major's reactions (**Figure 1.10A-C**): the light-dependent reactions and light-independent reactions (Singer et al., 2020). The light-dependent reaction takes place within the thylakoid membrane and requires a steady stream of sunlight, hence the name *light-dependent* reactions. The chlorophyll absorbs energy from the light waves, which is converted into chemical energy in the form of the molecules ATP and NADPH (**Figure 1.10C**). The light energy absorbed by chlorophylls associated with the photosystem II (PSII) reaction centers (RC) encounters three possible fates. It can be used to drive photochemistry in which an electron ( $e^-$ ) is transferred from the reaction center chlorophyll, P680, to the primary quinone acceptor of PSII, QA. Alternatively, absorbed light energy can be lost from PSII as chlorophyll fluorescence or heat (**Figure 1.10B**). The processes of photochemistry, chlorophyll fluorescence, and heat loss are in direct competition for excitation energy. If the rate of one process increases the rates of the other two will decrease (Baker, 2008). The light-independent reactions, also known as the Calvin–Benson–Bassham Cycle or Calvin cycle (or dark reactions), take place in the stroma which is the space between the thylakoid membranes and the chloroplast membranes, and consequently do not require light, hence the name *light-independent* reactions. During this reaction, energy from the ATP and NADPH molecules produced from light reactions is used to power the assimilation of  $\text{CO}_2$  to assemble carbohydrate molecules, like glucose (Long et al., 2015; Singer et al., 2020).

There are different types of photosynthesis. The C3 photosynthesis occurring in the majority of plants including wheat during which the first carbon compound produced under the catalysis of RuBisCo enzyme contains three carbon atoms called 3-phosphoglyceric acid (3PGA) which goes on to become glucose in the Calvin Cycle. The disadvantages of C3 plants are the photorespirations, by which RuBisCo fixes  $\text{O}_2$  instead of  $\text{CO}_2$ , thus, utilize energy that plants could have used to drive photosynthesis (Singer et al., 2020). Besides, when stomata are open,  $\text{CO}_2$  is entering at the expense of water loss, which is a disadvantage under drought-prone environments. Whereas, in C4 photosynthesis used by plants such as maize, sugarcane and sorghum, there is a four-carbon intermediate compound, which splits into carbon dioxide and a three-carbon compound during the Calvin Cycle. A benefit of C4 photosynthesis is the higher levels of carbon produced, allowing plants to thrive in environments without much light or water.

Severe drought conditions limit photosynthesis due to a decline in RuBisCo activity (Farooq et al., 2009). Further increase in wheat yield could be successfully achieved through research to enhance photosynthesis activity through manipulation of RuBisCo (Reynolds et al., 2011) or through

regulation of genes intervening in these process (Gupta et al., 2012). Under stress conditions, regulation of some stress-responsive genes could alleviate the stress negative impact of plant production. For instance, the upregulation of PsbH, PsbB and PsbD genes encoding PSII Core Proteins in wheat resulted in an increase in photosynthesis activity under heat stress, and hence produce a positive effect on grain yield (Zhang et al., 2020; Hassan et al., 2021).

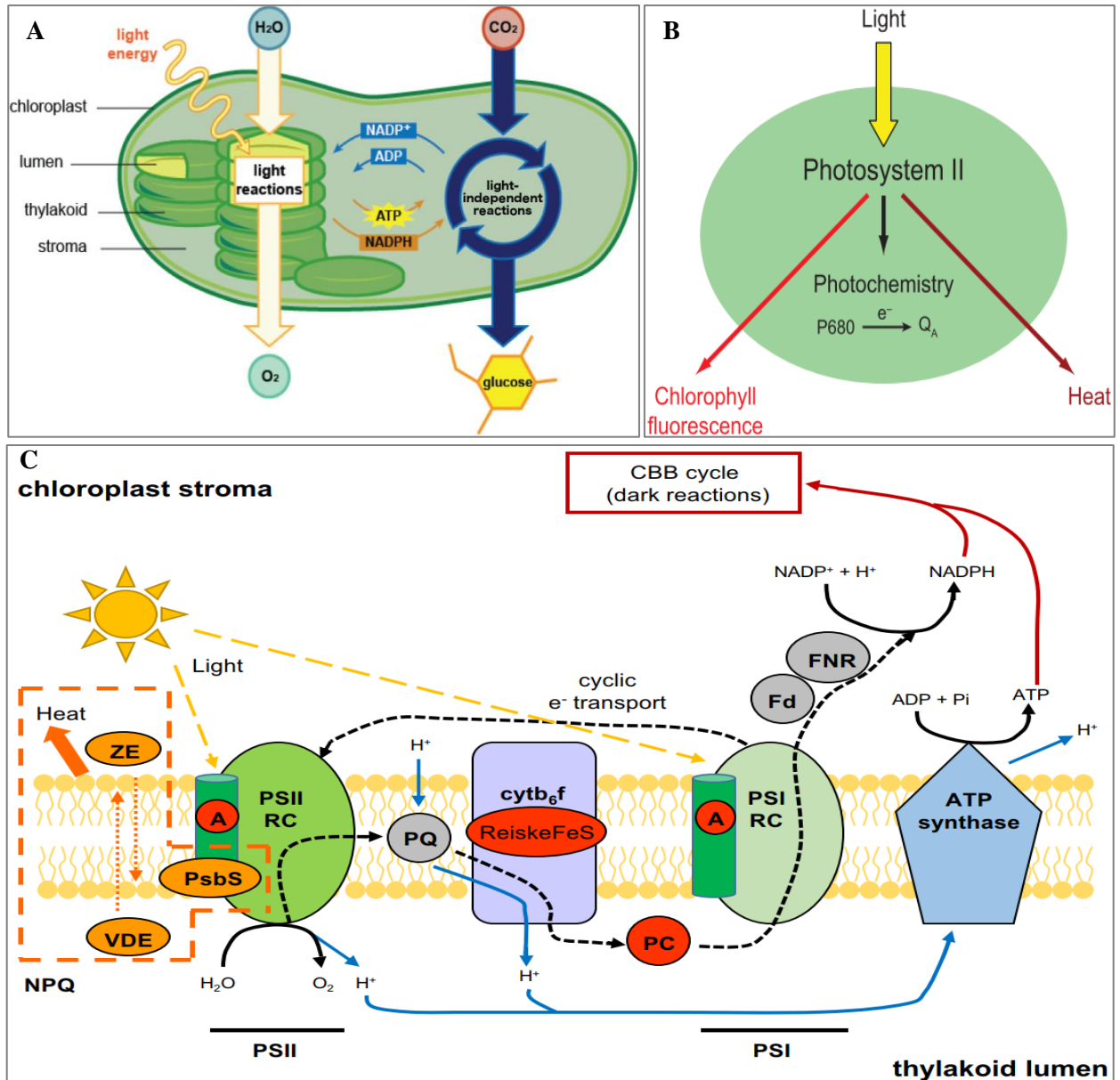


**FIGURE 1.10** | Overview of photosynthesis reactions. **(A)** Structure of chloroplast presenting the locations of both reactions of photosynthesis. **(B)** Simple model of the possible fate of light energy absorbed by photosystem II (PSII). **(C)** Schematic diagram of photosynthetic light reactions and non-photochemical quenching in C3 plants. Blue lines denote proton movement, black discontinuous lines denote movement of electrons, red lines denote movement to the Calvin cycle. Thermal dissipation of excess light energy via non-photochemical quenching (NPQ) is boxed in orange. Components of the light reactions and NPQ that have been modulated (either directly or indirectly) for improvement of photosynthetic efficiency are shown in red and orange, respectively. A light-harvesting antennae complexes, CBB Calvin–Benson–Bassham, cytb<sub>6</sub>f cytochrome b6f complex, Fd ferredoxin, FNR ferredoxin: NADP + reductase, NPQ non-photochemical quenching, PC plastocyanin, PQ plastoquinone, PSI photosystem I, PSII photosystem II, PsbS photosystem II subunit protein, RC reaction centre, ReiskeFeS component of the cytb<sub>6</sub>f complex encoded by PetC, VDE violaxanthin de-epoxidase, ZE zeaxanthin epoxidase. Source: **(B)**(Baker, 2008); **(C)**(Singer et al., 2020).

### 1.3.3. Sensor-based phenotyping of crop photosynthesis activity

High level of precision is necessary to record phenotypic data in plants, thus plant phenotyping of populations for QTL-studies can be laborious and time consuming for breeders aiming to release new varieties. Conventional phenotyping methods for water status in plant or chlorophyll parameters are destructive, nevertheless, the evaluation of crops tolerance to abiotic stress requires non-invasive measurements on the same plant/genotypes over growth stage to observe the kinetic of their stress-response (Sannemann, 2013; Dadshani, 2018). Therefore, the development and use of sensors in plant breeding could make advance in plant phenomics, which laid behind genomics data (Gupta et al., 2012). That will make the best use of DNA information level acquired through new high-throughput sequencing technologies (Churko et al., 2013; Sannemann, 2013). Sensor-based techniques have been used for recording data on complex traits such as tolerance to drought and heat. The methods used to monitor photosynthetic rates are based on spectroscopy. In this research project, we used several sensors such as, Mini-pam II (Walz, 2014), SPAD-502Plus (Minolta, 2009), Polypen RP410, Licor-6800, Ap4 porometer Delta-T to measure plant photosynthesis-related traits over growth stages.

The photosynthesis yield analyzer MINI-PAM-II is used to screen for chlorophyll fluorescence characteristics. The use of chlorophyll fluorescence to monitor photosynthetic performance in algae and plants is now widespread (Baker, 2008). The chlorophyll fluorescence parameters give insight on the changes in the photosystem II (PSII), the linear electron transport rates, and the CO<sub>2</sub> assimilation. The relationship between the PSII photochemistry efficiency and CO<sub>2</sub> assimilation in leaves enables to detect differences in the response of plants to environmental challenges and, consequently, to screen for tolerance to environmental stresses (Baker and Rosenqvist, 2004).

The use of spectral absorption index such as SPAD measured by SPAD-502Plus (Minolta, 2009) for estimating leaf chlorophyll content or plant healthiness or nitrogen status is also widely used in plant breeding. It determines the relative amount of chlorophyll present by measuring the absorbance of the leaf in two wavelength regions: the blue (400-500 nm) and the red (600-700 nm). This non-invasive method to measure chlorophyll content has shown strong correlation with the destructive one using acetone (Minolta, 2009; Su et al., 2010; Kumar, 2017). Other indices like Normalized Difference Vegetation Index (NDVI) measured by PolyPen RP 410 (Photon Systems Instruments, Drásov, Czech Republic) has been extensively used in agriculture as an indirect measure of photosynthetic activity and crop yield (Gupta et al., 2012). The NDVI is calculated using measurements of reflected light from the red (630–690 nm) and NIR (near infrared 750-2500 nm) bands as  $NDVI = (NIR-RED)/(NIR+RED)$  (Rouse et al., 1974). It is also an integrated measure of ground cover (leaf area) and the nitrogen (N) content of the canopy (an indirect measure of final crop

yield in small grains), under long-term water stress. Sensor phenotyping methods usually operate at leaf level, but new developments with aerial and mobile platforms are providing measurements on the whole canopy, hence giving a holistic status of plant response to external stress (**Figure 1.11**).

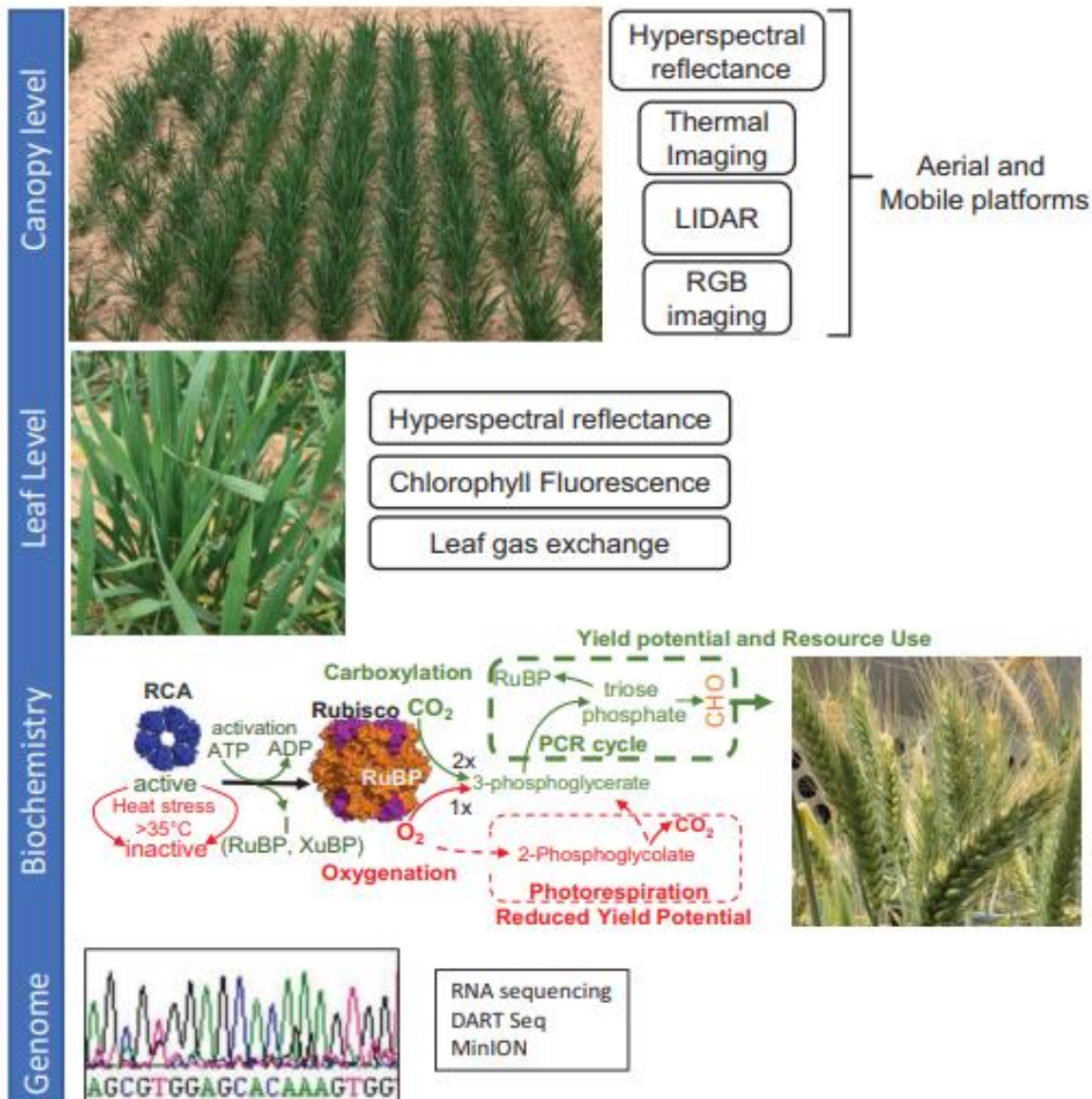


**FIGURE 1.11** | Genome to phenome and back: identification of photosynthetic traits for integration into breeding programs or gene technologies. Analysis of the photosynthetic CO<sub>2</sub> assimilation from the canopy and leaf level can be achieved through rapid phenotyping techniques. These techniques enable rapid determination of photosynthetic parameters that help select germplasm for detailed analyses. At the canopy level, LIDAR is used for non-destructive biomass determination, drones or unmanned aerial vehicles are used for imaging crop canopies which can include RGB cameras for crops coverage, and thermal imaging is used to estimate canopy temperature, which can be utilized for screening germplasm for differences in water use efficiency. At the leaf level, tools such as hyperspectral reflectance can be used to estimate electron transport capacity and V<sub>c</sub>max, in addition to leaf N and leaf mass per area. Tools such as MINI-PAM-II and SPAD provide surrogates for leaf N content, with the former measuring electron transport and non-photochemical dissipation of incoming light energy. Determining the underpinning biochemistry and gene sequence diversity is requisite to deploy traits crucial for improving CO<sub>2</sub> assimilation. Source: (Furbank et al., 2020).

#### 1.3.4. Molecular breeding

Molecular breeding, or marker assisted selection (MAS), refers to the technique of using DNA markers that are tightly linked to phenotypic traits to assist in a selection scheme for a particular breeding objective (Jaradat, 2016). This method has been successfully applied in plant breeding due to the characterization of several genetic markers, such as random amplified polymorphic DNA (RAPD), inter-simple sequence repeats (ISSRs), amplified fragment length polymorphism (AFLP), and notably single nucleotide polymorphism (SNP) (Cooper et al., 2014). In wheat, several generations of molecular markers have been identified for quantitative traits such as drought tolerance and can be used in marker-assisted breeding programs. The use of these markers in molecular breeding offer the possibility to improve wheat performance in diverse physio-morphological traits at different growth stages and also yield (Varshney et al., 2007; Khadka et al., 2020).

With the objective to be used in marker assisted selection, the discovery of QTLs/genes associated with target traits, including those associated with drought require the use of a mapping population, either a family-based linkage populations in traditional linkage mapping or a diversity panel in association mapping (Sallam et al., 2016; Khadka et al., 2020).

In contrast to the conventional linkage mapping approaches that uses two parents in the development of the population, hence has lower genetic variation resulting in low resolution QTLs, AM populations comprised diverse lines representing the diversity of natural or breeding populations of the crops (Zhu et al., 2008). Recently, advanced mapping populations named next-generation populations (NGPs), comprise Nested association mapping (NAM) populations, Multi-parent advanced generation intercross (MAGIC) population, and advanced intercross recombinant inbred lines (AIRILs), were developed to overcome the limitations posed by both previous mapping approaches. These mapping approaches has been successfully used in plant breeding and identified QTL regions harboring drought-responsive genes and transcription factors involved in drought tolerance (Table S1-S2-S3)(Mwadzingeni et al., 2016; Gupta et al., 2017; Kulkarni et al., 2017). Nevertheless, with the recent evolution in genomics that enable the detection of high number of SNP across the wheat genome (Shi and Ling, 2018), further research in QTL mapping is important to uncover the precise genetic architecture of drought tolerance.

## 1.4. Breeding progress and dissection of the genetic basis of traits of interest

### 1.4.1. Breeding progress

Wheat is a key cereal crop that impacts the global economy and food security. Continuous increase in grain related traits and tolerance to biotic and abiotic stress, together with higher nutritional value are critical for providing food to the growing population, and remain as the top priorities of wheat breeding programs (Baum et al., 2015; Mondal et al., 2016). Different approaches have been used to determine the breeding progress or the rate of genetic gain for grain yield and other traits. However, the method of linear regression of genotypes means over their year of release has been widely used in the literature (Sharma et al., 2012; Voss-Fels et al., 2019a; Lichthardt et al., 2020). (Tadesse et al., 2013) have determined a breeding progress of 110 kg/ha/year ( $R^2 = 0.66$ ;  $P = 0.001$ ) for the grain yield of the best line (BL) while the trial mean (TM) increased at a rate of 91.9 kg/ha/year ( $R^2 = 0.53$ ;  $P = 0.007$ ) indicating a continuous yield improvement at the International Winter Wheat Improvement Program (IWWIP). Breeding progress for grain yield was consistent across three various nitrogen cropping systems regardless of the baking quality classification (Voss-Fels et al., 2019). Recently, (Lichthardt et al., 2020) have reported a breeding progress of 9.85 t/ha/year when compared the cultivars from a European germplasm released between 1970 and 2010.

The assessment of the breeding progress in yield-related traits is valuable to recognize which of them are associated with GY, identify yield-limiting factors, and specially to plan future effective approaches to increase the genetic gains of GY in breeding programs. In addition, a regular assessment and upgrade of the yield progress are necessary to evaluate the performance of breeding programs on a global scale and incorporate new breeding strategies adapted to the new scenarios (Gerard et al., 2020). Given the current scenarios of climate change imposing drought stress in agricultural areas, evaluation of the breeding progress for grain yield and related traits is important to predict future genetic gain accordingly.

### 1.4.2. Association mapping

Association mapping is based on linkage disequilibrium (LD) and requires the use of a large number of genome-wide markers (Turuspekov et al., 2017). Based on the objectives of research, association mapping can be separated into two categories: candidate-gene association mapping and genome-wide association studies (GWAS) (**Figure 1.12**). Contrary to candidate-gene association mapping in which polymorphisms within candidate genes are correlated with the measured traits of interest, GWAS correlates the polymorphisms scanned across the whole genome to the measured traits (Risch and Merikangas, 1996).

LD is the non-random association of alleles at different loci in a given population. It is influenced by several factors such as selection, mutation rate, population structure, system of mating, sample size,

genetic drift, genetic recombination and diversity within a population (Chao et al., 2010). LD may be estimated different methods that are to some degree, confounded with allele frequencies or genetic diversity and are related to  $D$ , the coefficient of linkage disequilibrium. A commonly used method to quantify LD is with  $r^2$  (Ramakrishnan, 2013) that ranges between 0 and 1. The value  $r^2 = 0$  means that the loci are in complete linkage equilibrium, while  $r^2 = 1$  means that the loci are in complete LD. The LD may decay over a long or short distance based on the population under study and the chromosomal region.

The low costs for high throughput genotyping have enabled the discovery of high-density SNP marker across wheat genome that empower GWAS approaches for the detection of QTL (quantitative trait loci) associated with wheat traits of interest (Lopes et al., 2015; Cericola et al., 2017; Turuspekov et al., 2017). A QTL is a location on the genome that, in conjunction with other locations on the genome, is responsible for the variation of a quantitative characteristic (Collard et al., 2005). Compared to conventional linkage mapping, association mapping has three advantages: (1) it saves time and cost of the construction of a family-based segregating population that preserves only two variations of an allele, and it makes use of existing populations that comprise a wide diversity of genetic background; (2) it is able to detect multi-allelic variation, and thus helps to identify the most favorable alleles contributing to a target trait in a single analysis; and (3) its higher resolution resulting from exploration of all the ancestral recombination events present in a plant species, is more powerful for fine mapping of quantitative trait loci for several important traits (Breseghello and Sorrells, 2006; Atwell and Huang, 2010; Shi et al., 2017).

However, GWAS can exhibit higher rates of false positives than biparental populations (Yu and Buckler, 2006). To minimize the detection or occurrence of spurious or false-positive associations that might arise as a consequence of an unbalanced allele frequency distribution among individuals of diverse geographic origin or breeding, it is recommended to assess the population structure of an association panel and account for it in associations studies (Gajardo et al., 2015a; Zhang et al., 2018). Although, several models has been developed and used for QTL identification in association studies, the mixed linear model (equation 2) accounting for the population structure (Q) and the kinship among individuals (K) is more effective in the identification of true positive (Yue et al., 2006).

$$Y=X\alpha+Q\beta+K\mu+\varepsilon \quad (\text{Equation 1.2})$$

where  $Y$  is the phenotype of a genotype;  $\alpha$  and  $\beta$  are unknown vector containing fixed effects;  $X$  the matrix of fixed effect of the SNP;  $Q$  the matrix of fixed effect of population structure given by PCA or  $Q$  from STRUCTURE-analysis;  $K$  the random effect of relative kinship among individuals, and  $\varepsilon$  the error term, which is assumed to be normally distributed with mean = 0 and variance  $\delta_e^2$ .

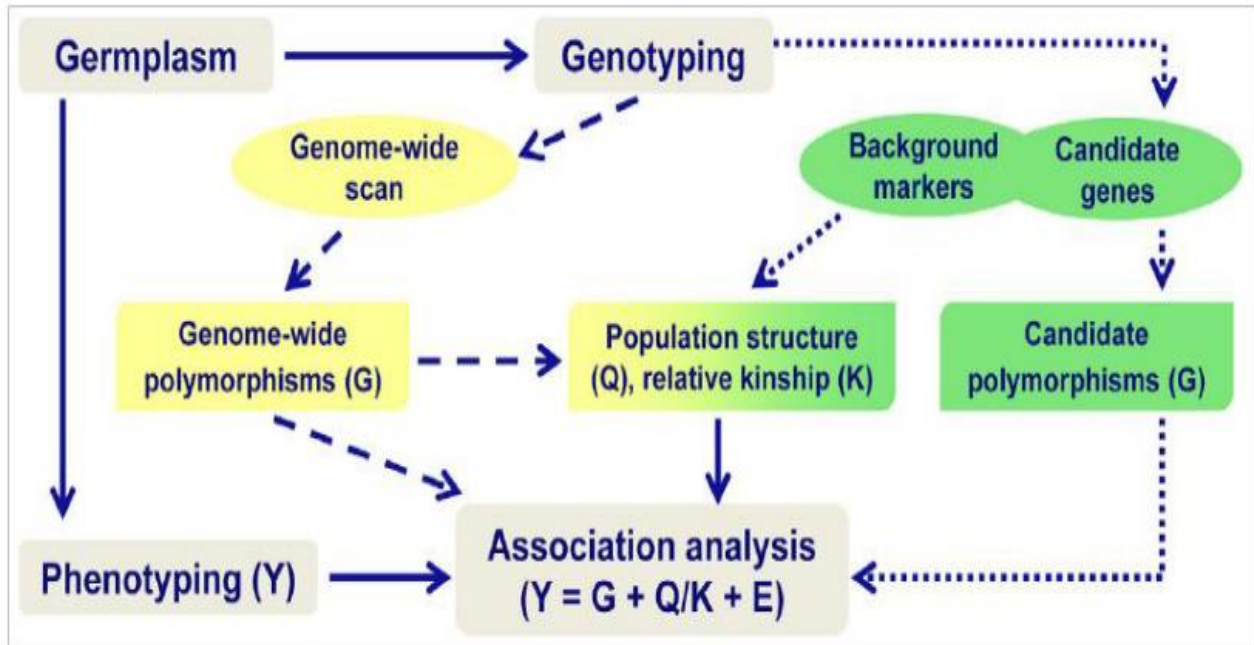


**FIGURE 1.12** | Scheme of contrast of GWAS and candidate-gene association mapping. The inclusion of population structure (Q), relative kinship (K), or both in final association analysis depends on the genetic relationship of the association mapping panel and the divergence of the trait examined. E: residual variance. Source: (Zhu et al., 2008a).

## 1.5. Research hypothesis and objectives

### 1.5.1. Hypothesis of this study

1. There is genetic variation in response to drought for agronomic traits.
2. Wheat photosynthesis efficiency related traits under different water regimes is genotypes specific and has an effect on the final biomass yield.
3. Breeding has contributed to improve wheat photosynthesis efficiency and agronomic performance.
4. There is a genetic variation in NUE, which is affected by N input levels, fungicide application, water limitation and root architectural traits.

### 1.5.2. Research objectives

Drought is a major abiotic stress factor causing prominent yield reduction in wheat, hence threatening the project to assure food security for the growing population by 2050 (Mohammadi, 2018). The development of drought tolerant and N use efficient genotypes has proven to be the most promising and economically sound strategy to increase wheat yield under new environmental constraints imposed by drought stress and political regulations to reduce nitrogen input. Therefore, gaining understanding of the agronomic, physiological, and the genetic basis underlying drought tolerance and NUE is of paramount importance to reach the desired breeding goal of developing high yielding wheat genotypes.

The major goal of this study was to determine the genetic variation among the studied wheat germplasm and evaluate the breeding progress in traits related to drought tolerance and NUE, and to identify genotypes and genomic regions with promising characteristics that can be exploited in breeding programs. The identification of superior genotypes and the dissection of the genetic architecture of relevant traits related to drought tolerance and NUE are the prerequisite for the application of marker assisted selection in the development of high yielding wheat genotypes.

The specific objectives of the proposed study were:

1. To assess and understand the genetic variation for drought tolerance in agronomic traits and dissect their genetic architecture;
2. To identify the growth stage where plant photosynthetic efficiency significantly impacts the final above ground yield and identify the relevant genetic markers associated with photosynthesis activity;
3. To evaluate the NUE and determine how it interacts with N input level, fungicide application, water-limitation, and root architectural traits;

4. To quantify the breeding progress made in agronomic and physiological traits under rainfed and drought stress, and in various nitrogen cropping systems;
5. To explore the candidate genes in the identified QTL regions for agronomic traits; drought tolerance, NUE and photosynthesis efficiency.
6. To identify the allelic variation in the promotor region of the gene NADH-ubiquinone oxidoreductase activity which is in the vicinity of the SNP marker *AX-158576783* associated with the photosynthesis activity.

The result of the study is divided into four chapters.

Chapter 2: Breeding driven enrichment of genetic variation for key yield components and grain starch content under drought stress in winter wheat.

Chapter 3: Chromosome 3A harbors several pleiotropic and stable drought-responsive genes for photosynthesis efficiency selected through breeding of wheat.

Chapter 4: Genome wide dissection and *in-silico* transcript analysis provides candidate loci for improved drought tolerance and nitrogen use efficiency in Winter Wheat.

Chapter 5: Fungicide application affects nitrogen utilization efficiency and grain yield and quality of winter wheat.

## **Chapter 2**

### **Breeding enriched genetic variants for drought tolerance of winter wheat for key yield components and grain starch content**

**P. A. Koua<sup>1</sup>, B. C. Oyiga<sup>1</sup>, M. M. Baig, J. Léon<sup>1, 2</sup> & A. Ballvora<sup>1</sup> ✉**

<sup>1</sup> INRES Pflanzenzüchtung, Rheinische Friedrich-Wilhelms-University, Bonn, Germany

<sup>2</sup> Field Lab Campus Klein-Altendorf, University of Bonn, Klein-Altendorf 2, 53359 Rheinbach, Germany

This chapter has been submitted in *Frontiers, Plant Breeding* (under review).

## **2.1. Abstract**

Drought is one of the major abiotic stress factors limiting wheat production worldwide, thus threatening food security. The dissection of the genetic footprint of drought stress response offers strong opportunities toward understanding and improving drought tolerance in wheat. In this study, we investigated the genotypic variability for drought response among 200 diverse wheat cultivars (genotypes) using agronomic, developmental, and grain quality traits, and conducted genome-wide association studies (GWAS) to uncover the genetic architectures of these important traits. Results indicated significant effects of genotype, water regime and their interactions for all agronomic traits. Grain yield was the most drought-responsive trait and was highly correlated with kernels number per meter square. GWAS revealed 17 and 20 QTL regions under rainfed and drought conditions, respectively, and identified one LD block on chromosome 3A and two others on 5D associated with breeding progress. The major haplotypes of these LD blocks have been positively selected through breeding and are associated with higher starch accumulation and grain yield under drought conditions. Upon validation, the identified QTL regions carrying favorable alleles for high starch and yield will shed light on mechanisms of tolerance to drought and can be used to develop drought resistant cultivars.

**Keywords:** Breeding progress, drought, GWAS, LD block, MTAs, QTL, yield components

## **2.2. Introduction**

Global crop production needs an increase of nearly 70% to meet demand by 2050 (Mohammadi, 2018; Semenov et al., 2014). Wheat is one of the world's most important staple food crops with an annual yield of 765.77 million tones in 2019 (FAO, 2021). Wheat plays a major role in global food security. However, its production is highly sensitive to climatic and environmental variations (Porter and Semenov, 2005; Semenov et al., 2014) and to various abiotic stress factors such as drought, excessive water, salinity, cold, etc. It is estimated that abiotic stress can lead to an average yield loss of more than 50% for most major crop plants (Boyer, 1982; Bray, 2000). Drought is one of the major stress factors limiting wheat yield in arid, semi-arid as well as temperate regions around the world (Hoseinlou et al., 2013; Nezhadahmadi et al., 2013). Compared to other natural disasters, drought has the largest spatial extent with nearly 80% of the total cultivated area worldwide (Mohammadi, 2018) and has the longest duration (Sheffield and Wood, 2012).

Drought affects the plant-water relations at all levels from molecular, cellular, and organ, to the whole plant levels (Oyiga et al., 2020). Moreover, drought stress affects plant nutrient uptake, as water is the transport medium from which nutrients are taken up by the plant root systems. Following drought incidence, stomata close progressively with a parallel decline in net photosynthesis owing to metabolic limitations and oxidative damage of chloroplasts (Farooq et al., 2014). The immediate consequence is the production of smaller organs, increased, flower abortion, and reduction in the grain filling period, which subsequently affect crop yield.

Grain filling has a significant effect on final grain production and greatly depends on photosynthesis and redistribution of assimilates from vegetative tissue to the reserve pools. Terminal drought accelerates leaf senescence and reduces photosynthesis (Farooq et al., 2011). Cultivars with the ability to stay green under prolonged drought remain photosynthetically active; thereby possess high spike fertility, which is often highly correlated to the number of kernels per spike (Reynolds et al., 2017; Würschum et al., 2018). Spike fertility and grain filling are major complex traits that could reduce grain yield by 58-92% under severe drought conditions (Dhanda & Sethi, 2002; Farooq et al., 2014). Modern cultivars had higher spike fertility hence, increased. grain number per spikelet than old ones due to their higher assimilates partitioning during pre-flowering periods (Royo et al., 2007). These characteristics are desired and useful in breeding programs (Tshikunde et al., 2019), to improve drought tolerance in cereals.

Although water deficit stress can occur at any time during the crops growing season, Liu et al. (2005) reported that water deficit at reproductive phase causes the most yield loss. Plants adopt various structural and functional adjustments to overcome the negative effects of water stress, ranging from their phenology, morphology, and anatomical structures to their physiological and biochemical reactions (Fang

and Xiong, 2015). These adjustments leading to plant tolerance involve four mechanisms, drought avoidance (DA) (or “shoot dehydration avoidance”), drought tolerance (DT), drought escape, and drought recovery (Fang and Xiong, 2015). DA and DT are the two major mechanisms employed by plants to tolerate mild, moderate, and severe drought (Yue et al., 2006). DA refers to morphological change such as leaf rolling, increasing wax accumulation, deep rooting system, and phenological change resulting in reduction or extension of the vegetative stage, while DT is the capability of plants to maintain physiological activities through regulation of genes to reduce or repair damages from drought stress (Yue et al., 2006; Luo, 2010). Presently, irrigation of agricultural areas is also employed to prevent substantial yield reduction imposed by drought. However, it is economically costly for small-scale farmers and a threat to the environment as water from irrigation could arouse land degradation and soil salinization (Stockle, 2001; Muli, 2014). The most relevant and economically sound solution is to breed crops with higher water use efficiency (WUE). Increasing plant water uptake and use efficiency for cultivation in drought-prone environments would require a broad understanding of the morphological, genetic, and physiological mechanisms adopted by plants to cope with water shortage.

The discovery of the genetic basis of grain yield (GY) and its component traits is essential for providing breeders with the tools necessary for the development of drought stress-tolerant cultivars (Kadam et al., 2018). Genetic dissection of complex traits such as GY and related traits has been possible through genome-wide association study (GWAS) based on linkage disequilibrium (Contreras-Soto et al., 2017; Fang et al., 2017). Recent technology developments have led not only to the identification of a high number of DNA-markers but also the production of the whole genome sequence draft of several crops including wheat with its large size of ~17 gigabases (Shi and Ling, 2018). Several QTL associated with yield related traits in winter wheat under drought stress conditions have been reported (Li et al., 2019; Xie et al., 2017; Xu et al., 2017). However, to the best of our knowledge this is the unique study done to uncover the genetic architectures of traits that are contributing to improved GY over the wheat breeding history between 1946 to 2013. QTL associated with water stress responses are valuable resources for exploitation in developing drought-tolerant (Farooq et al., 2009, Ashraf, 2010) and high-yielding cultivars. Recent findings suggest that breeding has increased GY through conserving favorable genetic factors and haplotypes involved in stress adaptation (Voss-Fels, Stahl, Wittkop et al., 2019).

In this research, we used a diversity panel of 200 winter bread wheat cultivars released from 1946 to 2013, and widely used in breeding programs around Germany to screen the genotypic variation in agronomic and grain quality traits under different water stress conditions. The main goal was to identify drought-tolerant cultivars and relevant QTL as well as shed some light on the drought tolerance mechanisms in wheat. The specific objectives of this study were to: (i) identify agronomic and developmental traits that contribute to enhance GY under drought conditions; (ii) highlight the role played

by breeding to enhance GY under drought conditions; (iii) identify QTL region linked to breeding progress and drought tolerance using years of release, agronomic, developmental and grain quality traits.

## 2.3. Materials and Methods

### 2.3.1. Plant materials and growth conditions

In this study, we tested 200 winter wheat cultivars originating from Europe, mostly Germany, USA, South America, and Asia, and previously described for their productivity under contrasting agrochemical input levels (Voss-Fels et al., 2019). The years of release of cultivars in the core set ranged from 1963 to 2013 including at least three cultivars per decade. These cultivars were assessed under drought and non-drought (control) conditions in 2016-2017 and 2017-2018 growing seasons. The drought stress treatment was under a rainout shelter and the control treatment under rainfed conditions, both at the same location in the experimental station of Campus Klein-Altendorf, University of Bonn (50.61° N, 6.99° E, and 187m above sea level). The plots under rainout shelter were irrigated by moveable overhead sprinklers set to deliver 36 L/m<sup>2</sup> water per week at the first 2-4 weeks of the experiment to enable germination and early establishment of the plants. Water stress was introduced by withholding water at BBCH40 [Biologische Bundesanstalt, Bundessortenamt und Chemische Industrie (Lancashire et al., 1991)], corresponding to the pre-booting growth stage and continued until harvesting (BBCH99). The difference of the volumetric content of water between rainfed and drought treatments was around 7% volume of soil, around heading growth stage (**Figure 2.S1**). The soil type of the experimental site is a Haplic Luvisol (World Reference Base for Soil Resources, WRB) derived from loamy silt (Perkons et al., 2014).

The plots were arranged in a randomized sub-block design with three repetitions. To reduce neighbor effects due to considerable differences among the cultivars in plant height and maturation period, the randomization was done within subgroups according to Voss-Fels et al. (2019). Each plot with a single row of 0.90 m and 60 seeds was assigned to one genotype, and a space of 0.20 m was kept between rows. To avoid border effects and plant damage by the machine while performing regular maintenance, four rows plots were flanked by two border rows. The weather data of the experimental site and the soil moisture content (0-30 cm) and temperature are provided in **Figure 2.S1**.

### 2.3.2. Phenotyping of agronomic, developmental, and grain quality traits

Agronomic traits included plant height (PH), spike number per meter square (SNms), shoot dry matter weight (SDW) which corresponded to the whole plant dry biomass weight (PBW) without grain yield (GY). Thousand kernels weight (TKW) was estimated as mean value multiplied by 2 after counting three repetitions of 500 seeds using an automatic seed counter. Harvest index (HI) was calculated as the ratio of GY to PBW which included grain yield. Visual scorings of developmental traits such as plant health state, homogeneity of growth, leaf rolling, and leaf greenness were done according to the methods described by Pask et al. (2012). The developmental growth stages of a core set of 20 cultivars that was selected by principal component analysis based on SNP makers to represent the genetic diversity of the wheat panel

were visually scored following the BBCH scale to assess the effect of drought on the duration of each stage. The grain quality traits (GQT) included ratios of grain protein content (GPC), grain starch content (GSC), and the neutral detergent fiber (NDF) measured using near infra-red spectrometry (NIRS) with Diode Array 7250 NIR analyzer (Perten Instruments, Inc., USA., 2021) by following the manufacturer's guidelines. Full description of evaluated traits is provided in **Table S1**.

### 2.3.3. Phenotypic data analyses

A mixed-linear-model was used to carry out a year-specific analysis of variance (ANOVA) to determine the effects of water regimes, cultivars (genotypes), and their interactions using SAS software (SAS Institute, 2015). Errors due to planting positions (row-and-column effects) in the field plots were corrected by including "Replication/Row\*Column" (Gilmour et al., 1995): rows crossed with columns nested within replication in the restricted maximum likelihood (REML) approach as random effects; whereas, the genotype and water regime treatment effects were considered to be fixed. Variance component estimation was based on REML (Searle et al., 2009). The best linear unbiased estimates (BLUES) were computed across each year for each water regime and cultivar according to the model (equation 2.1) and the resulting values were used in all the subsequent analyses.

$$P_{ijm} = \mu + G_i + T_j + GT_{ij} + R_m + \varepsilon_{ijm} \quad (\text{Equation 2.1})$$

where  $P_{ijm}$  is the response phenotype such as GY of the  $i$ th genotype, under the  $j$ th water regime, and the  $m$ th repetition.  $\mu$ , the general mean of the study,  $G_i$  the fixed effect of the  $i$ th genotype,  $T_j$ , the fixed effect of water regime,  $GT_{ij}$ , the fixed effect of the  $i$ th genotype under the  $j$ th water regime.  $R_m$ , the random effect of the  $m$ th repetition nesting row, column and Row\*Column, while  $\varepsilon_{ijm}$  is the error term.

The variance components due to genotypic ( $\sigma_g^2$ ) and water regime ( $\sigma_e^2$ ) effects were estimated using a mixed model procedure (SAS Institute, 2015) with both components set as random. The broad-sense heritability ( $H^2$ ) for all traits were calculated within each regime using equation 2.2 as described by Gitonga et al. (2014), and across water-regimes using equation 2.3 described by Piepho and Möhring (2007).

$$H^2 = (\sigma_g^2) / [\sigma_g^2 + \sigma_e^2/r] \quad (\text{Equation 2.2})$$

$$H^2 = \sigma_g^2 / \sigma_p^2 \text{ with } \sigma_p^2 = \sigma_g^2 + \sigma_{ge}^2/m + \sigma_e^2/rm \quad (\text{Equation 2.3})$$

where  $r$  is the number of replications of each genotype;  $\sigma_p^2$ , the phenotypic variance;  $\sigma_{ge}^2$ , the variance of genotype\*water regime interaction,  $\sigma_e^2$ , the residual error variance, and  $m$ , the number of water regimes.

Pearson correlation analysis of genotypic means was performed to assess the correlation between traits using the package *Performance Analytics* and the principal component analysis (PCA) was done by *Factominer* and *Factoextra*, both also implemented in R software (R Core Team, 2020). Thereafter, the relationships between GY and traits of interest under each water regime were evaluated with a regression model to quantify the contribution of the trait to GY. The regressions were conducted using *lm* function in R software.

#### 2.3.4. Drought stress tolerance estimation and quantification of the breeding progress in evaluated traits

The stress weighted performance (SWP) described by Saade et al. (2016) was used to identify the cultivars' drought tolerance status using the following formula.

$$SWP = YS/\sqrt{YP} \quad (\text{Equation 2.4})$$

where YS and YP are the means values of the trait of interest of the considered cultivar under drought stress and rainfed conditions, respectively. The 200 cultivars were ranked for each trait from the highest down to the lowest trait's SWP values and were classified as drought-tolerant and sensitive according to their overall SWP ranking as described by Oyiga et al. (2016).

The breeding progress was investigated by the absolute (ABP) and the relatives (BPr) indices using a panel of 192 cultivars with known release years. The absolute breeding progress (increase per year) was the slope (a) of the linear regression line between the traits of interest against the release years. The relative three decades breeding progress (Lichthardt et al., 2020) was considered as the result of changes in traits performance over years, and was calculated using the formula  $BPr=(Pi_{2010}- Pi_{1980})/Pi_{1980}$ ; where  $Pi_{2010}$  and  $Pi_{1980}$  were determined using the coefficients obtained with the following equation from the regression model of the absolute breeding progress.

$$Pi(x) = ax + b \quad (\text{Equation 2.5})$$

where x corresponds to 2010 or 1980; a is the slope representing the absolute breeding progress, and b, the intercept. For a trait of interest, we also test the significant difference between the means values of contrasting year of release cultivars groups to confirm the three decades breeding progress in the wheat panel. The group of oldest cultivars were released before 1980 (31 cultivars) and the newest were released after 2010 (30 cultivars).

#### 2.3.5. Genetic analysis of the 200 wheat diversity panel

We used for the genetic analysis, a set of 24216 SNP markers evenly covering all 21 chromosomes of wheat as described by Dadshani et al. (2021). Detailed information of SNP genotyping, population structure (PS), linkage disequilibrium (LD) analyses of the diversity panel, and the marker-trait

association tests through GWAS have been described in Koua et al. (Unpublished data). Briefly, the structure in the wheat panel was analyzed using Population structure of the wheat panel was inferred using the model-based clustering method implemented in STRUCTURE software (Pritchard and Przeworski, 2001; Falush et al., 2007), along with the delta K approach to identify the true K (Evanno et al., 2005).

The GWAS was performed with two software programs: TASSEL 5.2.13 (Bradbury et al., 2007) and *rrBLUP* package in R (R Core Team, 2020). Both GWAS were conducted following the model:

$$Y = X\alpha + P\beta + K\mu + \varepsilon \quad (\text{Equation 2.6})$$

where Y is the phenotype of a genotype;  $\alpha$  and  $\beta$  are unknown vector containing fixed effects; X the fixed effect of the SNP; P the fixed effect of population structure given by PCA matrix that included the first three components; K the random effect of relative kinship among cultivars, and  $\varepsilon$  the error term, which is assumed to be normally distributed with mean = 0 and variance  $\delta^2$ . Both Kinship matrix and PCA matrix were generated in TASSEL. GWAS for breeding progress was run with cultivars years of release used as phenotypic values. The congruent significant ( $P < 10^{-4}$ ) SNP loci identified by both programs were accepted as significant marker-traits associations. Also, FDR correction (Mangiafico, 2015) was applied to accept or reject MTAs with  $P < 10^{-4}$  obtained from only Tassel or rrBLUP. The Pvalue threshold of  $P < 10^{-4}$  to accept significant associations was determined based on the Q-Q plots and distribution of P-values.

Detection of significant loci interacting with water regimes through genome-wide locus by water regimes interactions was surveyed using the PROC MIXED procedure in SAS 9.4 (SAS Institute, Cary, NC, USA) which also included the Kinship matrix and PCA matrix from TASSEL. The P-value cutoffs for accepting highly significant marker\*treatment interaction associated with a trait were set at  $1 \times 10^{-5}$  for PBW, SNms, and GY and at  $1 \times 10^{-4}$  for kernels number per meter square (KNms), kernels number per spikes (KNSp), GPC, and GSC.

### 2.3.6. SNP clustering and candidate gene analysis

The detected marker-trait associations (MTAs) were considered to be in LD if they are located within the interval defined by the chromosomal LD (Breseghello & Sorrells, 2006; Pasam & Sharma, 2014), and were grouped in one SNPs-cluster according to Oyiga et al. (2019). The associated chromosomic regions were further explored using scripts written in R program to identify the probable functionally annotated putative candidate genes (iwgsc\_refseqv1.0\_FunctionalAnnotation\_v1\_\_HCgenes\_v1.0-repr.TEcleaned.TAB). The searches were performed in the genome assembly of *Triticum aestivum* cv. Chinese Spring (IWGSC et al., 2018) and only high confident genes were retained.

## 2.4. Results

### 2.4.1. Agronomic and grain quality traits were affected by drought stress

A mixed model ANOVA was carried out to estimate the variation components genotype (G), water regime (T) and their interaction effects on evaluated traits (**Table 2.1**). In both growing seasons, the agronomic and grain quality traits differed significantly ( $P < 0.001$ ) between water regimes (T) and among genotypes (G) except for SNms and NDF in 2018. Genotypes and water regimes were highly interacting in 2017, except for GSC and NDF, meanwhile, in 2018, G\*T interaction effects were highly significant for GY, kernels number per spike (KNSp), TKW, and GSC. Considering the combined ANOVA of both years, water regimes and genotypes, and their interactions effects were detected for all evaluated traits. Drought caused significant reductions in genotypes performance in most of the traits evaluated, and ranged from 0.11 (NDF) to 79.63% (GY) and from 2.25 (NDF) to 60.42% (GY) in 2017 and 2018, respectively. GY and KNms were the most affected traits by drought stress with 68.71% and 66.05% reduction, respectively. Furthermore, drought has significantly decreased the time to reach heading, anthesis, and fruit development growth stages compared to rainfed conditions (**Table 2.S1B**). The coefficients of variation (CV) for all traits were higher under drought compared to rainfed treatment in both years, except for TKW in both years and for PH, NDF in 2017. Broad-sense heritability ( $H^2$ ) estimates for some traits such as PBW could differ from control to drought treatment. Interestingly, GY recorded a consistently moderate  $H^2$  under control and drought conditions. Across both conditions, the higher  $H^2$  were obtained by PH, TKW, GPC, and GSC in both years. The developmental traits evaluated under drought conditions revealed a highly significant difference among genotypes with high CV of 30.07 and 55.86% in 2017 (**Table 2.S2**), for the relative healthy state (HSr) and relative leaf rolling (LRr), respectively.

The genetic relationship among traits under each water regime were evaluated using Pearson correlation coefficients based on cultivar means. Results showed significant ( $P < 0.001$ ) correlations among most of the traits under rainfed and water stress in 2017 and 2018 growing seasons (**Figure 2.S2AB**). The strongest associations were obtained between PBW and GY in 2017 ( $r = 0.91$ ) and 2018 ( $r = 0.84$ ) under rainfed conditions. However, under drought conditions, the highest associations were observed between PBW and GY ( $r = 0.87$ ) in 2017 and between GY and KNms ( $r = 0.95$ ) in 2018. Interestingly, the yield component KNms recorded the highest and consistent correlation with GY under both water regimes and growing seasons. However, in both planting seasons it was higher under drought compared to rainfed conditions. Among grain quality traits, GSC and NDF were positively correlated, and both exhibited negative associations with GPC under the two water regimes across growing seasons. For the developmental traits assessed under drought, leaves unrolled state (LRr) were significantly ( $P < 0.001$ )

associated with LGr in both years. LRr recorded the strongest relationship with GY in 2017, while LGr was the most correlated to GY in 2018 (**Figure 2.S2CD**).

The PCA performed showed the relationship among evaluated traits in growing seasons (**Figure 2.S3**). The first two principal components (PC1 and PC2) explained more than 50% of the total genetic variation under control and drought conditions in 2017 and 2018. The total variance explained by these two components is higher under drought stress when compared to rainfed conditions. The genotypic variation in the PC1 was explained by PBW, GY, and SDW under rainfed conditions in both years, while under drought stress, PC1 was consistently explained by PBW, GY, and KNms. The PC2 was explained by GPC, GSC, and PH under drought, whereas under rainfed it was differently explained in both years. Generally, PC1 characterized agronomic traits, while PC2 the grain quality traits (**Figure 2.S3**).

#### **2.4.2. Contribution of traits to grain yield**

The multiple linear regression approaches were exploited to ascertain the relative contribution of each yield component trait to GY. Under rainfed conditions, most agronomic traits such as SNms, KNms, KNSp, TKW and SDW contributed to GY in both years except SDW in 2018. However, under drought stress conditions, PH did not affect GY, but KNms and TKW had higher effects on GY in 2018 (**Table 2.S3**). Further, simple regression analysis confirmed that the yield components contribution to GY and to its variance differs upon water regimes. The variation in KNms, KNSp, and SNms significantly explained the variation in GY under drought rather than under rainfed conditions, whereas TKW and SDW explained rather the change in GY under rainfed than under drought conditions (**Figure 2.S4**). The regression GY intercepts under both water regimes were highly different, whereas the slopes under both conditions differed for KNms and TKW. The slope of KNms was higher under drought compared to the control conditions, while the contrary scheme was observed for TKW (**Table 2.S5**).

**TABLE 2.1** |ANOVA and descriptive statistics on agronomic, grain quality traits of 200 wheat genotypes (G) evaluated in two water regimes (T) across 2017 and 2018 years (Y).

Year	Statistics	Water Regime	Agronomic traits								Grain quality			
			PH (cm)	GY (g/row)	SDW (g/row)	PBW (g/row)	TKW (g)	SNms	KNms	KNSp	HI	GPC (%)	GSC (%)	NDF (%)
2017	Mean	Rainfed	78.93	203.99	192.42	396.21	39.10	708.16	27900	40.79	0.51	14.47	72.24	18.31
		Drought	56.47	41.51	66.17	109.20	34.74	286.42	6260	21.34	0.37	14.26	71.38	18.29
		Reduction (%)	28.46	79.65	65.61	72.44	11.15	59.55	77.56	47.68	27.21	1.46	1.19	0.11
	CV (%)	Rainfed	10.81	13.30	12.60	11.80	10.07	13.60	14.40	16.49	5.81	5.28	1.64	7.40
		Drought	8.59	31.40	20.70	24.20	9.70	17.23	38.30	24.49	16.38	6.65	1.67	4.81
	Heritability	Rainfed	0.95	0.51	0.75	0.65	0.87	0.68	0.50	0.70	0.42	0.72	0.28	0.33
		Drought	0.41	0.43	0.12	0.24	0.72	0.19	0.57	0.63	0.67	0.51	0.59	0.43
		H <sup>2</sup>	0.62	0.06	0.08	0.10	0.73	0.24	0.10	0.34	0.08	0.52	0.44	0.57
	Treatment effect	T	***	***	***	***	***	***	***	***	***	**	***	ns
		G	***	***	***	***	***	***	***	***	***	***	***	***
		T*G	***	***	***	***	***	***	***	***	***	*	ns	ns

(Continues)

TABLE 2.1 | (Continued)

Year	Statistics	Water Regime	Agronomic traits									Grain quality			
			PH (cm)	GY (g/row)	SDW (g/row)	PBW (g/row)	TKW (g)	SNms	KNms	KNSp	HI	GPC (%)	GSC (%)	NDF (%)	
2018	Mean	Rainfed	85.44	272.84	302.80	573.44	47.92	771.05	30307	39.98	0.48	14.26	72.91	18.20	
		Drought	76.88	107.71	134.05	241.64	42.13	414	13500	32.76	0.44	12.31	73.34	17.79	
		Lost (%)	10.02	60.52	55.73	57.86	12.07	46.31	55.45	18.05	7.34	13.63	-0.58	2.25	
	CV (%)	Rainfed	10.81	13.30	12.60	11.80	7.52	12.31	15.20	13.73	8.22	5.30	1.39	4.11	
		Drought	8.59	31.40	20.70	24.20	6.90	14.46	22.70	17.62	10.53	7.55	1.54	6.56	
	Heritability	Rainfed	0.67	0.32	0.06	0.17	0.72	NA	0.27	0.43	0.16	0.59	0.61	0.22	
		Drought	0.77	0.46	0.42	0.49	0.46	0.32	0.49	0.43	0.22	0.53	0.55	0.04	
		H <sup>2</sup>	0.85	0.33	0.34	0.39	0.68	0.12	0.39	0.22	0.42	0.65	0.64	0.12	
	Treatment effect	T	***	***	***	***	***	***	***	***	***	***	***	***	***
		G	***	***	**	***	***	ns	***	***	***	***	***	***	ns
		T*G	ns	**	ns	ns	*	ns	ns	***	ns	ns	*	ns	
	Overall	Mean	Rainfed	82.18	238.415	247.61	484.825	43.51	739.60	29100	40.38	0.50	14.36	72.58	18.25
Drought			66.67	74.61	100.11	175.42	38.44	350.21	9880	27.05	0.41	13.29	72.36	18.04	
Lost (%)			18.87	68.71	59.57	63.82	11.66	52.65	66.05	33.01	17.62	7.50	0.30	1.18	
Factors effect		Year (Y)	***	***	***	***	***	***	***	***	***	***	***	***	***
		T	***	***	***	***	***	***	***	***	***	***	***	**	***
		G	***	***	***	***	***	***	***	***	***	***	***	***	***
		T*G	*	***	***	***	***	***	***	***	***	***	***	*	ns
		Y*T	***	ns	***	***	***	***	***	***	***	***	***	***	*
		Y*G	ns	**	***	**	ns	*	ns	**	**	*	ns	ns	ns
		Y*T*G	ns	**	ns	**	ns	ns	ns	***	***	ns	ns	ns	ns

Abbreviations: PH, plant height; GY, grain yield; SDW, shoot dry weight; PBW, plant biomass weight; TKW, thousand kernels weight; SNms, spike number per meter square; KNms, grain number per meter square; KNSp, grain number per spike; HI, harvest index, GPC, grain protein content; GSC, grain starch content; NDF, neutral detergent fiber; CV, coefficient of variation; H<sup>2</sup>, trait heritability estimates; The significance level: \*P<0.05, \*\*P<0.01, \*\*\*P<0.001; ns = non-significant.

### 2.4.3. Modern cultivars perform better under both drought stress and control conditions

The absolute breeding progress (ABP) in the diversity panel was estimated by testing the significance of the slope (increase per year) from the regression model of the trait of interest against the years of release of cultivars. The results (**Figure 2.1, Figure 2.S5**) revealed three ABP patterns when the slopes of rainfed and drought treatments are compared (**Table 2.S4**). The first and second patterns were observed when both slopes are either positive or negative, while the third pattern occurs when the slope under drought is opposite sign compared to the one under rainfed (**Table 2.S4**). Although, GY was increasing with year of release in both control and drought conditions, the increase under drought was higher than under rainfed (**Figure 2.1A**). We didn't observe any case where breeding increased cultivars performance under rainfed while reducing it under drought. As shown in the scatter plots (**Figure 2.1**), the observed variation among cultivars across all regression lines was higher under drought than under control conditions. The relative three decades of breeding progress [BPr (%)] was described by the ratio between the trait value in 2010 and the one in 1980 (**Table 2.S4**). The highest increase was observed for GY and KNms with 12.16% and 9.27%, respectively under drought. Breeding has increased the HI, both under rainfed and drought conditions with a relative increase of 4.52% and 6.32%, respectively. The regressions models of traits vs year of release comparing the rates of breeding progress under both water regimes showed that the coefficients (intercepts and slopes) observed under drought significantly differed from the ones under rainfed conditions for PBW, SDW, PH, and SNms (**Table 2.S5**).

We compared the performance of the modern cultivars that are the newest (released after 2010) vs oldest (released before 1980) ones under each water regime using *t*-test of traits mean values between these two contrasting years of release (**Figure 2.2, Figure 2.S6**). Modern cultivars consistently performed better under both rainfed and drought stress conditions for yield components, GSC and NDF, except for PH and GPC where old cultivars recorded the highest performance (**Figure 2.2, Figure 2.S6**). SDW of old cultivars was higher than modern cultivars under rainfed while no significant difference was found under drought stress. Modern cultivars developed more spikes per m<sup>2</sup> than oldest cultivars under drought stress, whereas under rainfed conditions both groups did not show significant differences.

Further, we calculated the drought stress-weighted performance (SWP) to evaluate the drought tolerance status within the evaluated germplasm. Following the SWP index, cultivars with higher SWP values performed better under rainfed conditions and were more drought tolerant than cultivars with smaller values. As shown in **Figure 2.3A**, fifty cultivars obtained a SWP above the third quartile (20.62) and were considered drought-tolerant, whereas fifty cultivars with SWP average of 15.75 had their SWP smaller than the first quartile (16.95), hence were considered drought sensitive. The consistently selected tolerant (20) and sensitive (20) from the three categories of traits (agronomic, development, and grain

quality), and are presented in **Table 2.S6**. Among them, modern cultivars had the highest SWP indices, indicating they are more tolerant to drought (**Figure 2.3B**). The PC1 that explained 50.3% of the total variation in the PCA analysis separated the 20 tolerant and the 20 sensitive cultivars. The parameters that contributed to the difference between cultivars were KNms, GY, PBW, LGr, LRr, and GSC with the highest to the lowest in that order (**Figure 2.3C**).

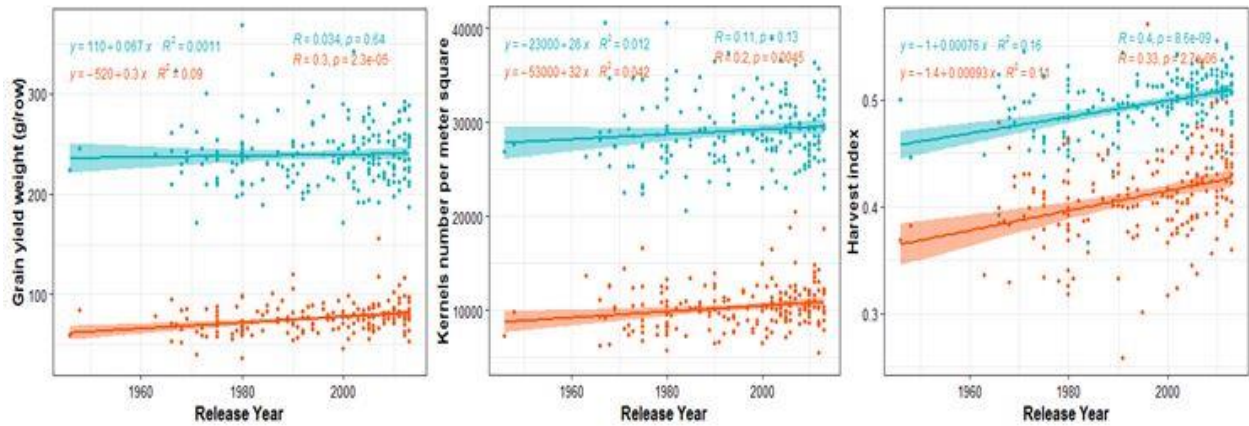


**FIGURE 2.1** | Regression plots showing breeding progress in agronomic traits on Blues values for two growing seasons. Each dot represents a BLUE value of a cultivars and the colored area represents the confidence interval of the regression line. The slopes of the linear regression lines (green lines for rainfed conditions and orange values for droughts stress field) are referred to absolute breeding progress and the relative breeding progress is the ratio between the values in 2010 and 1980 as show in Table 2.S4. A, B, and C are breeding progress in GY, KNms, SDW, respectively. The abbreviations of traits names are given in the legend of **Table 2.1**.

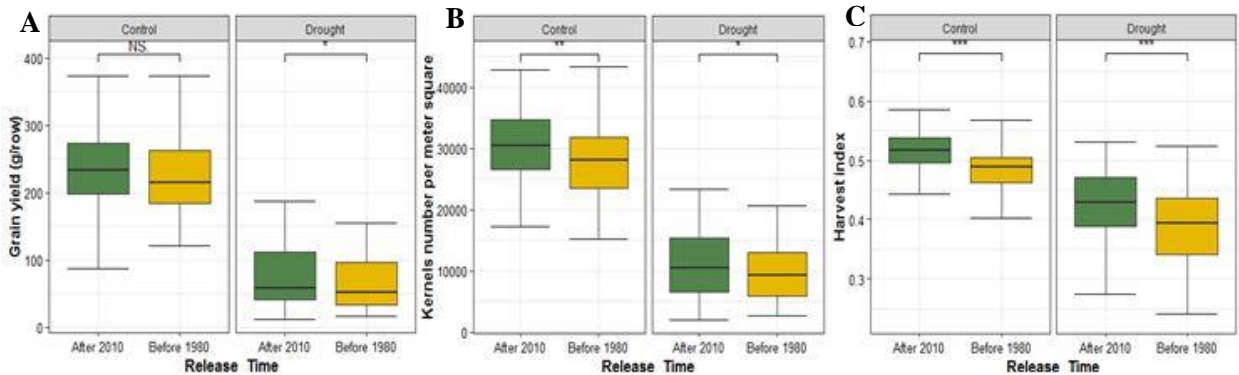


**FIGURE 2.2** | Comparison of breeding progress in agronomic and grain quality traits between two contrasting years of release groups under rainfed (control) and drought stress conditions. The oldest cultivars were released before 1980 (gold color) while the modern were released after 2010 (dark green). **A**, **B**, and **C** are illustrating the comparison of GY, KNms, and HI, respectively.

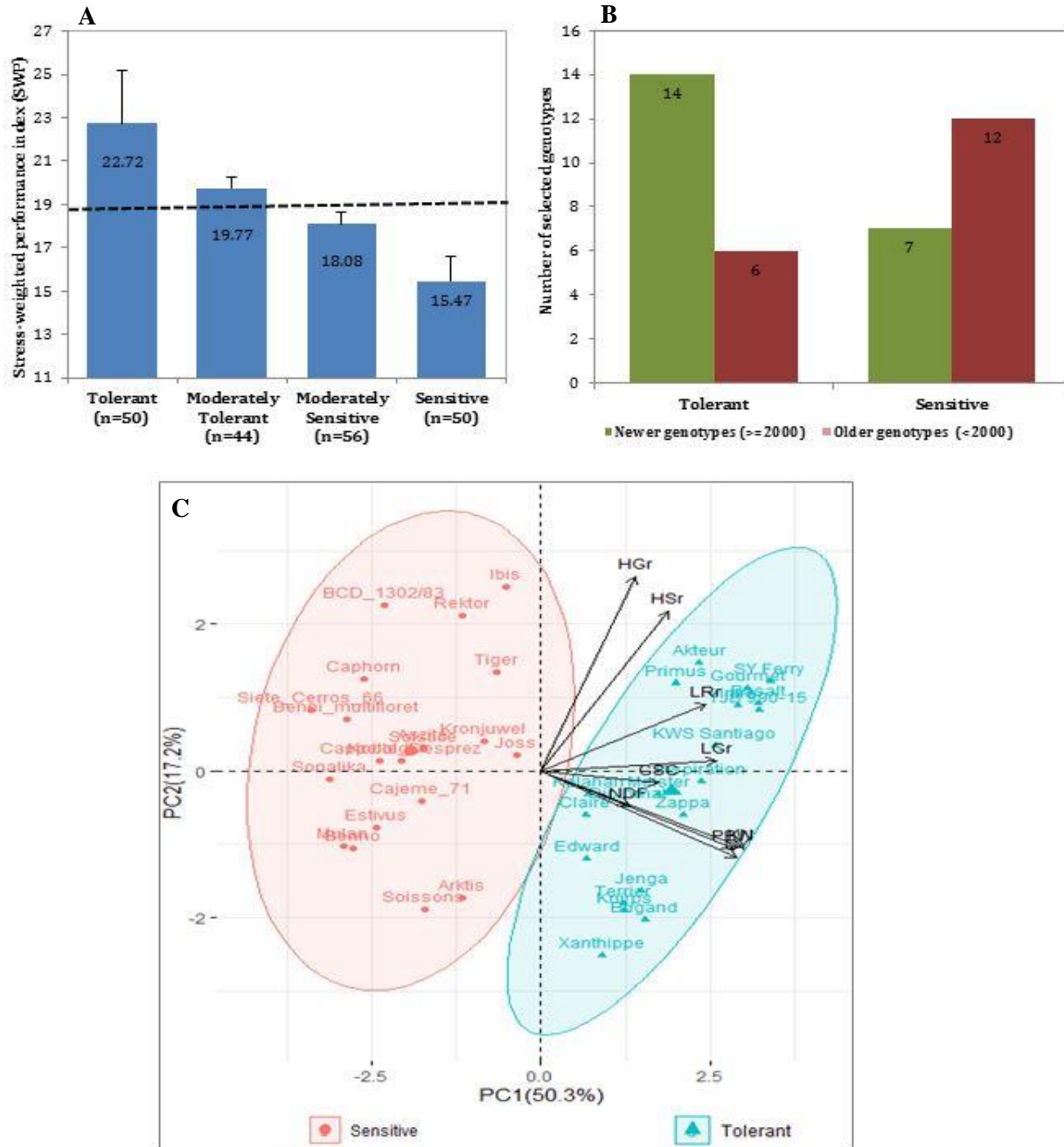


**FIGURE 2.3** | Representation of the studied cultivars based on SWP. **(A)** SWP representation of all the 200 cultivars classified into four drought tolerance groups. The dotted line represents the average SWP value of the entire population (SWP=18.96). **(B)** The number of selected twenty drought-tolerant and twenty drought-sensitive cultivars. Selected cultivars were classified into Newer (released in/or after 2000) or older (released before 2000). The selection was based on SWP of agronomic and grain quality traits, and the visual scores of developmental traits under drought stress conditions. **(C)** Scatter plot showing clustering of the tolerant (green) and sensitive (red) cultivars based on the PCA analysis of their SWP rankings of evaluated traits.

#### **2.4.4. Marker-trait associations (MTAs) detected under both water regimes and markers interacting with water regimes**

GWAS identified 78 significant MTAs ( $P < 10^{-04}$ ) across 26 QTL regions based on the chromosomal LD (Table 2.Sxl1; Table 2.Sxl2; Table 2.Sxl4). In total, 53 MTAs were found under drought and 26 under rainfed conditions. All QTL found under stress conditions are drought responsive since they were not detected under control conditions. The proportion of phenotypic variance explained (PVE) given by all SNP markers averaged 8.27% ranging from 6.84 to 10.27% under rainfed, and averaged 8.26% ranging from 6.12 to 11.29% under drought stress (Table 2.S7; Table 2.Sxl1). Chromosomes 7B, 1D, and 5D harbor the highest number of detected MTAs under drought conditions (Figure 2.S7). Interestingly, SNP marker *AX-109506123* on chromosome 5D at 528.819 Mbp exhibited a pleiotropic effect on SWD and PBW (Table 2.Sxl3). Among the 26 QTL regions, 9 and 4 of them comprised SNP-clusters with at least two MTAs, under drought and control conditions, respectively. The other 13 QTL regions included single MTAs (Table 2.Sxl4). A hotspot of 17 MTAs in SNP-clusters associated with SDW under drought conditions was found on chromosome 7B in a chromosomal region of 32 Mbp length, while under control conditions a hotspot of 7 MTAs for KNSp was found on 5A. The genetic region on 5D from 542.108 to 546.910 Mbp was a QTL hotspot for GSC under drought comprising 5 MTAs in the cluster (Figure 2.S7).

A total of 19 QTL regions comprising 87 MTAs were significantly interacting with water regimes for seven agronomic and grain quality traits. Among them, 10 harbor SNP-clusters, while 9 QTL regions comprised each a single MTAs (Table 2.Sxl6). PBW had the highest number of MTAs in SNPs-cluster on chromosome 2A (23) and 5D (16) in a region from 675.080 to 677.043 and from 559.729 to 562.834 Mbp, respectively. The SNP-cluster involved in GY was co-located with the QTL detected for PBW on chromosome 5A, which contained the highest number of interacting effect MTAs associated with GY, PBW, KNms, and GPC.

#### **2.4.5. Polymorphisms in relationship to breeding progress (BP)**

GWAS identified 28 congruent significant MTAs comprising 12 MTAs significant at  $P < 10^{-4}$  and 16 ( $P < 10^{-3}$ ) associated with breeding progress (Figure 2.4A,B). SNP markers explained from 5.86 to 11.34% of the observed phenotypic variation ( $R^2$ ) (Table 2.Sxl1). Among them, six and two SNPs detected on chromosomes 3A and 5D, respectively, were verified after FDR correction at  $Q = 0.05$  (Figure 2.4A). The associated SNPs on 3A were in a LD block located at 500.988–503.027 Mbp (Figure 2.4C). The ones on 5D were located within a chromosomal region composed of two LD blocks between 107.584 Mbp and 192.270 Mbp. The first LD block covers 15.58 Mbp interval, while the second LD block is 86.492 Mbp (Figure 2.4D).

We performed a principal component analysis based these 28 identified MTAs to determine the genetic relationship among cultivars from high and low SWP values. The PCA clearly separated the wheat cultivars based on their drought tolerance status (**Figure 2.5**). Most of the recently released cultivars were drought-tolerant and belong to one group, whereas the old cultivars were the drought-sensitive. The first three PCs explained 82.75% of the observed genetic variation. The PC1 accounted for 66.63% of the variation and mostly depicted the difference between drought-tolerant new and drought-sensitive old cultivars. This component obtained higher loadings values from SNPs makers located on chromosomes 3A and 5D. The biplot PC1 vs PC3 displayed drought-tolerant modern cultivars in the down left quadrant, whereas drought-sensitive, which were old released cultivars, were scattered randomly in the whole biplot.

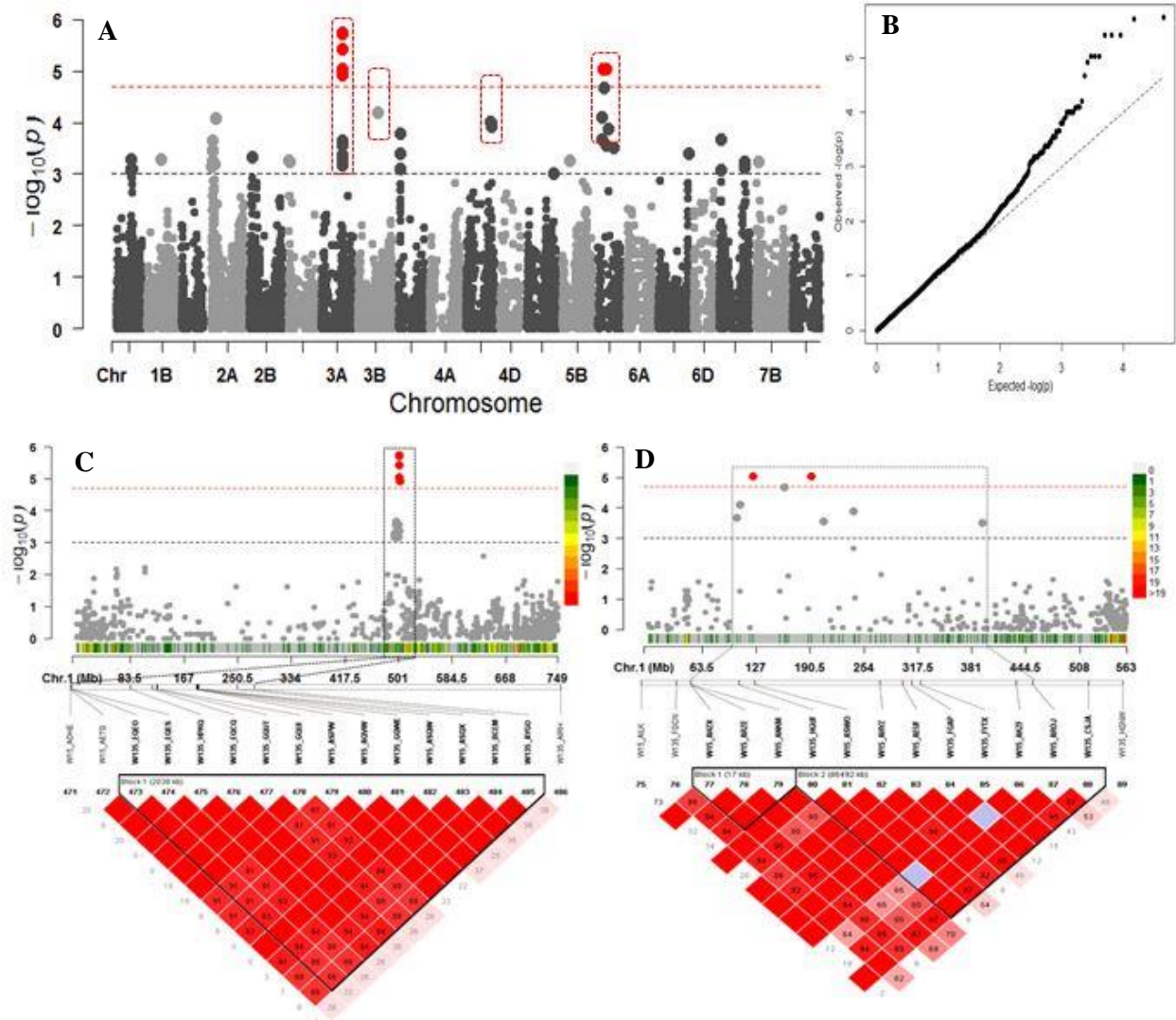


**FIGURE 2.4** | Association mapping for year of release. **(A)** Manhattan plot from association mapping using the MLM. The top 13 SNPs are shown in gray or dark gray (bigger size circle) and the SNPs exceeding the significance threshold of  $Q=0.05$  FDR correction are shown in red; the MTAs in dotted red squares are in common with GSC. **(B)** QQ plot of expected and observed P values. **(C)** The peak region on chromosome 3A span in a region of 0.643 Mbp from 502.398 to 503.027 Mbp harbored 6 MTAs in LD block. **(D)** The peak region on chromosome 5D spanning in a region of 15.58 Mbp size had two MTAs TA002565\_0478 and *wsnp\_Ex\_rep\_c67164\_65655648* in the first block, while the second block of 86.492 Mbp size comprised three MTAs *wsnp\_Ex\_c65985\_64188864*, *wsnp\_Ku\_rep\_c72922\_72561803*, and *Excalibur\_c10046\_579*. In **(C)** and **(D)**, pair-wise LD between SNP markers is indicated as  $r^2$  values: dark red indicates a value of 1 and white indicates 0. The dotted squares in **(C)** and **(D)** denote the linkage blocks that contain high significant SNPs on 3A and 5D. The color scaled legends at the right side of the Manhattans plots in c and d indicate the SNP density in a chromosomal region.

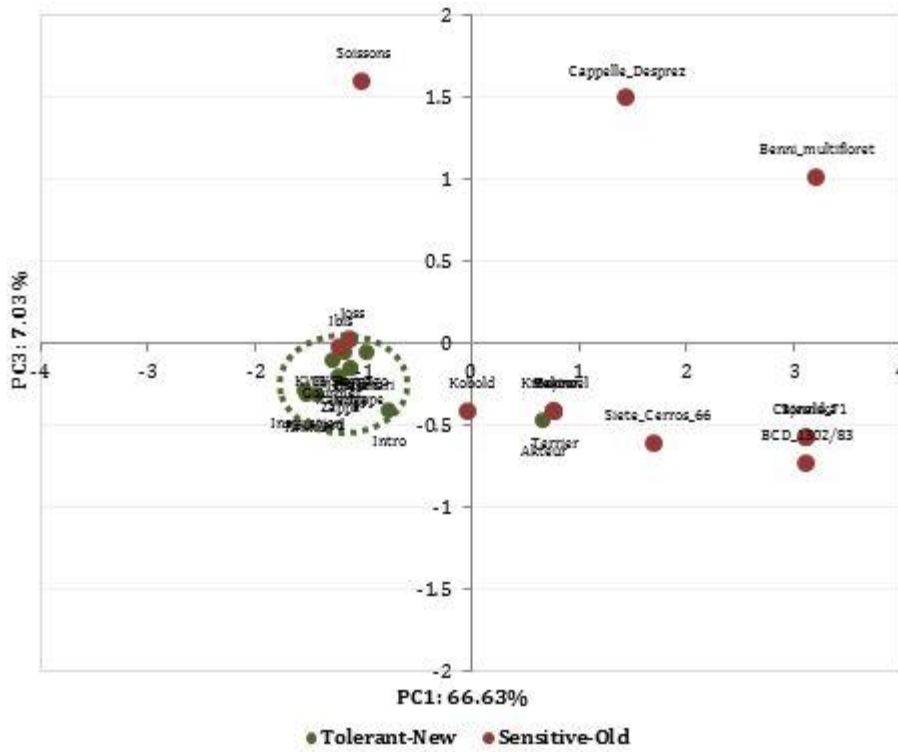


**FIGURE 2.5** | Principal component analysis (PCA) plot using a PCA matrix (Tassel 5.2) estimated with data from 30 SNPs involved in breeding progress of drought-tolerant (green color) and drought-sensitive (red color) wheat cultivars previously identified among the studied population.

#### 2.4.6. Haplotype CC selected through breeding has enhanced grain GSC and drought tolerance

Comparison of detected MTAs ( $P < 10^{-3}$ ) associated with BP and the ones associated with agronomic and grain quality traits under both water regimes revealed chromosome 3A harbors SNPs with pleiotropic effect on BP and GSC (**Table 2.Sx18**). Moreover, the QTL on chromosomes 3B and 4B showed drought inducible effect and were associated with GSC under drought conditions (**Table 2.Sx18**). The haplotype block on chromosome 3A located at 496.991 Mbp (**Figure 2.4C**), detected with AX-158576764 and AX-111076088 SNPs was associated with GSC under control and drought conditions (Figure S8). The haplotype representing their major allele (CC) significantly contributed to higher GSC than the minor allele (TT) under both water regimes (**Figure 2.6A,B**). Likewise, that major allele (CC) has contributed to higher GY under drought stress. However, under rainfed conditions, the difference between both alleles of the haplotype was not significant for GY (**Figure 2.S9**). The analysis of the allele frequencies of the associated haplotype-block 3A revealed that the allele "CC" conferring higher GSC were favorably selected against the alleles "TT" that is associated with low GSC throughout the wheat breeding history (**Figure 2.6C, Figure 2.S9**).

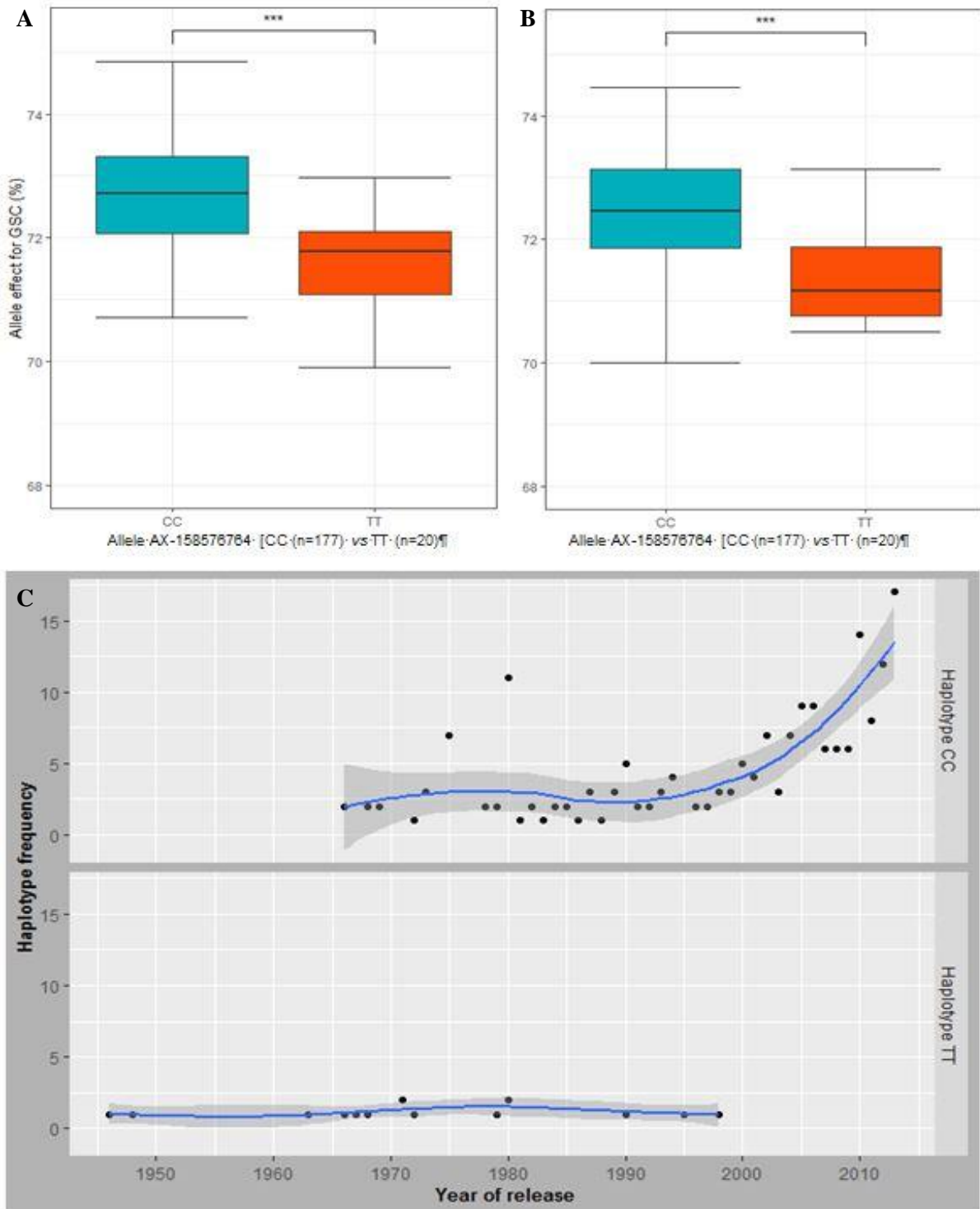


**FIGURE 2.6** | Allele AX-158576764 effect on GSC under (A) rainfed and (B) drought conditions. (C) The trend in the allele frequency of the haplotype block including the markers AX-158576764 and AX-111076088 over years of release of the cultivars is displaying an increase in the haplotype frequency (number of cultivars) having the favorable alleles or haplotype (CC).

#### 2.4.7. Identification of candidate genes located in QTL intervals

High confidence (HC) candidate genes at the vicinity of the detected SNP-clusters were retrieved from the genome assembly of *Triticum aestivum* cv. Chinese Spring. Under rainfed conditions, 94 HC genes were retrieved from six QTL regions (on 1D and 2A), whereas, under drought stress, 323 HC genes were obtained from nine QTL regions (on 4A, 4B, 4D, 5A, 5D, 7B). The chromosomal regions underlying breeding progress (BP) contain mostly antiporters and transmembrane proteins and are enriched in genes involved signal transduction, in redox homeostasis and detoxification, and included those associated with defense mechanisms against biotic and abiotic stress. Likewise, under drought conditions, the genes category that were present for BP were also significantly detected under drought conditions. However, under rainfed conditions, those genes were not notably present in the vicinity of the detected SNPs (**Figure 2.7**).

Specifically, QTL regions underlying traits under drought stress conditions were co-located with genes involved in primary metabolism such as photosynthesis activity namely electron transport, dehydrogenase, and oxidoreductase activity (GO:0004616; GO:0016491; GO:0055114) as well as cation and zinc transporter in stress response mechanism (**Table 2.Sxl5**). The genetic region of chromosome 7B associated with SDW (488.412 to 520.418 Mbp) with *AX-109411217* and *AX-109328820* as MTAs peak harbored 177 HC genes. Under rainfed conditions, marker *AX-108905462* on 5A for KN<sub>sp</sub>, *AX-109506123* on 5D for PWB, and *BS00101408\_51* on 7B co-segregate with genes involved in molecule transport activity such as oligopeptide, heavy metal, sugar, and nucleobase ascorbate transporter, and UDP-glycosyltransferase activity.

The analyses of the genomic regions of the SNP-clusters interacting with water regimes indicated that most of the candidate genes identified in this region belong to categories of genes involved in metabolic processes (GO:0008152), transferase activity (GO:0046912), and genes encoding for drought-responsive proteins. Further, chromosomal regions on 2B and 5D associated with KN<sub>ms</sub> and PBW co-segregate with genes involved in disease resistance whose gene ontology (GO:0043531) terms are related to protein and ADP binding (**Table 2.Sxl7**).

The QTL regions on 3A, which underlaid the breeding progress, harbors 8 HC candidate genes (Table 2.S2), including those whose functions are related to carbohydrate metabolic process (GO:0005975), protein phosphorylation (GO:0006468), and GTPase activity (GO:0003924). The chromosomal region on 5D, which showed significant association with BP, contains 267 HC genes, including some involved in stress response mechanism (GO:0006950), disease resistance, starch synthase, and photosynthesis activity including several dehydrogenases involved in oxidoreduction process (GO:0015979) (Table 2.Sx15).

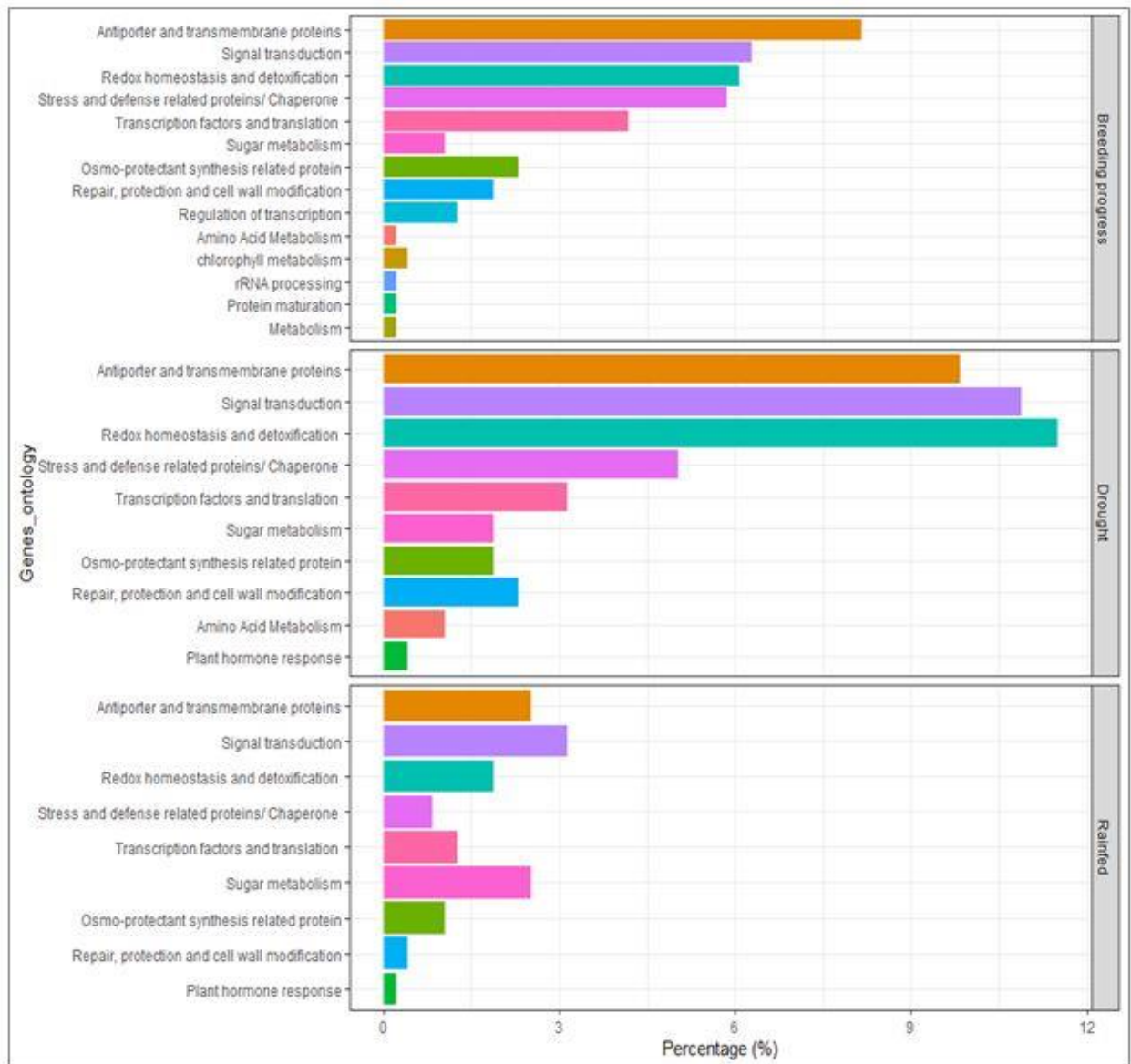


**FIGURE 2.7** | Genes annotation and ontological classifications of the associated DNA sequences underlying breeding progress and the traits of interest under drought and rainfed conditions using GWAS.

## 2.5. Discussion

The aim of this study was to evaluate the genetic variation for developmental, key yield components and grain quality traits, and link the observed phenotypic variation to QTL contributing to high GY, grain quality and improved drought tolerance in wheat. To the best of our knowledge, this is the first study using different types of quantitative traits and breeding progress information in a diverse wheat germplasm to identify drought tolerant genotypes and drought responsive QTL regions. The presented results reveal wide phenotypic variation in most of the agronomic, developmental, and grain quality traits evaluated and the detected heritability estimates ranged from low to high. This suggests that these traits can be exploited in developing drought-tolerant wheat cultivars.

### 2.5.1. Reduction of cultivars performance in agronomic, developmental, and grain quality traits under drought stress

Drought stress significantly reduced the GY by 68.71% and yield components, especially KNms by 66.05% compared to control conditions. The highest impact of drought on the GY may be partly due to the cumulative effects it exerts on the yield-related traits as well as the flowering and grain filling stage (Farooq et al., 2014, Mohammadi, 2018; Sallam et al., 2019). For instance, reports indicated that drought stress caused a significant reduction in yield component traits like plant growth, spike number due to early death of tillers, spike size, and TKW (Harris et al., 2002; Ozturk & Aydin, 2004; Daryanto et al., 2016). Following heading, prolonged drought can reduce the pollination of the ovary because of an increased ABA concentration in the spike, leading to an increased seed abortion and thus to a reduced seed set (Weldearegay et al., 2012). It is also known that drought can cause significant limitations during grain filling due to reduced net photosynthesis caused by oxidative damage to chloroplasts and stomatal closure (Farooq et al., 2014). As an example of limitations, we observed that drought stress has reduced time to reach growth stages, hence it has stimulated plant growth, which negatively impacted GY as reported in several previous studies (Barnabás et al., 2008; Munjonji et al., 2016; Sukumaran et al., 2018). Although, we did not measure the grain filling duration, the drought stress imposed at early growth stage may have reduced this stage, thus GY more in 2017 than in 2018 under drought conditions. The reduction in GY and yield-related traits under drought stress is a common phenomenon and is controlled by several complex molecular, physiological, and morphological factors across plant growth stages (Mohammadi, 2018; Kadam et al., 2018).

In the present study, drought had negative effect on GSC, as already reported (Barnabás et al., 2008), and also on GPC. Generally, drought stress reduces starch accumulation and increases the protein content (Flagella et al., 2010). The decrease of GPC detected in our study may be due to the application of drought at very early stage of plant development. Indeed, it has been reported that the effect of drought

stress on grain quality highly depends on its intensity and when it occurs (Rakszegi et al., 2019). Larger phenotypic variations were observed among the wheat cultivars under drought stress when compared to the rainfed conditions as indicated by higher CV and more dispersed scatter points across regression lines. That would suggest the existence of substantial genotypic differences in the response to drought in the studied population. This high genetic diversity is a valuable resource providing the fundamentals for future breeding for drought tolerance (Frei, 2015; Oyiga et al., 2016). Under rainfed field, it was not obvious to detect visually the difference between the genotypes for their developmental traits. Contrary to that, under drought conditions, a clear estimation of the genotypes' response to drought was possible. The visual scored developmental traits showed the highest CV in the study, hence confirmed the existence of huge genetic variation when plants are under stress conditions as reported (Oyiga et al., 2016). The lower heritability values observed under drought compared to rainfed conditions reflect the higher variation among repetitions. Also, the heritability calculated across treatments was generally lower compared to heritability within treatments. That could be explained by the significance difference between genotypes performance under drought and rainfed conditions.

The correlation between GY and KNms was higher under drought than under rainfed. Monneveux et al. (2012) reported that KNms is the most relevant trait among yield components contributing to high GY. The highest slope from the regressions GY vs KNms was found under drought conditions, suggesting the increase of KNms would enhance more the GY under drought than under rainfed conditions. Moreover, an increase in the grain starch correspondingly increased the GY, particularly under drought stress. Thus, could serve as an important proxy when breeding for drought tolerance. High starch deposition could be connected to higher photosynthetic activity and photosynthates assimilation, which would increase KNms and consequently GY. Starch availability is essential during embryo development, and sufficient starch greatly increases the number of fertile floret, hence the KNms (Boyer and Westgate, 2004). Our finding of lower correlation between TKW with GY observed under drought conditions compared to rainfed has been previously reported by Del Pozo et al. (2016) and that could be due to the decrease of TKW under drought conditions. NDF showed negative correlation with GPC, and positive association with GSC under both water regimes, but inconstantly associated with agronomic traits across water regimes. Drought effect on NDF was not significant in 2017, but it significantly decreased this nutritional parameter in 2018 in which no genotypic effect was observed. The effect of drought on fiber utilization by animals are less clear and limited (Ferreira and Brown, 2016; Vincent et al., 2005; Ferreira et al., 2021).

The present study showed that the relative values of leaf greenness were positively associated with the relative leaf rolling which is due to the loss of cell turgor pressure in leaves. Both traits were highly correlated with GY under drought treatment. The stay green of flag leaf provides insights on the ability of

leaves to remain photosynthetically active due to delayed senescence (Thomas and Howarth, 2000), and has been reported to be highly correlated with water use efficiency during grain development and with GY under drought conditions (Christopher et al., 2016). Cultivars with prolonged stay green ability are high yielding because up to 50% of the photosynthates needed during grain filling are contributed by flag-leaf photosynthesis (Larbi & Mekliche, 2004; Sylvester-Bradley et al., 1990).

### **2.5.2. Breeding contribution to cultivars performance and drought tolerance**

Contrary to the belief that crop improvement has reduced their potential to adapt to future challenges such as drought (Byrne et al., 2018; Swarup et al., 2020), our results showed that breeding has improved cultivars performance under both water regimes. We discovered that breeding has increased the KNMs, HI, and GY production under both rainfed and drought conditions as previously reported (Royo et al., 2007). Drought-tolerant cultivars differed from sensitive ones by showing higher performance under drought conditions, hence having higher SWP values. Interestingly, most of the identified drought-tolerant cultivars are the recently released cultivars. They showed high yielding potential than older cultivars under drought stress conditions. Reports have also shown that modern cultivars are higher yielding compared to older ones under low nitrogen application owing to accumulated genetic variants conferring favorable effects on key yield traits (Voss-Fels et al., 2019; Slafer & Araus 2007). Breeding has improved yield potential under optimum conditions as well as under stressful conditions through developing semi-dwarf cultivars with reduced plant height, which has improved resource allocation and increased green canopy duration (Lichthardt et al., 2020). Under rainfed conditions, the breeding progress for GY was low, whereas Voss-Fels et al. (2019) found high breeding progress for this trait under both limited conditions (drought, low agrochemical inputs) and optimal conditions (irrigated, high agrochemical inputs) using the same wheat panel. The low breeding progress obtained for GY under rainfed in the current experiment may be due to the small plot size, which in the absence of any stress may not favor detection of differences, as shown by low CV under rainfed than under drought conditions. The breeding progress on GPC was decreasing over years as reported in Voss-Fels et al. (2019). using the same panel. However, they found an increase of the total protein content per ha over year of release.

### **2.5.3. Marker traits association and SNP clustering**

The association mapping identified 25 and 53 MTAs under rainfed (PVE= 6.84-10.27%) and under drought (PVE= 6.12-11.29%) conditions, respectively. The higher PVE recorded under drought is indicating that the related genes are explaining more the observed variation under this condition than under control. This suggests that breeding for drought prone environment using genetic markers is achievable and promising to improve GY (Kumar et al., 2008; Mohammadi et al., 2014). The threshold for significant SNP set  $P < 10^{-4}$  enabled the identification of SNPs with strong effects on evaluated traits.

SNP-clusters under drought carried more MTAs than rainfed conditions, indicating an activation of great variety of genes with synergistic effect (Yang et al., 2010). As previously reported, drought stress is a major external stimuli that causes the overproduction of oxidative reactive oxygen species (ROS), which leads to the disruption of cells membrane integrity and later reduction in plant growth (Mohammadi, 2018). Plants respond to drought stress by producing several antioxidant enzymes such as catalase (CAT), ascorbate peroxidase (APX), guaiacol peroxidase (GPX) playing important role in ROS scavenging (Dudziak et al., 2019).

We found on 4B (marker *AX-110400483*), a QTL affecting PH. The homeologous locus on 4D, that led to a reduction of plant height has been recently reported (Alqudah et al., 2020). Likewise, the haplotype block on chromosome 4B including SNP markers associated with breeding progress, has reducing effect on plant height and TKW, but increased grain starch content and yield. The chromosome 4B and 4D have been reported to harbor the genes *Rht-B1b* (formerly *Rht1*) and *Rht-D1b* (*Rht2*) in wheat (Börner et al., 1996; Hedden, 2003).

#### **2.5.4. Genetic regions with hotspot QTL affecting multiple traits and related candidate genes**

The GWAS performed revealed that the QTL region on chromosome 3A has a pleiotropic effect on BP and GSC. QTL regions for grain quality traits such as seed loaf volume and crumb quality were identified on chromosome 3A (Kuchel et al., 2006). It has been reported that that chromosome 3A played an important role in wheat yield and harbors genes related to morphological and physiological traits such as tiller inhibition, a shoot architecture influencing trait (Araus et al., 2008; Kuraparthi et al., 2008; Czyczyło-Mysza et al., 2011; Farooq et al., 2014). The *in silico* analyses showed that this region located at 500.988–503.027 Mbp interval contains 8 HC genes, whose biological functions specify them as the probable candidate genes for the observed drought stress response (**Table 2.Sxl5**). These genes were found to regulate carbohydrate metabolic process, protein phosphorylation, and GTPase activity, etc. in wheat/or plant species, and might play a role in higher starch content in newer released genotypes. Likewise, some transcription factors like WRKY which mediates several abiotic stress responses (Phukan et al., 2016) and RING binding protein genes affecting ubiquitin protein ligase activity (GO:0005515; GO:0008270) were identified in the same chromosomal region.

QTL region on chromosome 5A spanning from 586.153 to 589.296 Mbp with the peak marker *AX-108905462*, which included a hotspot MTAs for KNSp under rainfed conditions, has been previously reported to have an association with leaves bronzing score (LBS) and ozone tolerance (Begum et al., 2020). QTL mapped for LBS of rice under ozone stress positively affected agronomic traits such as GY (Wang et al., 2014) and grain quality (Jing et al., 2016). Previous studies revealed the association of chromosomal 5A region to KNSp, GY, and flag-leaf rolling index (Czyczyło-Mysza et al., 2011; Farooq

et al., 2014). Therefore, the highest MTAs hotspot under rainfed in our study could be of high interest to increase the number of the kernel per spike, which has an important effect on wheat yield.

The linkage block on 5D detected also for breeding progress has been reported as a region harboring QTL associated with KNSp, TKW, and GY (Czyczyło-Mysza et al., 2011; Farooq et al., 2014). This linkage group co-segregates with genes involved in photosynthesis activity such as protein disulfide oxidoreductase activity, electron carrier activity and contains PSII reaction center protein complex that produces the ATP and reduces the NADP<sup>+</sup> to NADPH. Both ATP and NADPH are converted into glucose in the light-independent reaction of photosynthesis (Shi & Schröder, 2004). Reduction of net photosynthesis caused by oxidative damage to chloroplasts and stomatal closure under drought (Farooq et al., 2014) can cause significant limitations during grain filling, hence a limiting factor of higher yield. However, the activation of various drought responsive genes under enable some wheats genotypes to maintain physiological activities (Yue et al., 2006; Luo, 2010) and tolerate drought stress. The identified drought-responsive QTL regions and related candidate genes unraveled in our study should warrant further investigation as they may facilitate the molecular breeding of drought-tolerant wheat, thereby contributing to global food security.

## **2.6. Conclusion**

The present study identified KNms as the key component that importantly contributes to GY under drought stress conditions and uncovered genetic loci underlying GY under drought stress and rainfed conditions. The high density of SNPs mapped across the 21 chromosomes has enabled with precision the identification (less than 10 Mbp) of the genetic region associated with traits of interest. SNP-clustering approach was useful to identify chromosomal regions harboring QTL hotspots of MTAs with synergic effects. Our findings demonstrated the existence of huge genetic variation in the evaluated germplasm that could be used to develop drought-tolerant cultivars. Cultivar performance particularly for GY has been increased by breeding under rainfed and drought conditions through improving key yield components such as SNms and KNms, and incrementing favorable alleles for high grain starch accumulation, which afterward positively affects wheat yield. Breeding has contributed to conserve genomic regions that contain important genes playing role in detoxification against oxidative stress and in defense mechanisms against drought stress. Upon validation, these favorable alleles regulating these traits can be effectively used in breeding programs to improve yield under drought-prone environments.

## **Chapter 3**

### **Chromosome 3A harbors several pleiotropic and stable drought-responsive alleles for photosynthesis efficiency selected through breeding of wheat**

**Ahossi Patrice Koua<sup>1</sup>, Benedict Chijioke Oyiga<sup>1\*</sup>, Said Dadshani<sup>1\*</sup>, Salma Benaouda<sup>1</sup>, Uwe Rascher<sup>2</sup>, Jens Léon<sup>1,3</sup> & Agim Ballvora<sup>1</sup>✉**

1 INRES Pflanzenzüchtung, Rheinische Friedrich-Wilhelms-University, Bonn, Germany

2 Forschungszentrum Jülich GmbH, Leo-Brandt-Straße, 52425 Jülich, Germany

3 Field Lab Campus Klein-Altendorf, University of Bonn, Klein-Altendorf 2, 53359 Rheinbach, Germany

\* Both authors contributed equally to the manuscript.

Correspondence:

✉A. Ballvora INRES Plant Breeding Rheinische Friedrich-Wilhelms-University Bonn 53115 Germany

Tel.: +49228737400 Fax: +49-(0)228-73-2045 Email: [ballvora@uni-bonn.de](mailto:ballvora@uni-bonn.de)

To be submitted for publication in a peer-review Journal

### **3.1. Abstract:**

**Key message** Breeding has selected multiple pleiotropic and stable drought-responsive alleles on chromosome 3A conferring higher photosynthesis activity and grain yield under drought stress in winter wheat.

Water deficit is the most severe stress factor in agricultural crop production threatening global food security. In this study, we evaluated the genetic variation among 213 wheat cultivars for photosynthetic traits under different field drought stress scenarios. Significant genotypic, treatment and their interaction effects were detected for chlorophyll content and fluorescence parameters. Drought has reduced photosynthesis activities such as effective quantum yield of photosystem II (YII) from anthesis growth stage on. Leaf chlorophyll content (SPAD) were significantly correlated with YII and non-photochemical quenching under drought conditions measured at anthesis growth stages. Hence, it is an indicator of plant drought tolerance status that can be used for high throughput screening of plant physiological status. Breeding has significantly contributed to the increase in photosynthesis efficiency as newer released genotype had higher YII and SPAD values than the older ones. Genome-wide association study identified a QTL on chromosome 3A for YII under drought, while under rainfed conditions another QTL on chromosome 7A for SPAD across both growing seasons. Alleles TT of the haplotype-block on 3A, selected through breeding has significant contribution to higher YII and grain yield.

**Keywords:** Wheat, breeding progress, drought, GWAS, photosynthesis, SPAD, effective quantum yield of photosystem II

### **3.2. Introduction**

Frequent drought events is the most severe stress factor in agricultural crop production (Basu et al., 2016; Bray, 1997). It is estimated that by 2025 about 65% of the world population will be affected by drought conditions (Hoseinlou et al., 2013, Nezhadahmadi et al., 2013). Agriculture accounts for 80-90% of existing freshwater used by humans, mostly for crop production (Morison et al., 2008). Such use of water resources are considered unsustainable, especially in dry areas under increased pressure and water demand for other purposes (Schlosser et al. 2014; Munjonji et al., 2016). Due to the growing world population, expected to reach 9 billion by 2050, the global water and food production demand will undoubtedly continue to rise. FAO (2009) has predicted that an increase by at least 50% of the current food production is necessary to meet demand. Crop performance under water-limited conditions is determined by genetic factors controlling yield potential, drought resistance, and water use efficiency (Blum, 2005). Understanding the physiological basis and mechanisms involved in drought resistance is therefore of paramount importance.

Drought resistance can be achieved through several strategies that allow plants to adapt under different episodes of drought stress (Fang & Xiong, 2015). These strategies include drought avoidance (DA), drought tolerance (DT), drought escape (DE), and drought recovery (Levitt, 1972; Kneebone et al., 1992; Yue et al., 2006; Luo, 2010; Lawlor, 2013; Fang & Xiong, 2015). Often, plants combine different mechanisms to withstand water-deficit stress. Thus, breeding cultivars with high water use efficiency and drought tolerance are practical, economical and have shown promising results to enhance yield under stress conditions (Liu et al., 2010). However, the major challenge facing wheat breeders and geneticist are the lack of evaluation of appropriate traits (Araus et al., 1998), and the polygenic nature of traits associated with drought tolerance (Peleg et al., 2009). Various research programs aimed at improving wheat drought tolerance were mainly focused on direct selection for yield (Makino, 2011). Nonetheless, the improvement by physiological breeding which involves an indirect and rapid evaluation, selection, and mapping of genes for drought tolerance can be efficiently exploited.

Photosynthetic capacity and water use efficiency play a major role in wheat growth and productivity under drought conditions (Xu et al., 2017; Sallam et al., 2019). Moreover, Reynolds et al., (2000) have shown that grain yield is significantly and positively correlated with both photosynthetic rate and stomatal conductance. Makino (2011) and Sánchez et al. (2019) reviewed that more than 90% of crop biomass is derived from photosynthetic products. They reported that a genotype with improved photosynthetic activity under stress conditions could produce more biomass, suggesting that improving photosynthetic adaptation to environmental conditions will help to enhance crops biomass production. Drought is a major limiting factor of photosynthesis due to the effect of drought stress on the CO<sub>2</sub> diffusion as a result of

early stomatal closure. Hence it declines net CO<sub>2</sub> assimilation rate and restricts crop biomass accumulation (Centritto et al., 2009; Chaves et al., 2003). Other limiting factors are the decreased photochemical efficiency of photosystem II considering the decline in chlorophyll pigments under drought and the reduced activity of photosynthetic enzymes (Pandey & Shukla, 2015). Although the decrease of stomatal conductance as a result of stomatal closure limits transpirational water loss and aids plants to conserve water status under drought stress conditions.

Sensor-based phenotyping has been successfully used to evaluate simultaneously high numbers of genotypes for physiological traits associated with drought tolerance in wheat and barley (Araus et al. 2014, Ghanem et al., 2015). However, the cost and the lack of skilled personal in many institutes across the globe remain a major hindrance to using these new technologies in plant science. The most used method to phenotype plant physiological traits and evaluate drought tolerance under field or controlled conditions is the visual scoring of traits, such as leaf rolling, stay green, leaf wilting, *etc.* (Sallam et al., 2019).

To date, few studies have investigated the effect of drought on photosynthesis and transpiration rate across several growth stages on a wheat diversity panel that has been cultivated in the past 50 years. Given the importance of photosynthesis in plant growth, assimilates partition within the plant, and increasing yield production, it is essential to understand the genetics and gene action influencing this trait. The discovery of new traits and genetic markers associated with photosynthetic responses of wheat to drought will facilitate the identification of new genetic resources for increased yield and drought tolerance.

Recent technology developments have led not only to the identification of high numbers of DNA-markers but also the production of whole-genome sequence drafts of several crops including wheat with its large size of ~17 gigabases (Shi and Ling, 2018). Genome-wide association studies (GWAS) have been used in the past decade to dissect the genetic architecture of polygenic traits and identify significant marker-trait associations (MTAs). Compared to bi-parental mapping populations, GWAS panels can be developed faster and provide access to a wider range of alleles (Zhu et al., 2008).

In this research, we screened several photosynthetic related traits and evaluated their relationship with the aboveground yield and uncover the SNPs associated with photosynthesis activity under drought and rainfed conditions. The objectives of this study were to (1) evaluate the genotypic and drought effects on photosynthesis and transpiration dynamics and unravel the growth stage that mainly impacted the final aboveground biomass; (2) to provide information and highlight the key role played by breeding in improving photosynthesis activity; and (3) uncover the genetic architecture underlying photosynthesis-related traits.

### 3.3. Materials and Methods

#### 3.3.1. Plant materials, growth conditions, and management

The 200 wheat cultivars diversity panels and the experimental setup used in this study and the weather conditions have been described in Koua et al. (unpublished). Succinctly, the germplasm was grown under two water regimes in 2017 and 2018 growing seasons at the experimental station of Campus Klein-Altendorf, University of Bonn (50.61° N, 6.99° E, and 187m above sea level, Germany).

Among the 200 genotypes, a subset of 20 genotypes (core set) were selected based on the SNP markers data to represent the genetic diversity of the wheat panel (**Figure 3.S1**). This core set was used to phenotype the dynamic in photosynthetic traits across three and five growth stages in 2017 and 2018 planting seasons, respectively.

#### 3.3.2. Phenotyping of photosynthesis, agronomic, and grain quality traits

We screened several photosynthesis traits (**Table 3.S1-3.S2**) including the leaf chlorophyll content (SPAD) quantified by the SPAD-502Plus (Konica, Minolta, Japan) and the chlorophyll a fluorescence parameters (CFP) measured using MINI-PAM II (Mini-PAM; Effeltrich, Germany). Measurements were done on the core set at various growth stages considering pre-booting (BBCH30-39), booting (BBCH40-49), heading (BBCH50-59), anthesis (BBCH60-69), and postanthesis (BBCH70-85). At anthesis, we measured these photosynthesis traits on the 200 genotypes set.

Diffusion promoter leaf stomatal conductance (LSC<sub>p</sub>, mol.m<sup>-2</sup>.s<sup>-1</sup>) was measured using AP4-Porometer (AP4-Delta-T Eijelkamp, Giesbech, The Netherlands), while InfraRed Gas Analyzer (IRGA) based stomatal conductance (LSC<sub>i</sub>, mol.m<sup>-2</sup>.s<sup>-1</sup>), net photosynthetic rate (A, μmol.m<sup>-2</sup>.s<sup>-1</sup>), intercellular CO<sub>2</sub> concentration (C<sub>i</sub>, μmol.mol<sup>-1</sup>), transpiration rate (E, mmol.m<sup>-2</sup>.s<sup>-1</sup>), and leaf temperature (T, °C) were measured using LI-6800 (LI-COR, Lincoln, USA).

We performed visual scorings of developmental traits such as plant health state, homogeneity of growth, leaf rolling, and leaf greenness according to the methods described by Pask et al. (2012). Agronomic traits included grain yield (GY), shoot dry weight (SDW), plant biomass weight (PBW).

#### 3.3.3. Drought stress tolerance estimation

The stress weighted performance (SWP) status (Saade et al., 2016) was used to identify the genotypes' drought tolerance level for GY, SDW, SPAD and effective quantum yield of photosystem II (PSII) (YII) using the following formula

$$SWP = Y_S / \sqrt{Y_P} \quad (\text{Equation 3.1})$$

where Y<sub>S</sub> and Y<sub>P</sub> are the trait phenotypic value under drought and rainfed conditions, respectively.

Thereafter, the genotypes were ranked for each trait from the highest down to the lowest trait's SWP values and were separated into drought-tolerant and sensitive according to their overall SWP ranking as described by Oyiga et al. (2016).

### 3.3.4. Statistical analyses of the phenotypic data

A general linear model was used to carry out an analysis of variance (ANOVA) to determine the difference between water regimes (T), genotypes (G) as well as their interactions (T\*G) using R software. Proc Mixed (SAS Institute, 2015) adopting restricted maximum likelihood (REML) was used to compute the best linear unbiased estimates (BLUEs) across each year for each water regime and genotype while errors due to planting positions (row-and-column effects) in the field plots were corrected by including "Replication/Row\*Column" (Gilmour et al., 1995). These BLUEs were used in downstream analysis including GWAS.

The broad-sense heritabilities were calculated within each treatment, using the following equation as described by Gitonga et al. (2014).

$$H^2 = (\sigma_g)^2 / [\sigma_g^2 + \sigma_e^2 / r] \quad \text{(Equation 3.2)}$$

where  $\sigma_g^2$  the variance components due to genotypes, set as random in the mixed model procedure (SAS Institute, 2015)  $\sigma_e^2$ , the residual and r the number of replicates of each genotype in a treatment.

Narrow sens or marker-based estimation of heritability ( $h^2$ ) which included the kinship-matrix calculated in TASSEL (available at: <http://www.maizegenetics.net/tassel>) was estimated using the package "heritability" implemented in R software (Kruijjer et al., 2015).

Correlation coefficients (r) for each pair of evaluated traits from obtained using the R program with the package *performanceAnalytics* and the *corrplot* package was used to visualize the results. The principal component analysis of photosynthetic related and developmental traits was done with the package *FactoMineR* and the results were represented in a biplot using the package using the package *factoextra*. To evaluate the representation of a variable on the principal component, the square cosine ( $\text{Cos}^2$ ) for all variables was plotted using the *corrplot* package.

### 3.3.5. Evaluation of the breeding progress in evaluated traits

The breeding progress in physiological traits was investigated through linear regression of the trait of interest against the years of release of the genotypes. The adjusted mean values of each genotype under each water regime and growing season were used in the regression analysis. The absolute breeding progress (increase per year) was the slope of the linear regression line between the trait of interest and the year of release (Lichthardt et al., 2020).

### 3.3.6. SNP genotyping, population structure and linkage disequilibrium (LD) analysis

The diversity panel was genotyped with 15K Illumina Infinium iSelect chip, and with the 135K Affymetrix genotyping array at TraitGenetics GmbH (SGS GmbH Gatersleben, Germany) and described by (Dadshani et al., 2021). We used for the genetic analysis, a set of 24,216 SNP markers evenly covering all 21 chromosomes of wheat.

Population structure of the diversity set was determined using 2,769 unlinked SNPs ( $r^2 < 0.7$ ) selected through SNP pruning with Plink software, which adopted the indep-pairwise algorithm considering a window of 3500 SNPs that shifted by 350 SNPs forward after each calculations (Purcell, 2010). The admixture model using the Bayesian clustering method implemented in STRUCTURE v.2.3.4 (Pritchard et al., 2000) was run with the obtained 2,769 SNPs, with the inferred number of sub-population K ranging from 1 to 10, with 10 replications in each test. The true number of K was determined in the structure harvester (Evanno et al., 2005; Earl 2012). Principal component analysis (PCA) was performed using TASSEL with 24,216 SNP markers set to identify the genetic relatedness behind the existing sub-populations. Prior imputation of missing SNP values by the mean was done before the PCA analysis.

The linkage disequilibrium (LD) among SNP pairs within a defined sliding window equal to 10% of the total number of SNPs on the considered chromosome was estimated for A, B, and D genomes in TASSEL. The LD decay was determined by plotting LD ( $r^2$ ) values against the distance (megabase pairs) between SNPs on the same chromosome. Thereafter, we deployed a non-linear regression function (Remington et al., 2001) to fit the trend of LD decay across chromosomes, and A, B, and D genomes. The genetic distance corresponding to  $r^2 = 0.1$  for each genome and chromosomes was estimated and was considered as the critical distance up to which a QTL could extend.

### 3.3.7. GWAS and genetic relationship among drought tolerance contrasting wheat cultivars

To determine the marker-trait associations (MTAs), we used the mixed linear model (MLM-P+K) accounting for population structure (P-matrix) calculated by the PCA and kinship (K-matrix), both implemented in software program TASSEL 5 (Yu et al., 2005; Zhang et al., 2010). Variance component analysis was set to P3D and compression level was set to the optimum level. The association tests were also performed using rrBLUP R package (Endelman 2011). Both GWAS studies were conducted following the model:

$$Y = X\alpha + P\beta + K\mu + \varepsilon \quad (\text{Equation 3.3})$$

where Y is the phenotype of a genotype;  $\alpha$  and  $\beta$  are unknown vectors containing fixed effects; X the fixed effect of the SNP; P the fixed effect of population structure given by PCA matrix that included the first three components; K the random effect of relative kinship among cultivars, and  $\varepsilon$  the error term,

which is assumed to be normally distributed with mean = 0 and variance  $\delta_e^2$ . GWAS for breeding progress was run with cultivars years of release used as phenotypic values.

To minimize false positives, only congruent significant ( $P < 10^{-4}$ ) MTAs in both analyses were retained and reported as significant MTAs in the present study. Thereafter, Benjamini–Hochberg algorithm, which is the false discovery rate (FDR) correction procedure adopted in rrBplup (Mangiafico, 2015) was used to remove false positive at  $Q = 0.05$  using the equation:

$$p = (i/m)Q, \quad \text{(Equation 3.4)}$$

where  $i$  is the SNP p-value's rank, from the smaller to the biggest,  $m$  the total number of tests corresponding to the total number of SNP 24,216  $Q$  the false discovery rate at 0.05 significance level.

We compared significant MTAs ( $10^{-3}$ ) underlying agronomic, photosynthesis traits, and BP to identify SNPs that have pleiotropic effects on these traits and/or are collocating in the same genomic region.

Detected SNP loci associated with breeding progress were subsequently used in a principal-components analysis (PCA) performed in Tassel to analyze the genetic relationships among older and newer released cultivars *vis-à-vis* their tolerance level. The significant ( $P < 10^{-4}$ ) SNP loci detected at genetic intervals defined by the chromosomal LD were considered to be in LD (Brescaglio and Sorrells 2006; Pasam and Sharma 2014) and were grouped into one SNP cluster.

Genome-wide locus by water regimes interactions was surveyed to detect significant loci interacting with water regimes using the PROC MIXED procedure in SAS 9.4 (SAS Institute, Cary, NC, USA). The mixed model included the Kinship matrix and PCA matrix calculated in TASSEL as already described. The FDR  $Q$ -value cutoffs for accepting highly significant marker\*treatment interaction associated with a trait were set at  $1 \times 10^{-4}$  and only the first fifty significant SNP within this threshold for each trait were reported. We also performed a genome-wide SNP-SNP epistatic interaction through multilocus approach (Afsharyan et al., 2020). The LogP value cutoff was set at 4 under control to retain at least some significant interactions loci against 15 drought conditions to retain the most significant interactions. The interaction graph was drawn using the package *Circlize* implemented in R (Gu et al., 2014).

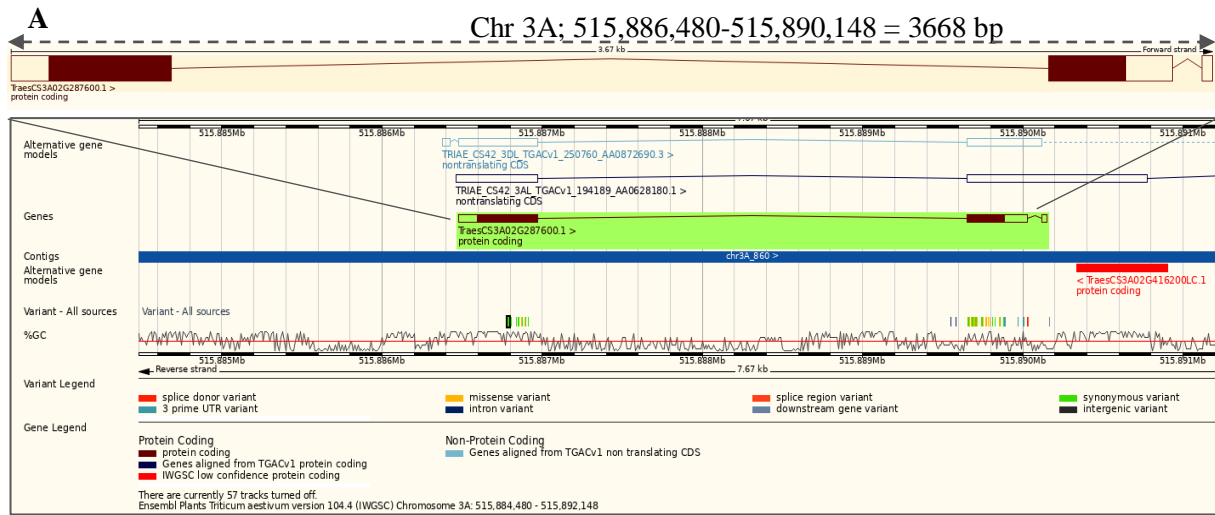
### 3.3.8. Identification of candidate genes in QTL intervals

We searched for candidate genes in the interval region of stable or pleiotropic MTAs that were in LD with the peak SNP markers. We took the positions of adjacent SNPs that were not in LD with the SNP-cluster or with the MTAs of interest as the boundary. The searches were performed in the genome assembly of *Triticum aestivum* cv. Chinese Spring (IWGSC et al., 2018) and only high confident (HC) genes were retained.

### 3.3.9. Analysis of the promoter regions of NADH-ubiquinone oxidoreductase genes

To understand the mechanistic regulation of photosynthesis efficiency, we amplified and analyzed the promoter region of the genes *TraesCS3A02G287600* (**Figure 3.1**) located near the marker *AX-158576783* (515.889 Mbp) that is associated with high YII under drought conditions. This gene encodes for oxidoreductase activity, NADH dehydrogenase (ubiquinone) activity, and involved in electron transport coupled proton transport. It starts from 515.886 until 515.890 Mbp, and is made of three exons *TraesCS3A02G287600.1-E1*, 490 Bp; *TraesCS3A02G287600.1-E2*, 379 Bp and *TraesCS3A02G287600.1-E3*, 30 Bp.

We extracted genomic DNA from two selected drought-tolerant cultivars Gourmet (T057), Inspiration (T080), respectively released in 2013 and 2007, and two drought-sensitive ones Mironovska 808 (S176) and Ivanka (S190), released in 1963 and 1998, respectively (in chapter 2, **Table 2.S6; Figure 3.S3**). The DNA extraction was done from leaf using a PeqGold plant DNA extraction kit (Pepqab, Erlangen, Germany). The PCR amplification reactions were performed in a 25 µL reaction volume containing 100 ng of genomic DNA, 5×Taq DNA polymerase reaction buffer, 10 µM of forward and reverse primers, 100 µM of dNTP, and 0.5 unit of Taq DNA polymerase (NEB, Frankfurt, Germany). The PCR were conducted in thermocycler Flex cyler (Analytik GmbH, Jena, Germany). The following conditions were used for the amplification PCR, Heat lid to 110.0°C; 95°C for 4 min and 40 cycles of 94°C for 30 s, 58°C for 50 s, and 72 °C for 1.5 min, followed by an additional 72°C extension for 10 min, and the sample was stored forever at 4°C. The primer sequences were 5'-CATGTGCAAAGGGGAAGAT-3' (forward) and 5'-AAGCATACAGGAGGGGTGTG-3' (reverse). The PCR profiles were visualized by electrophoresis on a 1 to 2% agarose gel stained with ethidium bromide. Then, the PCR product was purified using an Invitrogen PureLink Genomic Plant DNA Purification Kit (Fisher Scientific GmbH, Germany). Finally, the purified DNA was sequenced using the strand of the primers used for the PCR. The obtained sequences analyzed were using MAFFT software (Kato et al., 2019), SeqMan Pro software, Bioedit (<https://bioedit.software.informer.com/7.2/>), MegaX alignment explorer and expasy for DNA to protein translation (<https://web.expasy.org/translate/>), and insilico.ehu (<http://insilico.ehu.eus/translate/index2.php>). The transcription factors binding sites were analyzed insilico using PlantRegMap/PlantTFDB v5.0 (Jin et al., 2016) and the function Gene Group Analysis of PlantPAN 3.0 (Chow et al., 2019).



**B**



**FIGURE 3.1** | NADH-ubiquinone oxidoreductase genes *TraesCS3A02G287600*. **(A)** Overview of drought-responsive genes in QTL intervals in chromosome 3A in the vicinity of the maker *AX-158576783* detected associated with effective quantum yield of PSII. **(B)** The three economic regions of the genes. The chromosome regions were retrieved from Ensembl Plants release and expanse web application.

### 3.4. Results

#### 3.4.1. The dynamic in photosynthesis-related traits are affected by drought stress

To determine the effect of drought stress on the photosynthesis efficiency, we measured the chlorophyll content and fluorescence, several photosynthetic-related traits across growth stages under rainfed and drought conditions in 2017 and 2018 growing seasons. Analysis of variance indicated significant effects of water regimes (T), genotypes (G), and their interactions (W\*G) on SPAD in 2017 and on YII and other fluorescence parameters in both years and across growth stages (**Figure 3.2; Table 3.S3-3.S4**). Drought stress application has significantly reduced SPAD values from heading growth stage afterwards. The effective quantum yield of PSII was declined by 13.95% from booting (in 2017) and heading by 12.08% (2018), whereas, under control conditions, it was increasing from heading till anthesis and postanthesis in both years (**Figure 3.2AB**). The non-photochemical quenching (NPQ) which describes plants' protection from excess absorbed light, was decreased by almost 50% under drought stress in both years (**Table 3.S4**).

The diffusion-based leaf stomatal conductance (LSC<sub>p</sub>) declined from booting by 60.21% to anthesis and by 72.78% to postanthesis under drought stress, while it was increasing significantly under control conditions (**Figure 3.2C; Table 3.S5**). IRGA-based leaf stomatal conductance (LSC<sub>l</sub>), photosynthetic rate (A), transpiration rate (E), and intercellular CO<sub>2</sub> (C<sub>i</sub>), were significantly (P<0.01) decreased by 50.23, 29.53, and 8.95%, respectively, under drought stress at anthesis (**Figure 3.2D; Table 3.S6**).

The standard deviations of traits under drought were higher than the ones under rainfed conditions (**Figure 3.2**). The CV among the genotypes ranged from 5.95% for SPAD at booting to 67.41% for F<sub>min</sub> at heading under rainfed and from 6.20% (SPAD) to 79.87% (F<sub>min</sub>) under drought conditions. The broad-sense (H<sup>2</sup>) and narrow-sense heritability (h<sup>2</sup>) ranged from low values for F<sub>min</sub> under drought (h<sup>2</sup>=4.38%) to high values for SPAD under control (H<sup>2</sup>=92.57%) (**Table 3.S3**).

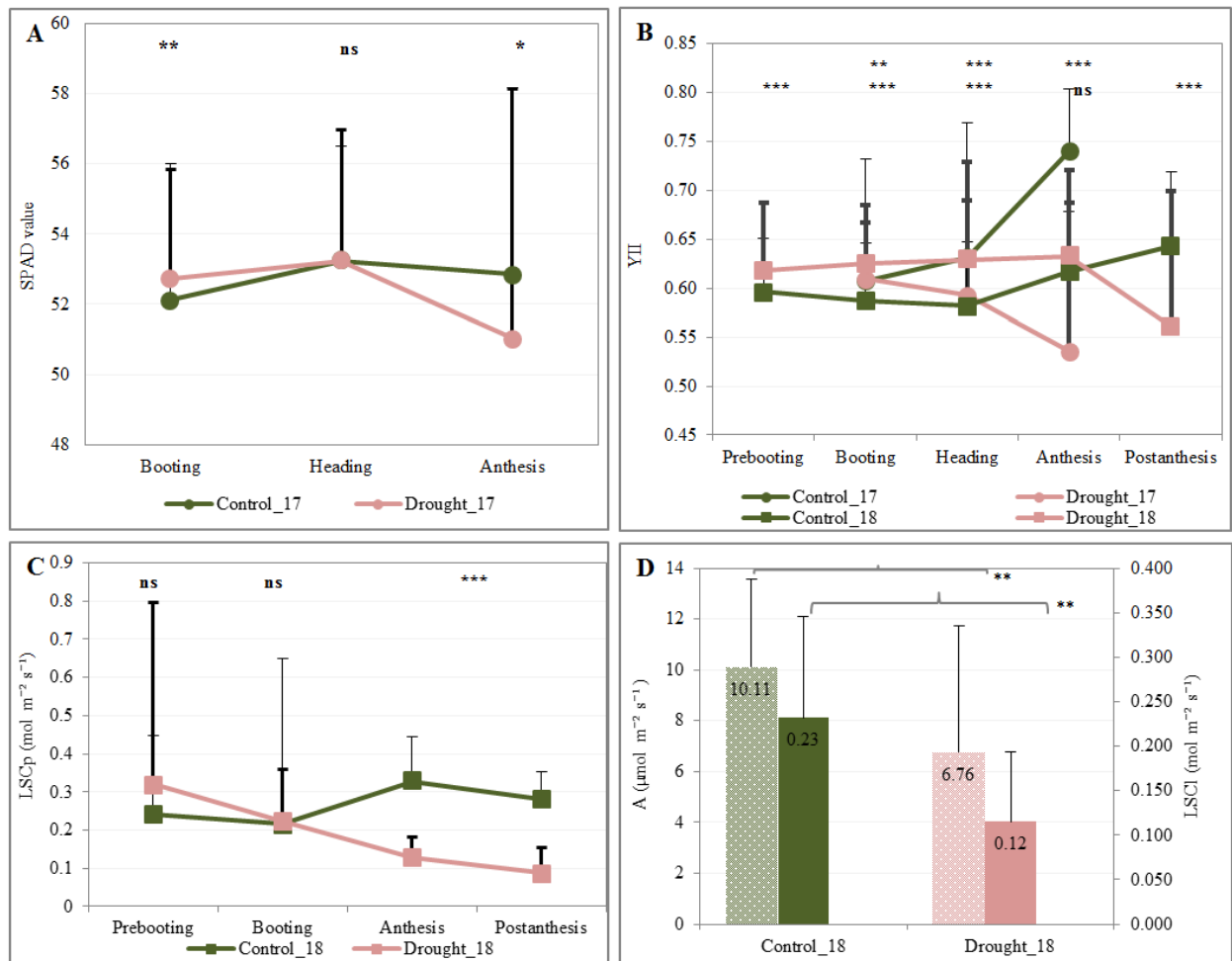


**FIGURE 3.2** | Drought stress effect on the photosynthesis related traits across growth stages. **(A)** Chlorophyll content in 2017; **(B)** effective quantum yield of PSII under drought (red curve) vs control (green curve), in 2017 (circle-shaped) and 2018 (squared shaped). **(C)** Diffusion porometer based leaf stomatal conductance in 2018. **(D)** Drought stress effect on photosynthetic rate (stars filled barplot) and leaf stomatal conductance (full colored barplot). The significance between both water regimes is given above the graphs in Table S3. In sub-panel A, the first line of significance level is for 2017, while the second line is for 2018. The error bars of the curves represent the standard deviation. The thicker one is under drought conditions.

### 3.4.2. Relationship between photosynthetic traits and drought tolerance in wheat

Pearson coefficient correlation and PCA analysis were performed to examine the relationship between the photosynthetic traits and the wheat response to prolonged drought. Results indicate that SPAD was significantly correlated with NPQ,  $F_v/F_m$  and YII under drought, and negatively correlated to NPQ under rainfed conditions (**Figure 3.3, Figure 3.S2**). Leaf temperature (DTLA) correlate negatively with transpiration rate (E), photosynthesis rate (A) and IRGA-based stomatal conductance (LSCI) under both water regimes, and with NPQ and  $F_v/F_m$  under drought conditions. Leaf greenness significantly and positively correlated with NPQ and  $F_v/F_m$ , but negatively associated with DTLA under drought stress. Photosynthesis rate correlated significantly with LSCI and transpiration rate under control and drought stress conditions. The slopes of the regressions A vs LSCI and A vs E indicated that one unit increase in LSCI and E enhanced the photosynthetic rate under much more drought than under control conditions (**Figure 3.3AB**). The first two principal components (PC) explained 50.2% of the cumulative variance in eleven photosynthesis traits and four developmental traits scored under drought stress conditions (**Figure 3.3CD**). PC1 constituted a gradient of drought tolerance oriented from the left with sensitive genotypes (Ivanka, BCD\_1302/83, and Mironovska\_808) towards the right side of the biplot with tolerant genotypes (Einstein, Gourmet, and Zentos). Comparison of PCA biplot under drought and control conditions revealed that genotypes could show different performance across both water regimes (**Figure 3.S3**).

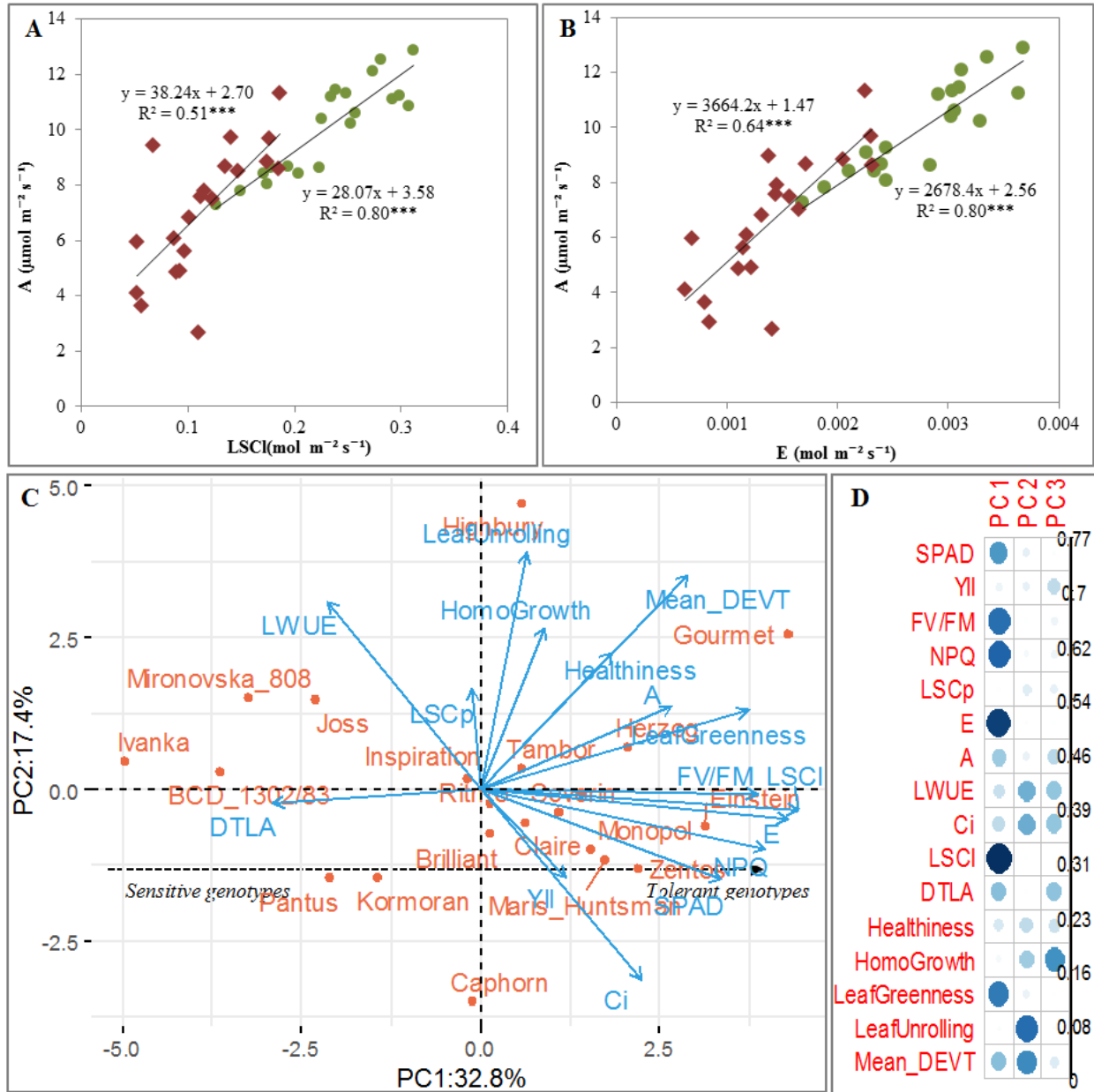


**FIGURE 3.3** | Relationship between photosynthesis rate vs (A) stomatal conductance; (B) and transpiration rate after anthesis growth stage in 2018 growing season. Red diamond-shape and green circle-shape indicate the genotypes data points under drought and rainfed conditions, respectively. (C) Principal component analysis biplot using 11 photosynthesis related variables and 4 visual scored developmental traits under prolonged drought stress condition. Cosines square of the variables contributing to the newly constructed principal components (D). The size of the circle in **Figure D** indicates the intensity of the variable. The abbreviations of traits name are listed in **Table S2**.

### **3.4.3. GY is significantly related to plant photosynthesis traits at post-anthesis under drought stress**

To evaluate the relationship between photosynthesis traits with plant biomass weight (PBW) and grain yield, Pearson correlation coefficients based on cultivars means under each water regime were calculated. We observed that the correlation between GY and YII measured at postanthesis i.e. grain filling stage was stronger than the ones of GY and YII measured at earlier stages under control conditions (**Figure 3.4A**). Similarly, associations between GY with YII measured at earlier growth stage were lower than the one with YII screened at grain filling under drought conditions. Under this condition, significant correlations were detected between  $F_v/F_m$  with GY and PBW at anthesis. Although not significant, NPQ had higher correlation with GY under drought than under control conditions (**Figure 3.4A**). Further regression analysis between GY vs YII and  $F_v/F_m$  showed that YII significantly explained the variation in GY under rainfed, while under drought the change in GY was rather explained by  $F_v/F_m$ . The dispersions of scatter points across the regression lines indicated higher genetic variation for both traits under drought than rainfed conditions (**Figure 3.4B**).

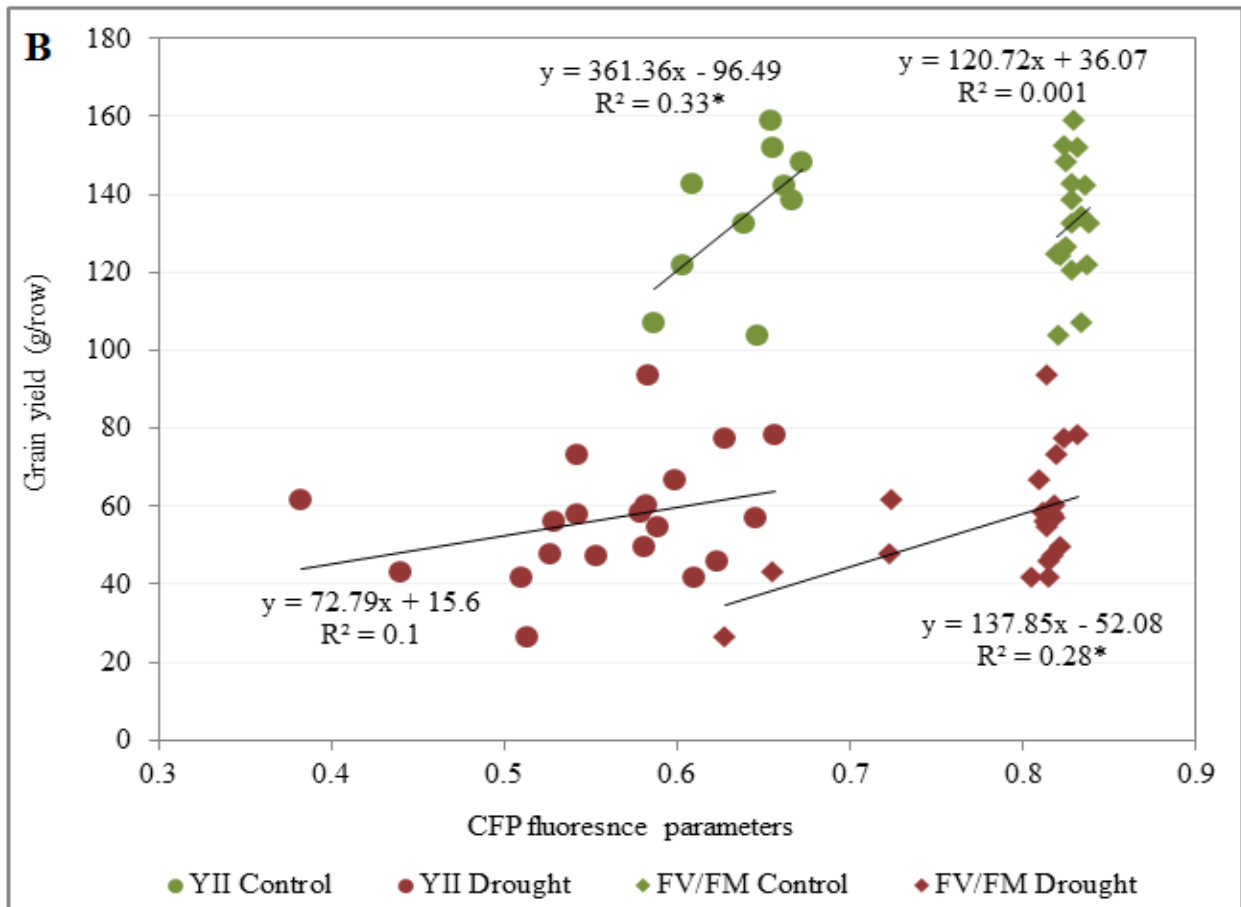
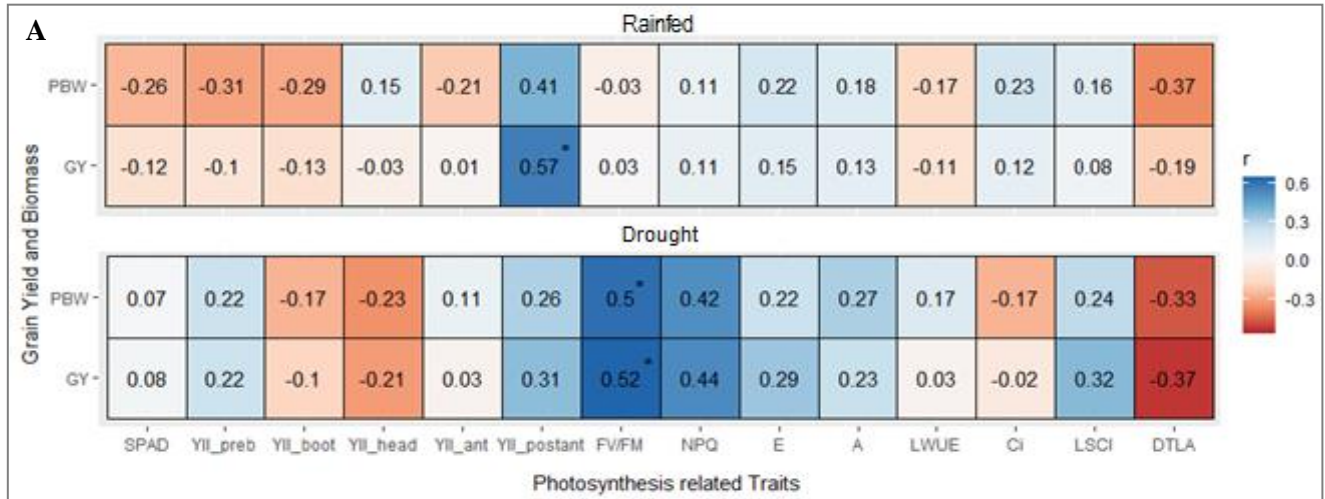


**FIGURE 3.4** | Relationship among evaluated traits. (A) Pearson correlation coefficient of photosynthesis traits vs aboveground yield (grain yield and plant biomass weight) under rainfed control (**up panel**) and drought conditions (**down panel**). The legend on the right indicates the correlation coefficients. (B) Relationship between GY vs YII and F<sub>v</sub>/F<sub>m</sub>. The abbreviations of traits name are listed in Table S2-S3.

#### **3.4.4. Breeding progress has contributed to improve photosynthesis and drought stress tolerance in wheat**

We investigated the contribution of breeding to photosynthesis and drought tolerance in wheat by comparing slopes of the linear regression between the year of release and the cultivars mean value of the traits of interest. The result indicated that breeding from 1963 to 2014 has improved the effective quantum yield of PSII (**Figure 3.5A**). The newer released cultivars showed higher photosynthetic activity potential than the old cultivars across all growth stage (GS), with the highest slopes detected at anthesis under drought conditions. The years of release significantly explained 32% of the variations ( $R^2$ ) observed for YII at anthesis and 23% at booting under drought stress. Under rainfed conditions, year of release explained 62%, and 18% of the variation for YII at anthesis, and booting, respectively. Moreover, the modern (newest) cultivars had significantly higher in YII and SPAD than older ones when their values were compared. Interestingly, for YII the difference between the newest and oldest cultivars groups is higher under drought than rainfed conditions (**Figure 3.5BC**). In addition, recently released cultivars were all among the ones with higher leaf greenness, healthiness, and leaf unrolling traits scores, suggesting their higher resilience to drought over the older cultivars (**Figure 3.5D**).

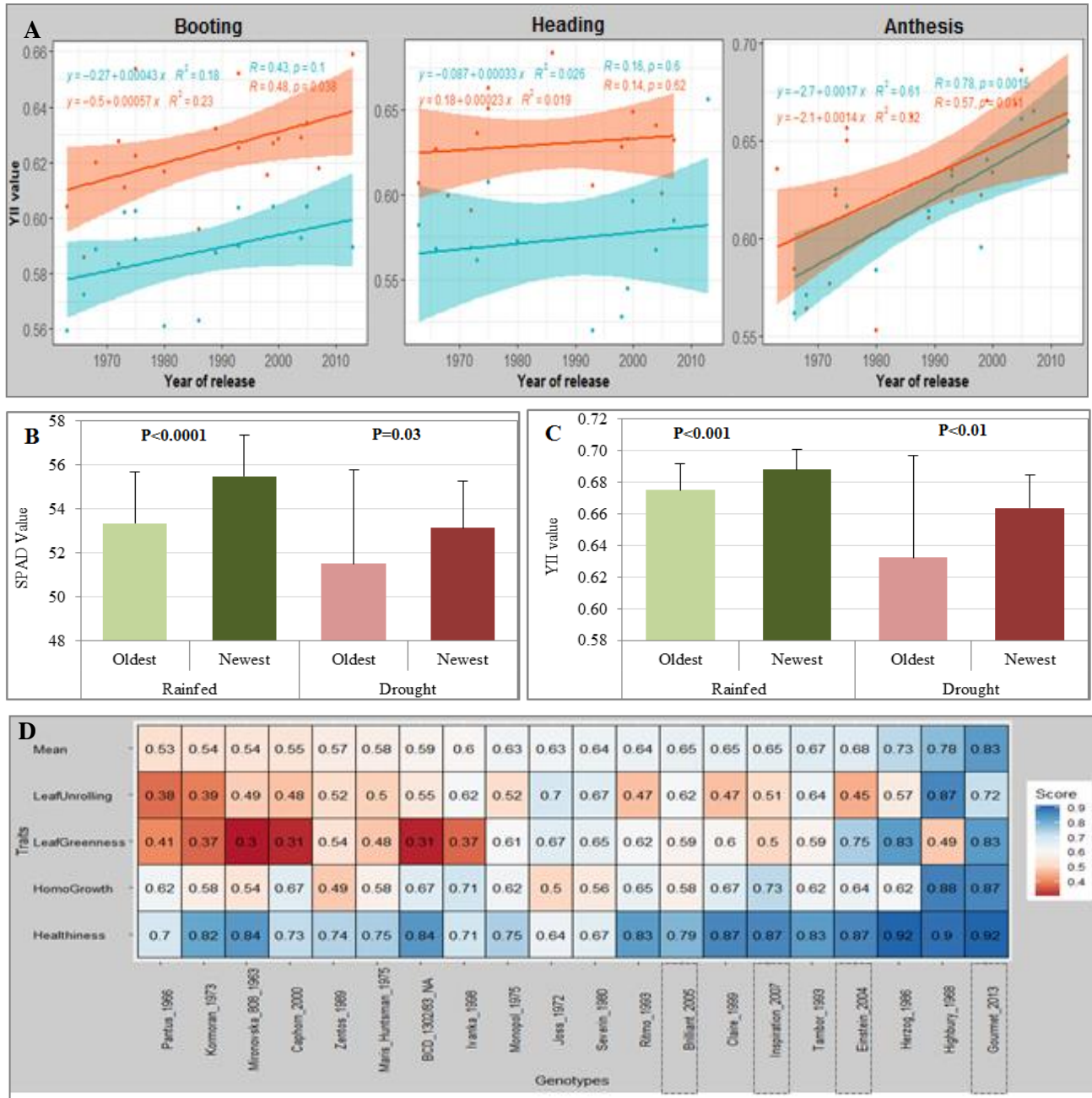


**FIGURE 3.5** | Illustration of breeding progress of evaluated traits. **(A)** Regression plots showing temporal trends in effective quantum yield of PSII among 20 winter wheat cultivars in relation to the year of cultivar registration under two contrasted water regimes. The slopes of the linear regression lines (orange line for drought and green line for rainfed) are referred to as absolute breeding progress. Boxplots of oldest vs newest released cultivars under rainfed and drought conditions for **(B)** YII, and **(C)** SPAD screened at heading/anthesis for the whole population; **(D)** Heatmap representation of the average of visual scores of developmental traits screened over both experimental years showing a gradient of cultivar with lower relative score in red (sensitive cultivars) to high relative scores in blue (tolerant cultivars).

### 3.4.5. Genome-wide association studies uncover QTL of photosynthetic traits for drought tolerance on chromosome 3A

The analysis of the genetic data revealed the subgenome B had the highest number of SNP markers (11,887) with chromosome 5B being the largest (2,131), while Genome D (2,364), especially 4D (104) had the lowest number of SNPs (**Figure 3.S4**). The LD decay which determines the resolution of association mapping was estimated at 19, 38, and 17.5 megabase pairs (Mbp) to background level of  $r^2 = 0.1$ , across the A, D and B genome, respectively (**Table 3.Sx11; Figure 3.S5**).

Relative kinship within the diversity panel was evaluated based on pairwise kinship between cultivars calculated with 24,216 SNP markers set. From 19,900 pairwise kinships calculated among cultivars of the panel, 61.20% of the total number of kinship estimates were below 0, and 38.35% were higher than 0 and less than 1 (**Figure 3.S6A**). The decline in the frequency of higher pairwise kinship coefficient was continuous till 1, and few estimates were higher than 1, suggesting a weak genetic relationship among the cultivars of the panel (**Figure 3.S6B**). Population structure inferred using the STRUCTURE algorithm and Evano test ( $\Delta K$ ) methods indicated two sub-populations within the 200 wheat cultivars (**Figure 3.S7AB**), with the first and second PCs explaining 11.09 and 4.15% of the genetic variance, respectively. With membership coefficient allotments of  $Q > 0.8$ , 99 and 25 cultivars were inferred to belonging to sub-population 1 and 2, respectively, and 76 cultivars with  $Q < 0.8$  were designated as admixture. The two distinct defined sub-groups related to the origins of the cultivars with sub-group 1 comprising entries originating from Europe ( $F_{st} = 0.3133$ ), while sub-group 2 included entries outside Europe ( $F_{st} = 0.0745$ ). The cultivars were color coded according to this structure result and plotted with PC1 vs. PC2 (**Figure 3.S7C**). The Q1 values of ancestry coefficient (Q matrix) given by population structure analysis at  $K = 2$  were color coded and mapped with the geographic origins of cultivars (**Figure 3.S7D**).

GWAS were conducted to identify QTL that are significantly ( $P < 10^{-4}$ ) associated with the response of the photosynthetic traits to drought stress (**Table 3.Sx12**). A total of 51 and 117 MTAs, representing 11 and 23 QTL regions, respectively, were significantly associated with the photosynthetic traits under control and drought conditions, respectively. All the detected 117 MTAs were induced by drought effect as they were not present under control conditions. The highest number of significant MTAs was obtained for YII under both water regimes (**Table 3.Sx12**). The drought inducible QTL interval ranging from 510.691 to 533.624 Mbp on chromosome 3A was associated with  $F_{max}$  and YII traits (**Figure 3.6; Table 3.Sx12**). The QTL regions on chromosome 7A covering genetic interval between 267.570-286.152 Mbp was associated with SPAD under control conditions (**Figure 3.S8**), while another one spanning on 10.480 Mbp length from 583.204 to 593.684 Mbp was detected for YII (**Table 3.Sx12**).

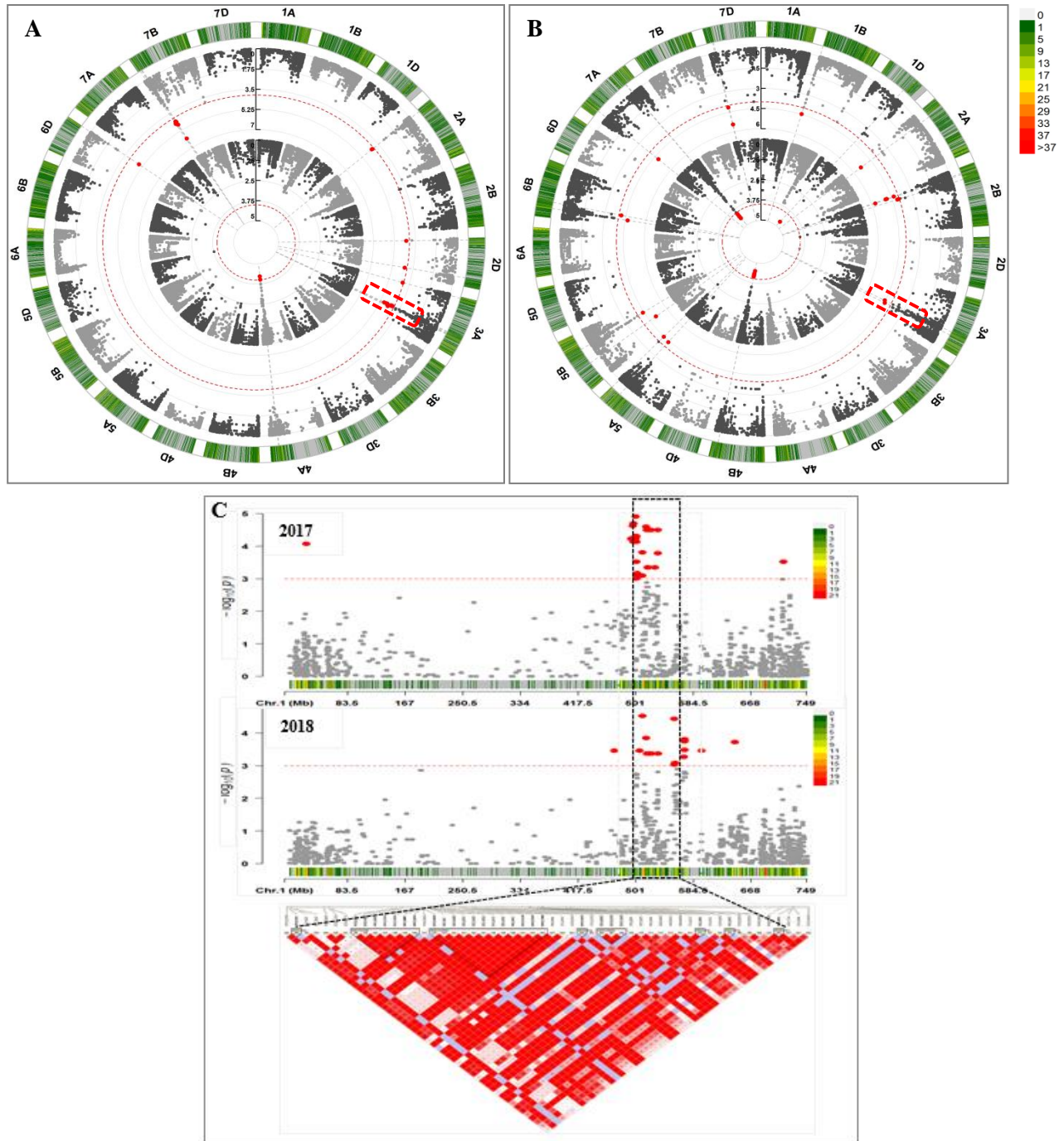


**FIGURE 3.6** | Presentation of GWAS results for YII and SPAD. (A) Cmplot for YII under control (inside track) and drought (outside track) including significant MTAs in 2017 and (B) 2018 showing drought inducible QTL on chromosome 3A. (C) Manhattan plot showing a hotspot of associated SNPs on 3A region of 22 Mbp length delimited from *AX-158597824* (510.691 Mbp) to *wsnp\_Ex\_rep\_c66865\_65263145* (533.624 Mbp) associated with YII under drought stress in 2017 and 2018. The legends on the right side show the SNP density per chromosomal region

#### 3.4.6. Analysis of QTL involved in marker by treatment and SNPs epistatic interactions for photosynthetic traits

GWAS was run to detect QTL involve in marker by treatment interactions effect. Eleven QTL regions involving 128 significant markers ( $FDR < 10^{-4}$ ) were interacting with water-treatment for SPAD, Fmax and YII (**Table 3.Sxl3**). The highest number (100) of marker\*treatment interactions was detected on chromosome 3A for SPAD, Fmax and YII traits (**Table 3.Sxl3-4**). The marker\*treatment interaction effect analysis on the associated chromosome 3A LD-block between the interval (515.889-516.803 Mbp) with the SNP peak *AX-158576783* indicated that genotypes with major alleles (TT) recorded significantly higher values than those with minor alleles (CC) under drought conditions, whereas the contrary pattern was observed under rainfed condition (**Figure 3.S9**).

Drought has triggered 19 epistatic interactions between SNP loci at 25 QTL regions for both YII and SPAD (**Figure 3.7; Table Sxl8**). Specifically, 26 SNPs located on 12 chromosomes were involved in 15 epistatic interactions for effective quantum yield of photosystem II, while 4 epistatic interactions included 7 SNPs on 6 chromosomes for SPAD. Among SNPs with epistatic interactions were 4 SNPs that as well detected for the main-effects in the GWAS analysis performed for YII (**Table 3.Sxl8**). SNP locus *AX-111134276* located at 556.662 Mbp on 3A, which had significant effect on YII via GWAS under drought conditions exerted high epistatic interactions with *w SNP\_Ku\_c28854\_38769308* at 690.958 Mbp on 6B. Likewise, the locus *AX-111134276* interacted epistatically with *AX-158588791* at 695.492 Mbp on 6B for SPAD. Both *w SNP\_Ku\_c28854\_38769308* and *AX-158588791* are located in the same QTL region.

Analysis of the effect of the interacting SNP pairs [*w SNP\_Ku\_c28854\_38769308* (G/A) at 690.958 Mbp on 6B and *AX-111134276* (G/A) at 556.662 Mbp on 3A] on YII indicated that combination A\*G (minor allele\* major allele) increased the YII value with 17.72% higher than the combination G\*A (major allele\* minor allele) which decreased it. In the same order, the combination of G\*G (minor allele\* major allele) of SNP pairs [*AX-158588791* (T/G) at 695.492 Mbp on 6B and *AX-111134276* (G/A) at 556.662 Mbp on 3A] increased the SPAD by 14.60% compared to T\*A combination (**Table Sxl8**). In addition, *AX-109950638* (G/A) interacted epistatically with *AX-109950638* (G/T) at 699.434 Mbp on 2A for YII. Genotypes with alleles pairs G\*G (major allele\*major allele) had higher YII than the one with A\*G and A\*T (**Table 3.Sxl8**).

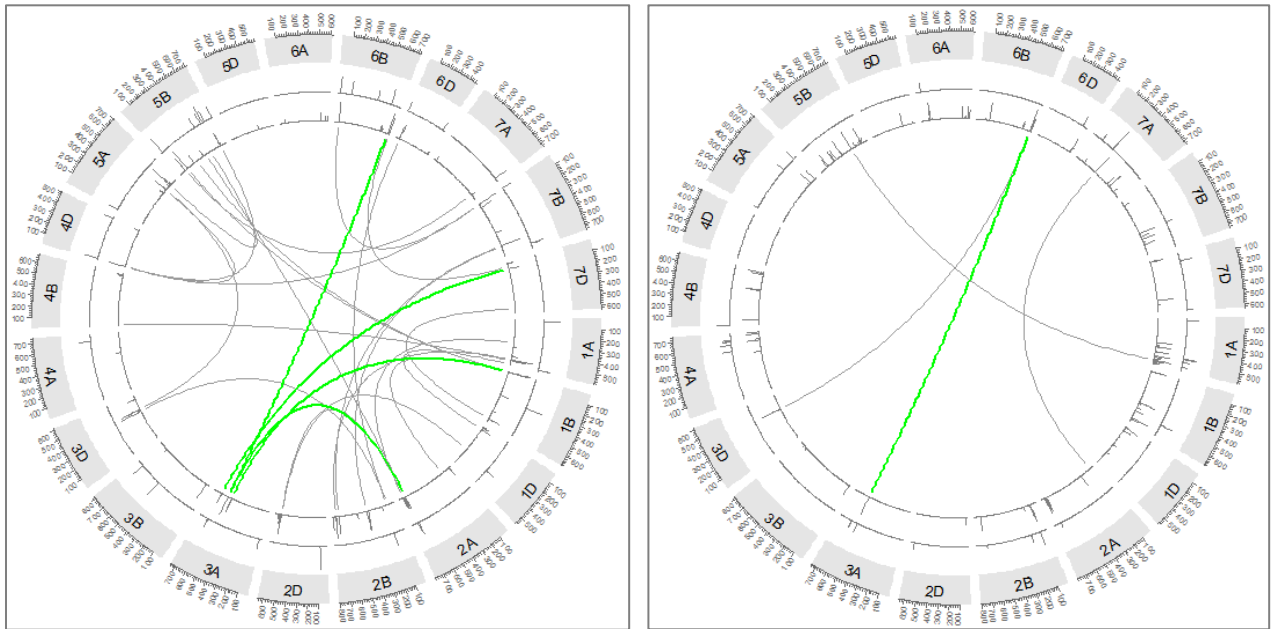
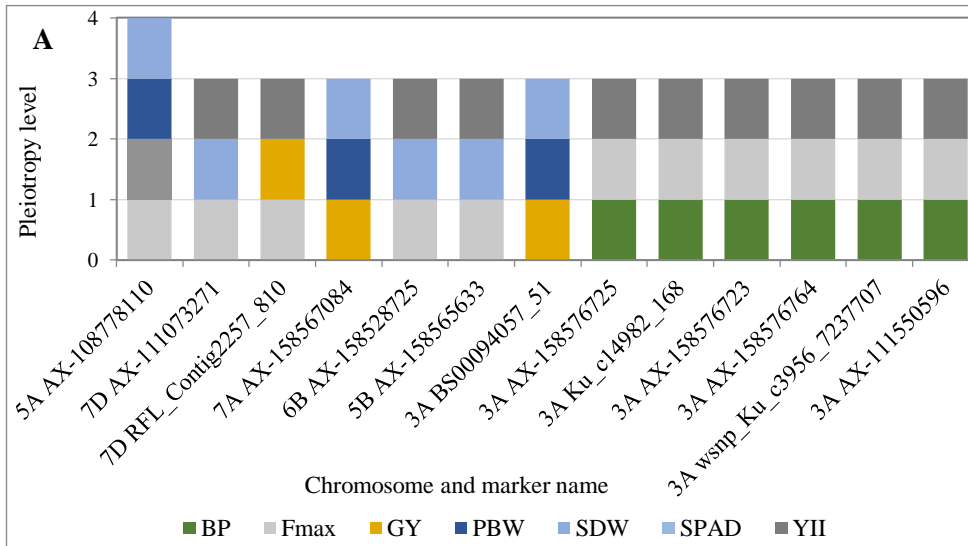


**FIGURE 3.7** | Circular plot showing the epistatic interactions SNPs with the corresponding positions on the genetic map of wheat. Wheat chromosomes 1A–7D are shown in a clockwise direction in the Circos diagram. Green colored connections represent epistatic loci on chromosome 3A controlling YII (**left panel**) and SPAD (**right panel**). Gray colored connections represent epistatic interactions on other chromosomes. The first track line after the chromosome name track is showing the significant ( $10^{-4}$ ) epistatic loci detected under rainfed while the following track is showing the ones detected under drought conditions.

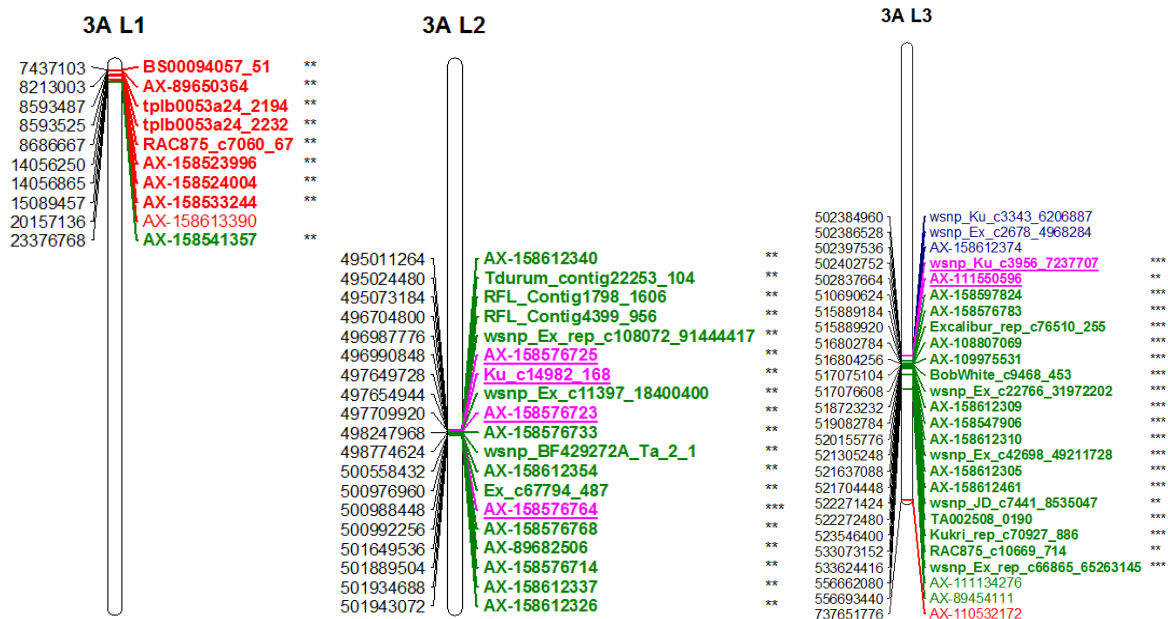
### 3.4.7. Breeding has improved genetic factors involved in photosynthesis and drought tolerance

Stable QTL that were detected in 2017 and 2018 trials and/or showed pleiotropic effect on several traits including SDW, PBW, and GY were identified and further analyzed. A total of 57 and 15 SNPs located on chromosome 3A and 7A, respectively were stable QTL and/or exhibited pleiotropic effects on the traits (**Table 3.Sxl5**). A QTL region spanning 5.847 Mbp from *RFL\_Contig4399\_956* (496.705 Mbp) to *AX-111076088* (503.027 Mbp) on chromosome 3A had a pleiotropic effect on BP and YII (**Figure 3.8AB**). The LD analysis performed showed that the associated genomic region on chromosome 3A that showed pleiotropic effect on YII and BP are in high LD ( $r^2 > 0.86$ ) (**Figure 3.8C**). Comparison of the allelic effects on traits of the SNPs in 3A haplotype-block region (peak marker *AX-158576783* at 515.889 Mbp) revealed that genotypes with TT (major) alleles significantly contributed to higher YII and GY when compared to genotypes with the CC (minor) alleles. The observed allele effect was found to be stronger under drought conditions (**Figure 3.9; Figure 3.S10A-D**). Further analysis showed that the favorable (TT) alleles were prominently present in the newer released cultivars, whereas the unfavorable alleles (CC) were present in old cultivars (**Figure 3.9EF**). The mean GY and YII of genotypes with TT alleles are 76.68 g/row and 0.66, respectively, while the genotypes with CC alleles had 65.92 and 0.53 for GY and YII, representing 16.33% (GY) and 23.11% (YII) increase in crop productivity between 1963 and 2013 (**Figure 3.9**).

The drought tolerance status of the cultivars in the studied panel were calculated for GY, SDW, PDW, SPAD and YII using the SWP index and cultivars were ranked as tolerant (highest SWP) to sensitive (lowest SWP). Based on the SWP index, 10 cultivars with SWP index  $> 31.99$  were considered tolerant, while those with SWP index  $< 27.03$  were identified as sensitive genotypes. Interestingly, most selected drought tolerant cultivars were recently released, while the old release cultivars were mostly observed in the sensitive group (**Figure 3.10AB**). PCA constructed with the selected tolerant and sensitive cultivars using the SNP markers associated with breeding progress trait separated the cultivars into two groups. The first two components explaining 75.01% of the total variation and the grouping was based on the drought tolerance status of the cultivars. The recently released cultivars being drought tolerant (in green/circle-shaped) were mostly clustered in the left side of the plot, while the old released cultivars and most sensitive were distributed at the right side of the plot (**Figure 3.10C**).



**B**



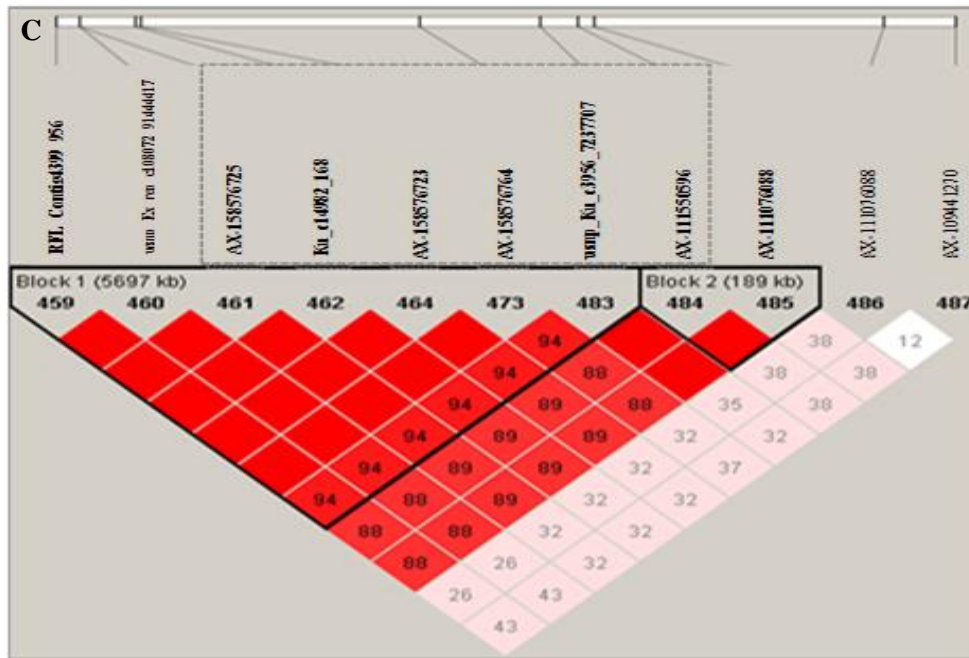


**FIGURE 3.8** | Representation of most pleiotropic SNPs detected under drought. **(A)** Pleiotropic SNP involved in breeding progress. **(B)** Map positions of drought inducible SNPs associated with evaluated traits. Map distance (in base pairs) is shown on the left. ‘Underlined and bold’ SNPs are pleiotropic and the numbers of stars indicated the number of traits the SNP was underlying; The color of SNPs indicated the category of traits the SNP is associated with [“red” = agronomic traits (SDW, PDW or GY); “green” = photosynthesis traits (SPAD, Fmin, Fmax or YII); “blues” = breeding progress (BP); “light-blue” = pleiotropic Agro+Physio; “purple” = BP+Physio; “dark-red” = Agro+Physio+BP]. **(C)** Chromosomal region of 5.847 Mbp length on 3A from *RFL\_Contig4399\_956* (496.705 Mbp) to *AX-111076088* (503.027 Mbp) harbored six SNPs (grey square) associated with BP progress and YII. Two haplotypes blocs were found in this region, pairwise  $D'$  between SNPs of LD block are displayed.

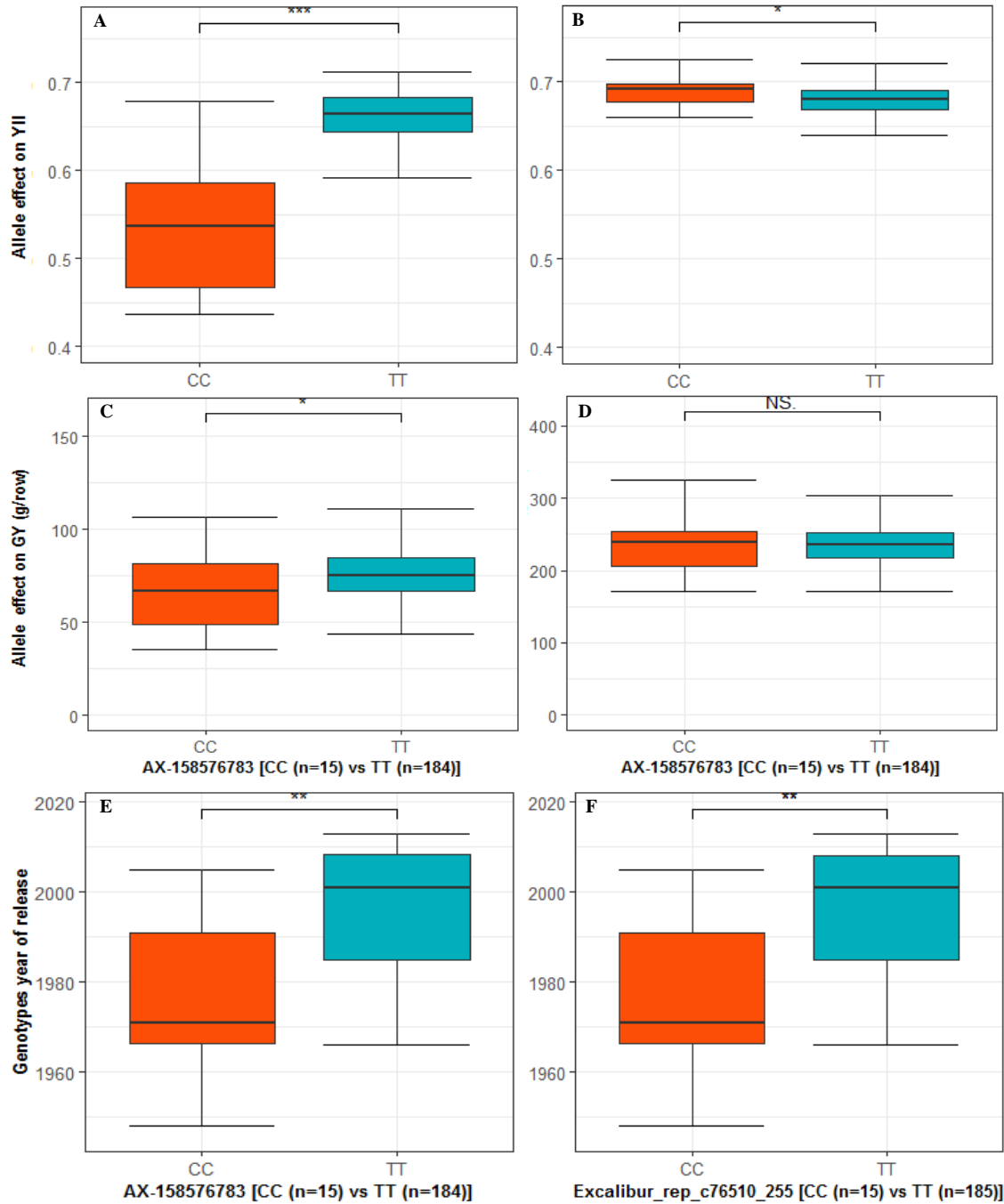


**FIGURE 3.9** | Allelic effect of AX-158576783 on YII and GY. (A) Allelic effect on YII under drought and (B) rainfed; and on GY under drought (C) and rainfed (D); (E-F) Chromosome 3A SNPs AX-158576783 (515.889-516.804 Mbp) alleles distribution by cultivars year of release in the wheat panel. Two-sample *t*-test P-value shows significant difference between major (TT) and minor (CC) alleles.

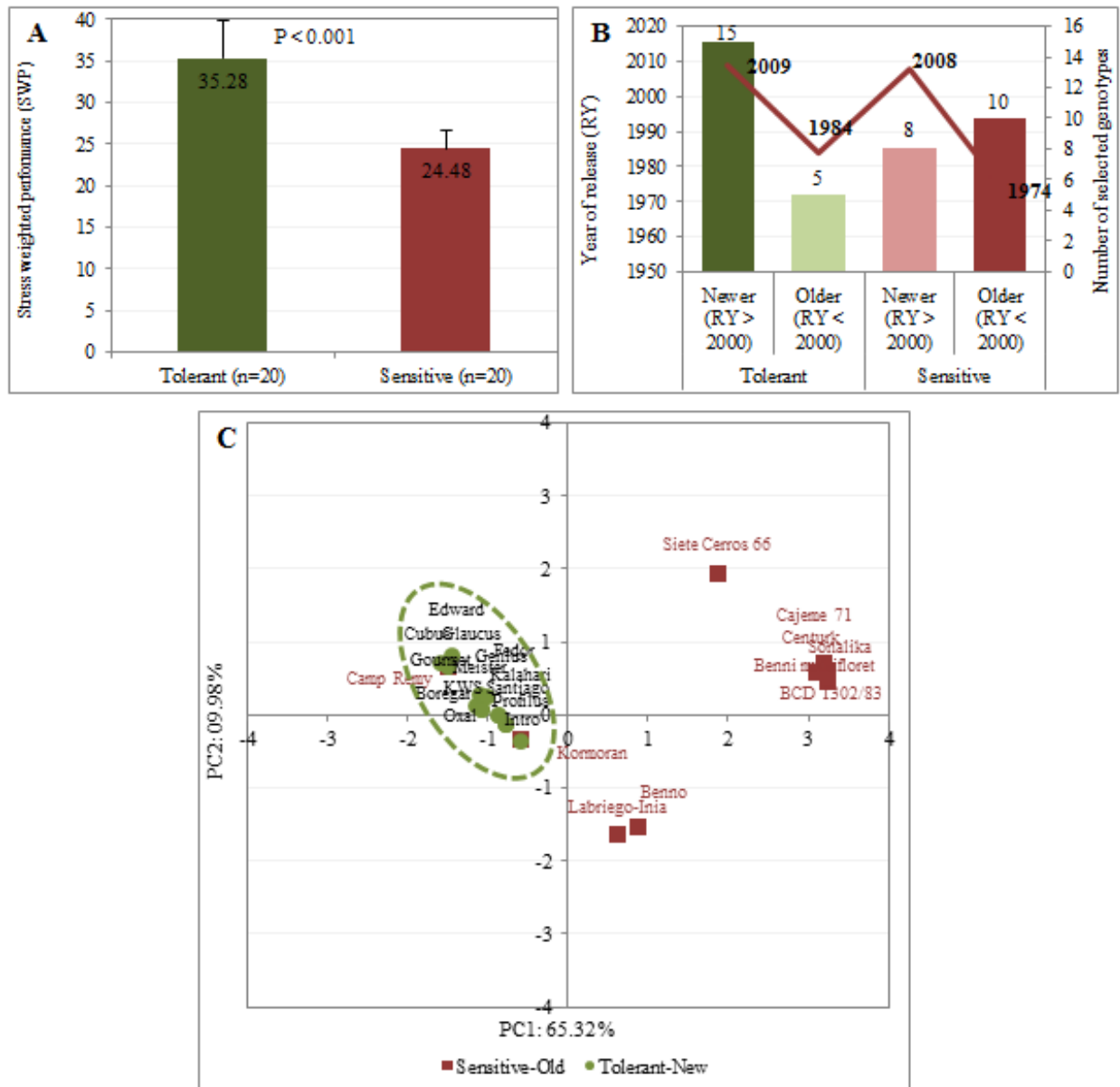


**FIGURE 3.10** | Representation of forty contrasting cultivars. **(A)** Barplot of 20 drought-tolerant (green) and 20 drought-sensitive cultivars groups based on their SWP estimates; the P value indicates significant difference between both groups. **(B)** Barplot of new (green) and old (dark-red) released cultivars based on SWP estimates. The dark-red color showed new released cultivars are prominent among the drought-tolerant cultivars while older ones are mostly present in the drought-sensitive group. **(C)** Principal component analysis based on 28 MTAs of BP separating thirteen drought-tolerant and new released (in green circle) and ten drought-sensitive and old cultivars (dark-red square).

### 3.4.8. Candidate genes in the chromosomal regions harboring stable and pleiotropic MTAs

The candidate genes in the region harboring stable and pleiotropic MTAs were retrieved and the result is presented in **Table 3.Sxl6**. A total of 225 HC genes including 58 on chromosomes 3A were retrieved from associated QTL regions. The associated region for YII spanning 12.912 Mbp on chromosome 3A contain 42 genes involved in response to oxidative stress. The 3A *AX-158576783* haplotype-block (515.889-516.804 Mbp) contains genes whose gene ontology (GO) terms are related to cellulose synthase, electron transport, coupled proton transport mitochondrial respiratory chain complex I assembly, contain WRKY transcription factors, and chaperone protein dnaJ which protect proteins from external stress. Chromosomal region of the stable SNP peak *Excalibur\_rep\_c68899\_1400* on chromosome 2B underlying GY, YII harbored 31 genes (**Table 3.Sxl3**) mainly involve in peroxidase and non-specific serine/threonine protein kinase activity, and stress protector genes such as heat shock 70 kDa protein. SNP peak *RFL\_Contig2257\_810* on chromosome 7D, although not in LD block with other significant candidate loci was pleiotropic for Fmax, YII and GY under drought. This SNP co-segregates with 13 HC genes majorly involved in carbonic anhydrase and oxidation-reduction process heme binding, carbonate dehydratase activity, ATP binding protein BP: protein phosphorylation; recognition of pollen.

The *in silico* analysis of the 3A and 5B chromosomal regions with high interaction marker\*treatment effect revealed high sequence homologies to genes involved in drought stress response and photosynthesis activity (**Table 3.Sxl7**). A total of 536 HC genes were found in the five regions where SNP peak for interaction effect were located. Thirty-two of these genes are involved in plant response to environmental stress and defense mechanisms including heat shock protein and transcription factors, zinc finger C3H1 domain, disease resistance protein. We found genes category involved in phosphorylation, glycerol metabolic process, electron transport, whose actions play important role in photosynthesis activity.

BLAST searches indicate that most of significant epistatic loci are located in the vicinity of genes involved in photosynthesis activity, particularly in oxidation-reduction process and phosphogluconate dehydrogenase (decarboxylating). These QTL regions harbor ferredoxin reductase-type FAD-binding domain and alternative NADH-ubiquinone oxidoreductase which catalyzes the oxidation of mitochondrial NADH. In addition, universal stress proteins, disease resistance protein and nucleotide-diphospho-sugar transferases were found (**Table 3.Sxl9**).

#### 3.4.9. Allelic variation in the promoter regions of NADH-ubiquinone oxidoreductase genes

Comparison of the four sequences of the *TraesCS3A02G287600* promoter region with reference sequence revealed four polymorphic sites +70, +212, +241, and +435. The drought-tolerant cultivars possess the allele A, C, G, and A at the positions +70, +212, +241, and +435, respectively like the reference allele, whereas the drought sensitive had G, T, A, and G at these respective positions (**Figure 3.11**). The similarity among the promoter sequences of the contracting cultivars were assessed through comparison of their amino acid sequences. The sequences of drought-tolerant cultivars were more similar; hence, they clustered together, while the drought sensitives were clustered in another group (**Figure 3.12**).

Analysis of the transcription factors binding sites (TFBS) in the promoter region of *TraesCS3A02G287600* using PlantTFDB indicated six TFBS overlapping with the polymorphisms site at +212 and eight TFBS at +435 (**Table 3.Sxl11**). Most of the TFBS were in the family of APETALA2/ETHYLENE RESPONSIVE FACTOR transcription factors (AP2/ERFs) (**Table 3.Sxl11**). For, instance, the transcriptions factors TFmatrixID\_0719 (ID: AT5G18560) binding sites located at +212 is an ethylene-responsive transcription factor involved in the regulation of gene expression by stress factors and by components of stress signal transduction pathways.

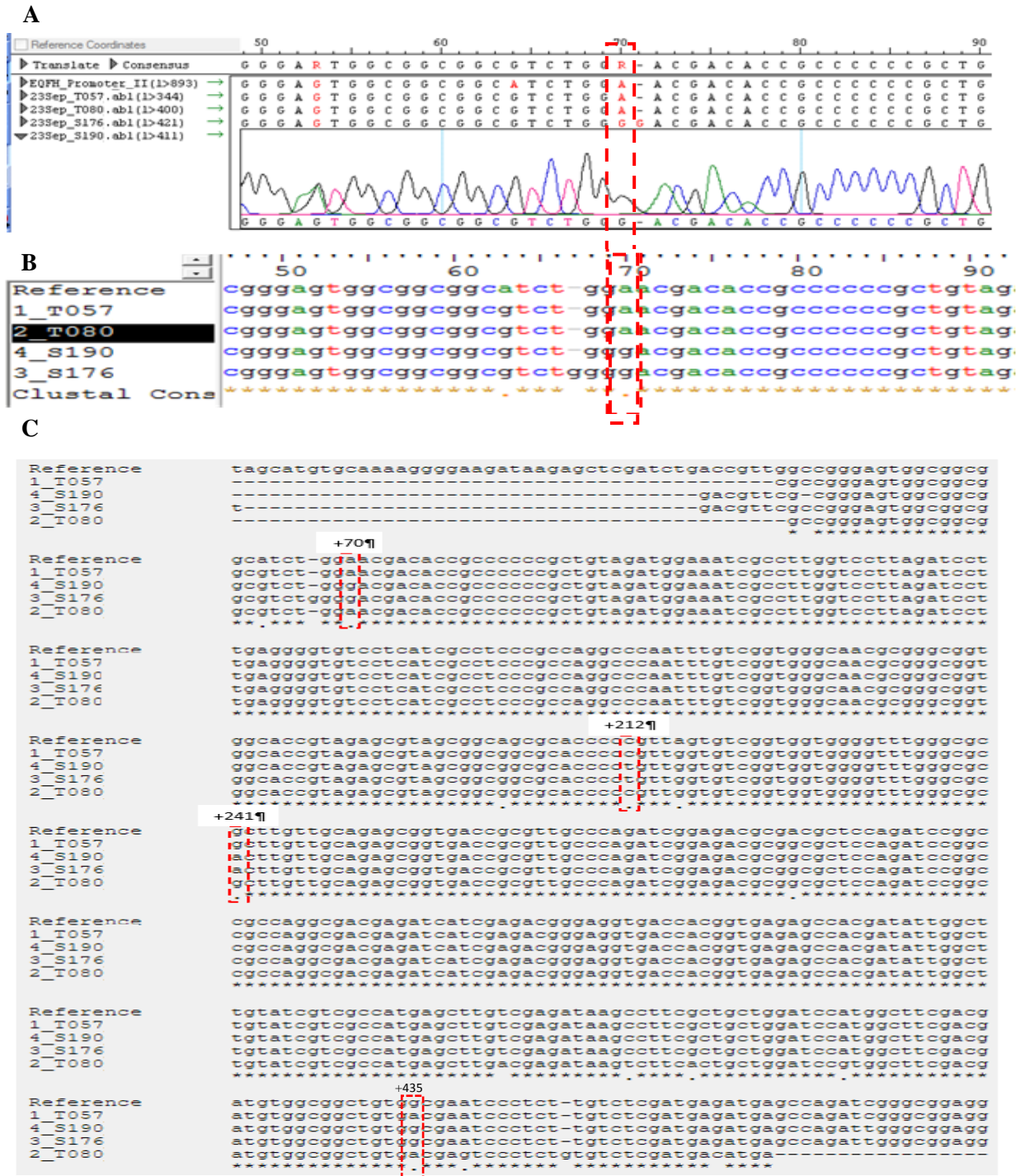


**FIGURE 3. 11** | DNA alignment displaying positions of allelic variation in the promoter region of two groups of contrasting cultivars. Alignment were made using SeqMan Pro (A), BioEdit (B), and MAFFT (C). In panel A, “.” indicate nucleotide exchanges marked by the red boxes showing non-conserved substitutions. “\*” indicates the identical nucleotide in all sequences.

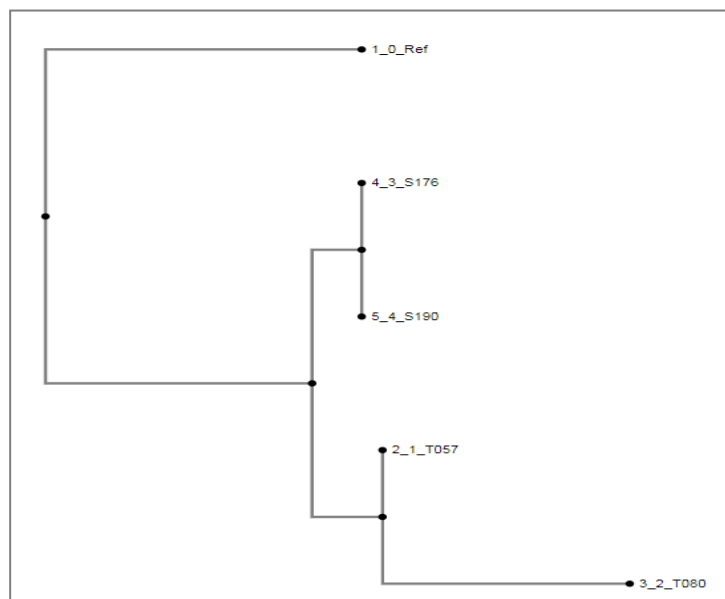


**FIGURE 3.12** | Dendrogram displaying similarities among the four cultivars based on the amino-acid sequence of the promoter region analyzed with MAFFT. The drought-sensitive cultivars [*Mironovska* 808 (S176) and *Ivanka* (S190)] are classified in one group and the drought-tolerant [*Gourmet* (T057), *Inspiration* (T080)] were in another group.

### **3.5. Discussion**

Water stress is a major threat on wheat yield thus threatening global food security. The use of diverse wheat panel is important to assess plant physiological and morphological response under prolonged drought stress and uncover new genetic variants that contribute to drought tolerance. Considerable effort has been made to quantify drought effect on yield lost, but few studies have focused on unveiling the genetic factors underlying breeding progress for drought tolerance vis-a-vis physiological traits i.e. photosynthesis activity. In this research, we aimed to investigate the genetic variation and dynamic in photosynthesis activity of wheat traits under drought stress, identify pleiotropic and stable QTL over the two years underlying photosynthesis traits and yield, and shed a light on the contribution of breeding to drought tolerance.

#### **3.5.1. Phenotypic variation in response to drought stress**

Drought has significant effect on chlorophyll content and fluorescence parameters across GS with the observed effect of 3.47 and 27.03%.for chlorophyll content and effective quantum yield of PSII, respectively. Drought caused a significant effect on plant photosynthesis rate (29.53%), resulting in reduced crop productivity. The reduction of photosynthetic parameters under prolonged drought conditions is expected at several levels as drought affects all biological processes in chloroplast including disorder of the electron transfers in PSII (Yang et al., 2007; Balla et al., 2014). Excessive drought may rise leaf temperature which was the case in our study. High temperature caused accelerated aging, leading to the activation of proteolytic enzymes, protein degradation, and chlorophyll losses (Harding et al., 1990). The reduction of chlorophyll content leads to a decrease in the chlorophyll fluorescence level, which in turn lessened the effective quantum yield of PSII and prevented the reduction of NADP<sup>+</sup> to NADPH and the formation of ATP (Pinto et al., 2020). Another reason for the reduction of photosynthesis under stress conditions is the stomatal closure to prevent water loss, leading to a lower internal CO<sub>2</sub>/O<sub>2</sub>, hence making carbon assimilation less efficient during the Calvin Cycle reaction of photosynthesis (Araus et al., 2008). Under drought stress conditions, the correlations among photosynthetic- related traits was higher than those under rainfed, suggesting drought stress would affect most physiological mechanisms. Specially, chlorophyll content exhibited higher correlations with CFP under drought conditions, suggesting that high leaf chlorophyll content, which maintain “leaf stay-green” properties, was very important to tolerate dehydration in wheat as previously reported (Yang et al., 2007). The CV among the genotypes ranged from 5.95 to 67.41% under controlled condition and from 6.20 to 79.87% under drought conditions. The recorded heritability estimates of the traits ranged from moderate to high, with the exception of Fmin that showed low heritability, suggesting that the observed trait response to drought can be attributed to the genotypic effect. Thus, can be exploited for drought tolerance

characterization among the studied genotype. The marker based heritability which is relevant in dissection of complex traits (Kruijer et al., 2015) revealed that a larger portion of phenotypic variance is ascribed to genotypic variance for SPAD and F<sub>max</sub>. These results highlight the existence of high variability in cultivar's responses to drought stress that can be exploited through GWAS to develop drought tolerant cultivars (Oyiga et al., 2019).

The presented investigations revealed plant photosynthetic-related traits such as YII, F<sub>v</sub>/F<sub>M</sub>, and NPQ at the post-anthesis growth stage were strongly correlated with the plant biomass weight and grain yield. Higher photosynthetic activity of plants at anthesis and post-anthesis GS is relevant for increased GY as it affects the key yield components, the number of grains per spike, and per square meter (Lichthardt et al., 2020). Similar relationships between photosynthetic related traits namely chlorophyll content, leaf CO<sub>2</sub> assimilation (A), and effective quantum yield of PSII and grain yield were reported in previous studies on triticale and bread wheat under drought stress in Mediterranean climates, (Méndez-Espinoza et al., 2019). Their research revealed that triticale obtained higher yield than bread wheat owing to his higher photosynthesis activity at grain filling stage. The assimilates necessary for filling the grain are provided by photosynthesis in the leaves (Evans et al., 1975) and spikes (Tambussi et al., 2007; Maydup et al., 2012), and the redistribution of reserves stored in vegetative tissues during the pre- and/or post-anthesis periods, which are translocated to the growing grains (Schnyder, 1993; Zhang et al., 2006). Farooq et al. (2014) reported the principal reasons for lower yield under drought conditions are reduced rates of net photosynthesis owing to metabolic limitations, oxidative damage to chloroplasts and stomatal closure, causing poor grain set and development. Reduction of photosynthesis activity under drought stress is caused by accelerated leaf senescence due to the breakdown of chlorophyll molecules, affecting the stay green state of the plant, particularly the flag leaf (Yang et al., 2001). Almost half of the photosynthates needed during grain filling in wheat are contributed by flag-leaf photosynthesis, which reduction induced the dilution of sucrose in the ear and floret abortion and subsequent low yield (Sylvester-Bradley et al., 1990; Barnabás et al., 2008).

We detected a strong correlation between SPAD and other photosynthetic-related traits such as NPQ, F<sub>v</sub>/F<sub>M</sub>, and YII traits mainly at post anthesis under drought conditions. These results suggest SPAD, non-invasive and rapid assessment of leaf chlorophyll content could be a suitable surrogate to screen plant physiological status of the plant under drought condition. Particularly under drought conditions where water and nutrient uptake are limited, cultivars with largest root mass, hence high nitrogen status at grain filling would have higher photosynthesis activity, assimilate partition and higher yield (Kaggwa, 2013).

An increase in the photosynthesis efficiency correlated with the breeding progress. Modern cultivars have higher chlorophyll content and effective quantum yield of PSII values than the old cultivated cultivars as shown by their significant positive slopes (**Figure 4**). The latter exhibited a high correlation with

grain yield under drought conditions, indicating that the effective quantum yield of PSII is positively associated with grain yield. Previous studies reported high yield performance of modern over older cultivars owing to their higher photosynthetic capacity or canopy longevity, radiation use efficiency, stay green traits during the milk-grain stage to maturity (Araus et al., 2008; Sanchez-Garcia et al., 2015). Since grain growth is supported by transient photosynthesis and translocation of assimilates stored in vegetative organs prior to anthesis (Maydup et al., 2010; Sanchez-Bragado et al., 2014). Similar to our findings, Lichthardt et al. (2020) reported SPAD value around anthesis as one of the relevant traits for progress in German winter wheat breeding in the past five decades. Comparison of SPAD and YII values of cultivars released before 1980 vs the ones released after 2010 confirmed that modern cultivars have significantly higher values in both photosynthetic parameters. Interestingly, for YII the difference between these two contrasting groups was higher under drought than under control, suggesting breeding might even have increased cultivars photosynthetic efficiency under drought than under control condition. Breeding has accumulated genetic variants conferring favorable effects on photosynthetic activity, and disease resistance, which subsequently have enhanced GY under less optimal conditions (Voss-Fels et al., 2019).

### **3.5.2. Population structure and linkage disequilibrium pattern**

We identified two main sub-populations relating to the geographic origin of cultivars including Europe and outside Europe clusters, and an admixture group between both sub-populations. The  $F_{ST}$  value among cultivars originating from Europe was weak (0.3133), while the one outside Europe was weaker (0.0745). This result is an indication of high genetic diversity in this set due to germplasm exchange between breeding programs, and limited selection pressure and genetic drift (Chao et al., 2017; UPOV, 1991). The low intra-population  $F_{ST}$  values suggested a weak population structure in the evaluated panel and the individuals in both subpopulations share a high number of alleles. Assessing the population structure of a diversity panel is relevant to minimize the occurrence of spurious or false-positive associations (Gajardo et al., 2015). Therefore, we included three first principal components as population structure matrix and a kinship matrix in the mixed model for association mapping. The LD of the studied wheat panel decayed after 19.0, 38, and 17.5 Mbp for A, B, and D genomes, respectively, revealing that the LD decay of genome B was slower than A and D. Similar trends in the genomes LD decay were found in earlier studies performed the same germplasm genotyped with 15K chip SNP marker set (Voss-Fels, Stahl, Wittkop et al., 2019).

### **3.5.3. Genetic variant with improved photosynthesis activity has conferred drought tolerance**

GWAS of chlorophyll content and fluorescence parameters identified 51 MTAs and 117 MTAs corresponding to 11 and 23 QTL regions under rainfed and drought, respectively, with the highest number of MTAs on chromosome 3A. Most of the detected MTAs were only present under drought stress

conditions, suggesting that they might be drought inducible QTL. The genetic control of CFP could vary considerably between drought-stressed and non-stressed plants (Czyczyło-Mysza et al., 2011), indicating that the identified QTL performed different expression patterns under rainfed and drought conditions. Previous research successfully mapped CFP on almost all chromosome under well-watered, moderate, and severe drought using a double haploid biparental population. Interestingly, chromosome 3A harbored QTL associated with all evaluated CFP under drought conditions as found in our study for Fmax and YII (Czyczyło-Mysza et al., 2011). However, some chromosomes such as 1B, 7A, 7B and 7D has similarly been mapped for important physiological traits including chlorophyll content, water use efficiency, osmotic adjustment, and chemical desiccation tolerance in several studies (Börner et al. 2003; Hao et al. 2003, Cao et al. 2004). Contrary to the present research, most of these QTL mapping for physiological traits used biparental mapping population consisting of double haploids (Christopher et al., 2016; Czyczyło-Mysza et al., 2011). Although, chromosome 3A was not found in many reported studies, the consistency of the QTL hotspot in the chromosomal region from *AX-158597824* (510.691 Mbp) to *wsnp\_Ex\_rep\_c66865\_65263145* (533.624 Mbp) in the present study make this region a good candidate for higher photosynthetic activity under drought conditions. The analysis of the promoter region of the genes *TraesCS3A02G287600* near *AX-158576783* (515.889 Mbp) has revealed several TFBS including APETALA2/ETHYLENE RESPONSIVE FACTOR transcription factors (AP2/ERFs) that overlapped with the polymorphic sites. The AP2/ERFs are known as key regulators of various stress responses, and they improved plant survival during stress conditions (Xie et al., 2019). Similar to our results, chromosome 7A (263.733 to 285.609 Mbp) harbored QTL hotspot constantly associated with SPAD, YII under rainfed conditions as reported in previous studies (Börner et al. 2003; Hao et al. 2003, Cao et al. 2004).

The identified QTL in our study are quite conclusive as they co-segregate with genes involved in plant response to abiotic stress such as production of stress-related proteins under drought stress conditions and in oxidation-reduction processes and Carbohydrate metabolism-related proteins (Cheuk et al., 2020). Specifically, on chromosome 7D, *RFL\_Contig2257\_810* pleiotropic for Fmax, YII, and GY co-segregated with carbonate dehydratase activity and  $\beta$ -galactosidase activity. With reduced photosynthetic activity, it has been observed that the galactosidase activity could enhance sugars needed as energy source when photosynthates production is lower (Pandey et al., 2017).

### **3.6. Conclusion**

Prolonged drought has resulted in a reduction of chlorophyll content, fluorescence parameters, and photosynthetic capacity. Significant genotypic variation was found in plant physiological and morphological response to drought stress. The positive relationship between most photosynthetic traits such as SPAD, YII,  $F_v/F_M$  screened at anthesis or post anthesis GS and the plant biomass weight and grain yield confirm the importance of high photosynthesis in increasing biomass production not only under well-watered field but under drought prone environment. Our results suggest the combination of physiological traits and agronomic traits under drought can efficiently to select for drought tolerant cultivars. Comparatively to most yield components and GY, breeding has significantly contributed to improve photosynthetic related traits across all growth stages, but importantly at anthesis, under prolonged stress. GWAS unravel a hotspot of stable QTL on chromosome 3A involved in effective quantum yield of PSII, which is directly link to photosynthesis activity under drought conditions. Interestingly, several MTAs in LD block on 3A associated with breeding history showed pleiotropic effects with YII. Some of these MTAs had significant allelic effect on GY under drought condition and co-segregate with genes related to response to oxidative stress, cellulose synthase, aerobic respiration, and electron transport rate in the PSII chain. The loci and candidate genes identified in this study may facilitate the molecular breeding of drought-tolerant wheat, and improve wheat production under drought prone environment.

## Chapter 4

### Genome wide dissection study and *in-silico* transcript analysis provides candidate loci for improved drought tolerance and nitrogen use efficiency in winter wheat

Ahossi Patrice Koua<sup>1</sup>, Md. Nurealam Siddiqui<sup>1</sup>, Katrin Heß<sup>1</sup>, Nikko Klag<sup>1</sup>, Diana Duarte-Delgado<sup>1</sup>, Benedict Chijioke Oyiga<sup>1</sup>, Jens Léon<sup>1,2</sup> & Agim Ballvora<sup>1</sup>✉

1 INRES Pflanzenzüchtung, Rheinische Friedrich-Wilhelms-University, Bonn, Germany

2 Field Lab Campus Klein-Altendorf, University of Bonn, Klein-Altendorf 2, 53359 Rheinbach, Germany

Correspondence:

✉Agim Ballvora

Katzenburgweg 5, 53115 Bonn

ballvora@uni-bonn.de

Tel. +49 228 737400

INRES Plant Breeding Rheinische Friedrich-Wilhelms-University Bonn 53115 Germany Tel.: +49228737400 Fax: +49-(0)228-73-2045 Email: [ballvora@uni-bonn.de](mailto:ballvora@uni-bonn.de)

To be submitted in a peer reviewed journal.

#### **4.1. Abstract**

**Key message** A genome wide association study has identified haplotypes on chromosomes 1B and 5A associated with drought tolerance in winter wheat, whose neighboring genes showed higher transcript abundance under various biological conditions including drought.

Nitrogen (N) is the crucial nutrient element for plant growth and productivity. Climate change across the globe is the source of extreme conditions like prolonged drought, which result in higher yield losses due to its effect on nutrients uptake, including nitrogen. The understanding of the mechanistic basis of nitrogen use efficiency (NUE) under drought conditions, is essential to improve wheat yield. Here, we evaluated the genetic variation of NUE-related traits and photosynthesis response in diversity panel of 200 wheat genotypes under drought and nitrogen stress to identify quantitative trait loci (QTL) underlying these traits through genome-wide association study (GWAS). The results indicated significant genetic variations in the response to drought and nitrogen deprivation in the evaluated traits. Drought has reduced more the plant performance than N deprivation due its effect on water and nutrients uptake. A total of 27 potential QTL with main effect were detected by GWAS, while 10 QTL regions were interacting with N availability. Significance differences were found between both haplotypes variants on chromosome 1B that included SNP markers associated with N uptake and use efficiency. The transcript abundance analysis showed that the cold shock protein gene expression was higher under various biological conditions including drought. Upon validation this genomic could be used as N and drought adaptive marker simultaneously.

**Keywords:** Drought, nitrogen deficiency, GWAS, root architecture, photosynthesis, allele effect, transcript abundance.

## 4.2. Introduction

Winter wheat (*Triticum aestivum* L.) is one of the most widely cultivated crops in the world with an area of around 215.902 million hectares (FAO, 2020). Both nitrogen (N) and water availability have a strong influence on the wheat yield. Nitrogen deficiency and drought stress lead to severe yield losses (Farooq et al., 2014; Han et al., 2015). To increase crop production, the amount of N fertilizer supply has increased in the recent times. Meanwhile, about 50% of the N fertilizer applied to cropping systems is not absorbed by plants, but is lost as ammonia (NH<sub>3</sub>), nitrate (NO<sub>3</sub><sup>-</sup>), and nitrous oxide (N<sub>2</sub>O) (Ciampitti & Vyn, 2014; Maeoka et al., 2020). Therefore, the extensive use of nitrogen fertilizers, which was largely responsible for the large increase in yields of the last few decades, has nonetheless negatively threatened the environment. Nitrogen leaching and runoff contaminate ground and surface water causing eutrophication, soil salinization and threatening the quality of air (Han et al., 2015; Thompson et al., 2019). When eutrophication occurs, biodiversity decreases and drinking water production is endangered. N pollution poses an even greater challenge than carbon (C), because of the complex effects of reactive N cascade through its many chemical forms (Xu et al., 2012).

In the past, the focus in plant breeding was on increasing yields and improving quality. The introduction of the “dwarfing genes” and the improvement in the use of nitrogen fertilizers resulted in yield rise by the Green Revolution (Good and Beatty, 2011). For instance, the production of cereal crop tripled during this period, with only 30% increase in land area cultivated (Wik et al., 2008; Pingali, 2012). By reducing plant height, the resistance to lodging was increased and the plants were able to absorb more nitrogen and translocate it to the grain (Le Gouis, 2011), hence increasing the harvest index (Jobson et al., 2019). The current focus of plant breeding is the improvement of the nitrogen use efficiency (NUE), the reduction of fertilizer use and the maintenance or increase of the yield under abiotic stress conditions such as drought (Hirel et al., 2011). Breeding cultivars with high nutrient use efficiency for grain production would require breeding for high N uptake and utilization efficiency. This breeding approach is not only important for developing countries with drought prone environments and nutrient-deficient soils, but it is essential for developed countries due to the environmental consequences of extensive nitrogen fertilizer use. Improved NUE will contribute to reduce the environmental problems and costs associated with N fertilization and increase yield to face the increasing global demand for food. Increased crop productivity at low N supply is associated with higher N uptake, whereas yield gain under high N supply is more associated with the ability of crops to convert N fertilizer into grain dry matter (Nehe et al., 2018). The challenge is therefore to improve the N uptake and N utilization efficiency in the context of reduced water availability due to drought (Lawlor, 2002). The mobility of N in the soil-plant system is controlled by factors and complex interactions, including the soil moisture content and the plant root system architecture (Fageria et al., 2010).

Optimization of the root system architecture (RSA), especially under low input and drought conditions, will significantly improve crop productivity (Zhu et al., 2011; Xie et al., 2017). The root system provides the plant anchorage, competitiveness and adaptation to stress. Furthermore, roots also have significant roles in soil exploration, stand establishment, belowground carbon sequestration, soil structure improvement and maintenance of soil fertility by driving microbial processes (Siddiqui et al., 2020; Richard et al., 2015; Kaggwa, 2013). Improving RSA-traits such as root length, biomass and area have shown positive effects on plant photosynthetic features like high stomata density and to lower canopy temperature. These effects on the aboveground tissues contribute to increase drought-tolerance status. Despite the importance of roots, direct selection for optimal RSA characteristics in the field has not been routine because of the complex interactions between the root system and rhizosphere.

To date, few studies have focused on the nitrogen mobility from soil to the grain under drought stress conditions. To the best of our knowledge, there is not much studies carried out to uncover QTL underlying NUE-related traits in wheat, especially under drought conditions. Therefore, our present study was conducted to (1) evaluate the genetic variation for nitrogen use-related traits under drought and rainfed conditions, (2) assess the root system attributes under drought and nitrogen deprivation to determine its key role in improving plant photosynthetic traits, and (3) identify the QTL associated with these traits and their plausible candidate genes.

### 4.3. Materials and methods

#### 4.3.1. Plant Material

A total of 200 winter wheat cultivars were grown at the experimental station of Campus Klein Altendorf, University of Bonn (50.61° N, 6.99° E, and 187m above sea level, 113 Germany) in 2017 and 2018 seasons. The soil of the experimental site was a Haplic Luvisol (World Reference Base for Soil Resources, WRB) derived from loamy silt (Perkons et al., 2014). Two water regimes (drought stress under rainout shelter and a rainfed treatment), and two nitrogen applications rates including a medium N supply (MN) which corresponded to 110 kg/ha and high N supply (HN) with 220 kg/ha, both adjusted to the N<sub>min</sub> in soil. In 2017, only the variant 220 kg/ha was applied. The experimental set-up of the water supply under rainout shelter and drought treatment is described in Koua et al. (unpublished).

A pot experiment was grown in the Poppelsdorf Campus of the University of Bonn (50.73° N, 7.09° E, and 63 m above sea level) in 2019, including 30 selected winter wheat cultivars from which 20 genotypes represented the genetic diversity of the panel, five were drought-tolerant and five drought-sensitive (**Table 4.S1**). This experiment was carried with the two water regimes and two nitrogen levels as described for the field trial (**Figure 4.1**). We aimed to investigate the influence of drought on NUE and root architectural features. The NUE-related traits were calculated according to the formula described in Foulkes & Murchie (2011). The traits evaluated are fully described in **Table 4.S2**.

#### 4.3.2. Above-ground biomass and root architecture features

The aboveground parts of the plants were harvested at postanthesis (BBCH70-85) [Biologische Bundesanstalt, Bundessortenamt und Chemische Industrie (Lancashire et al., 1991)] followed by the fresh biomass weight (FPBW) measurement. Thereafter, the samples were dried in oven for three days at 65 °C for the dry plant biomass weight (DPBW) estimation. The belowground part of the plant (root) was also harvested and gently washed. The fresh and dry biomass of the roots of two plants per pot was weighed as described for the aboveground part. The root angle was measured using a shovelomics scoreboard (Trachsel et al., 2011). The part within 5 cm from the crown down the root system of one plant was cut off and placed on the scoreboard to measure the right ( $\alpha$ ) and left ( $\beta$ ) angles (**Figure 4.1**). Thereafter, the root area was calculated using the following formula.

$$\text{Root area} = 180 - (\text{root angle } \alpha + \text{root angle } \beta) \quad (\text{Equation 4.1})$$

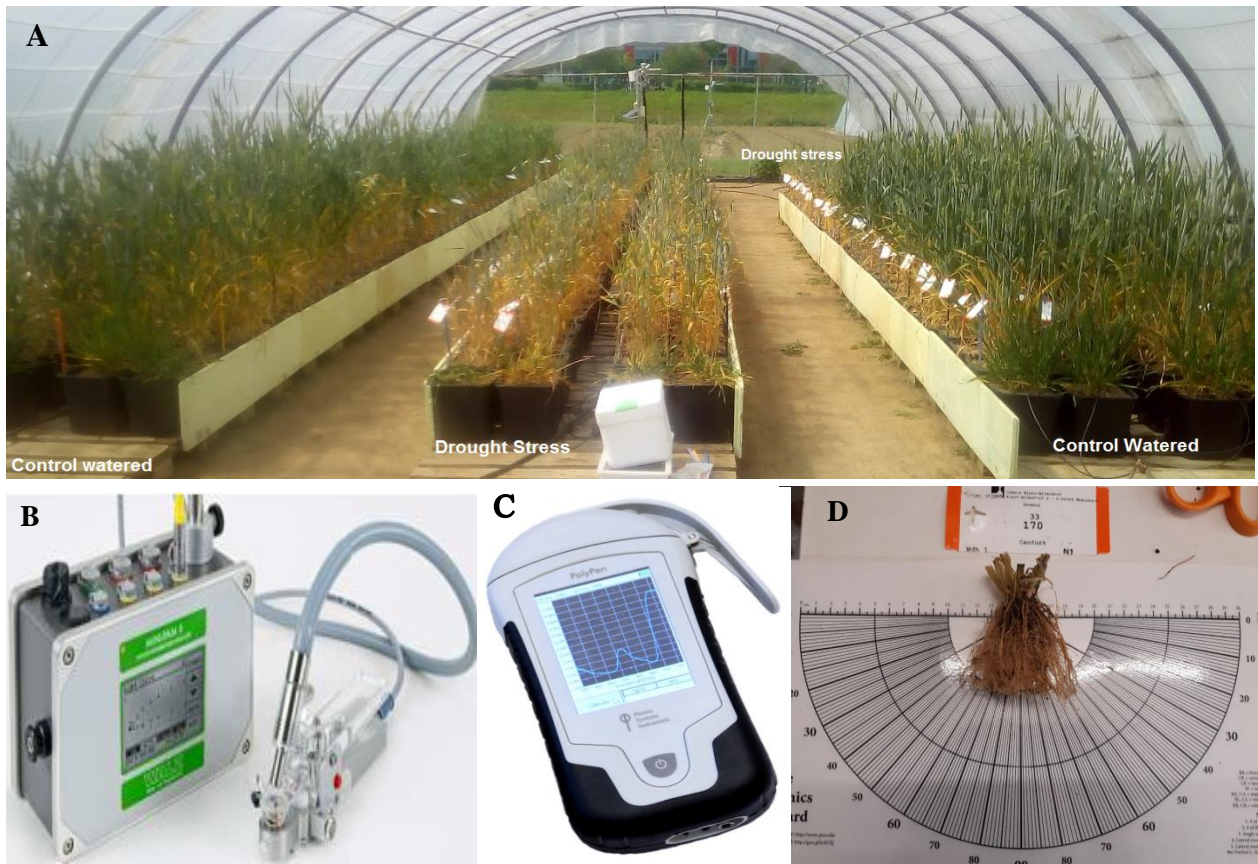


**FIGURE 4.1** | Overview of experimental setup and phenotyping tools. Picture of the “polytunnel” with watered plants and plants under drought stress (A), chlorophyll fluorometer MINI-PAM II (Walz) with leaf clip (B), Polypen Rp410 (C), Shovelomic template for root angle measurement (D)

#### 4.3.3. Estimation of plant nitrogen content

The N content in dry grinded shoot and grain was determined using the near-infrared spectrometer (NIRS) from Perten (Perten Instruments, Inc., USA). The measurement of the nitrogen content was performed in leaves harvested at anthesis growth stage (BBCH61-69) with the C/N analyzer (Euro EA 3000, EuroVector S.p.A., Italy). Before the C/N measurement, the leaves were dried in an oven at 65 °C for three days and ground. Thereafter, the samples were cut into pieces and added to 2ml microtubes with two small metal balls to finely grind the tissue in the MM400 vibrating mill from Retsch (Retsch AG, Arzberg, Germany) or in the Tissue Lyser II from Qiagen (Qiagen, CA, USA) for 10 to 15 minutes at 30 tours/s. The grounded tissue was dried again overnight at 65 °C in order to remove the residual moisture. For the measurement, two technical replicates of  $1.75 \pm 0.25$  mg were weighed for each sample with  $1.10 \pm 0.10$  mg from the acetanilide standard in tin cups.

#### 4.3.4. Identification of drought-tolerant or NUE-efficient genotypes

To identify high performing cultivars under drought and low N input conditions, the stress weighed performance (SWP) index (Saade et al., 2016) was calculated using the following formula:

$$SWP = P_s / \sqrt{P_k} \quad (\text{Equation 4.2})$$

where  $P_s$  is the mean value of the cultivar for a trait under stress (drought stress or reduced N fertilization), and  $P_k$  is the mean value of the cultivar for the trait under control conditions (rainfed or full N-fertilization). The mean values of the SWP of all trait was calculated and ranked. The cultivars with the higher indices were defined as the most stress-tolerant.

#### 4.3.5. Statistical analyses

The analysis of variance (ANOVA) for each trait of interest was performed including the factors water regimes, nitrogen levels, and genotypes in R software (R Core Team, 2020) and the best linear unbiased estimates (BLUEs) per genotypes within treatments was generated. For the field experiment of 2017, the ANOVA included the factors water regimes and genotypes as we had only one N level. The correlation between traits was evaluated with the BLUEs values using the “chart.correlation” function from the “*PerformanceAnalytics*” package implemented in R software (R Core Team, 2020). The Principal component analysis (PCA) of the SWP index of N use relevant traits was used to evaluate the relationship among cultivars *vis-à-vis* their nitrogen use efficiency under rainfed and drought stress conditions. The cultivars with contrasting NUE traits were determined according to their SWP values.

#### 4.3.6. Genome wide association study for marker-traits association (MTAs) identification

GWAS with 24,216 informative SNP markers with defined physical positions (Dadshani et al., 2021) was carried out for NUE-related traits under the different water regimes and N treatments to

determine genomic regions (QTL) associated with these traits. The SWP index for each trait under rainfed and drought-stress conditions was used as phenotypic data in the GWAS model to uncover the QTL interacting with the nitrogen treatment.

The GWAS was performed with the mixed linear model (MLM-P+K) as described in Koua et al. (unpublished) including the population structure (P-matrix) and kinship (K-matrix) (Yu et al., 2005; Zhang et al., 2010). To minimize false positives, only congruent SNPs in both TASSEL (Bradbury et al., 2007) and “*rrBLUP*” package in R (Endelman, 2011) were reported. The GWAS threshold of  $-\log(p) = 3$  which was determined based on the Q-Q plots and distribution of p-values was set to declare significant associations (Sukumaran et al., 2018). Both analyses followed the model:

$$Y = X\alpha + P\beta + K\mu + \varepsilon \quad (\text{Equation 4.3})$$

where Y is the vector phenotypic value of a genotype;  $\alpha$  and  $\beta$  are unknown vectors that contain fixed effects including genetic marker SNP and population structure; X is the fixed effect of the SNP; P is the fixed effect of the population structure given by the PCA matrix containing the first three components; K is the random effect of the relative relationship between the genotypes and  $\varepsilon$  is the error term which is assumed to be normally distributed with mean = 0 and variance  $\delta_e^2$ .

#### **4.3.7. Identification of candidate genes in the regions with identified QTL and Gene Ontology (GO) enrichment analysis**

The detected MTAs within a LD threshold of  $r^2 > 0.8$  were assigned to one LD block delimited by the position of two adjacent SNPs. Thereafter, the candidate genes within the LD block were downloaded from the Ensemble Plants database ([https://plants.ensembl.org/Triticum\\_aestivum/Info/Index/](https://plants.ensembl.org/Triticum_aestivum/Info/Index/)). For MTAs that were not in a LD block, the chromosome segment with a span of 1 megabase pairs (Mbp) upstream and downstream the position of the considered marker was examined for genes retrieval. The gene annotation was retrieved from the Uniprot database (<https://www.uniprot.org/uniprot/>). The GO enrichment analysis of the genes in the QTL regions was performed using the ShinyGO graphical gene-set enrichment tool (Ge et al., 2020), to classify them according to the underlying molecular pathways and functional categories. This GO tool implemented a multiple testing correction analysis to control the false discovery rate (FDR) with adjusted P-value  $\leq 0.05$  (Benjamini and Hochberg, 1995). The expressions levels of 24 candidate genes involved in stress response such as chemical, biotic and abiotic stimulus, and molecule transport, were analyzed using the transcriptome evaluated under multiple biological conditions, and available in the expVIP database (Borrill et al., 2016) and Expression Atlas (available at <https://www.ebi.ac.uk/gxa/home> ;Papatheodorou et al., 2020) databases. Some of the studies corresponded to the temporal transcriptome profiling of homeologous genes contributing to heat and drought acclimation in wheat (Liu et al., 2015) and the analysis of seedlings grown under PEG-simulated drought stress (Borrill et al., 2016).

## 4.4. Results

### 4.4.1. Phenotypic variation in response to drought stress and nitrogen deficiency

The analysis of variance (ANOVA) was carried out to assess the effect of genotype (G), water regimes (W), nitrogen (N) treatments, and their interactions on the phenotypic variation (**Table 4.1**). In 2017 and 2018 growing seasons, the variation in the SPAD, YII, GY, PBW, and most NUE-related traits differed significantly among genotypes (G;  $P < 0.001$ ) and treatments (W and N,  $P < 0.01$ ). The interactions W\*G and W\*N were significant for most of the studied traits, while N\*G and W\*N\*G interactions were not significant except for N harvest index (NHI) ( $P < 0.01$ ). The detailed descriptive statistics of these traits revealed that drought significantly decreased genotype performance, and the highest reductions were observed for GY and NUE-traits such as NUEGr, NupE and NAB (**Table 4.2**). When comparing the coefficient of variation (CV) of treatments combination rainfed plus medium N (RMN) vs drought plus medium N (DMN) and rainfed plus high N (RHN) vs drought plus high N (DHN), the highest CV among genotypes occurred under drought conditions, independently of the nitrogen levels. The Tukey HSD comparison showed that the treatment combination DHN and DMN are in the same group of lowest means (group a) for SPAD, YII, PBW and GY, while for NUE-related traits, both DHN and DMN were in different groups (**Figure 4.2**).

To analyze how the different traits were interrelated, we conducted a correlation analysis based on the BLUEs values (**Figure 4.3**). Significant and strong correlations were observed between GY and NUEBio, NUEGr, and PBW under all four treatments. As expected NHI index was positively correlated with grain N content and negatively correlated with N content in straw. Year of release was positively associated with SPAD, YII, and NUEGr but had negative correlation with NGr. The YII was positively correlated to NUE-related traits under drought conditions (low N and high), but had low associations with these traits under rainfed conditions.

**TABLE 4.1** ANOVA and descriptive statistics on agronomic, grain quality traits of 200 wheat genotypes (G) evaluated under two water regimes (T) in 2017 and 2018.

Growing seasons	2017			2018							
	Treatments	Water (W)	Genotype (G)	W*G	Water (W)	Nitrogen (N)	Genotype (G)	W*G	W*N	N*G	W*N*G
<b>Traits</b>											
<b>SPAD</b>		***	***	***	***	***	***	*	**	ns	ns
<b>YII</b>		***	ns	ns	***		***	***	ns	ns	ns
<b>PBW</b>		***	***	***	***	***	***	***	***	ns	ns
<b>GY</b>		***	***	***	***	*	***	***	ns	ns	ns
<b>SDW</b>		***	***	***	***	***	***	*	***	ns	ns
<b>NUEBio</b>		***	***	***	***	***	***	***	***	ns	ns
<b>NUEGr</b>		***	***	***	***	***	***	***	***	ns	ns
<b>NUpE</b>		***	ns	ns	***	***	***	ns	*	ns	ns
<b>NUtE</b>		*	ns	ns	ns	***	***	ns	***	ns	ns
<b>NAB</b>		***	ns	ns	***	***	***	ns	***	ns	ns
<b>NLf</b>		NA	NA	NA	***	***	***	ns	ns	ns	ns
<b>NSt</b>		***	***		***	*	***	*	***	ns	ns
<b>NGr</b>		**	***	*	***	***	***	***	***	ns	ns
<b>NRE</b>		NA	NA	NA		***	*	*	***	ns	ns
<b>NHI</b>		***	***		***		***	*	***	*	ns

PBW, Plant biomass weight; GY, Grain yield, SDW, Shoot dry weight; SWaP, Shoot water potential at anthesis; SPAD, Chlorophyll Content; YII, Effective photochemical quantum yield of PS II; NUEBio, Nitrogen use efficiency for Biomass production; NUEGr, Nitrogen use efficiency for Grain Yield production; NAB, Nitrogen in aboveground plant biomass; NUpE, Nitrogen uptake efficiency; NUtE, Nitrogen utilization efficiency; NGr, N content in grain; NSt, N content in straw; NLf, N content in leaves at anthesis; NRE, Nitrogen remobilization efficiency; NHI, Nitrogen harvest index. The significance level \*P<0.05, \*\*P<0.01, \*\*\*P<0.001; ns is not significant at 0.05. NA means not available.

**TABLE 4.2** | Descriptive statistics of evaluated traits in the field experiment from 2018 under drought and N stress.

STATS	Treatment	SPAD*	YII	PBW*	GY	SDW	NUEBio	NUEGr	NUpE	NUtE	NAB	NLf	NSt	NGr	NRE	NHI
<b>Mean</b>	RHN	54.73 <sup>c</sup>	0.62 <sup>b</sup>	573.38 <sup>c</sup>	272.87 <sup>b</sup>	302.12 <sup>c</sup>	120.66 <sup>b</sup>	57.42 <sup>c</sup>	1.84 <sup>c</sup>	35.55 <sup>a</sup>	405.00 <sup>c</sup>	4.18 <sup>d</sup>	0.53 <sup>d</sup>	2.51 <sup>d</sup>	0.87 <sup>a</sup>	0.83 <sup>a</sup>
	DHN	52.25 <sup>a</sup>	0.58 <sup>a</sup>	241.10 <sup>a</sup>	107.69 <sup>a</sup>	134.23 <sup>a</sup>	50.60 <sup>a</sup>	22.6 <sup>a</sup>	0.66 <sup>a</sup>	38.18 <sup>c</sup>	144.74 <sup>a</sup>	3.56 <sup>b</sup>	0.40 <sup>a</sup>	2.20 <sup>a</sup>	0.88 <sup>b</sup>	0.85 <sup>c</sup>
	Reduction (%)	4.53	6.45	57.95	60.53	55.57	58.06	60.64	64.26	-7.39	64.26	14.87	24.53	12.28	-1.48	-2.41
	RMN	53.37 <sup>b</sup>	0.62 <sup>b</sup>	545.52 <sup>b</sup>	264.73 <sup>b</sup>	280.18 <sup>b</sup>	262.39 <sup>c</sup>	127.33 <sup>d</sup>	2.19 <sup>d</sup>	39.24 <sup>d</sup>	358.86 <sup>b</sup>	3.83 <sup>c</sup>	0.46 <sup>c</sup>	2.34 <sup>c</sup>	0.88 <sup>b</sup>	0.84 <sup>b</sup>
	DMN	51.82 <sup>a</sup>	0.59 <sup>a</sup>	241.30 <sup>a</sup>	105.36 <sup>a</sup>	137.00 <sup>a</sup>	116 <sup>b</sup>	50.68 <sup>b</sup>	0.91 <sup>b</sup>	36.51 <sup>b</sup>	149.72 <sup>a</sup>	3.26 <sup>a</sup>	0.42 <sup>b</sup>	2.25 <sup>b</sup>	0.87 <sup>a</sup>	0.84 <sup>b</sup>
	Reduction (%)	2.89	4.84	55.77	60.20	51.10	55.79	60.20	58.28	6.96	58.28	14.80	8.70	3.70	1.31	0.00
<b>CV (%)</b>	RHN	4.9	3.93	15	16	25.71	15	16	24.76	12.83	24.76	15.50	12.47	5.47	3.05	2.14
	DHN	7	15.9	19	22	24.08	19	22	28.52	11.36	28.52	12.19	12.71	7.6	2.62	1.92
	RMN	4.1	4.12	14	15	21.33	14	15	21.78	12.19	21.78	16.20	12.97	5.89	2.64	2.43
	DMN	5.5	15.59	20	25	22.73	20	25	24.85	12.89	24.85	13.85	9.81	8	2.84	1.68

\* The traits names are given in caption of **Table 4.1**; RHN, rainfed high N; DHN, drought high N; RMN, rainfed medium N; DMN drought medium N supply

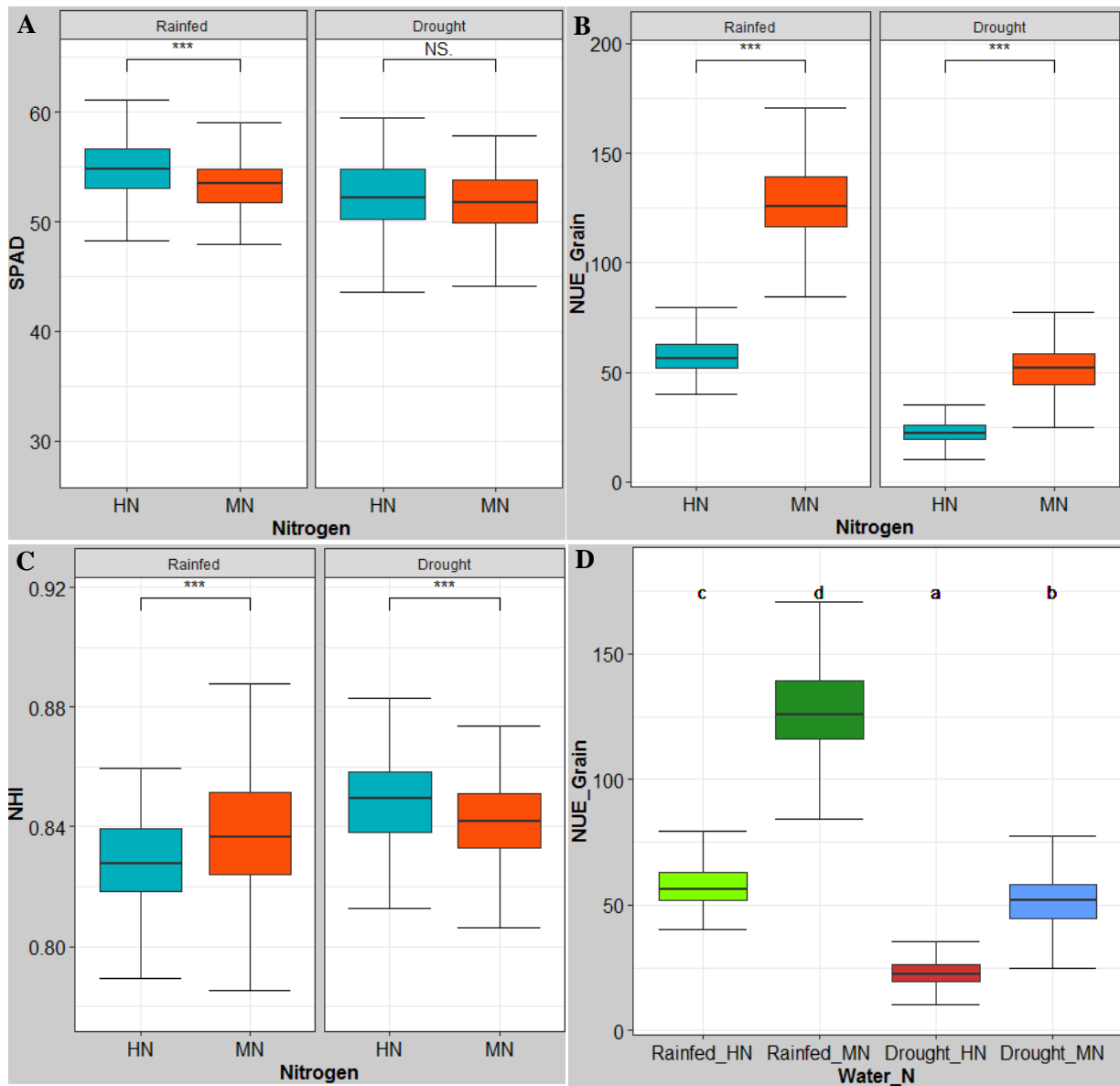


**FIGURE 4.2** | Comparison of means between both N treatments under rainfed and drought for (A) SPAD; (B) NUE for grain production; (C) nitrogen harvested index. (D) Means comparison of the four levels of combined treatments for NUE for grain production. HN and MN mean high N and medium N supply, respectively.

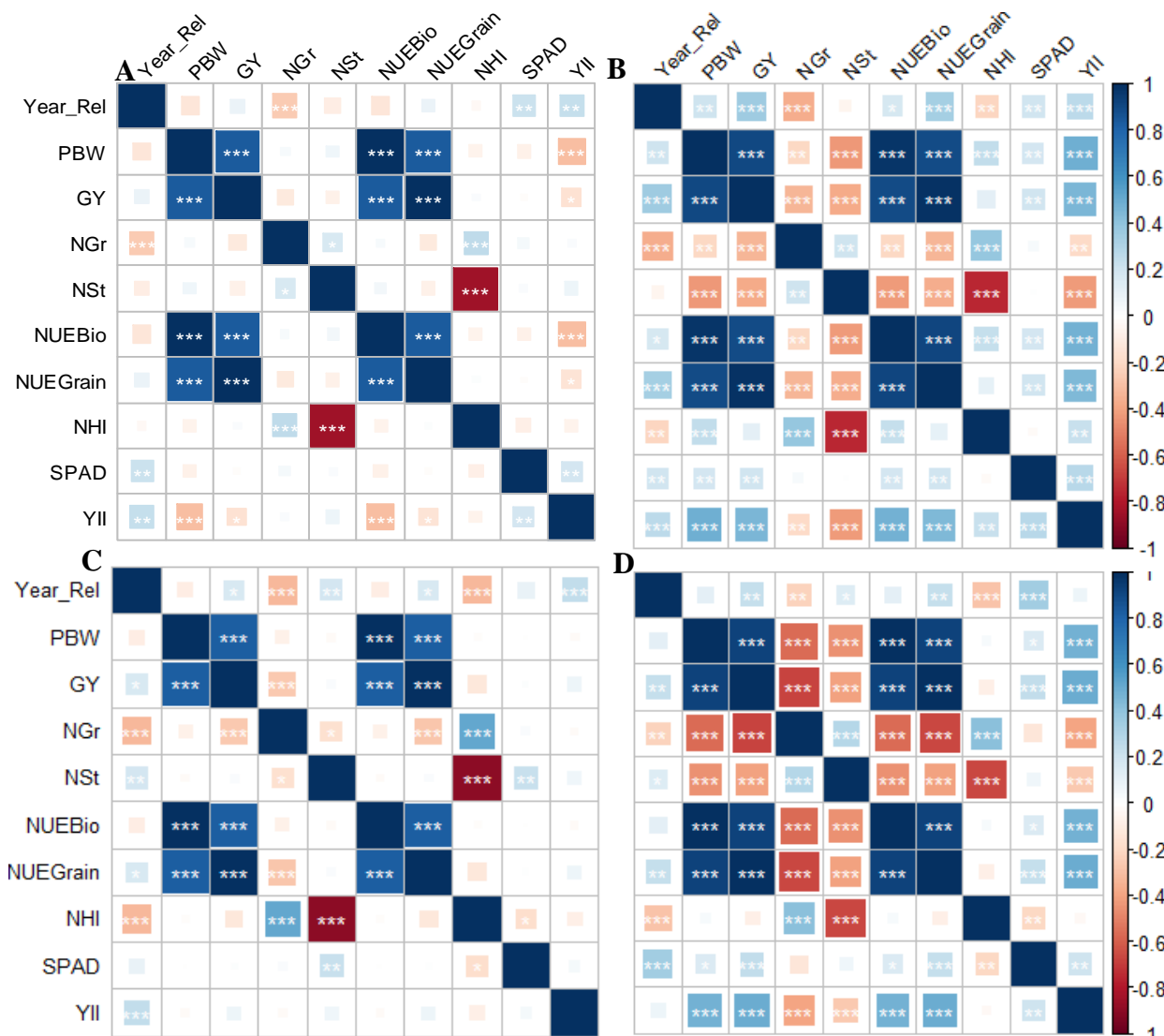


**FIGURE 4.3** | Pearson correlation matrix for phenotypic traits of 200 different wheat genotypes grown under 4 treatments. **(A)** Rainfed with high nitrogen; **(B)** drought with high nitrogen; **(C)** rainfed with low nitrogen; **(D)** drought with low nitrogen. Asterisk indicates statistically significant correlation at \* $p < 0.05$ ; \*\*  $p < 0.01$ ;  $n = 200$ .

#### 4.4.2. Variation in plant biomass and root architectural traits under drought and nitrogen deficiency

The ANOVA from the pot experiment indicated that the water regime and genotype had a significant effect on all shoot and root traits, and also on NDVI. For the other photosynthesis-related traits, only G had effect on YII variation while W influenced NDVI and SPAD (**Table 4.3**). The W\*G interaction affected all shoot, root and photosynthesis-related traits, except root area and YII. N application had significant effect on YII, SPAD and shoot traits. Interactions W\*N, N\*G, and W\*N\*G were significant for NLF. Drought stress has significantly reduced plant shoot and root traits under high N and low N treatments. However, reduction due to N deprivation under each water regime was not significant (**Table 4.4, Figure 4.4**). The shoot and root biomass were significantly higher under control than under drought stress treatment. The ratio of the root biomass weight over the total biomass was significantly higher under water deficiency (55.87%) than under control conditions (37.25%) (**Figure 4.4**), suggesting the ratio root/shoot was higher under drought than watered conditions. N treatment did not affect the root area (RA), as the variants high N and medium N were classified the same Tukey mean group, both under control and drought treatments. The Tukey HSD comparison showed that with high N supply, control and drought treatments were in two different groups, which indicate an effect of drought on RA (**Table 4.4**).

The highest NLF content (3.42%) was observed under drought with high N, while the lowest value (2.07%) was under rainfed with low N. When both nitrogen fertilization treatments are compared. Also, the treatments with high N application presented the highest N content in leaves (**Table 4.4**).

Pearson correlations were calculated to assess the relationship among the evaluated traits of wheat genotypes grown under rainfed and drought stress conditions with a high nitrogen level (**Figure 4.5**). The strongest correlations were observed among different shoot traits, or among different root traits. The photosynthesis-related traits were significantly and positively correlated between each other under both water regimes. Likewise, the NDVI trait showed higher associations with shoot and root traits under drought than under control conditions (**Figure 4.5**).

**TABLE 4.3** | Anova table for the root and shoot traits of the pot experiment 2019.

Traits	Water (W)	Nitrogen (N)	Genotypes	W*N	W*G	N*G	W*N*G
<i>Shoot traits</i>							
FSW	***	*	***	**	***	ns	ns
SDW	***	ns	***	ns	***	ns	ns
SWaP	***	***	***	***	***		
NLf	***	***	***	***	***	***	***
<i>Root traits</i>							
FRW	***	ns	***	Ns	*	ns	ns
RDW	***	NA	***	NA	***	NA	NA
RWaP	***	NA	***	NA	*	NA	NA
Root area (RA)	***	ns	***	Ns	ns	ns	ns
<i>Photosynthesis related traits at anthesis growth stage</i>							
SPAD	ns	***	**	Ns	*	ns	ns
YII	***	*	ns	**	ns	ns	ns
NDVI	***	NA	***	NA	***	NA	NA

FSW, fresh shoot weight; SDW, shoot dry weight; SWaP, shoot water potential; NLf, N content in leaf; FRW, Fresh root weight; DRW, Root dry weight; RWaP, Root water potential; RA, root area; SPAD, Chlorophyll Content; YII, Effective photochemical quantum yield of PS II; NDVI, Normalized difference vegetation index The significance level \*P<0.05, \*\*P<0.01, \*\*\*P<0.001, ns and NA mean non-significant and not available, respectively.

**TABLE 4.4** | Descriptive statistics for the root and shoot traits of the pot experiment 2019.

Stats	Env	SPAD	YII	NDVI	FSW	SDW	SWaP	NLf	RA	FRW	RDW	RWaP
Mean	CHN	49.36 <sup>bc*</sup>	0.38 <sup>c</sup>	0.71 <sup>b</sup>	194.84 <sup>c</sup>	78.30 <sup>b</sup>	116.20 <sup>c</sup>	2.90 <sup>b</sup>	82.24 <sup>b</sup>	114.30 <sup>b</sup>	23.71 <sup>b</sup>	93.20 <sup>b</sup>
	DHN	50.53 <sup>c</sup>	0.28 <sup>b</sup>	0.57 <sup>a</sup>	49.68 <sup>a</sup>	25.84 <sup>a</sup>	23.85 <sup>a</sup>	3.42 <sup>d</sup>	70.74 <sup>a</sup>	65.25 <sup>a</sup>	13.75 <sup>a</sup>	50.24 <sup>a</sup>
	Reduction (%)	-2.37	24.90	19.67	74.50	67.00	79.48	-17.94	13.98	42.91	42.00	46.09
	CMN	45.61 <sup>a</sup>	0.36 <sup>c</sup>	NA	184.13 <sup>b</sup>	77.21 <sup>b</sup>	106.92 <sup>b</sup>	2.07 <sup>a</sup>	83.33 <sup>b</sup>	NA	NA	NA
	DMN	46.46 <sup>ab</sup>	0.19 <sup>a</sup>	NA	51.12 <sup>a</sup>	26.56 <sup>a</sup>	24.56 <sup>a</sup>	3.18 <sup>c</sup>	68.81 <sup>a</sup>	NA	NA	NA
	Reduction (%)	-1.86	48.37	NA	72.24	65.60	77.03	-53.70	17.42	NA	NA	NA
CV (%)	CHN	8.77	22.16	5.01	13.00	12.12	14.86	10.52	14.55	23.91	29.24	23.20
	DHN	21.91	28.58	24.90	11.96	11.50	15.28	19.89	18.29	20.69	20.81	21.78
	CMN	11.36	23.78	NA	13.03	12.22	14.90	14.41	15.41	NA	NA	NA
	DMN	26.60	43.66	NA	13.67	11.03	19.16	18.44	14.30	NA	NA	NA

\* Turkey groups of means comparison between treatments for each trait. Group a is the lowest mean value while group d is the highest mean. CHN, control high N; drought high N; CMN, control medium N, DMN, drought medium N. Traits names are on given in Table 3.

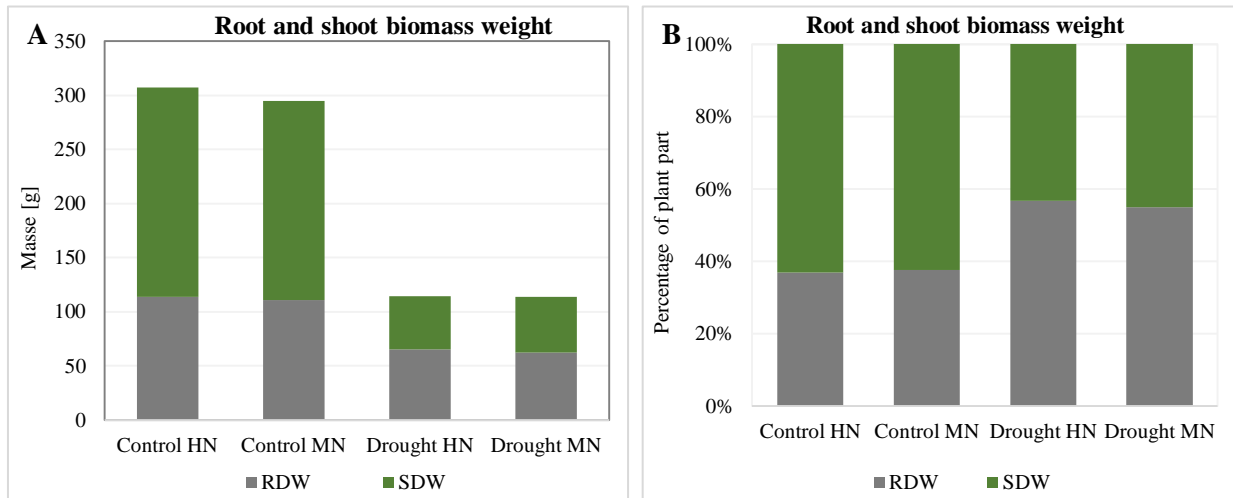


**FIGURE 4.4** | Bar graphs of the root and shoot mass. (A) mean values of the root biomass, (B) percentage of the shoot and root biomass per treatment. RDW, Root dry weight; SDW, shoot dry weight; HN, high N supply; MN, medium N supply.

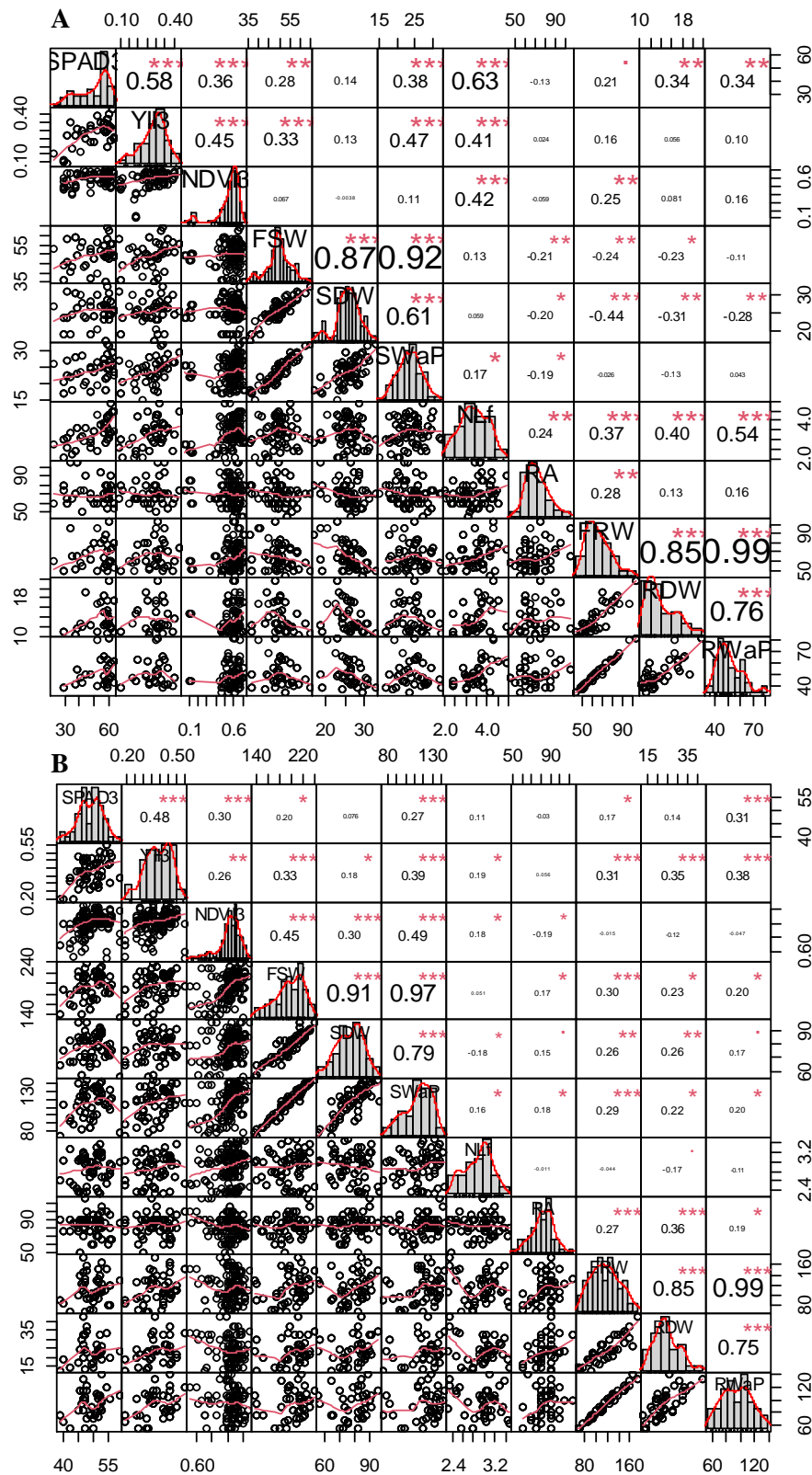


**FIGURE 4.5** | Phenotypic correlations of 30 different wheat genotypes. (A) under control watered with high nitrogen; (B) drought with high nitrogen. Asterisk indicates statistically significant correlation at \* $p < 0.05$ ; \*\*  $p < 0.01$ ;  $n = 60$ .

#### 4.4.3. Genome wide association study for drought and nitrogen deficiency tolerance related traits in wheat

The GWAS performed on 15 phenotypic traits during the growing seasons of 2017 and 2018 under rainfed + high nitrogen (RHN), drought + high nitrogen (DHN), rainfed + medium nitrogen (RMN), and drought + medium nitrogen (DMN) conditions identified 442 MTAs. These associations involved 372 SNP markers explaining from 5.10 to 14.99% of the phenotypic variation ( $R^2$ ) in traits (**Table 4.Sx11**). A total of 73, 179, 60 and 130 MTAs were detected in both growing seasons for DMN, DHN, RMN and RHN, respectively. The MTAs detected for traits of interest measured under drought or medium N were induced by stress conditions as they were not detected under control environments (**Table 4.Sx11**). A total of 27 QTL regions harbored SNPs with pleiotropic effects on the evaluated traits (**Table 4.Sx12**). For instance, the QTL region spanning from 470.936 to 489.207 Mbp on 1B contained nine pleiotropic SNPs for NAB and NUpE. The genotypes with the allele TTTTCC from the haplotype (*Hap1B*) had higher NUpE under drought stress than those with the variant GGCCAA (**Figure 4.6A,B**). This haplotype included the marker *Tdurum\_contig59449\_249* and two adjacent pleiotropic SNPs. On the other hand, the marker *AX-111561744*, located on chromosome 2D (23.416 Mbp), displayed pleiotropic effects on six traits under drought and on SPAD under control conditions (**Table 4.S3**; **Table 4.Sx13**). Some genomic regions, such as the interval in the vicinity of *AX-108817594* (575.723 Mbp) on 1B, were associated with NAB and NUpE under DMN while under RMN they influenced PBW, NUEBio and SDW variation.

GWAS was performed on SWP for NUE-related traits to identify significant SNP markers that were interacting with the N supply level. From the 639 MTAs that interacted with nitrogen levels, 321 (266 SNPs) were exclusively detected under drought and 318 (239 SNPs) under rainfed conditions. Therefore, these MTAs were water regime-specific. The  $R^2$  explained by these markers ranged from 5.37% to 18.36%. The highest number of N level-interacting MTAs were found on chromosome 5A (49 MTAs) and 1A (94 MTAs) under drought and rainfed conditions, respectively (**Figure 4.S1**). The markers *Tdurum\_contig50355\_269* and *Tdurum\_contig29280\_216* located in the same QTL region (1A from 33.021 to 33.376 Mbp) were interacting with N treatment in four traits under rainfed (i.e. NAB, NUE, NUpE, and GY) (**Table 4.S3**; **Table 4.Sx14**). The chromosomal region on 5A, comprising the SNPs *w SNP\_Ex\_c23795\_33033150* and *w SNP\_Ex\_c23795\_33033010*, interacted with the N supply level for NUEGr and GY under drought conditions. The genotypes containing the minor allele (GGCC) from the haplotype produced by these two SNPs (i.e. *Hap5A*), had significantly increased NUEGr under low N conditions (**Figure 4.6C,D**). The average NUEGr value estimated for these genotypes was 36.86, compared to the mean calculated for the genotypes with the major allele AATT (32.48), representing an increase of 13,49% (**Figure 4.6D**). However, these alleles of the haplotype *Hap5A* did not show significant difference for NUpE and NUEGr under both water regimes plus high N supply (**Figure 4.6C**; **Figure 4.S2A,B**). These results indicate that low N supply induced

the activity of this genomic region under drought conditions. The analysis of the year of release from the cultivars revealed that the genotypes carrying the haplotype GGCC are more recent than the ones with AATT haplotype (**Figure 4.S2C,D**).

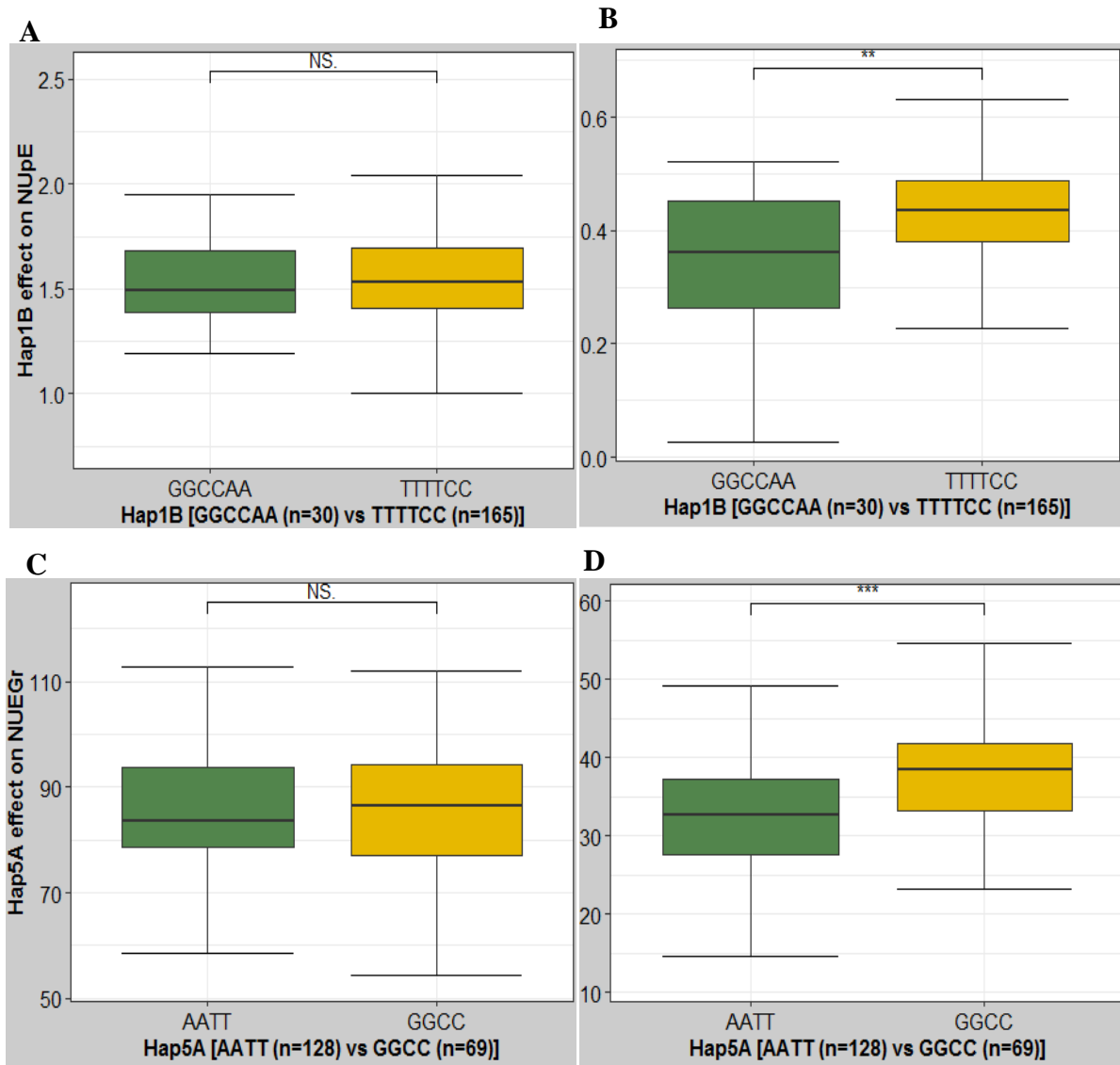


**FIGURE 4.6** | Allelic effects of the haplotype *Hap1B* and *Hap5A*. (A) *Hap1B* effect on NUpE under rainfed with high nitrogen and (B) drought with high nitrogen; (C) *Hap5A* effect on NUEGr under rainfed with medium nitrogen and (D) drought with medium nitrogen.

#### 4.4.4. Candidate genes in the vicinity of pleiotropic QTL regions

We retrieved the candidate genes in the vicinity of MTAs which had pleiotropic effects on the evaluated traits. A total of 2,653 genes were present in the 27 QTL regions harboring significant pleiotropic SNPs detected in the GWAS under each treatment (**Table 4.Sxl5**). The genes ontology (GO) enrichment analysis performed in ShinyGO (P-value FDR cutoff =0.05) classified 1469 genes in diverse categories. Among them, 19.67% (289 genes) were involved in response to stress and abiotic, endogenous, exogenous and chemical stimuli, followed by 18.45% (271 genes) that were involved in cellular component organization and biogenesis. Some genes were classified in the detoxification category (11 genes) (**Figure 4.8; Table 4.Sxl6**). Regarding the biological process, pathways related to regulation and transcription contained the highest number of genes with 1817 entries. A total of 103 genes (Enrichment FDR = 3.1E-03) were involved in carbohydrate metabolism process (**Figure 4.S3A; Table 4.Sxl7**). In terms of the molecular function sub-ontology, 17.15% (218 genes) of retrieved genes were involved in transporter and transmembrane transporter activity and 24 % in transferase activity (**Figure 4.S3B; Table 4.Sxl8**). The genomic intervals of 21 MTAs of interest, including five markers with pleiotropic effects, six induced by medium N supply, and ten that showed an interaction with nitrogen level in soil, were further analyzed (**Table 4.S3**). For instance, the region in the vicinity of *Tdurum\_contig59449\_249* on chromosome 1B harbored 96 genes, which corresponded to Myb transcription factor, aminotransferase, cytochrome P450, F-box and cold shock protein families (**Table 4.S3; Table 4.Sxl9**). The QTL region of *AX-158577204* located at 714.294 Mbp on chromosome 3A, marker with pleiotropic effect on NAB, NUEGr, NUpE and GY harbored genes such as *TraesCS3A02G484700* encoding for amino acid transporters (AATs) (**Table 4.S3, Table 4.Sxl4**).

The *in silico* analysis of 10 QTL regions that interacted with nitrogen supply under both water regimes revealed they co-located with 221 genes (**Table 4.S3; Table 4.Sxl9**). Among those 10 QTL, the one including the haplotype block *Hap5A* harbored transcription factors, kinase family and endoribonuclease dicer-like proteins.

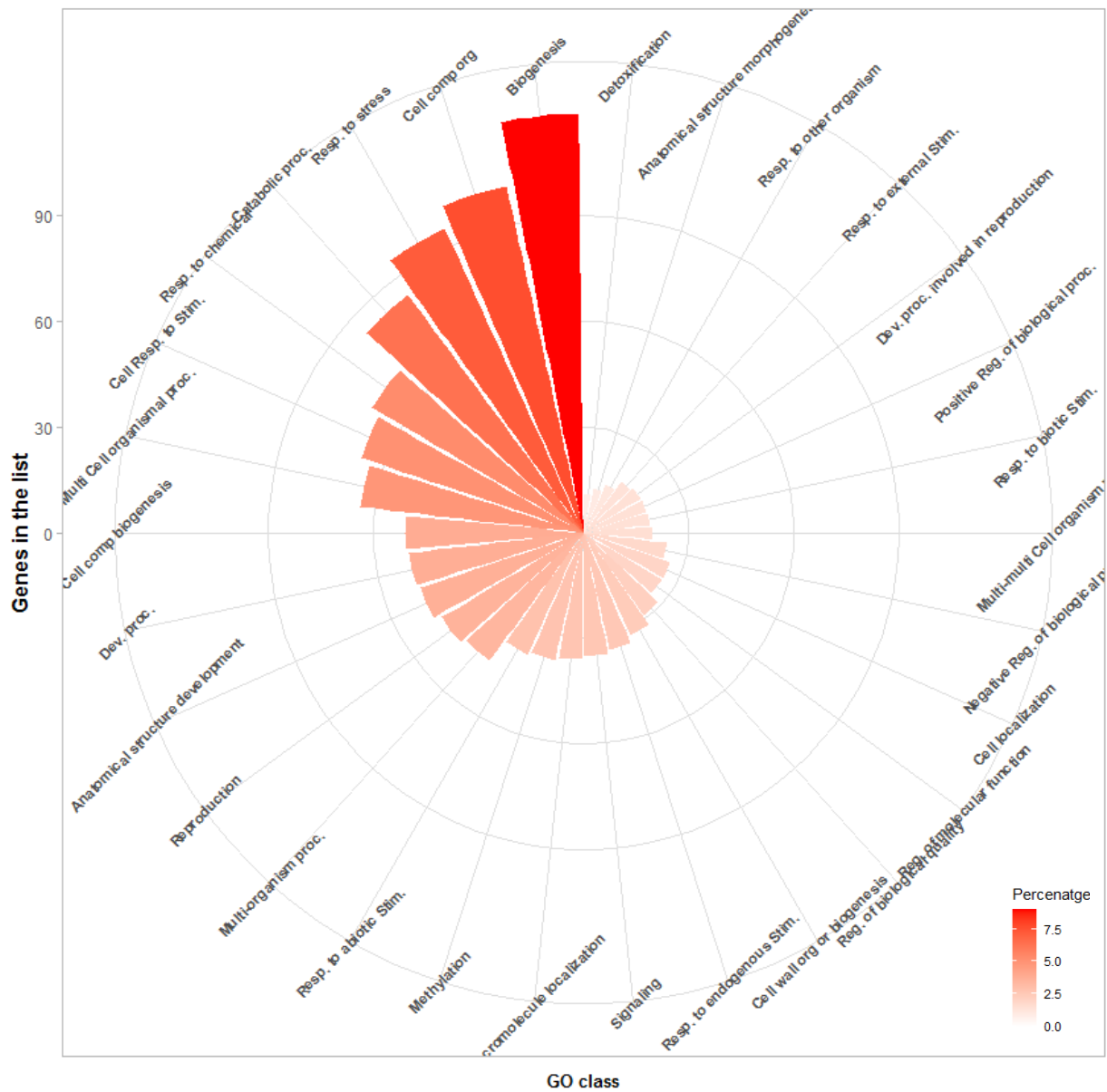


**FIGURE 4.7** | Gene Ontology classification group of 2653 genes retrieved from 27 QTL regions. The genes are grouped by functional categories defined by high-level GO terms.

#### 4.4.5. Transcript abundance pattern of candidate genes

The transcript abundance associated to 24 candidate genes in the category of response to stress and chemical, abiotic, endogenous and external stimuli was investigated in two databases (in expVIP and Expression Atlas). The results (**Figure 4.9**) showed that the gene *TraesCS1B02G273000*, which co-segregated with the haplotype *Hap1B*, was abundant under all biological conditions. This gene coding a cold shock protein, intervenes in the regulation of transcription and has a zinc-binding role. Another one, *TraesCS7A02G429600* in the neighboring of *Excalibur\_c20307\_654* on 7A is an Adaptin ear-binding coat-associated protein is upregulated under septoria, magnaporthe diseases conditions (**Figure 4.9**). The gene *TraesCS1B02G352400*, located within the interval of *AX-108817594* on chromosome 1B, showed the highest transcript abundance under drought+heat conditions. This gene codes for an ATP-dependent chaperone ClpB which intervene in protein metabolic process. In addition, the neighboring region of the previous MTAs is enriched with genes encoding for peroxidase, cytochrome P450, WRKY transcription factor, senescence regulator, ABC (ATP-binding) transporter, sugar transporter SWEET and magnesium transporter protein types. According to the Expression Atlas database, *TraesCS1B02G273000* obtained the highest transcript abundance at two nodes visible stage and inflorescence stage, in most plant tissues and developmental stage. While *TraesCS7A02G429600* was higher in the whole plant fruit formation stage 30-50%, and in leaf (**Figure 4.S4**).

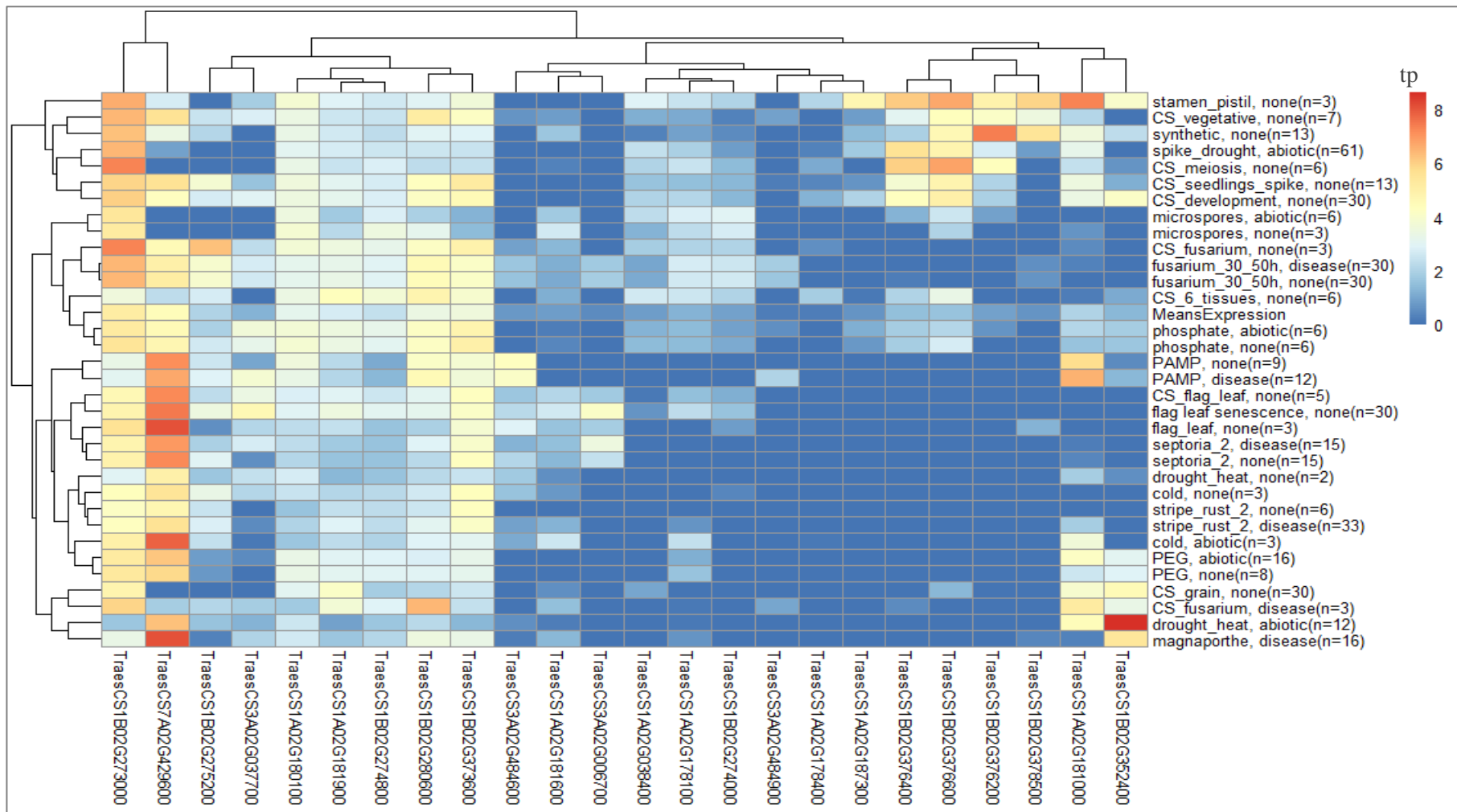


**FIGURE 4.8** | Transcript abundance of 24 candidate genes under different biological conditions deposited in the expVIP database (Borrill et al., 2016).

## 4.5. Discussion

This study evaluated the cumulative effect of drought and nitrogen stress on agronomic traits, and the effect of drought on nitrogen use efficiency related traits. We aimed to link the observed phenotypic variation with genetic markers to uncover promising candidate genes controlling NUE, particularly under drought conditions. The key findings of this research are discussed below.

### 4.5.1. Drought and nitrogen treatments effect on evaluated under field and glasshouse

The existence of high genetic variation in our wheat panel is supported by the significant genotypic effect on the evaluated traits in response to water regime and nitrogen application, and the high values of coefficient of variation calculated under drought. High genetic variation in a diversity panel is required for dissecting the genetic architecture of complex traits through GWAS (Hall et al., 2010; Rasheed and Xia, 2019). Compared to the nitrogen deficiency condition, drought stress resulted in a higher reduction of plant's performance for all measured traits. Although, an effect of N supply on the traits was detected under rainfed conditions, no significant differences were observed between both nitrogen levels under drought stress, for most traits. These results corroborate that plant nitrogen uptake and use strongly depend on the soil moisture. The dynamic of nutrients in soil and plant water uptake are limited under low soil moisture, which result in low nutrient uptake independently of nutrient availability (da Silva et al., 2011; Kagawa, 2013). The values of the NUE-relevant traits (i.e. NUpE, NUtE; NRE, NUEBio, and NUE) were lower with high nitrogen fertilization, as described in various articles, reporting low NUE traits, as the result of low values of the numerator, and high denominator (available N or applied N) in NUE calculation (Voss-Fels et al., 2019). NUpE, NUEGr and NUEBio values decrease with increasing nitrogen fertilization, as these indices are calculated as a ratio of harvested biomass or grain to the available nitrogen. Despite considerable available N in the soil under high nitrogen supply, the N uptake could be limited by drought; while under rainfed the nitrogen uptake is not remobilized and used for grain production. In fact, higher NUE is a product of higher N uptake and utilization, particularly under drought conditions.

Similar to the field conditions, in the glasshouse, plants exposed to the cumulative effects of drought and medium nitrogen supply showed lower performance than plants under watered conditions plus high nitrogen. Under drought conditions, N content in leaves was higher with low N input than with high N fertilization. This outcome is explained by the dilution effect, which refers to increase of the mineral concentration due to low water content (Guttieri et al., 2015).

Drought stress has resulted in the reduction of the root biomass and root area. As the drying rate is more pronounced in superficial than in the deeper soil layers, plants tend to develop a deeper root system to obtain more water under drought conditions (Alsina et al., 2010; Ding et al., 2018). The proportion of

the root mass in the total biomass was significantly higher under DHN than under CHN conditions, indicating the importance of favoring root over shoot development under drought to increase drought tolerance. However, nitrogen application levels did not affect root traits. The examination of roots from plants growing in pots may have prevented their full development in depth and diameter. This and other difficulties such as extracting the entire root system as it is in field to evaluate its features been reported (Garnett et al., 2009). The correlations between YII and root system traits were significant and stronger under drought stress than under control conditions. This result highlight the key role played by root in the photosynthesis efficiency, especially under drought conditions.

#### **4.5.2. Genetic architecture controlling NUE and candidate genes for drought-nitrogen deficiency tolerance**

The GWAS threshold was set at P-value <0.001 for accepting significant MTAs (Sukumaran et al., 2018), and identifying the MTAs exerting pleiotropic effect on evaluated traits. Significant and strong correlations among some traits at phenotypic level, were confirmed with the GWAS analysis by the detection of common MTAs regulating those traits. For instance, strong relationships were found at both levels between GY & NUEGr, NUEBio & PBW, and NAB & NUPE. Besides, cultivars year of release was positively associated with NUEGr, SPAD and YII. That findings were approved at genetic level. For example, the haplotype form GGCC of *Hap5A*, which has been selected through breeding at the detriment of the AATT form (**Figure 4.S2**), increased significantly the NUEGr under drought conditions with medium N (**Figure 4.6D**). Selection by breeding of increment favorable alleles for a trait explain the higher performance of newer released cultivars over the older ones (Voss-Fels et al., 2019).

Several genes adjacent to the identified MTAs with pleiotropic effects, play a role in transport or response to stress. For, instance, a sugar transporter from the SWEET family, which co-located with the marker *Tdurum\_contig59449\_249* on chromosome 1B, has been reported to play crucial roles in plant development and stress responses in wheat (Gautam et al., 2019). Under severe drought stress, wheat genotypes accumulate more soluble sugars that become an essential replacement for water (Farshadfar et al., 2008; Hussain et al., 2018; Sallam et al., 2019). This phenomenon of sugars accumulation is known as osmotic adjustment, allows cells to manage their dehydration and membrane structural integrity to give tolerance against drought and cellular dehydration (Loutfy et al., 2012). In previous report on expression analysis involving both *insilico* and *in planta*, the TaSWEET, a subgroup of SWEET genes, was upregulated in water/heat sensitive and leaf rust resistant genotypes (Gautam et al., 2019; Han et al., 2015). Besides, the number and effectiveness of the transporters play a major role in the uptake and translocation of nitrogen (Xu et al., 2012). An ABC transporter encoded by the *TraesCS1A02G051800* gene, is located on chromosome 1A and shares homology sequence with the marker

*Tdurum\_contig29280\_216*, that was interacting with N treatment under rainfed conditions. This marker could be used to develop NU efficient genotypes under rainfed conditions.

The genomic region in the vicinity of *AX-158577204* located at 714.294 Mbp on chromosome 3A, pleiotropic marker for NAB, NUEGr, NUpE and GY harbored genes such as *TraesCS3A02G484700* encoding for amino acid transporters (AATs) (**Table 4.S3, Table 4.SxI9**). AATs are relevant in the uptake of asparagine synthetase (AS) from the soil, in their transport over great distances, their remobilization from the vegetative tissue, and their accumulation in the grain. Much of the nitrogen in the grain comes from the remobilization of AS from the vegetative tissues. Almost 70% of the remobilized nitrogen is translocated into the grain (Wan et al., 2017). The markers *w SNP\_Ex\_c23795\_33033150* and *w SNP\_Ex\_c23795\_33033010* could be associated to N-efficiency and drought stress tolerance, as they are within a region of genes encoding for protein kinases and transcriptions factors (MADS-box and basic helix-loop-helix). Protein kinases belong to a large superfamily that play an important role in plant development, plant growth and stress tolerance. These include biological processes such as mitosis, cell wall biosynthesis, regulation of the time of flowering, photosynthesis and the hormone response (Wei and Li, 2019).

The expression atlas analyses highlighted a gene coding a cold shock protein (*TraesCS1B02G273000*) in the region of the haplotype *Hap1B*, with a higher transcript abundance under most biological conditions, including drought, heat and pathogen infection. This gene could play important role in response to external and endogenous stress. Overexpression of exogenous cold shock proteins (i.e. SeCspA and SeCspB) in transgenic arabidopsis lines increased germination and survival rates, and increased primary root length compared to control plants under drought and salt stress (Yu et al., 2017; Kim et al., 2013), and in maize (Castiglioni et al., 2008). The analysis of several stress-related traits in SeCspA and SeCspB transgenic wheat lines evidenced stress tolerance characteristics such as lower malondialdehyde (MDA) content, lower water loss rates, lower relative Na<sup>+</sup> content, higher chlorophyll and proline content than the control wheat plants grown under drought and salt stresses (Yu et al., 2017).

#### **4.6. Conclusion**

Improving NUE is a foremost target of plant breeding owing to the ecological consequences of excessive N application and the economic advantages of reducing N fertilization. This improvement can be achieved by combining genetic selection with crops management practices. This study has shown that wheat yield loss, and reduction in shoot and root traits due to drought stress were significantly higher than nitrogen deprivation, because drought affect plants water uptake and nutrient uptake, which depends on the availability of water in soil. Also, we have found that cultivars genetic make-up also plays important role in NUE under low N, and high N when plants are exposed to drought. We demonstrated through GWAS that genetic factors on chromosome 1B and 5A have contributed to higher NUE under drought conditions. These regions harbor candidate genes such as amino acid transporters, cold shock proteins and transcription factors that are relevant for drought tolerance and NUE. Upon validation, these genes can be used to develop drought-tolerant and N use-efficient genotypes. Similarly, particular attention should be paid to the root system characteristics, as this organ is the most important contributing to N uptake and drought stress tolerance.

## **Chapter 5**

### **Fungicide application affects nitrogen utilization efficiency, grain yield, and quality of winter wheat**

**Ahossi Patrice Koua<sup>1\*</sup>, Mirza Majid Baig<sup>1\*</sup>, Benedict Chijioke Oyiga<sup>1</sup>, Jens Léon<sup>1,2</sup> & Agim Ballvora<sup>1</sup>✉**

1 INRES Pflanzenzüchtung, Rheinische Friedrich-Wilhelms-University, Bonn, Germany

2 Field Lab Campus Klein-Altendorf, University of Bonn, Klein-Altendorf 2, 53359 Rheinbach, Germany

\* Both authors contributed equally to the manuscript.

Correspondence:

✉ Tel.: +49228737400 Fax: +49-(0)228-73-2045 Email: ballvora@uni-bonn.de

This chapter has been submitted to MDPI Agronomy (under review)

## 5.1. Abstract

**Key message:** Synergistic effect of nitrogen and fungicide on grain yield (GY) and the differences in yield stability levels of (recently released) winter wheat cultivars across three cropping systems (CS) suggest that resource use efficiency can be improved via cultivar selection for targeted CS.

Nitrogen (N) is a vital component of crop production. Wheat yield varies significantly under different soil available N. Knowing how wheat responds to or interacts with N to produce grains is essential in the selection of N use efficient cultivars. We assessed in this study the variations among wheat genotypes for productivity-related traits under three CS, high-nitrogen with fungicide (HN-WF), high-nitrogen without fungicide (HN-NF), and low-nitrogen without fungicide (LN-NF) in 2015, 2016, 2017 seasons. ANOVA results showed genotypes, CS, and their interactions significantly affected the agronomic traits. The grain yield (GY) increased with higher leaf chlorophyll content, importantly under CS without N and fungicide supply. Yellow rust disease reduced the GY by 20% and 28 % in 2015 and 2016, respectively. Moreover, averaged over growing seasons, GY was increased by 23.78% under CS with N supply, while it was greatly increased by 52.84%, under CS with both N and fungicide application, indicating a synergistic effect of N and fungicide on GY. Fungicide supply greatly improved the crop ability to accumulate N during the grain filling, hence the grain protein content. Recently released cultivars outperform the older ones in most agronomic traits including GY. Genotype performance and stability analysis for GY production showed differences in their stability levels under the three CS.

**Key-words:** Nitrogen fertilization, fungicide treatment, cropping systems, yield components, yield performance, yield stability

## 5.2. Introduction

Wheat is one of the world's most important staple food crops (Oyiga et al., 2019), and it plays a major role in global food security. Thus, improving wheat grain yield is germane towards feeding the growing population (Ma et al., 2019). Nitrogen fertilizer is a key factor in the determination of the cropping system (CS), and has a strong effect on plant metabolism and biological processes that regulate plant growth and development (Gregory, 2011; Barraclough et al., 2014). It also affects wheat grain quality including gluten, protein, and starch contents (Wang et al., 2004).

Considering the importance of nitrogen (N) in ensuring higher crop yield and productivity, farmers tend to overuse it (Yadav et al., 1997; Good and Beatty, 2011), but paying little attention on important aspects like plant N uptake and utilization. An excessive application of nitrogen may lead to overstimulation of tillering and plant vegetation (i.e., haying-off) that locks up the carbohydrates in the structural materials rather than transporting them to the storage organs for later use at the grain filling stage. Effectively, only one third of the applied N is utilized by plants for grain production, resulting in a huge waste of resources that would harm the environment (Hawkesford, 2017; SHEN et al., 2017). Buckwell and Nadeu (Buckwell and Nadeu, 2016) reported that based on estimations between 2004 and 2011, apart from the northeast regions of Europe and mountain areas, most of the European Union (EU) is characterized by surpluses of nitrogen in agricultural land with an average of 49 to 80 kg. ha<sup>-1</sup>.

Wheat cultivation and productivity are limited by diverse biotic and abiotic stress factors such as soil water content, soil and air temperatures, and disease occurrence (Hailu and Fininsa, 2007). A direct relationship has been established between the N application and the incidence of yellow rust (*Puccinia striiformis* f. sp. *tritici*) (Danial and Parlevliet, 1995; Bryson et al., 1997), indicating that application of fungicides would decrease pathogen-related yield losses, especially under CS with higher amounts of fertilizers (Carlton et al., 2012). Improvement of wheat yield would require development of resilient CS (Lamichhane et al., 2015), including selection of genetic resources that would significantly increase plant productivity under limited and optimal nitrogen and agrochemical inputs. In the context of political and environmental constraints on agrochemical inputs and climatic changes, the reduction of agricultural inputs will contribute to reducing the negative impacts of agriculture on the environment (Gregory, 2011). Therefore, breeding to increase crops nitrogen use efficiency (NUE) in different crop management systems will assure high productivity along with lower economical costs and environmental threat (Ma et al., 2019).

A better understanding of the relationships existing among wheat productivity related traits, N fertilization and fungicides application would facilitate the identification and selection of high yielding cultivars for different targeted N application rates and CS. Several studies have revealed key components of NUE including N uptake and N use efficiency (Barraclough et al., 2014; Hawkesford, 2017). They

indicated that genetic variation exists among cultivars for traits related to NUE and recommended the use of broader germplasm including new and old varieties, landraces, and wild relatives to gain insights into NUE in crops. The breeding progress in wheat has resulted in increasing yield under less optimum condition *via* the identification and conservation of favorable genetic factors and haplotypes involved in stress adaptation in crops while eliminating detrimental genetic variants (Voss-Fels et al., 2019). On contrary, it has been also reported that newer released wheat cultivars perform poorly under less optimal conditions compared to the older released wheat cultivars (Kahiluoto et al., 2019). To date, few studies have investigated the main and cumulative effects of fungicide and nitrogen on wheat productivity as well as their interactions under different CS at vegetative and reproductive stages. In the context of breeding for low and high input CS, sufficient research information needs to be provided to wheat growers to improve productivity under both conditions. In this study, 220 winter wheat cultivars released from the last 50 years with variable phenotypic traits were grown in three CS including one conventionally managed system with high nitrogen, fungicides and growth hormones. The aims of this study were to (1) explore the genetic variability existing among 220 cultivars for agronomic traits, disease response, and seed grain quality under effect of nitrogen and fungicide CS; (2) identify the GY most contributing traits among its components under each CS and (3) provide information on the breeding progress made in important traits to assure high productivity under less and high input conditions.

### 5.3. Materials and Methods

#### 5.3.1. Plant material, experimental design, and treatment

A total of 220 winter wheat cultivars described by Voss-Fels et al. (2019) were used in this study. They were grown in the field at the Campus Klein-Altendorf, University of Bonn (50.61° N, 6.99° E, and 187 m above sea level) in 2014/2015, 2015/2016 and 2016/2017 growing seasons. The experiments were performed in an alpha design consisting of 1,320 plots under three CS with two replications each, using plot-in-plot systems. The CS treatments adopted were: LN-NF (no N fertilization, without fungicide), HN-NF [semi-intensive system with 220 kgN.ha<sup>-1</sup> mineral fertilizer adjusted for soil mineral nitrogen (Nmin), plant growth regulators, and no fungicide application], and HN-WF (intensive system with 220 kgN.ha<sup>-1</sup> adjusted for soil Nmin, plant growth regulators plus fungicide application). The soil information including Nmin of the experimental site, the amount of N fertilizer applied, and the agro-chemical input including fungicide are provided in Table S1, S2 and S3, respectively. Each plot was 6 m long and 2.5 m wide with a sowing density of 330 viable seeds per m<sup>2</sup> in rows spaced by 10.4 cm and the harvested plot was 5.0 m long and 1.65 m wide. The weather conditions during the experimental periods are summarized in Figure S1.

#### 5.3.2. Soil sampling and fertilization

After seed sowing, soil samples were taken from 0 to 90 cm depth in 30 cm increments and analyzed for the available Nmin in the soil. Soil Nmin was determined by micro-Kjeldhal digestion method (Jackson, 1958). Ammonium N (NH<sub>4</sub><sup>+</sup>N) was extracted by 2 M KCl and analyzed by using phenate method (Apha, 1985). Nitrate N (NO<sub>3</sub><sup>-</sup>N) was extracted by 1g/100ml CaSO<sub>4</sub> and analyzed by phenol disulphonic acid method (Jackson, 1958). The soil characteristics of the experimental site are shown in Table S1.

#### 5.3.3. Phenotypic evaluation

The traits evaluated include: agronomic [plant height (PH), heading date (HD), spikes per m<sup>2</sup> (SNms), kernels per spikes (KNSp), kernels per m<sup>2</sup> (KNms), thousand kernels weight (TKW), harvest index (HI), plant biomass per m<sup>2</sup> weight (PBWms), and GY], physiological [chlorophyll content (SPAD)], disease response [yellow rust visual score (YR)], and grain quality [grain crude protein (GPC), grain starch content (GSC) and sedimentation]. The heading date (HD) indicated the duration of vegetative period from germination until heading growth stage at BBCH59 (Biologische Bundesanstalt, Bundessortenamt und Chemische Industrie (Lancashire et al., 1991)). The severity of yellow rust was scored in 2015 and 2016 growing seasons under all three cropping systems according to Pask et al. (2012). The full description of evaluated traits is given in Table S4.

#### 5.3.4. Statistical analyses of the evaluated traits

The analysis of variance (ANOVA) for all the traits was performed with a mixed-linear-model to determine the effect of CS, genotypes (cultivars), and their interactions across the three growing seasons. Restricted maximum-likelihood (REML) was adopted to estimate the variance parameters, and the best linear unbiased estimate (BLUES) of all traits for each genotype under different CS were generated. The resulted BLUES were used for the subsequent downstream analyses. BLUES of three CS for each trait were compared using Tukey's honestly significant differences (HSD) test to obtain significance groups (Sheskin, 2020). A three ways analysis of variance was carried out especially for GY and GNY to estimate the existence of variation among genotypes, CS, years, and their interaction effects using ANOVA Procedure in SAS software (SAS Institute, 2015).

A mixed-linear model with restricted maximum-likelihood (REML) was used to estimate the variance components due to genotypes ( $\sigma_g^2$ ), CS ( $\sigma_c^2$ ), and their interaction G\*CS ( $\sigma_{ge}^2$ ). These components were set as random effects in the model (SAS Institute, 2015). Thereafter, the broad-sense heritability ( $H^2$ ) for all traits across growing seasons were calculated as described by Piepho and Möhring (Piepho and Möhring, 2007) ) using the equation

$$H^2 = \sigma_g^2 / \sigma_p^2 \quad (\text{Equation 5.1})$$

with  $\sigma_p^2 = \sigma_g^2 + \sigma_{ge}^2 / m + \sigma^2 / rm$

where  $\sigma_p^2$  is the phenotypic variance,  $m$  the number of studied CS,  $r$  the number of replicates per CS and  $\sigma^2$  the residual error variance.

Pearson correlation analysis of genotypic means was performed using “*Performance Analytics*” package in R (R Core Team, 2020) to assess the correlation between evaluated traits. We tested the significant difference among CS correlation coefficients of GY and its components through `r.test` function for two independent correlations in a Fisher's z-test in “*psych*” R package. Thereafter, the relationships between GY and traits of interest were evaluated using linear regression to quantify the contribution of the trait to GY. The regressions were conducted using `lm` function as implemented in R and path models analysis using “*lavaan*” and “*semPlot*” packages as described by Rosseel (Rosseel, 2012). The differences among regression coefficients namely slopes and intercepts of the three CS were tested using linear regression models which included CS as categorical variables.

#### 5.3.5. Effects of nitrogen and fungicide on the evaluated traits

The effect of nitrogen and fungicide on the evaluated traits was calculated with traits average values under each CS using the following formula.

$$N_{\text{eff}} = [P_{(\text{HN-NF})} - P_{(\text{LN-NF})}] / P_{(\text{LN-NF})} \quad (\text{Equation 5.2})$$

$$NF_{\text{eff}} = [P_{(\text{HN-WF})} - P_{(\text{LN-NF})}] / P_{(\text{LN-NF})} \quad (\text{Equation 5.3})$$

$$F_{\text{eff}} = [P_{(\text{HN-WF})} - P_{(\text{HN-NF})}] / P_{(\text{HN-NF})} \quad (\text{Equation 5.4})$$

Where:  $N_{\text{eff}}$ , represents the nitrogen effect;  $NF_{\text{eff}}$ , the combined nitrogen plus fungicide effect and  $F_{\text{eff}}$  the fungicide effect under high nitrogen CS.

Two indicators including NUE (Nitrogen use efficiency) and NAE (Nitrogen agronomy efficiency) were estimated according to (Ma et al., 2019), and used to determine the N requirements for GY production. NUE and NAE were calculated as:

$$NUE \left( \frac{\text{kg}}{\text{kg}} \right) = Y_{N_{av}} / N_{av} \quad (\text{Equation 5.5})$$

$$NAE \left( \frac{\text{kg}}{\text{kg}} \right) = (Y_N - Y_0) / A_N \quad (\text{Equation 5.6})$$

where  $Y_{N_{av}}$  (kg) is the GY harvested under respective CS;  $N_{av}$  (kg) the available nitrogen (Fertilizer and  $N_{\text{min}}$ ) in respective CS;  $Y_N$  (kg) indicates the GY under high N;  $Y_0$  (kg) the GY obtained under low N;  $A_N$  the amount of applied N fertilizer under high N.

The effect of fungicide on NAE under HN-NF and HN-WF was investigated to evaluate how fungicide application could improve N use. We defined four classes of NAE depending on the amount of N used for GY production. The genotype with the highest GY under HN-NF or HN-WF was considered as having converted 100% of the available nitrogen into GY, hence had the highest NAE ( $NAE_{\text{max}}$ ). A genotype  $i$  was class one (class1) when  $k = NAE_i / NAE_{\text{max}} * 100$  was less than 25%, class2 when  $k$  was more than 25% and less than 50%, class3 when  $k$  was between 50% and 75%, and with  $k$  greater than 75% was assigned class4.

### 5.3.6. Estimation of the breeding progress using the wheat diversity panel

The breeding progress in the winter wheat panel for each trait was investigated with 209 cultivars whose year of release are known by the linear regression function. The BLUEs values of each genotype averaged over three years growing seasons were used in the regression analysis. The absolute breeding progress (increase per year) was the slope of the linear regression line between the year of release and the trait of interest as described by Lichthardt et al. (2020).

### 5.3.7. GY performance and stability analysis

To measure the GY performance of each genotype under three CS across three years, the genotype performance measure ( $P_i$ ) was calculated as described by Lin and Binns (1988) as:

$$P_i = \sum_{j=1}^q \frac{(X_{ij}-M_j)^2}{2q} \quad (\text{Equation 5.7})$$

where  $P_i$  of a genotype  $i$  under a CS or agro-environment  $j$  is defined as the mean square between the genotype's GY ( $X_{ij}$ ) and the maximum harvested GY ( $M_j$ ) in the CS ( $j$ ), averaged over the total number of CS ( $q$ ) for the three years of trial. The smaller the mean square, higher achievement in GY is the genotype. The  $P_i$  were ranked and twenty-two cultivars with smallest  $P_i$  values were selected in each of the three CS.

Thereafter, the GY stability under each CS was carried out with 46 consistently high yielding cultivars previously selected with  $P_i$  measure. The stability of these cultivars was ascertained under each CS in the three years taken as environments. A combined analysis with the three CS over three years was carried out to estimate the cultivars' stability performance under all CS. Genotype stability index was estimated using the GEA-R software program as described by Pacheco et al. (2015). Francis coefficient of variation CV (%) and the mean value were used as stability and performance indices, respectively (Francis and Kannenberg, 1978). With this approach, cultivars with high GY and low CV across environments are considered high yielding and stable.

The additive main effects and multiplicative interaction (AMMI) model analysis of variance for GY from the 46 selected high yielding cultivars was performed by GEA-R (Pacheco et al., 2015) to evaluate the cultivars and CS interactions. The model was

$$Y_{ij} = \mu + g_i + e_j + \sum_{n=1}^N \tau_n \gamma_{in} \delta_{jn} + \varepsilon_{ij} \quad (\text{Equation 5.8})$$

where  $Y_{ij}$  is the yield of the  $i$ -th genotype ( $i=1,\dots,I$ ) in the  $j$ -th yearly CS considered as environment ( $j=1,\dots,J$ );  $\mu$  the grand mean;  $g_i$  and  $e_j$  are the genotype and CS deviations from the grand mean, respectively;  $\tau_n$  the eigenvalue of the PC analysis axis  $n$ ;  $\gamma_{in}$  and  $\delta_{jn}$  the genotype and environment principal components scores for axis  $n$ ;  $N$  the number of principal components retained in the model and  $\varepsilon_{ij}$  the error term. GGE biplots were generated by R with the Package *GGEbiplotGUI* using the first two principal components (IPCA1 and IPCA2) that explained the higher variation in the AMMI analysis for visual interpretation of Gx E interaction.

The CS were classified based on the predicted means obtained from the AMMI analysis and the Biplot were visualized. Thereafter, the function *which won where* was used to identify best cultivars and group CS with high similarity. The biplots were based on an environment-centered (centering = 2) G by E table without any scaling (scaling = 0), and it was environment-metric preserving (SVP = 2) and the axes were drawn to scale (default feature of *GGEbiplot*).

### 5.3.8. Cropping system performance and discriminating level

We classified CSs based on their performance indices and identified the least discriminative CS. The least discriminative CS is the CS where cultivars better utilized the available nitrogen. We calculated two CS performance indices. The first used the whole set of 220 cultivars, while the second used the set of 46 high yielding cultivars. The CS performance indices were calculated using the following formula.

$$P(cs) = \sum_{j=1}^n \frac{P_i}{n} \quad (\text{Equation 5.9})$$

where  $P(cs)$  is the performance index of the CS,  $n$  the total number of considered cultivars,  $P_i$  the performance index of  $j$ th genotype as described by Lin and Binns (Lin and Binns, 1988).

## 5.4. Results

### 5.4.1. Nitrogen and fungicide application effect on phenotypic traits

The phenotypic traits expression differed significantly ( $P < 0.001$ ) among genotypes and CS (**Table 5.S5**). The interactions of G\*CS across the three growing seasons were also significant ( $P < 0.001$ ). Means comparison by Tukey HSD test showed that the cultivars grown under HN-WF and HN-NF showed better performance for most traits evaluated than cultivars grown under LN-NF (**Figure 5.1; Figure 5.S2; Table 5.S6**). GY ranged from 6.455 Mg.ha<sup>-1</sup> under LN-NF in 2016 to 11.225 Mg.ha<sup>-1</sup> under HN-WF in 2015 (**Table 5.S7**). GY was increased due to N, NF and F applications, with a range from 6.39% for N<sub>eff</sub> in 2016 to 68.03% for NF<sub>eff</sub> in 2015 (**Figure 5.2A,C; Table 5.S6,S7**). Results indicated that kernel number per m<sup>2</sup> (KNms) was highly increased by N (30.24% in 2016 and 27.94% in 2017) and by NF (53.21% in 2016 and 32.81% in 2017), while TKW was reduced by N and NF applications (**Table 5.S6**).

SPAD values increased under HN-NF and HN-WF in 2016, indicating an increasing effect of nitrogen and fungicides on leaves chlorophyll content. However, a decrease (-2.2%) of chlorophyll content due to fungicide effect was observed in 2017. The yellow rust (YR) effect on the cultivars reduced by 26.59% and 32.3% under HN-NF compared to LN-NF in 2015 and 2016, respectively. In addition, the cultivation under HN-WF reduced plant rust infection by 41.29% in 2015 and 38.08% in 2016. In 2017 season, the infection of yellow rust was not observed, therefore, it was not scored. Regarding grain quality traits, N, NF, and F had an increasing effect on grain crude protein content with NF having the highest effect followed by N effect. Sedimentation volume was significantly increased by N application over the three growing seasons, whereas it was not affected by fungicide application in 2015 and 2017. However, grain starch content was decreased by nitrogen and fungicide applications (**Table 5.S6**).

Coefficient of variation of evaluated traits ranged from 0.237% for kernels per spike in 2017 to 62.73% for YR in 2016. Heritability estimates ( $H^2$ ) ranged from 0.22 for biomass in 2015 to 0.95 for Heading date (HD) in 2017.  $H^2$  estimates for YR were consistently high with 0.84 in 2015 and 0.92 in 2016 (**Table 5.S5**).

We further investigated yield performance through three ways ANOVA and variance components analysis with year (Y), Genotypes (G) and CS as factors, to evaluate the effect of each factor and identify the highest source of variation in yield. Results revealed significant ( $P < 0.001$ ) differences among years, cropping systems, genotypes, and their interactions (**Table 5.S8,S9**). Cropping system was the most important source of variation in grain yield, with 54.45% followed by the genotypes and years, explaining 16.22% and 10.38% of the total variance, respectively (**Figure 5.2D; Table 5.S9**).

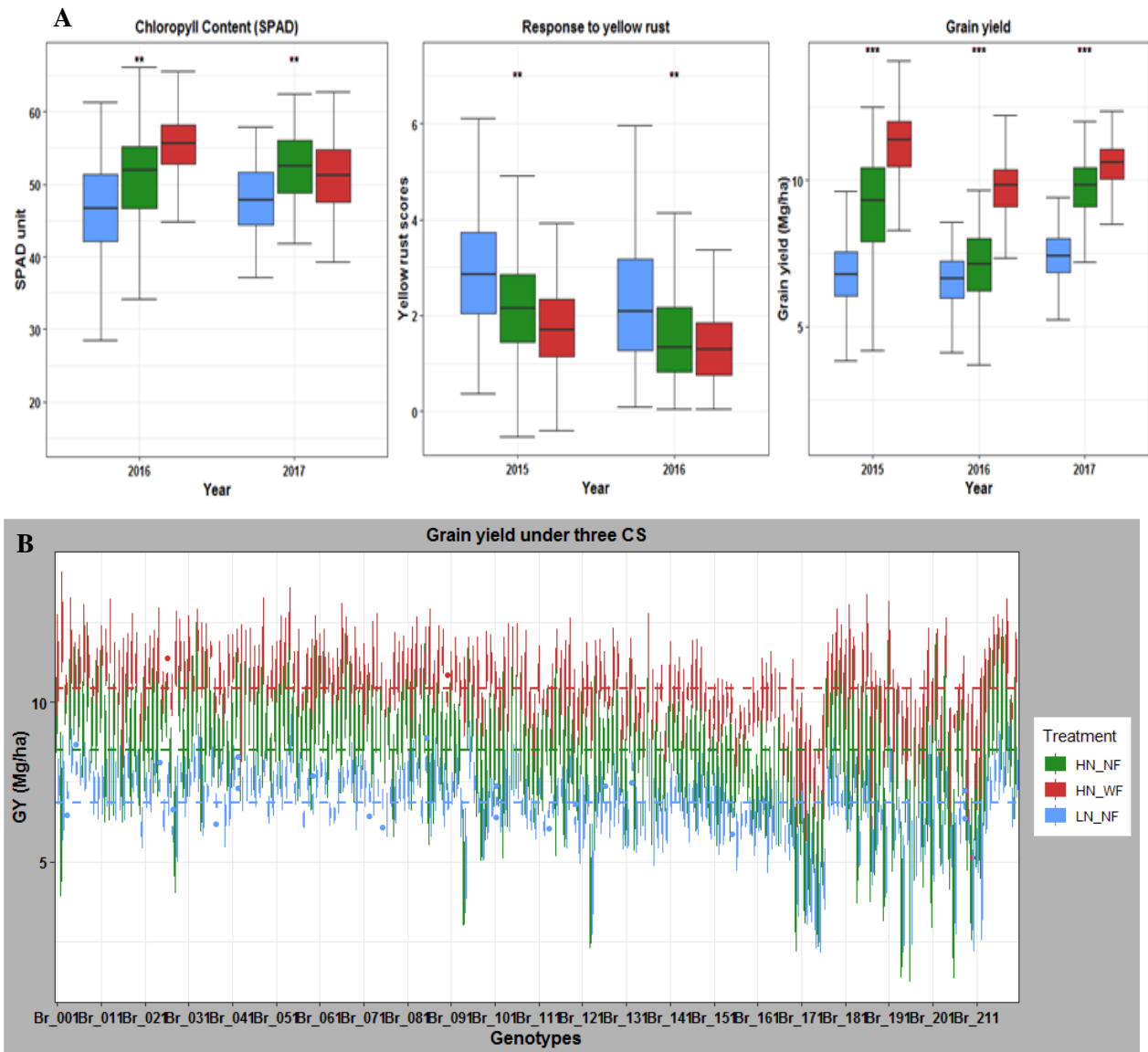


**FIGURE 5. 1** | Differences between the three cropping systems. **(A)** leaf chlorophyll content, plant response to yellow rust, and GY traits. **(B)** Three years averaged grain yield production (Mg.ha<sup>-1</sup>) of 220 cultivars under the three cropping systems. The dashed lines indicate the GY mean under each CS: blue: LN-NF (6.850 Mg.ha<sup>-1</sup>); green: HN-NF (8.507 Mg.ha<sup>-1</sup>), and red: HN-WF (10.447 Mg.ha<sup>-1</sup>). The symbol \*\* means significant at p=0.01.

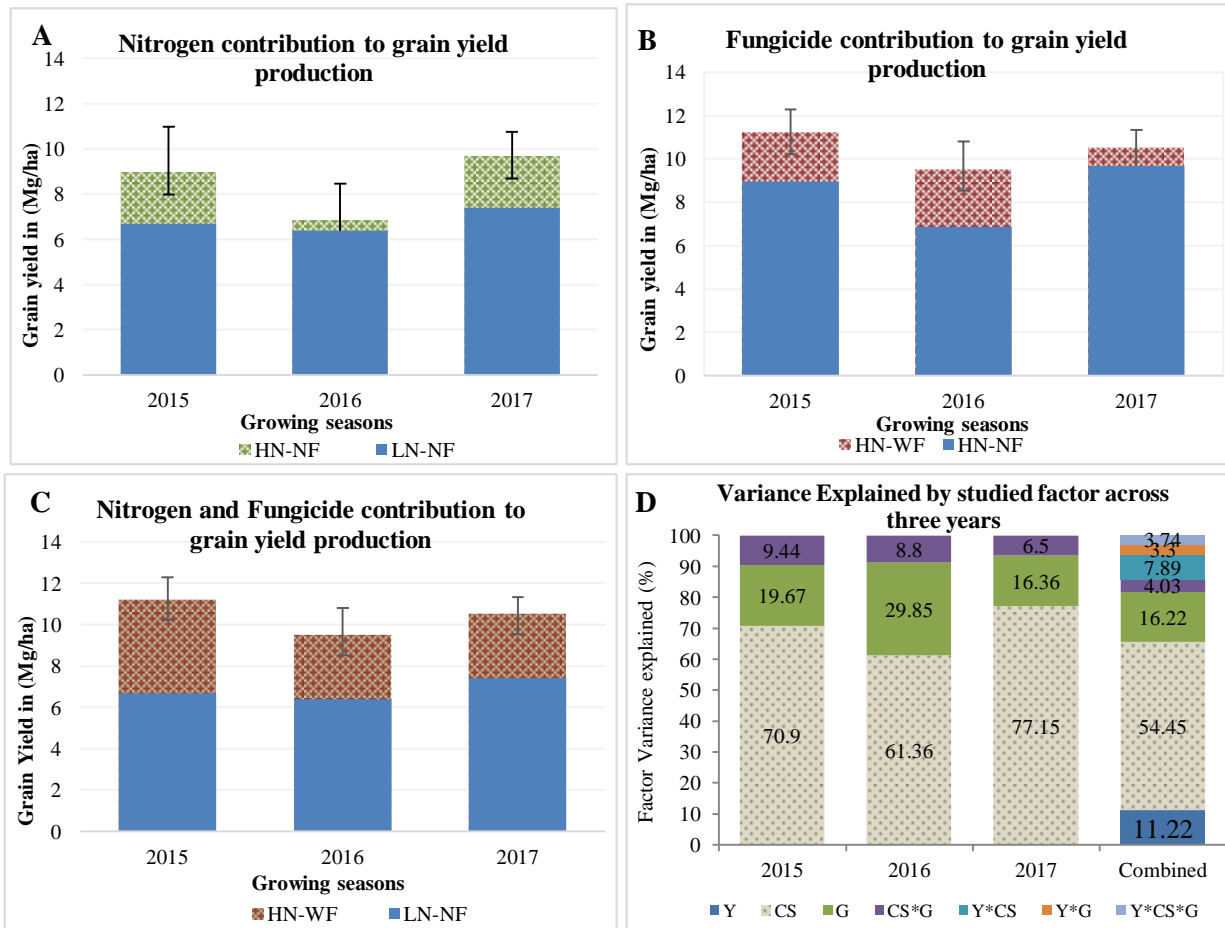


**FIGURE 5.2** | Contribution of nitrogen and fungicide to grain yield ( $\text{Mg}\cdot\text{ha}^{-1}$ ) production in 2015, 2016, and 2017 growing seasons and variance components of each factor. **(A)** blue bars are showing the grain yield harvested under LN-NF and green/white bar above is showing grain yield gained from additional fertilization. **(B)** Blue bars are grain yield from HN-NF used as control and the above red/white show gained grain yield owing to fungicide application. **(C)** Blue bars are grain yield harvested under LN-NF (Control) and the above red/green bars show gained grain yield due to combined effect of additional nitrogen fertilization and fungicide application. **(D)** Proportion of the variance components of factors years (Y), cropping systems (CS), and genotypes (G) and their interactions.

#### 5.4.2. Application of nitrogen and fungicide improve GY and grain N yield (GNY)

The NUE and NAE estimates were used to examine the proportion of N used for grain production. The results indicated that both estimates varied significantly ( $p < 0.001$ ) among genotypes and CS in the three growing seasons. Significant  $G*CS*Y$  interactions were also observed (**Table 5.S10A**). NUE was twice higher under LN-NF than under HN-NF and HN-WF, indicating that higher amounts of N fertilization do not lead to an increase in NUE. The estimates of NAE was significantly higher under HN-WF when compared to the HN-NF (**Figure 5.3**). Moreover, the classification of cultivars based on their NAE values revealed that a total of 14, 10 and 73 cultivars are efficient N utilizers nitrogen for grain production under HN-WF in 2015, 2016, and 2017, respectively. However, under HN-NF, only 12 cultivars efficiently utilized the available nitrogen in 2017 (**Figure 5.S3**). The grain nitrogen yield (GNY) differed significantly among cultivars, CS, and years. Similarly, a significant  $Y*G*CS$  and  $G*CS$  interaction was detected for GNY (**Table 5.S10A**). Compared to LN-NF, GNY increased under HN-NF and HN-WF in all growing seasons. Nitrogen plus fungicide increased the GNY compared to the system when N was supplied alone across the three years of trials (**Figure 5.S4A**). GNY strongly correlated with GY under all CS (HN-NF = 0.98; HN-WF = 0.90, LN-NF = 0.97) (**Table 5.S10**).

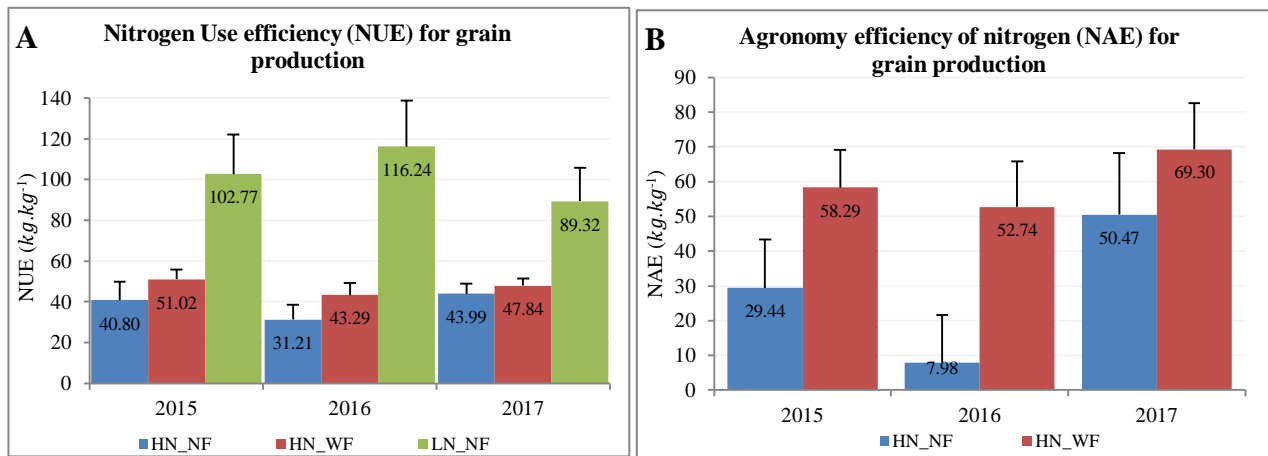


**FIGURE 5.3** | (A) Nitrogen use efficiency; (B) Agronomy efficiency of Nitrogen in three years of trial.

### 5.4.3. Genetic relationship between GY and evaluated traits

The genetic relationship between GY and each traits of interest across cropping systems was evaluated through Pearson correlations coefficients and linear regression analysis based on cultivar means. For cultivars response to yellow rust infection, we noticed that an increase in the disease infection reduced the GY in 2015 ( $r=-0.52^{***}$ ) and 2016 ( $r=-0.51^{***}$ ) seasons (**Figure 5.S5**). The response to YR explained 36.4%, 31.7%, and 11.14% of the variation in GY under LN-NF, HN-NF and HN-WF, respectively. Under LN-NF and HN-WF, GY decreased 0.5333 and 0.4517 Mg.ha<sup>-1</sup> per unit increase in YR infestation. Whereas, GY reduction was significantly higher under HN-NF with 0.9665 Mg.ha<sup>-1</sup> decrease per unit increase in YR infestation compared to HN-WF and LN-NF (**Figure 5.4A; Table 5.S11**). Cultivars with low YR infestation recorded higher yield under all three CS (**Figure 5.S4B**).

The correlation and regression analyses performed showed significant and positive relationships between GY and leaf chlorophyll content (SPAD) in 2016 ( $r= 0.62^{***}$ ) and 2017 ( $r= 0.33^{***}$ ) (**Figure 5.S5; Figure 5.S6A,B**). Independent of the CS, leaf chlorophyll content explained 41.52% and 3.56% of the variation in GY in 2016 and 2017, respectively. The increase in GY was estimated to 0.2098 Mg.ha<sup>-1</sup> in 2016 and 0.0747 Mg.ha<sup>-1</sup> in 2017 per unit increase in SPAD value (**Figure 5.S6A,B**). Leaf chlorophyll content more explained the variation in GY under LN-NF ( $R^2 = 0.4196$  in 2016 and  $R^2 = 0.059$  in 2017) than under HN-NF and HN-WF (**Figure 5.4B,C**). In 2016, GY increased equivalently under LN-NF and HN-NF with 0.1332 and 0.1518 Mg.ha<sup>-1</sup> per unit increase in SPAD, respectively, and both were significantly higher than the one observed s under HN-WF which amounted to 0.0717 Mg.ha<sup>-1</sup>.SPAD<sup>-1</sup> in the same year (**Table 5.S12**). Cultivars with higher SPAD obtained higher GY than the ones with lower SPAD values under LN-NF (**Figure 5.S4C**).

HD was positively correlated with GY ( $r= 0.19^{**}$ ,  $r= 0.33^{***}$ ;  $r= 0.41^{***}$  in 2015, 2016 and 2017, respectively), while negative correlations were detected between GY and PH ( $r= -0.46^{***}$ ,  $r= -0.26^{***}$  and  $r= -0.51^{***}$  in 2015, 2016 and 2017, respectively) (**Figure 5.S5**). Longer vegetative period due to delay of HD was beneficial to increase cultivar GY, more importantly under LN-NF with an increase of 0.2607 Mg.ha<sup>-1</sup> per one additional day. The delay in HD equally affected GY under HN-WF and HN-NF (**Figure 5.4D; Table 5.S12**). On the other hand, the increase in PH reduced GY under all three CS, including a pronounced yield reduction under HN-WF with 0.0669 Mg.ha<sup>-1</sup> decrease per cm increase in PH. The reduction in GY per increase in PH was significant only when compared HN-WF to LN-NF (**Figure 5.S6C; Table 5.S12**).

GY positively correlated with most of the yield components across the three growing seasons (**Figure 5.S5**). Result indicated that GY is positively and significantly ( $P<0.001$ ) correlated with kernels per spike ( $r= 0.35- 0.42$ ), and KNms ( $r= 0.52-0.53$ ). GY exhibited positive correlation with HI ( $r= 0.59-0.79$ ) and with PBWms ( $r= 0.41-0.64$ ) across the growing seasons. Under each CS, GY recorded significant and

positive correlations with its key components, especially with KNms ( $r= 0.36-0.56$ ), except SNms and TKW (under HN-WF) as shown in **Figure 5.5**. Like KNms, GY harvested under one CS positively and significantly correlated with the ones from the two other CSs (**Figure 5.S5D,E**). Results of the comparisons among correlations (GY vs its components) coefficients from the three CS indicated significant ( $P < 0.001$ ) differences. Correlation coefficients obtained under HN-WF was different with, HN-NF and LN-NF for PBWms, TKW, and KNms. The cropping system did not affect the relationship between SNms and GY as shown by insignificant differences among correlations coefficients (**Table 5.S11**).

The genetic link between GY and grain quality traits such as grain protein (GPC), grain starch (GSC), and sedimentation investigated revealed significant positive associations between GY and GSC ( $r= 0.34-0.65$ ,  $P < 0.001$ ) across growing seasons. However, GY negatively correlated with GPC ( $r= -0.18^{**}$ ,  $r= -0.46^{***}$ ,  $r= -0.27^{**}$ ) and sedimentation ( $r= -0.19^{**}$ ,  $r= -0.22^{**}$ ,  $r= -0.30^{***}$ ) across three years (**Figure 5.S5**). The regression analysis revealed that the variation in GSC significantly explained the variation in GY across all three CS, but importantly under HN-WF with 48.13% of variance ( $R^2$ ) explained in GY (**Figure 5.S6D**). A unit increase in GSC enhanced GY by 0.8573, 0.7954 and 0.7765  $\text{Mg}\cdot\text{ha}^{-1}$  under HN-NF, HN-WF, and LN-NF, respectively, whereas GY decreased by 1.5502, 1.0854 and 1.2532  $\text{Mg}\cdot\text{ha}^{-1}$  when GPC increased by one unit under LN-NF, HN-NF, and HN-WF, respectively (**Figure 5.S6E; Table 5.S12**). GY reduction per unit increase in GPC was significantly higher under LN-NF than under HN-NF, and HN-WF. Therefore, the highest trade-off relationship between GY and grain protein content occurred under LN-NF.

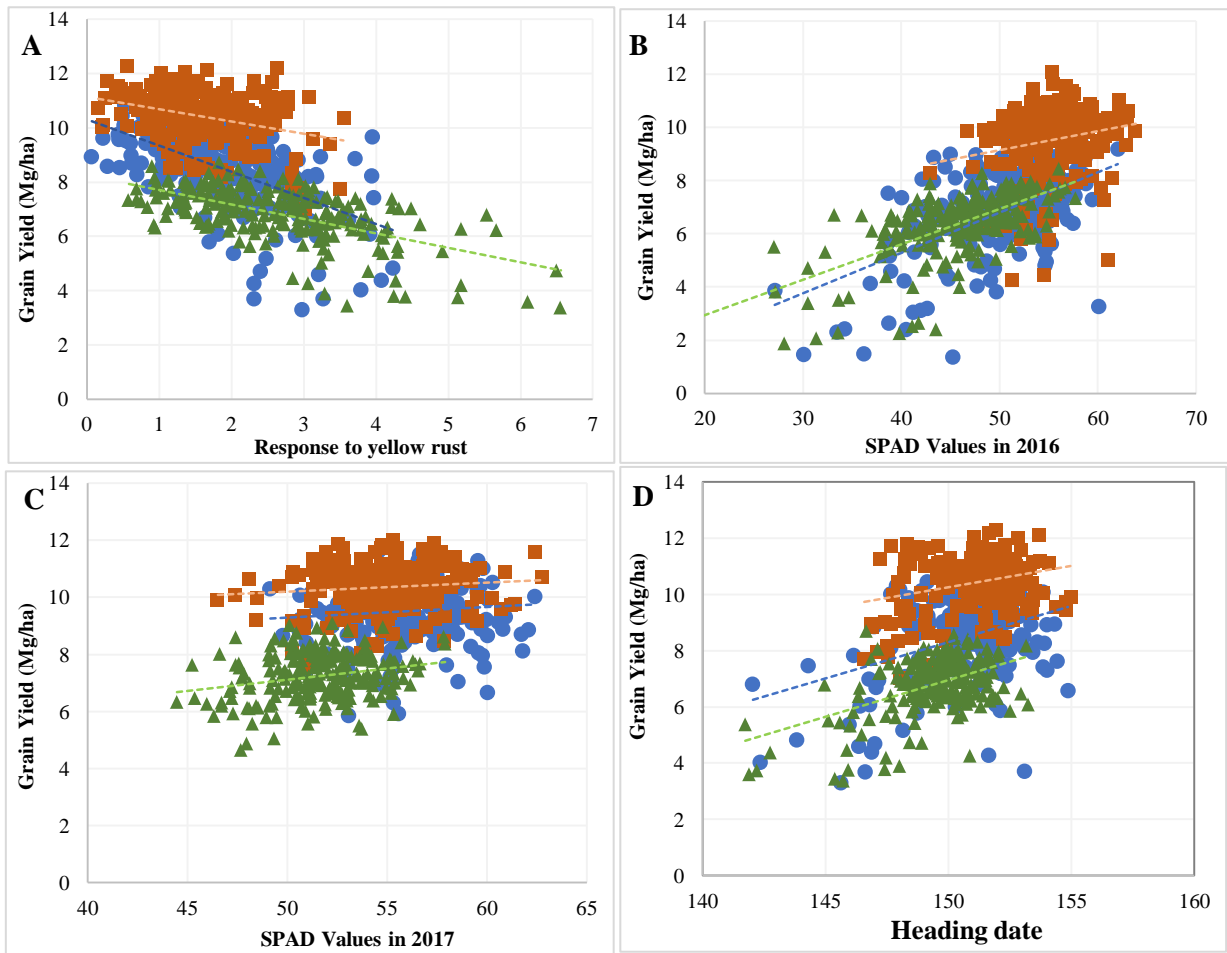


**FIGURE 5.5** | Relationship between GY and evaluated traits. (A) Response to yellow rust (score); (B) SPAD in 2016; (C) SPAD in 2017; (D) Heading date. Colour-shape symbols: green-triangle for the cropping system LN-NF, blue-circle for HN-NF, and red-square for HN-WF. The regressions equations, the significance of the slopes and comparison among slopes of the three CS is given in **Table 5.S12**.

Yield Components	Cropping Systems		
	GY (HN-NF)	GY (HN-WF)	GY (LN-NF)
PBWms	0.74	0.21	0.53
HI	0.78	0.7	0.67
TKW	0.42	0.1 <sup>-</sup>	0.4
KNms	0.55	0.36	0.56
KNSp	0.44	0.23	0.38
SNms	0.16 <sup>-</sup>	0.02 <sup>-</sup>	0.2 <sup>-</sup>

**FIGURE 5.5** | Correlations between GY and yield components traits under each CS. Traits were measured in a wheat population containing 220 cultivars grown under three CS between 2015 and 2017. The correlations coefficients are ranged low values (blues color) to high values (red colored). The numbers crossed with minus<sup>(-)</sup> are not significant at P< 0.05.

#### 5.4.4. GY was significantly affected by indirect effects of several agronomic traits

Full regression and path analysis were used to quantify the effect of several agronomic traits on GY (Table 5.S13A). The full regression model captured 86.2, 81.6, and 84.7% of the total variation in GY under HN-NF, HN-WF, and LN-NF, respectively. HD, SPAD, YR, HI, PBWms, and GSC had significant ( $p < 0.001$ ) effects on GY. As revealed by the path coefficients (Table 5.S13B), most traits had higher indirect effects on GY than direct effects, except HI and PBWms under all CS. The path correlation coefficients relating YR to GY were made of sizeable negative indirect effects (-0.405 under HN-NF; -0.179 under HN-WF and -0.359 under LN-NF) via other traits, and direct effects (-0.158 under HN-NF; -0.128 under HN-WF and -0.243 under LN-NF).

#### 5.4.5. Few cultivars achieved maximum yield under HN-NF, the most discriminating CS

We defined least discriminative CS as the CS under which most cultivars had their GY close to the highest yielding cultivar, hence having a CS performance index ( $P_{cs}$ ) close to zero.  $P_{cs}$  describes how well, cultivars come to achieve the maximum yield potential under a CS. The  $P_{cs}$  calculated with 220 cultivars (Figure 5.6A) and with 46 high yielding cultivars (Figure 5.6B) showed similar trends in the performance of the CS. Averaged over three years, LN-NF recorded the lowest performance index, therefore was more suitable for many cultivars to reach a GY close to the maximum yield, and HN-WF was the second least discriminative CS. While, HN-NF recorded the highest  $P_{cs}$  indices calculated with 220 cultivars (12,154), and with 46 cultivars (591), therefore the most discriminating CS. Further biplots from AMMI analysis revealed the discriminating ability and the representativeness of tested CS taken as different environments (Figure 5.6C). The two first principal components of the biplots explained 83.67% of the total variation of the environment-centered G by E table (G+GE) and revealed that LN-NF is more representative of other tested CS, thus less discriminating. The length of the vectors of HN-NF is greater than LN-NF and HN-WF indicating that HN-NF had the highest discriminating ability. Thereafter, the function “*which won where*” identified high similarity between LN-NF and HN-NF, making then one mega environment with cultivars Hybery and Tabasco as winning cultivars. The cropping system HN-WF was considered as one mega environment with Tobak as winning cultivars.

#### 5.4.6. High yielding cultivars showed different stability level under the three cropping systems

The performance index of Lin and Binns (1988) was used to identify high performing cultivars across growing seasons under different CS. A total of 81 cultivars highest yielding were selected across the three CS over the three growing seasons. Among them, 46 were selected at least under 5 agro-environments, and comprised 43 newer and 3 older released cultivars (Figure 5.S8). Results of GY stability (Francis CV) of these 46 high yielding cultivars are presented in Figure 5.S9, and Table 5.S14. Among them, 19



### 5.4.7. Newer released cultivars outperformed older cultivars in most traits and GY under all CS

The breeding progress in the studied wheat panel was quantified by the slope of the regression between years of release of 209 cultivars and the values of traits of interest. Under each CS, breeding progress for all traits evaluated were significant, except for the HD and SNms. Breeding had increased GY via increasing the key yield components, most importantly on KNSp and KNms, while reducing the PH and the response to disease over years (Figure 5.7; Figure 5.S7). For SPAD and YR, significance differences of the breeding progresses among the three CS were detected, which indicate that cultivars behaved differently under the three CS depending on their years of release. The highest increase in breeding progress trends for SPAD was observed under LN-NF, while the breeding progress for YR observed under HN-WF was the weakest among the three CS (Table 5.S15). For GY, the breeding progress was significantly higher under HN-NF than both HN-WF and LN-NF, where the breeding progresses recorded similar trend (Figure 5.7A). Breeding has also decreased the coefficient of variation of GY, hence it has increased the yield stability (Figure 5.7B). KNms and sedimentation recorded slow breeding progress under LN-NF than under HN-NF and HN-WF (Figure 5.S7). The correlations between cultivars years of release and the evaluated traits were significant and almost equal under all three CS, suggesting that breeding had increased the cultivar adaptability under low, semi, and high input CS (Figure 5.7C).

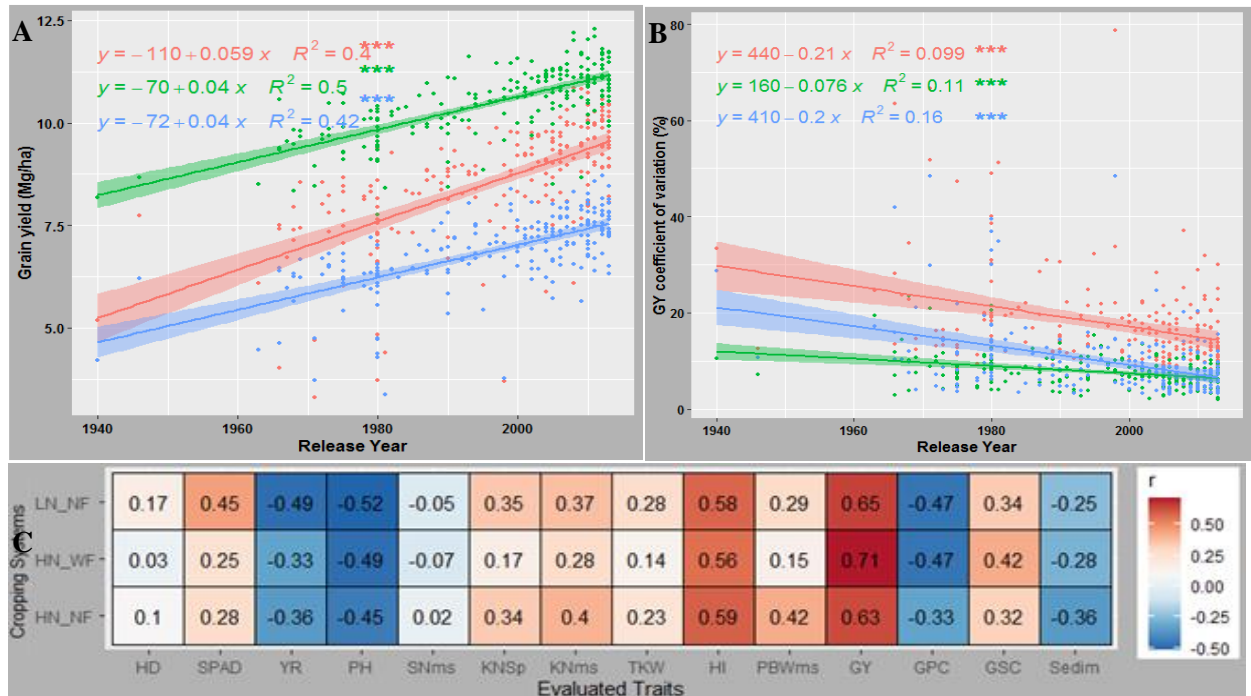


**FIGURE 5.7** | Temporal trends observed in traits of interest. (A) GY; (B) GY coefficient of variation in relation to year of registration among 220 cultivars under three CS, HN-WF in green, HN-NF in red and LN-NF in blue color. (C) Correlations coefficients between year of release and fourteen traits of interest under three CS. The center lines represent the regression lines and the shaded regions in A and B represent the 95% confidence intervals. The ns means not significant at 0.05; (\*) (\*\*) significant at 0.05 and 0.01, respectively.

## 5.5. Discussion

Few studies were done on the joint effect nitrogen with other important crop management element like fungicide. The main aim of this study was to evaluate the genotypic response of 220 cultivars released in the last five decades to nitrogen and fungicide application, in order to provide information on substantial resource loss when cultivars and CS elements are not adequately managed. The key findings from our research are discussed below.

### 5.5.1. Variation in agronomic traits and GY under the effect of nitrogen and fungicide

Nitrogen and fungicide application increased wheat yield. Higher GY following N fertilization was due to the increase of grain number (Gooding and Davies, 1997; Litke et al., 2018). GY improvement under intensive CS could be explained by a synergistic effect of nitrogen and fungicide to increase grain numbers (kernel per m<sup>2</sup>, kernel per spike). Fungicide supply positively contributed to GY owing to the maintenance of green leaf area particularly flag leaf life extension after anthesis, affecting photosynthates partitioning within the plant, which enhances grain weight (Gooding et al., 2005; Royo et al., 2007). In fact, fungicide application contributed to plant protection against disease invasion, particularly YR which was more pronounced in the two first years of trial, and very known for his effect on yield lost (FAO, 2017). In 2017 growing season, the infection of yellow rust was not observed; hence it was not scored. The lower infestation yellow rust could be related to the weather conditions at the experimental site (**Figure 5.S1**) which was drier in 2017 with higher temperatures and lower rainfall compared to 2016 and 2015 growing seasons. Lower temperatures and high relative humidity increase the infection levels with yellow rust (Te Beest et al., 2008). Nitrogen application enhanced plant resilience to YR infestation, whereas earlier studies reported higher rust infestation under high N application rates owing to increased plant canopy size (Danial and Parlevliet, 1995; Bryson et al., 1997; May et al., 2020). Our result could find explanation in the fact that we supplied N fertilization in the form of ammonium, which decreases stem and YR, while nitrate-N increases them (Neumann et al., 2004). Plant height was decreased under nitrogen and fungicide supply due to the application of growth regulator hormones in these CS (Tripathi et al., 2004).

Most evaluated traits recorded moderate to high heritability ( $H^2$ ) estimates across the three growing seasons, thus, they can be exploited to identify QTL underlying variation in traits in the evaluated diversity panel using the GWAS approach (Oyiga et al., 2019). GY recorded high  $H^2$  across all growing seasons suggesting that selecting for high yielding cultivars for each CS could be simplified in our panel, particularly TKW with  $H^2= 0.84$  were observed under several nitrogen supply experiments (Guttieri et al., 2015).

### 5.5.2. Nitrogen and fungicide application effects on N flow from soil to the grain

Nitrogen and fungicide lead to increased leaf chlorophyll content and grain quality. Under high N input CS, the amount of nitrogen molecule required for the constitution of chloroplasts was satisfied, and sufficient nitrogen would imply high chlorophyll molecules (Tucker, 2004). Besides, nitrogen has large effect on leaf growth, increases leaf area, and the intensity of photosynthesis (Bojović and Marković, 2009). In line with the present study, Bryson et al. (1997) have reported that fungicide sprayed on wheat plants increased chlorophyll content of leaves.

Nitrogen and fungicide are contributing to high GPC and GNY, owing to high N relocation from the shoot to the growing grain (Gooding et al., 2005). Fungicide application increased the grain N accumulation through the improvement of nitrogen uptake from soil, and the remobilization of nitrogen from plant green tissues to the grain (Gregory et al., 2005). We obtained 13.95%, 13.66%, and 11.17% GPC under HN-WF, HN-NF, and LN-NF. However, the standard minimum GPC for bread baking is 12%, which required an amount of 180 kg.ha<sup>-1</sup> fertilized N (Litke et al., 2018). Lowest grain crude protein (GPC) and grain N yield (GNY) recorded under LN-NF CS would indicate a deficiency of most cultivars to remobilize N to the grain in the absence of sufficient nitrogen and fungicide (**Table 5.S15A**). Even under sufficient N, the use of high yielding genotype is a requisite to obtain higher GNY (**Table 5.S15B**). Hawkesford (Hawkesford, 2017) reported that only a third of nitrogen inputs to cereal crops worldwide are recovered in grain for consumption. These findings attest the necessity to breed for cultivars with improved N use efficiency and confirm that high nitrogen supply is not synonymous with high yields. Cultivation of cultivars adapted and selected for low input CS *i.e.* organic farming resulted in improvement of GY under this CS (Reganold and Wachter, 2016). However, growing of less N uptake efficient cultivars will result in high amount of residual N. Likewise, higher GNY obtained under HN-WF compared to HN-NF although they had the same amount of N indicated the existence of important residual N that was not removed from HN-NF.

Ladha et al. (2016) reported that wheat harvested total N comprised 48% of applied fertilizer N and 52% of other source like non-symbiotic N<sub>2</sub> fixation (24%), manure (14%), and atmospheric deposition (6%). Therefore, almost half of 155, 165 and 135 kg.ha<sup>-1</sup> N fertilizer applied in 2015, 2016, and 2017, respectively (**Tables 5.S2**) were recovered in grain, resulting in a loss of 80.6 , 85.8 and 70.2 kg.ha<sup>-1</sup> N fertilizer in the agro ecosystem that later can undergo N leaching, runoff or erosion (Reganold and Wachter, 2016). Nitrogen loss from N fertilizer is increasing with the increasing amount of applied fertilizers (Reganold and Wachter, 2016). (Angus, 2001) reported ~20 kg.ha<sup>-1</sup> N (including all sources of N) is needed to produce one tone of wheat grain, and 6 kg.ha<sup>-1</sup> N for one tone of straw production. According to this benchmark of 20 kg.ha<sup>-1</sup> N, under our field conditions, a total of 25.86 and 21.07 kg.ha<sup>-1</sup> N was utilized to produce one tone of grain out of the available 220 kg.ha<sup>-1</sup> N for HN-NF and HN-WF,

respectively, whereas 9.56 kg.ha<sup>-1</sup> N was utilized out of 65.43 kg.ha<sup>-1</sup> for LN-NF (**Table 5.S15c**). Therefore, higher amount of N under HN-NF was required N to produce the same quantity of grain compared to HN-WF and LN-NF, showing low NUE under HN-NF. Moreover, nitrogen loss in the agro-ecosystem following over fertilization which decreased the NUE is reported (Hawkesford, 2017). In a previous report on global nitrogen budgets in cereals, total amount of N input in the agro-ecosystem consisted of 51% of N fertilizer, 15% and 19% of biological fixation and manure, respectively, followed by crop residue (8%) and deposition (about 7%). Considering the importance of N in increasing GY and the environmental damage following huge N rate application, combining N application with fungicide (May et al., 2020), using the optimum amount of N (Ma et al., 2019) or exploring other sources of N like biological N<sub>2</sub> has lately raised interest in agriculture (Roper and Gupta, 2016). The estimates of NAE was significantly higher under HN-WF when compared to the HN-NF, implying that fungicide had an increasing effect on NAE, and that demonstrates a synergic effect of N and F on cultivars performance to produce grain.

A trade-off relationship was observed between GY and grain protein content (GPC). The negative correlation between GY and grain quality parameters, particularly GPC is well known and constitute a constraint in breeding for high GPC and GY (KOKSAL et al., 2007). Genetic factors may be responsible for the undesirable associations between these traits (Stuber et al., 1962; Miezani et al., 1977). That could be a consequence of a dilution effect that caused a reduction in GPC as yield increased (Guttieri et al., 2015). To select high GY while maintaining high GPC, the deviation from the GPC–yield relationship (GPD) has been suggested as a metric for selection (Oury and Godin, 2007). The GPD is related to post-anthesis N uptake, and might be associated to genotypic differences in access to soil N (Bogard et al., 2010). Under low N CS, nitrogen would primarily be allocated to GY, which was a primary breeding goal in cereals during last decades (Michel et al., 2019). However, eleven cultivars comprising three new released and six old cultivars, and two unknown released years were among the low yielding cultivars and had their GPC 12.14%, 14.40, and 15.03% under LN-NF, HN-NF, and HN-WF, respectively.

### **5.5.3. Agronomic traits contribution to GY across cropping systems**

Most of the agronomic traits exhibited higher indirect effects than direct effects on GY, except HI under the three CS and biomass under HN-NF and HN-WF, which direct effects were significantly higher as previously reported (Mansouri et al., 2018). Our results revealed that GY was more influenced by kernels number per m<sup>2</sup> rather than kernels' weight and number of spikes among its components, independently of the CS. Nevertheless, Mansouri et al. (2018) reported spikes number as the most significant variable, influencing GY under south Mediterranean conditions. However, low correlation observed between spikes number and GY in some cases is due to the number of infertile florets on spikes (Royo et al.,

2007). The delay in HD was beneficial to high GY under the three CS, importantly under LN-NF. Early HD of a genotype may lead to early maturity, which is a limiting factor for high GY due to reduced time period for assimilates translocation to the grain. Increased GY obtained from late heading cultivars are attributed to the increased number of fertile florets as a result of higher assimilate accumulation during the pre-flowering period (Royo et al., 2007).

SPAD index measured at heading growth stage as an indication of leaf nitrogen content was positively correlated with GY as reported in several studies (Islam et al., 2014; Sanchez-Bragado et al., 2014). The variation in the leaf chlorophyll content highly explained the variation in GY under LN-NF, and cultivars with higher SPAD obtained higher GY under this CS. These results showed that leaf chlorophyll content under low nitrogen is a physiological indicator to select nitrogen uptake and utilization efficient cultivars.

GY was negatively correlated with the susceptibility of cultivars to YR infestation, consistently across CS. Similarly to our results, it has been reported that YR disease is a major cause of wheat yield loss worldwide (Chen et al., 2014). Although, YR infestation under HN-NF was lower compared to LN-NF, its effect on GY reduction under the former was greater. Similarly, previous research reported significant negative effects of YR on GY under high nitrogen input CS. High nitrogen increases crop size and canopy density, which creates favorable conditions for YR invasion (Danial and Parlevliet, 1995; Bryson et al., 1997). To control the negative effect of YR and other diseases (Gregory et al., 2005) suggested the use of fungicide, and the use of YR tolerant cultivars is a valuable resource to increase GY.

#### 5.5.4. Breeding progress in agronomic traits and yield stability across cropping systems

The regression results together with the correlation between traits and genotype release year provide evidence that breeding has enhanced genotype performance not only under optimal conditions but under production systems with reduced agrochemical inputs. Breeding has accumulated genetic variants conferring favorable effects on key yield parameters, photosynthetic activity, and disease resistance, which subsequently have enhanced GY (Voss-Fels et al., 2019). GY was negatively correlated with PH, which can be due to the reduction in PH through incorporating the dwarfing genes (*Rht1 (Rht-B1b)*, *Rht2 (Rht-D1b)*, *Rht-D1c*, and *Rht8*) in modern high yielding cultivars (Mashilo et al., 2019).

The contribution of breeding to GY was not related to the increase in HD, because as opposed to GY, day to heading has not been increased in the breeding history, even though, a strong correlation occurred between vegetation duration with high GY. Although not shown, our results revealed a low decline in the shoot dry weight over years. Similarly, it has been reported that breeding improved GY by increasing the HI through allocation of resource to grain number per m<sup>2</sup> rather than shoot biomass production (Maeoka et al., 2020). Despite significant, the breeding progress in TKW was lower compared to other yield components. Similar results were found by Lichthardt (Lichthardt et al., 2020), reporting that TKW is not affected by breeding, unlike other traits such as green canopy duration and other source components that have increasing effects on GY.

The highest yielding cultivars across CS comprised only three old and 43 recently released cultivars registered in/or after 2000. This result highlighted the tremendous role played by breeding in increasing GY. These improved cultivars showed differences in their stability levels under the three CS, indicating high interaction G\*CS, and support the necessity to use convenient cultivars for targeted CS. Kadhem and Baktash (Kadhem and Baktash, 2016) have reported that selecting for promising cultivars must include the criteria of high yield and the stability performance of the genotype, because some cultivars may be high yielding but unstable across growing seasons and/or CS. We defined least discriminative CS as the one with most cultivars having their GY means closed the highest yielding genotype, hence a CS with performance index ( $P_{cs}$ ) close to zero. HN-NF was the most discriminative CS, indicating that most cultivars could not make use of the available nitrogen fertilizer. Under HN-NF CS, N use efficient cultivars are more likely to achieve high yield. It has been recommended to use superior cultivars for the best use of the available nitrogen and other resources to avoid resource waste (Kaggwa, 2013).

The results of AMMI analysis are very useful in determining specific adaptation, genotype stability, and choice of the best CS (Gauch Jr, 2006; Zhe et al., 2010). The association of LN-NF and HN-NF into one mega CS could be explained by the absence of fungicide which was a determinant factor in the agronomy efficiency use of nitrogen. Under these two CS, many cultivars could not adequately use the available nitrogen and express their yielding potential. Further study should be done with several nitrogen

application levels to identify the optimum level of N input to obtain better GY and grain quality as 65.43 kg.ha<sup>-1</sup> was too low, while 220 kg.ha<sup>-1</sup> was too high.

## 5.6. Conclusion

The present study revealed that the leaf chlorophyll content measured by SPAD meter around heading growth stage could serve as a proxy to estimate GY under low nitrogen conditions. The results showed that nitrogen and fungicides have synergistic effects on GY production and grain protein content (GPC). In the absence of fungicide application, YR highly decreased GY, mostly under high nitrogen input CS. Under our field conditions, most cultivars obtained an average GY close to the cultivars with maximal yield under LN-NF and HN-WF compared to HN-NF. HN-NF was more selective in GY production as few cultivars were close to the highest yielding cultivar. HN-WF achieved the best GY production because of fungicide that played an important role in extending plant life cycle, and photosynthesis activity. Among 46 high performing cultivars used in the stability analysis, 19, 14, and 10 cultivars were stable under HN-NF, HN-WF, and LN-NF, respectively. The leaf chlorophyll content and the cultivar resilience to YR infection played an important in enhancing GY. Therefore, selection for these traits and identification of genetic factor underlying them could be considered in wheat breeding program in future genetic studies to improve GY. The AMMI Analysis confirmed the discriminating power of HN-NF, indicating that fewer cultivars could make use of the additional fertilizer. These results suggest and recommend the cultivation of nitrogen use efficient cultivars, and to associate different nitrogen levels with fungicide to maximize nitrogen use and avoid resource waste. New breeding strategies for high GY should promote selection of cultivars for specific CS *i.e.* for high and low input CS, and include leaf chlorophyll content and resilience to YR as selection criteria. Released cultivars should be labeled with their NUE level and its favorable CS to enable organic or conventional agriculture farmers make a better choice when growing a cultivar.

## **Chapter 6**

### **General Discussion**

Drought is the major abiotic stress factor causing prominent yield losses in wheat due to its effects on plant water and nutrients uptake (Mohammadi, 2018). Nitrogen (N) is the most important nutrient for plants to maintain high yield (McElrone et al., 2013b; Nezhadahmadi et al., 2013). Developing drought tolerant genotypes with an efficient utilization of nitrogen is the most promising strategy to increase wheat GY under the new environmental constraints imposed by water deficit and regulations to reduce N fertilization. The available genetic variability could help to evaluate plants traits in response to drought and to select tolerant genotypes that could serve as parents in breeding programs. The main aim of this study was to evaluate the phenotypic variation for agronomic, photosynthesis-related and grain quality traits under effect of drought, to highlight the breeding progress on these traits in the last 70 years and link the observed traits variations to genetic region using GWAS. Knowing the complexity of drought tolerance which depends not only on the plant physiology, genetics and molecular mechanisms but also on the growth stage of at which the stress occurs, stress tolerance evaluation should be considered at different developmental stage in a breeding program (Sallam et al., 2019). To the best of our knowledge, this is the first study of drought-N stress tolerance that includes different types of traits such as agronomic and photosynthesis-related. Besides, the study considers the breeding history of the germplasm, coupled with GWAS in winter wheat to identify drought tolerant genotypes, drought responsive QTL and genomic regions regulating N stress tolerance.

#### **6.1. Drought stress has reduced plant agronomic performance by reducing photosynthesis efficiency**

In chapter 2, we found that drought reduced plant performance, from stem elongation to grain filling growth stages, resulting in a reduction of key yield components and grain yield. This reduction was especially important for grain number per meter square. Likewise, drought has significantly decreased the number of tillers compared to rainfed conditions. The reduction of this key yield component explained the lower GY under drought. Our results were in line with previous studies reporting that yield reduction under drought was due to the cumulative effects it exerts on yield-related traits (Farooq et al., 2014a; Mohammadi, 2018; Sallam et al., 2019). A possible explanation for the reduction of key yield components, is the increase of infertile florets under drought conditions due to the increase of abscisic acid (ABA) concentration in the spike, which led to an increased seed abortion (Weldearegay et al., 2012). Also, the photosynthesis efficiency of the genotypes under drought plays a significant role in grain

filling, thus on the seed set. Oxidative damage of chloroplast and stomatal closure under drought would reduce net photosynthesis activity (Farooq et al., 2014). To find out at which growth stage the photosynthesis efficiency mostly influenced yield and its components, we evaluated in chapter 3 the dynamic of the photosynthesis access growth stages. We found that photosynthetic-related traits measured at post-anthesis, such as the effective quantum yield of photosystem II (PSII), the maximum quantum yield of PSII, and NPQ, had strong correlation with the final aboveground yield (i.e. GY and plant biomass weight). Similar results were found in a previous study, highlighting the importance of photosynthesis efficiency during grain filling for higher yield (Evans et al., 1975; Méndez-Espinoza et al., 2019).

## **6.2. Breeding has increased yield through improving photosynthesis performance over years**

We estimated the breeding progress for each trait of interest through regression analysis. The use of linear regression algorithm to calculate the breeding progress has been previously used to determine the genetic gain over years of breeding (Sharma et al. 2012, Voss-Fels et al. 2019, Lichthardt et al. 2020). For agronomic traits in chapter 2 and for photosynthesis related traits in chapter 3, newly released genotypes have shown better performance than older released ones. Contrary to most traits, the shoot dry weight has decreased over year of breeding, while the GY have and the harvest index have been increased. The increase in the harvest index is the result of the improvement of the photosynthetic machinery, the green canopy duration, and the radiation use efficiency (Tian et al., 2011; Lichthardt et al., 2020). This improvement in plant physiological features resulted in the improvement of key yield components such as kernel number, tiller number, and consequently the grain yield as previously reported (Sanchez-Garcia et al., 2015; Würschum et al., 2018). The higher performance of recently released genotypes was not only observed under optimal conditions, but also under drought or reduced N input as shown in chapter 5. Similar to the study of Voss-Fels et al.(2019), we found out that the genetic improvement of wheat to maintain high yield under environmental constraint is due to the increment of genetic regions and alleles with increased effect on grain yield, whereas detrimental alleles have been reduced or lost over breeding.

## **6.3. Population structure and linkage disequilibrium pattern**

The identification of the structure of a population, including the number of subpopulations in the GWAS model, enables to control false positives and reduce spurious marker-traits associations (Haldar and Ghosh, 2012; Dodig et al., 2012; Zhao et al., 2014). In chapter 3, we identified two main sub-populations through the STRUCTURE algorithm and PCA analyses that were implemented based on SNP markers data. The cultivars were clustered according to their geographic origin as European or non-European, and

additionally there was an admixture group between both sub-populations. The  $F_{ST}$  values among cultivars originating from Europe was weak ( $F_{ST}=0.3133$ ), while the one outside Europe was weaker ( $F_{ST}=0.0745$ ). These results are an indication of high genetic diversity in this panel due to germplasm exchange among breeding programs, limited selection pressure and genetic drift (Chao et al., 2017; UPOV, 1991). The low intra-population  $F_{ST}$  values suggested a weak population structure in the evaluated panel and suggests that the genotypes in both subpopulations share a high number of alleles. Assessing the population structure of a diversity panel is relevant to minimize the occurrence of spurious or false-positive associations (Gajardo et al., 2015). Therefore, we included the three first principal components of PCA as the population structure matrix and a kinship matrix in the mixed model for association mapping. The LD from genome B decayed after 38 Mbp, which was slower than for A (19.0 Mbp) and D (17.5 Mbp) genomes. Similar trend in the LD decay was found in an earlier study performed with the same germplasm genotyped with a 15K SNP chip set (Voss-Fels et al., 2019).

#### **6.4. Genome wide association scan analysis**

GWAS for agronomic, photosynthesis, and NUE-traits were performed under rainfed and drought regimes to identify chromosomal regions associated with the observed trait variation. Moreover, the added value of our study was the identification of genomic regions associated with the breeding history through GWAS. The inclusion of the population structure (PCA matrix) and relatedness (kinship matrix) in the GWAS multilocus mixed linear model (Zhao et al., 2007), has improved our mapping resolution and reduced the detection of false positives. We excluded from the genotypic dataset all the alleles that had less than 5% of minor allele frequency (Dadshani et al., 2021), as these rare variants are more likely to result in the detection of false positives in the GWAS (Broer et al., 2015; Abondio et al., 2019). We performed GWAS using TASSEL software and rrBLUP package in R, and reported only congruently detected marker-traits association from both analyses, which is beneficial for the detection of true positives (Oyiga, 2017). The SNP-clustering method adopted in this study enabled the identification of hotspot QTL regions linked to trait variation. In each chapter, one of the objectives was to dissect the genetic architecture underlying the traits of interest. These results were presented and discussed in chapters 2, 3, and 4 highlighting the important genomic regions associated with phenotypic variations. In chapter 2, significant MTAs for breeding history (i.e. release year) were found on chromosomes 3A and 5D. The SNPs associated with this trait were in a LD block and have exerted pleiotropic effects on grain starch content under drought conditions. Change of allele frequency over years of breeding confirmed the increment of favorable alleles and the loss of detrimental alleles for starch accumulation. This result is in line with a previous study using the same population (Voss-Fels et al., 2019). An added value of our study was the estimation of markers by treatment interactions effects, and SNP-SNP epistatic interactions,

which rarely are included on GWAS models. An added value of our study was the estimation of markers by treatment interactions effects, and SNP-SNP epistatic interactions analyzed with Proc mixed SAS. That is very unique and few studies adopting such approaches were found in the literature. The classic GWAS model that analyzed the marker by treatment effect, confirmed that chromosome 3A harbors drought-responsive alleles.

### **6.5. Candidate gene in the region of associated polymorphisms**

The *in-silico* analysis of the DNA sequence harboring detected MTAs has facilitated the discovery of high confident genes controlling drought stress tolerance and plant abiotic stress responses. Most of the detected QTL regions co-located with genes involved in the regulation of metabolic processes. The transcription factor family WRKY is known to mediate several abiotic processes. One member of that family was found in the genomic region (chromosome 5D) associated with breeding progress. WRKY transcription factors *TaWRKY1* and *TaWRKY33* have been reported to enhance drought tolerance in wheat and tobacco (Wang et al., 2013; He et al., 2016; Kulkarni et al., 2017). The linkage block associated with breeding progress on chromosome 5D contained genes involved in photosynthesis activity categories such as protein disulfide oxidoreductase activity, electron carrier activity and PSII reaction center protein complex. In chapter 3, genes involved in cellulose synthase, serine acetyltransferase, NADH dehydrogenase (ubiquinone) activity, and from the WRKY family were discovered in the vicinity of the SNP *AX-158576783* on chromosome 3A. This region from 515.741 to 516.804 Mbp also included novel candidate loci for photosynthesis activity. The presence of these genes in pleiotropic QTL regions with effects on breeding progress, agronomic traits or photosynthesis related traits, can explain the contribution of the favorable alleles in that region to higher yields under drought conditions as shown in chapter 3. In chapter 4, GWAS coupled with the analysis of transcript abundance from candidate genes targeted loci on chromosome 1B and 5A in haplotype blocks associated with higher NUE under drought conditions.

In conclusion, the present study has demonstrated that the available genetic variation can be successfully used to breed for drought tolerance and NUE. In chapter 2, we showed that there is significant genetic variation in the studied germplasm in response to drought for agronomic traits. Our first hypothesis under study was accepted. Similarly, in the chapter 3, we tested the hypothesis of significant genetic variation for the photosynthesis efficiency. It has been found significant differences among evaluated cultivars for photosynthesis efficiency, both under drought and rainfed conditions. We identified post-anthesis as the growth stage where plant photosynthetic efficiency significantly affects the final aboveground yield. In the whole study, we analyzed the contribution of breeding to drought tolerance. We found breeding has contributed to genetic gain in traits partly due to the accumulation of genetic regions with favorable alleles and the loss of deleterious alleles. We proved that alleles whose frequencies have been increased

over years showed higher allelic effect on traits than deleterious alleles. The drought/nitrogen SWP index calculated for each trait was useful to select the most drought-tolerant and drought-sensitive genotypes of the wheat panel at the phenotypic level. Subsequent GWAS performed for traits of interest identified relevant QTL regions. The exploration of candidate genes within QTL intervals identified the presence of transcriptions factors of drought responsive genes, which are genetic factors explaining drought tolerance. Further allelic variation analysis in the promoter regions of the gene *TraesCS3A02G287600* coding an NADH-ubiquinone oxidoreductase activity which in the vicinity of the SNP marker *AX-158576783* contributed to higher photosynthesis activity. The presense of polymorphic sites in the binding sites of transcriptions factors in the promoter regions of this gene might explain the lower photosynthesis in both sensitive genotypes. Upon validation at the expression level, this locus can be used to develop genotypes with higher photosynthesis and hence higher GY under drought conditions. In chapter 4 and 5, we tested and acted the hypothesis of existence of genetic variation for NUE. We showed that NUE is affected by the N and/or fungicide supply in the agrosystem. Moreover, water limitation in soil had significant effect on NUE. The discovery of genetic regions associated with high NUE under drought stress conditions (chapter 4) is of great importance to improve simultaneously NUE and drought tolerance.

## References

- Abondio, P., Sazzini, M., Garagnani, P., Boattini, A., Monti, D., Franceschi, C., et al. (2019). The genetic variability of APOE in different human populations and its implications for longevity. *Genes* 10, 222.
- Abrahám, E., Rigó, G., Székely, G., Nagy, R., Koncz, C., and Szabados, L. (2003). Light-dependent induction of proline biosynthesis by abscisic acid and salt stress is inhibited by brassinosteroid in *Arabidopsis*. *Plant Mol. Biol.* 51, 363–372.
- Abreu, J. D. M., Flores, I., De Abreu, F., and Madeira, M. (1993). Nitrogen uptake in relation to water availability in wheat. *Plant Soil* 154, 89–96.
- Afsharyan, N. P., Sannemann, W., León, J., and Ballvora, A. (2020). Effect of epistasis and environment on flowering time in barley reveals a novel flowering-delaying QTL allele. *J. Exp. Bot.* 71, 893–906.
- Allahyari, M. S., Poursaeed, A., and Branch, R. (2019). Sustainable Agriculture: Implication for SDG2 (Zero Hunger).
- Alqudah, A. M., Haile, J. K., Alomari, D. Z., Pozniak, C. J., Kobiljski, B., and Börner, A. (2020). Genome-wide and Snp network analyses reveal genetic control of spikelet sterility and yield-related traits in wheat. *Sci. Rep.* 10, 1–12.
- Alsina, M. M., Smart, D. R., Bauerle, T., De Herralde, F., Biel, C., Stockert, C., et al. (2010). Seasonal changes of whole root system conductance by a drought-tolerant grape root system. *J. Exp. Bot.* 62, 99–109.
- Angus, J. (2001). Nitrogen supply and demand in Australian agriculture. *Aust. J. Exp. Agric.* 41, 277–288.
- Anjum, F., Yaseen, M., Rasul, E., Wahid, A., and Anjum, S. (2003). Water stress in barley (*Hordeum vulgare* L.). II. Effect on chemical composition and chlorophyll contents. *Pak J Agric Sci* 40, 45–49.
- Apha (1985). *Standard methods for the examination of water and wastewater*. Apha.
- Araus, J., Amaro, T., Casadesus, J., Asbati, A., and Nachit, M. (1998). Relationships between ash content, carbon isotope discrimination and yield in durum wheat. *Funct. Plant Biol.* 25, 835–842.
- Araus, J. L., Slafer, G. A., Royo, C., and Serret, M. D. (2008). Breeding for yield potential and stress adaptation in cereals. *Crit. Rev. Plant Sci.* 27, 377–412.
- Asada, K. (2006). Production and scavenging of reactive oxygen species in chloroplasts and their functions. *Plant Physiol.* 141, 391–396.

- Ashraf, A., Rehman, O. U., Muzammil, S., León, J., Naz, A. A., Rasool, F., et al. (2019). Evolution of Deeper Rooting 1-like homoeologs in wheat entails the C-terminus mutations as well as gain and loss of auxin response elements. *PLoS One* 14, e0214145.
- Ashraf, M. (2010). Inducing drought tolerance in plants: Recent advances. *Biotechnol. Adv.* 28, 169–183. doi:10.1016/j.biotechadv.2009.11.005.
- Atwell, S., and Huang, Y. (2010). vilhjalmsjon BJ, willems G. Horton M Li Meng Platt Tarone AM Hu TT Jiang R Mulyati Nw Zhang X Amer MA Baxter Brachi B Chory J Dean C Debieu M Meaux J Ecker JR Faure N Kniskern JM Jones JD Michael T Nemri Roux F Salt Tang C Todesco M Traw MB Weigel Marjoram P Borevitz JO Bergelson J Nord. *M*, 627–631.
- Baker, N. R. (2008). Chlorophyll fluorescence: a probe of photosynthesis in vivo. *Annu Rev Plant Biol* 59, 89–113.
- Baker, N. R., and Rosenqvist, E. (2004). Applications of chlorophyll fluorescence can improve crop production strategies: an examination of future possibilities. *J. Exp. Bot.* 55, 1607–1621.
- Balla, K., Bencze, S., Bónis, P., Árendás, T., and Veisz, O. (2014). Changes in the photosynthetic efficiency of winter wheat in response to abiotic stress. *Cent. Eur. J. Biol.* 9, 519–530.
- Barnabás, B., Jäger, K., and Fehér, A. (2008). The effect of drought and heat stress on reproductive processes in cereals. *Plant Cell Environ.* 31, 11–38.
- Barracough, P. B., Lopez-Bellido, R., and Hawkesford, M. J. (2014). Genotypic variation in the uptake, partitioning and remobilisation of nitrogen during grain-filling in wheat. *Field Crops Res.* 156, 242–248.
- Basu, S., Ramegowda, V., Kumar, A., and Pereira, A. (2016). Plant adaptation to drought stress [version 1; referees: 3 approved]. *F1000Research* 5, 1–10. doi:10.12688/F1000RESEARCH.7678.1.
- Baum, M., Tadesse, W., Nachit, M., Abdalla, O., Rajaram, S., Singh, R., et al. (2015). “Global crop improvement networks to bridge technology gaps,” in *Advances in Wheat Genetics: From Genome to Field* (Springer, Tokyo), 387–399.
- Begum, H., Alam, M. S., Feng, Y., Koua, P., Ashrafuzzaman, M., Shrestha, A., et al. (2020). Genetic dissection of bread wheat diversity and identification of adaptive loci in response to elevated tropospheric ozone. *Plant Cell Environ.*
- Benjamini, Y., and Hochberg, Y. (1995). Controlling the false discovery rate: a practical and powerful approach to multiple testing. *J. R. Stat. Soc. Ser. B Methodol.* 57, 289–300.
- Bi, H., Kovalchuk, N., Langridge, P., Tricker, P. J., Lopato, S., and Borisjuk, N. (2017). The impact of drought on wheat leaf cuticle properties. *BMC Plant Biol.* 17, 1–13.
- Blum, A. (2005). Drought resistance, water-use efficiency, and yield potential—are they compatible, dissonant, or mutually exclusive? *Aust. J. Agric. Res.* 56, 1159–1168. doi:10.1071/AR05069.

- Bogard, M., Allard, V., Brancourt-Hulmel, M., Heumez, E., Machet, J.-M., Jeuffroy, M.-H., et al. (2010). Deviation from the grain protein concentration–grain yield negative relationship is highly correlated to post-anthesis N uptake in winter wheat. *J. Exp. Bot.* 61, 4303–4312.
- Bojović, B., and Marković, A. (2009). Correlation between nitrogen and chlorophyll content in wheat (*Triticum aestivum* L.). *Kragujev. J. Sci.* 31, 69–74.
- Börner, A., Plaschke, J., Korzun, V., and Worland, A. (1996). The relationships between the dwarfing genes of wheat and rye. *Euphytica* 89, 69–75.
- Borrill, P., Ramirez-Gonzalez, R., and Uauy, C. (2016). expVIP: a customizable RNA-seq data analysis and visualization platform. *Plant Physiol.* 170, 2172–2186.
- Boyer, J. S. (1982). Plant productivity and environment. *Science* 218, 443–448.
- Boyer, J., and Westgate, M. (2004). Grain yields with limited water. *J. Exp. Bot.* 55, 2385–2394.
- Bradbury, P. J., Zhang, Z., Kroon, D. E., Casstevens, T. M., Ramdoss, Y., and Buckler, E. S. (2007). TASSEL: software for association mapping of complex traits in diverse samples. *Bioinformatics* 23, 2633–2635.
- Braun, H.-J., Atlin, G., and Payne, T. (2010). Multi-location testing as a tool to identify plant response to global climate change. *Clim. Change Crop Prod.* 1, 115–138.
- Bray, E. A. (1997). Plant responses to water deficit. *Trends Plant Sci.* 2, 48–54.
- Bray, E. A. (2000). Response to abiotic stress. *Biochem. Mol. Biol. Plants*, 1158–1203.
- Breseghello, F., and Sorrells, M. E. (2006). Association mapping of kernel size and milling quality in wheat (*Triticum aestivum* L.) cultivars. *Genetics* 172, 1165–1177.
- Broer, L., Buchman, A. S., Deelen, J., Evans, D. S., Faul, J. D., Lunetta, K. L., et al. (2015). GWAS of longevity in CHARGE consortium confirms APOE and FOXO3 candidacy. *J. Gerontol. Ser. Biomed. Sci. Med. Sci.* 70, 110–118.
- Bryson, R., Paveley, N., Clark, W., Sylvester-Bradley, R., and Scott, R. (1997). “Use of in-field measurements of green leaf area and incident radiation to estimate the effects of yellow rust epidemics on the yield of winter wheat,” in *Developments in Crop Science* (Elsevier), 77–86.
- Buckwell, A., and Nadeu, E. (2016). Nutrient recovery and reuse (NRR) in European agriculture. *Rev. Issues Oppor. Actions RISE Found. Bruss.*
- Byrne, P. F., Volk, G. M., Gardner, C., Gore, M. A., Simon, P. W., and Smith, S. (2018). Sustaining the future of plant breeding: The critical role of the USDA-ARS National Plant Germplasm System. *Crop Sci.* 58, 451–468.
- Cai, W.-J., Hu, X., Huang, W.-J., Murrell, M. C., Lehrter, J. C., Lohrenz, S. E., et al. (2011). Acidification of subsurface coastal waters enhanced by eutrophication. *Nat. Geosci.* 4, 766–770.

- Cao, P., Ren, Y., Zhang, K., Teng, W., Zhao, X., Dong, Z., et al. (2014). Further genetic analysis of a major quantitative trait locus controlling root length and related traits in common wheat. *Mol. Breed.* 33, 975–985.
- Carlton, R. R., West, J. S., Smith, P., and Fitt, B. D. (2012). A comparison of GHG emissions from UK field crop production under selected arable systems with reference to disease control. *Eur. J. Plant Pathol.* 133, 333–351.
- Carmo-Silva, A. E., Keys, A. J., Andralojc, P. J., Powers, S. J., Arrabaça, M. C., and Parry, M. A. (2010). Rubisco activities, properties, and regulation in three different C4 grasses under drought. *J. Exp. Bot.* 61, 2355–2366.
- Castiglioni, P., Warner, D., Bensen, R. J., Anstrom, D. C., Harrison, J., Stoecker, M., et al. (2008). Bacterial RNA chaperones confer abiotic stress tolerance in plants and improved grain yield in maize under water-limited conditions. *Plant Physiol.* 147, 446–455.
- Centritto, M., Lauteri, M., Monteverti, M. C., and Serraj, R. (2009). Leaf gas exchange, carbon isotope discrimination, and grain yield in contrasting rice genotypes subjected to water deficits during the reproductive stage. *J. Exp. Bot.* 60, 2325–2339.
- Cericola, F., Jahoor, A., Orabi, J., Andersen, J. R., Janss, L. L., and Jensen, J. (2017). Optimizing training population size and genotyping strategy for genomic prediction using association study results and pedigree information. A case of study in advanced wheat breeding lines. *PloS One* 12, e0169606.
- Chao, S., Dubcovsky, J., Dvorak, J., Luo, M.-C., Baenziger, S. P., Matnyazov, R., et al. (2010). Population- and genome-specific patterns of linkage disequilibrium and SNP variation in spring and winter wheat (*Triticum aestivum* L.). *BMC Genomics* 11, 1–17.
- Chao, S., Rouse, M. N., Acevedo, M., Szabo-Hever, A., Bockelman, H., Bonman, J. M., et al. (2017). Evaluation of genetic diversity and host resistance to stem rust in USDA NSGC durum wheat accessions. *Plant Genome* 10, 1–13.
- Chaves, M. M., Maroco, J. P., and Pereira, J. S. (2003). Understanding plant responses to drought—from genes to the whole plant. *Funct. Plant Biol.* 30, 239–264.
- Chen, W., Wellings, C., Chen, X., Kang, Z., and Liu, T. (2014). Wheat stripe (yellow) rust caused by *Puccinia striiformis* f. sp. *tritici*. *Mol. Plant Pathol.* 15, 433–446.
- Cheuk, A., Ouellet, F., and Houde, M. (2020). The barley stripe mosaic virus expression system reveals the wheat C2H2 zinc finger protein TaZFP1B as a key regulator of drought tolerance. *BMC Plant Biol.* 20, 1–34.

- Chow, C.-N., Lee, T.-Y., Hung, Y.-C., Li, G.-Z., Tseng, K.-C., Liu, Y.-H., et al. (2019). PlantPAN3. 0: a new and updated resource for reconstructing transcriptional regulatory networks from ChIP-seq experiments in plants. *Nucleic Acids Res.* 47, D1155–D1163.
- Christopher, J. T., Christopher, M. J., Borrell, A. K., Fletcher, S., and Chenu, K. (2016). Stay-green traits to improve wheat adaptation in well-watered and water-limited environments. *J. Exp. Bot.* 67, 5159–5172.
- Churko, J. M., Mantalas, G. L., Snyder, M. P., and Wu, J. C. (2013). Overview of high throughput sequencing technologies to elucidate molecular pathways in cardiovascular diseases. *Circ. Res.* 112, 1613–1623.
- Ciampitti, I. A., and Vyn, T. J. (2014). Understanding Global and Historical Nutrient Use Efficiencies for Closing Maize Yield Gaps. *Agron. J.* 106, AGJ2AGRONJ140025. doi:<https://doi.org/10.2134/agronj14.0025>.
- Collard, B. C., Jahufer, M., Brouwer, J., and Pang, E. (2005). An introduction to markers, quantitative trait loci (QTL) mapping and marker-assisted selection for crop improvement: the basic concepts. *Euphytica* 142, 169–196.
- Condon, A. G., Richards, R., Rebetzke, G., and Farquhar, G. (2004). Breeding for high water-use efficiency. *J. Exp. Bot.* 55, 2447–2460.
- Contreras-Soto, R. I., Mora, F., de Oliveira, M. A. R., Higashi, W., Scapim, C. A., and Schuster, I. (2017). A genome-wide association study for agronomic traits in soybean using SNP markers and SNP-based haplotype analysis. *PloS One* 12, e0171105.
- Cooper, M., Messina, C. D., Podlich, D., Totir, L. R., Baumgarten, A., Hausmann, N. J., et al. (2014). Predicting the future of plant breeding: complementing empirical evaluation with genetic prediction. *Crop Pasture Sci.* 65, 311–336.
- Cruz de Carvalho, M. H. (2008). Drought stress and reactive oxygen species: production, scavenging and signaling. *Plant Signal. Behav.* 3, 156–165.
- Czyczyło-Mysza, I., Marcińska, I., Skrzypek, E., Chrupek, M., Grzesiak, S., Hura, T., et al. (2011). Mapping QTLs for yield components and chlorophyll a fluorescence parameters in wheat under three levels of water availability. *Plant Genet. Resour.* 9, 291–295.
- da Silva, E. C., Nogueira, R., da Silva, M. A., and de Albuquerque, M. B. (2011). Drought stress and plant nutrition. *Plant Stress* 5, 32–41.
- Dadshani, S. A. W. (2018). Genetic and physiological characterization of traits related to salinity tolerance in an advanced backcross population of wheat.
- Dadshani, S., Mathew, B., Ballvora, A., Mason, A. S., and León, J. (2021). Detection of breeding signatures in wheat using a linkage disequilibrium-corrected mapping approach. *Sci. Rep.* 11, 1–12.

- Dai, A. (2011). Drought under global warming: a review. *Wiley Interdiscip. Rev. Clim. Change* 2, 45–65.
- Danial, D., and Parlevliet, J. (1995). Effects of nitrogen fertilization on disease severity and infection type of yellow rust on wheat genotypes varying in quantitative resistance. *J. Phytopathol.* 143, 679–681.
- Daryanto, S., Wang, L., and Jacinthe, P.-A. (2016). Global synthesis of drought effects on maize and wheat production. *PloS One* 11, e0156362.
- Daszkowska-Golec, A., and Szarejko, I. (2013). Open or close the gate—stomata action under the control of phytohormones in drought stress conditions. *Front. Plant Sci.* 4, 138.
- Del Pozo, A., Yáñez, A., Matus, I. A., Tapia, G., Castillo, D., Sanchez-Jardón, L., et al. (2016). Physiological traits associated with wheat yield potential and performance under water-stress in a Mediterranean environment. *Front. Plant Sci.* 7, 987.
- Dhanda, S., and Sethi, G. (2002). Tolerance to drought stress among selected Indian wheat cultivars. *J. Agric. Sci.* 139, 319.
- Ding, L., Lu, Z., Gao, L., Guo, S., and Shen, Q. (2018). Is nitrogen a key determinant of water transport and photosynthesis in higher plants upon drought stress? *Front. Plant Sci.* 9, 1143.
- Dodig, D., Zoric, M., Kobiljski, B., Savic, J., Kandic, V., Quarrie, S., et al. (2012). Genetic and association mapping study of wheat agronomic traits under contrasting water regimes. *Int. J. Mol. Sci.* 13, 6167–6188.
- D’Odorico, P., Chiarelli, D. D., Rosa, L., Bini, A., Zilberman, D., and Rulli, M. C. (2020). The global value of water in agriculture. *Proc. Natl. Acad. Sci.* 117, 21985–21993.
- Dudziak, K., Zapalska, M., Börner, A., Szczerba, H., Kowalczyk, K., and Nowak, M. (2019). Analysis of wheat gene expression related to the oxidative stress response and signal transduction under short-term osmotic stress. *Sci. Rep.* 9, 1–14.
- Earl, D. A. (2012). STRUCTURE HARVESTER: a website and program for visualizing STRUCTURE output and implementing the Evanno method. *Conserv. Genet. Resour.* 4, 359–361.
- Endelman, J. B. (2011). Ridge regression and other kernels for genomic selection with R package rrBLUP. *Plant Genome* 4.
- Evanno, G., Regnaut, S., and Goudet, J. (2005). Detecting the number of clusters of individuals using the software STRUCTURE: a simulation study. *Mol. Ecol.* 14, 2611–2620.
- Evans, L., Wardlaw, I., and Fischer, R. (1975). Wheat. p. 101–149. LT Evans (ed.) Crop physiology. Cambridge Univ. Press, New York. *Wheat P 101–149 LT Evans Ed Crop Physiol. Camb. Univ Press N. Y.*
- Fageria, N., and Baligar, V. (2005). Enhancing nitrogen use efficiency in crop plants. *Adv. Agron.* 88, 97–185.

- Fageria, N., De Morais, O., and Dos Santos, A. (2010). Nitrogen use efficiency in upland rice genotypes. *J. Plant Nutr.* 33, 1696–1711.
- Falush, D., Stephens, M., and Pritchard, J. K. (2007). Inference of population structure using multilocus genotype data: dominant markers and null alleles. *Mol. Ecol. Notes* 7, 574–578.
- Fang, C., Ma, Y., Wu, S., Liu, Z., Wang, Z., Yang, R., et al. (2017). Genome-wide association studies dissect the genetic networks underlying agronomical traits in soybean. *Genome Biol.* 18, 1–14.
- Fang, Y., and Xiong, L. (2015). General mechanisms of drought response and their application in drought resistance improvement in plants. *Cell. Mol. Life Sci.* 72, 673–689.
- FAO (2009). How to Feed the World in 2050. *Insights Expert Meet. FAO* 2050, 1–35. doi:10.1111/j.1728-4457.2009.00312.x.
- FAO (2017). *The future of food and agriculture: trends and challenges*. doi:10.4161/chan.4.6.12871.
- FAO (2020). Food and Agriculture Organization of the United Nations.
- FAO (2021). FAOSTAT. *Food Agric. Organ. U. N.* Available at: <http://www.fao.org/faostat/en/#data/QC/visualize>. (Accessed 29 April 2021) [Accessed April 29, 2021].
- Farooq, M., Bramley, H., Palta, J. A., and Siddique, K. H. (2011). Heat stress in wheat during reproductive and grain-filling phases. *Crit. Rev. Plant Sci.* 30, 491–507.
- Farooq, M., Hussain, M., and Siddique, K. H. (2014). Drought stress in wheat during flowering and grain-filling periods. *Crit. Rev. Plant Sci.* 33, 331–349.
- Farooq, M., Wahid, A., Kobayashi, N., Fujita, D., and Basra, S. (2009). “Plant drought stress: effects, mechanisms and management,” in *Sustainable agriculture* (Springer), 153–188.
- Farshadfar, E., Ghasempour, H., and Vaezi, H. (2008). Molecular aspects of drought tolerance in bread wheat (*T. aestivum*). *Pak. J. Biol. Sci. PJBS* 11, 118–122.
- Ferreira, G., and Brown, A. N. (2016). Environmental factors affecting corn quality for silage production. *Adv. Silage Prod. Util.*
- Ferreira, G., Martin, L., Teets, C., Corl, B., Hines, S., Shewmaker, G., et al. (2021). Effect of drought stress on in vitro neutral detergent fiber digestibility of corn for silage. *Anim. Feed Sci. Technol.* 273, 114803.
- Flagella, Z., Giuliani, M. M., Giuzio, L., Volpi, C., and Masci, S. (2010). Influence of water deficit on durum wheat storage protein composition and technological quality. *Eur. J. Agron.* 33, 197–207.
- Fleury, D., Jefferies, S., Kuchel, H., and Langridge, P. (2010). Genetic and genomic tools to improve drought tolerance in wheat. *J. Exp. Bot.* 61, 3211–3222.
- Foulkes, M. J., and Murchie, E. H. (2011). Optimising canopy physiology traits to improve the nutrient-utilization efficiency of crops. *Mol. Basis Nutr. Use Effic. Crops Wiley-Blackwell*, 65–82.

- Francis, T., and Kannenberg, L. (1978). Yield stability studies in short-season maize. I. A descriptive method for grouping genotypes. *Can. J. Plant Sci.* 58, 1029–1034.
- Frei, M. (2015). Breeding of ozone resistant rice: Relevance, approaches and challenges. *Environ. Pollut.* 197, 144–155.
- Friedrich, T. (2015). A new paradigm for feeding the world in 2050 the sustainable intensification of crop production. *Resour. Mag.* 22, 18–18.
- Friso, G., Giacomelli, L., Ytterberg, A. J., Peltier, J.-B., Rudella, A., Sun, Q., et al. (2004). In-depth analysis of the thylakoid membrane proteome of *Arabidopsis thaliana* chloroplasts: new proteins, new functions, and a plastid proteome database. *Plant Cell* 16, 478–499.
- Gajardo, H. A., Wittkop, B., Soto-Cerda, B., Higgins, E. E., Parkin, I. A., Snowdon, R. J., et al. (2015). Association mapping of seed quality traits in *Brassica napus* L. using GWAS and candidate QTL approaches. *Mol. Breed.* 35, 1–19.
- Garnett, T., Conn, V., and Kaiser, B. N. (2009). Root based approaches to improving nitrogen use efficiency in plants. *Plant Cell Environ.* 32, 1272–1283.
- Garnett, T., Plett, D., Heuer, S., and Okamoto, M. (2015). Genetic approaches to enhancing nitrogen-use efficiency (NUE) in cereals: challenges and future directions. *Funct. Plant Biol.* 42, 921–941.
- Gauch Jr, H. G. (2006). Statistical analysis of yield trials by AMMI and GGE. *Crop Sci.* 46, 1488–1500.
- Gautam, T., Saripalli, G., Gahlaut, V., Kumar, A., Sharma, P., Balyan, H., et al. (2019). Further studies on sugar transporter (SWEET) genes in wheat (*Triticum aestivum* L.). *Mol. Biol. Rep.* 46, 2327–2353.
- Ge, S. X., Jung, D., and Yao, R. (2020). ShinyGO: a graphical gene-set enrichment tool for animals and plants. *Bioinformatics* 36, 2628–2629.
- Gerard, G. S., Crespo-Herrera, L. A., Crossa, J., Mondal, S., Velu, G., Juliana, P., et al. (2020). Grain yield genetic gains and changes in physiological related traits for CIMMYT's High Rainfall Wheat Screening Nursery tested across international environments. *Field Crops Res.* 249, 107742.
- Ghanem, M. E., Marrou, H., and Sinclair, T. R. (2015). Physiological phenotyping of plants for crop improvement. *Trends Plant Sci.* 20, 139–144.
- Gill, S. S., and Tuteja, N. (2010). Reactive oxygen species and antioxidant machinery in abiotic stress tolerance in crop plants. *Plant Physiol. Biochem.* 48, 909–930.
- Gilmour, A. R., Thompson, R., and Cullis, B. R. (1995). Average information REML: an efficient algorithm for variance parameter estimation in linear mixed models. *Biometrics*, 1440–1450.

- Gitonga, V. W., Koning-Boucoiran, C. F., Verlinden, K., Dolstra, O., Visser, R. G., Maliepaard, C., et al. (2014). Genetic variation, heritability and genotype by environment interaction of morphological traits in a tetraploid rose population. *BMC Genet.* 15, 146.
- Gonzalez-Dugo, V., Durand, J.-L., and Gastal, F. (2010). Water deficit and nitrogen nutrition of crops. A review. *Agron. Sustain. Dev.* 30, 529–544.
- Good, A. G., and Beatty, P. H. (2011). Fertilizing nature: a tragedy of excess in the commons. *PLoS Biol* 9, e1001124.
- Good, A. G., Shrawat, A. K., and Muench, D. G. (2004). Sources and fates of nitrogen in plants and the environment. *Trends Plant Sci.* 12, 597–605.
- Gooding, M., Gregory, P., Ford, K., and Pepler, S. (2005). Fungicide and cultivar affect post-anthesis patterns of nitrogen uptake, remobilization and utilization efficiency in wheat. *J. Agric. Sci.* 143, 503–518.
- Gooding, M. J., and Davies, W. P. (1997). *Wheat production and utilization: systems, quality and the environment*. CAB international.
- Gregersen, P. L. (2011). Senescence and nutrient remobilization in crop plants. *Mol. Physiol. Basis Nutr. Use Effic. Crops*, 83–102.
- Gregory, P. J. (2004). Agronomic approaches to increasing water use efficiency. *Water Use Effic. Plant Biol.*, 142–170.
- Gregory, P. J. (2011). Crop root systems and nutrient uptake from soils. *Mol. Physiol. Basis Nutr. Use Effic. Crops John Wiley Sons Inc Chichester UK*, 21–45.
- Gregory, P. J., Gooding, M., Ford, K., Clarke, M. P., and Pepler, S. (2005). Managing roots, nitrogen and fungicides to improve yield and quality of wheat. *HGCA Proj. Rep.* 359.
- Gu, Z., Gu, L., Eils, R., Schlesner, M., and Brors, B. (2014). circlize implements and enhances circular visualization in R. *Bioinformatics* 30, 2811–2812.
- Gupta, P., Balyan, H., Gahlaut, V., and Kulwal, P. (2012). 2 Phenotyping, Genetic Dissection, and Breeding for Drought and Heat Tolerance in Common Wheat: Status and Prospects. *Plant Breed. Rev.* 36, 85.
- Gupta, P. K., Balyan, H. S., and Gahlaut, V. (2017). QTL analysis for drought tolerance in wheat: present status and future possibilities. *Agronomy* 7, 5.
- Guttieri, M. J., Baenziger, P. S., Frels, K., Carver, B., Arnall, B., and Waters, B. M. (2015). Variation for grain mineral concentration in a diversity panel of current and historical Great Plains hard winter wheat germplasm. *Crop Sci.* 55, 1035–1052.
- Hailu, D., and Fininsa, C. (2007). Epidemics of stripe rust (*Puccinia striiformis*) on common wheat (*Triticum aestivum*) in the highlands of Bale, southeastern Ethiopia. *Crop Prot.* 26, 1209–1218.

- Haldar, T., and Ghosh, S. (2012). Effect of population stratification on false positive rates of population-based association analyses of quantitative traits. *Ann. Hum. Genet.* 76, 237–245.
- Hall, D., Tegström, C., and Ingvarsson, P. K. (2010). Using association mapping to dissect the genetic basis of complex traits in plants. *Brief. Funct. Genomics* 9, 157–165.
- Han, M., Okamoto, M., Beatty, P. H., Rothstein, S. J., and Good, A. G. (2015). The genetics of nitrogen use efficiency in crop plants. *Annu Rev Genet* 49, 269–289.
- Han, M., Wong, J., Su, T., Beatty, P. H., and Good, A. G. (2016). Identification of nitrogen use efficiency genes in barley: searching for QTLs controlling complex physiological traits. *Front. Plant Sci.* 7, 1587.
- Harding, S. A., Guikema, J. A., and Paulsen, G. M. (1990). Photosynthetic decline from high temperature stress during maturation of wheat: I. Interaction with senescence processes. *Plant Physiol.* 92, 648–653.
- Harris, D., Tripathi, R., and Joshi, A. (2002). On-farm seed priming to improve crop establishment and yield in dry direct-seeded rice. *Direct Seeding Res. Strateg. Oppor. Int. Res. Inst. Manila Philipp.*, 231–240.
- Hassan, H., Alatawi, A., Abdulmajeed, A., Emam, M., and Khattab, H. (2021). Roles of Si and SiNPs in Improving Thermotolerance of Wheat Photosynthetic Machinery via Upregulation of PsbH, PsbB and PsbD Genes Encoding PSII Core Proteins. *Horticultrae* 2021, 7, 16.
- Hawkesford, M. J. (2017). Genetic variation in traits for nitrogen use efficiency in wheat. *J. Exp. Bot.* 68, 2627–2632.
- Hawkesford, M. J., Araus, J., Park, R., Calderini, D., Miralles, D., Shen, T., et al. (2013). Prospects of doubling global wheat yields. *Food Energy Secur.* 2, 34–48.
- He, Y., Mao, S., Gao, Y., Zhu, L., Wu, D., Cui, Y., et al. (2016). Genome-wide identification and expression analysis of WRKY transcription factors under multiple stresses in *Brassica napus*. *PLoS One* 11, e0157558.
- Hedden, P. (2003). The genes of the Green Revolution. *TRENDS Genet.* 19, 5–9.
- Hirel, B., Lea, P. J., Hawkesford, M., and Barraclough, P. (2011). The molecular genetics of nitrogen use efficiency in crops. *Mol. Physiol. Basis Nutr. Use Effic. Crops*, 139–164.
- Hoerling, M., Eischeid, J., and Perlwitz, J. (2010). Regional precipitation trends: Distinguishing natural variability from anthropogenic forcing. *J. Clim.* 23, 2131–2145.
- Hoseinlou, S. H., Ebadi, A., Ghaffari, M., and Mostafaei, E. (2013). Nitrogen use Efficiency under Water Deficit Condition in Spring Barley. 4, 3681–3687.
- Hu, H., and Xiong, L. (2014). Genetic engineering and breeding of drought-resistant crops. *Annu. Rev. Plant Biol.* 65, 715–741.

- Huang, C. Y., Kuchel, H., Edwards, J., Hall, S., Parent, B., Eckermann, P., et al. (2013). A DNA-based method for studying root responses to drought in field-grown wheat genotypes. *Sci. Rep.* 3, 1–7.
- Hussain, H. A., Hussain, S., Khaliq, A., Ashraf, U., Anjum, S. A., Men, S., et al. (2018). Chilling and drought stresses in crop plants: implications, cross talk, and potential management opportunities. *Front. Plant Sci.* 9, 393.
- IPCC (2014). Synthesis report summary chapter for policymakers. *IPCC Geneva Switz.* 31.
- Islam, M. R., Haque, K. S., Akter, N., and Karim, M. A. (2014). Leaf chlorophyll dynamics in wheat based on SPAD meter reading and its relationship with grain yield. *Sci. Agric.* 8, 13–18.
- IWGSC, A. R., Eversole, K., Feuillet, C., Keller, B., Rogers, J., and Stein, N. (2018). Shifting the limits in wheat research and breeding using a fully annotated reference genome. *Science* 361, eaar7191–eaar7191.
- Jackson, M. (1958). Soil chemical analysis prentice Hall. *Inc Englewood Cliffs NJ* 498, 183–204.
- Jaradat, A. A. (2016). “Breeding oilseed crops for climate change,” in *Breeding oilseed crops for sustainable production* (Elsevier), 421–472.
- Jin, J., Tian, F., Yang, D.-C., Meng, Y.-Q., Kong, L., Luo, J., et al. (2016). PlantTFDB 4.0: toward a central hub for transcription factors and regulatory interactions in plants. *Nucleic Acids Res.*, gkw982.
- Jing, L., Dombinov, V., Shen, S., Wu, Y., Yang, L., Wang, Y., et al. (2016). Physiological and genotype-specific factors associated with grain quality changes in rice exposed to high ozone. *Environ. Pollut.* 210, 397–408.
- Jobson, E. M., Johnston, R. E., Oiestad, A. J., Martin, J. M., and Giroux, M. J. (2019). The impact of the wheat Rht-B1b semi-dwarfing allele on photosynthesis and seed development under field conditions. *Front. Plant Sci.* 10, 51.
- Joshi, A., Mishra, B., Chatrath, R., Ferrara, G. O., and Singh, R. P. (2007). Wheat improvement in India: present status, emerging challenges and future prospects. *Euphytica* 157, 431–446.
- Joshi, R. K., and Nayak, S. (2010). Gene pyramiding-A broad spectrum technique for developing durable stress resistance in crops. *Biotechnol. Mol. Biol. Rev.* 5, 51–60.
- Kadam, N. N., Struik, P. C., Rebolledo, M. C., Yin, X., and Jagadish, S. K. (2018). Genome-wide association reveals novel genomic loci controlling rice grain yield and its component traits under water-deficit stress during the reproductive stage. *J. Exp. Bot.* 69, 4017–4032.
- Kadhem, F., and Baktash, F. (2016). AMMI analysis of adaptability and yield stability of promising lines of bread wheat (*Triticum aestivum* L.). *Iraqi J. Agric. Sci.* 47, 35–43.
- Kaggwa, R. J. (2013). Field Root Biomass, Morphology And Nitrogen Use Efficiency Of Pavon 76 And Its Wheat-Rye (1RS) Translocations.

- Kahiluoto, H., Kaseva, J., Balek, J., Olesen, J. E., Ruiz-Ramos, M., Gobin, A., et al. (2019). Decline in climate resilience of European wheat. *Proc. Natl. Acad. Sci.* 116, 123–128.
- Kang, Y., Khan, S., and Ma, X. (2009). Climate change impacts on crop yield, crop water productivity and food security—A review. *Prog. Nat. Sci.* 19, 1665–1674.
- Khadka, K., Raizada, M. N., and Navabi, A. (2020). Recent Progress in Germplasm Evaluation and Gene Mapping to Enable Breeding of Drought-Tolerant Wheat. *Front. Plant Sci.* 11, 1149.
- Kim, M.-H., Sato, S., Sasaki, K., Saburi, W., Matsui, H., and Imai, R. (2013). COLD SHOCK DOMAIN PROTEIN 3 is involved in salt and drought stress tolerance in Arabidopsis. *FEBS Open Bio* 3, 438–442.
- Kneebone, W., Kopec, D., and Mancino, C. (1992). Water requirements and irrigation. *Turfgrass* 32, 441–472.
- KOKSAL, Y., Sozen, E., and CI, E. A. (2007). Heritability and correlation of yield and quality traits in durum wheat (*Triticum durum*). *Indian J. Agric. Sci.* 77, 565–8.
- Kruijer, W., Boer, M. P., Malosetti, M., Flood, P. J., Engel, B., Kooke, R., et al. (2015). Marker-based estimation of heritability in immortal populations. *Genetics* 199, 379–398.
- Kuchel, H., Langridge, P., Mosionek, L., Williams, K., and Jefferies, S. (2006). The genetic control of milling yield, dough rheology and baking quality of wheat. *Theor. Appl. Genet.* 112, 1487.
- Kulkarni, M., Soolanayakanahally, R., Ogawa, S., Uga, Y., Selvaraj, M. G., and Kagale, S. (2017). Drought response in wheat: key genes and regulatory mechanisms controlling root system architecture and transpiration efficiency. *Front. Chem.* 5, 106.
- Kumar, A., Bernier, J., Verulkar, S., Lafitte, H., and Atlin, G. (2008). Breeding for drought tolerance: direct selection for yield, response to selection and use of drought-tolerant donors in upland and lowland-adapted populations. *Field Crops Res.* 107, 221–231.
- Kumar, P. (2017). Estimation of Chlorophyll by Non-destructive method (SPAD). *Man. ICAR Spons. Train. Programme Tech. Staff ICAR Inst. "Physiological Tech. Anal. Impact Clim. Change Crop Plants,"* 23.
- Kuraparthi, V., Sood, S., and Gill, B. S. (2008). Genomic targeting and mapping of tiller inhibition gene (*tin3*) of wheat using ESTs and synteny with rice. *Funct. Integr. Genomics* 8, 33–42.
- Ladha, J., Tirol-Padre, A., Reddy, C., Cassman, K., Verma, S., Powlson, D., et al. (2016). Global nitrogen budgets in cereals: A 50-year assessment for maize, rice, and wheat production systems, *Sci. Rep.-UK*, 6, 19355.
- Lamichhane, J. R., Barzman, M., Booiij, K., Boonekamp, P., Desneux, N., Huber, L., et al. (2015). Robust cropping systems to tackle pests under climate change. A review. *Agron. Sustain. Dev.* 35, 443–459. doi:10.1007/s13593-014-0275-9.

- Lancashire, P. D., Bleiholder, H., Boom, T. van den, Langelüddeke, P., Stauss, R., WEBER, E., et al. (1991). A uniform decimal code for growth stages of crops and weeds. *Ann. Appl. Biol.* 119, 561–601.
- Larbi, A., and Mekliche, A. (2004). Relative water content (RWC) and leaf senescence as screening tools for drought tolerance in wheat. *Options Méditerranéennes Sér. Sémin. Méditerranéens* 60, 193–196.
- Lawlor, D. W. (2002). Carbon and nitrogen assimilation in relation to yield: mechanisms are the key to understanding production systems. *J. Exp. Bot.* 53, 773–787.
- Lawlor, D. W. (2013). Genetic engineering to improve plant performance under drought: physiological evaluation of achievements, limitations, and possibilities. *J. Exp. Bot.* 64, 83–108.
- Lawlor, D. W., and Cornic, G. (2002). Photosynthetic carbon assimilation and associated metabolism in relation to water deficits in higher plants. *Plant Cell Environ.* 25, 275–294.
- Le Gouis, J. (2011). Genetic improvement of nutrient use efficiency in wheat. *Mol. Physiol. Basis Nutr. Use Effic. Crops Hawkesford MJ Barraclough P Eds*, 123–138.
- Levitt, J. (1972). Water deficit (or drought) stress. In ‘Responses of plants to environmental stresses’.(Ed. J Levitt) pp. 322–352.
- Li, F., Wen, W., Liu, J., Zhang, Y., Cao, S., He, Z., et al. (2019). Genetic architecture of grain yield in bread wheat based on genome-wide association studies. *BMC Plant Biol.* 19, 168.
- Licausi, F., Ohme-Takagi, M., and Perata, P. (2013). APETALA 2/Ethylene Responsive Factor (AP2/ERF) transcription factors: Mediators of stress responses and developmental programs. *New Phytol.* 199, 639–649.
- Lichthardt, C., Chen, T., Stahl, A., and Stützel, H. (2020). Co-Evolution of Sink and Source in the Recent Breeding History of Winter Wheat in Germany. 10, 1–15. doi:10.3389/fpls.2019.01771.
- Lin, C., and Binns, M. (1988). A method of analyzing cultivar x location x year experiments: a new stability parameter. *Theor. Appl. Genet.* 76, 425–430.
- Litke, L., Gaile, Z., and Ruža, A. (2018). Effect of nitrogen fertilization on winter wheat yield and yield quality. *Agron. Res.* 16, 500–509.
- Liu, F., Jensen, C. R., and Andersen, M. N. (2005). A review of drought adaptation in crop plants: changes in vegetative and reproductive physiology induced by ABA-based chemical signals. *Aust. J. Agric. Res.* 56, 1245–1252.
- Liu, Y. A., Dou, Q. W., Chen, Z. G., and Zhao, D. Y. (2010). Effect of drought on water use efficiency, agronomic traits and yield of spring wheat landraces and modern varieties in Northwest China. *Afr. J. Agric. Res.* 5, 1598–1608.

- Liu, Z., Xin, M., Qin, J., Peng, H., Ni, Z., Yao, Y., et al. (2015). Temporal transcriptome profiling reveals expression partitioning of homeologous genes contributing to heat and drought acclimation in wheat (*Triticum aestivum* L.). *BMC Plant Biol.* 15, 1–20.
- Lobell, D. B., Schlenker, W., and Costa-Roberts, J. (2011). Climate trends and global crop production since 1980. *Science* 333, 616–620.
- Long, S. P., Marshall-Colon, A., and Zhu, X.-G. (2015). Meeting the global food demand of the future by engineering crop photosynthesis and yield potential. *Cell* 161, 56–66.
- Lopes, M., Dreisigacker, S., Peña, R., Sukumaran, S., and Reynolds, M. P. (2015). Genetic characterization of the wheat association mapping initiative (WAMI) panel for dissection of complex traits in spring wheat. *Theor. Appl. Genet.* 128, 453–464.
- Lopes, M. S., and Reynolds, M. P. (2010). Partitioning of assimilates to deeper roots is associated with cooler canopies and increased yield under drought in wheat. *Funct. Plant Biol.* 37, 147–156.
- López-Maury, L., Marguerat, S., and Bähler, J. (2008). Tuning gene expression to changing environments: from rapid responses to evolutionary adaptation. *Nat. Rev. Genet.* 9, 583–593.
- Loutfy, N., El-Tayeb, M. A., Hassanen, A. M., Moustafa, M. F., Sakuma, Y., and Inouhe, M. (2012). Changes in the water status and osmotic solute contents in response to drought and salicylic acid treatments in four different cultivars of wheat (*Triticum aestivum*). *J. Plant Res.* 125, 173–184.
- Luo, L. (2010). Breeding for water-saving and drought-resistance rice (WDR) in China. *J. Exp. Bot.* 61, 3509–3517.
- Ma, G., Liu, W., Li, S., Zhang, P., Wang, C., Lu, H., et al. (2019). Determining the Optimal N Input to Improve Grain Yield and Quality in Winter Wheat With Reduced Apparent N Loss in the North China Plain. *Front. Plant Sci.* 10, 1–12. doi:10.3389/fpls.2019.00181.
- Maccaferri, M., El-Feki, W., Nazemi, G., Salvi, S., Canè, M. A., Colalongo, M. C., et al. (2016). Prioritizing quantitative trait loci for root system architecture in tetraploid wheat. *J. Exp. Bot.* 67, 1161–1178.
- Maeoka, R. E., Sadras, V. O., Ciampitti, I. A., Diaz, D. R., Fritz, A. K., and Lollato, R. P. (2020). Changes in the Phenotype of Winter Wheat Varieties Released Between 1920 and 2016 in Response to In-Furrow Fertilizer: Biomass Allocation, Yield, and Grain Protein Concentration. *Front. Plant Sci.* 10, 1786.
- Makino, A. (2011). Photosynthesis, Grain Yield, and Nitrogen Utilization in Rice and Wheat. *Plant Physiol.* 155, 125–129. doi:10.1104/pp.110.165076.
- Mangiafico, S. S. (2015). An R companion for the handbook of biological statistics, version 1.3. 2. rcompanion. org/rcompanion. Pdf Version Rcompanion OrgdocumentsRCompanionBioStatistics Pdf.

- Mansouri, A., Oudjehih, B., Benbelkacem, A., Fellahi, Z. E. A., and Bouzerzour, H. (2018). Variation and Relationships among Agronomic Traits in Durum Wheat [ *Triticum turgidum* (L.) Thell. ssp. *turgidum* conv. *durum* (Desf.) MacKey] under South Mediterranean Growth Conditions: Step-wise and Path Analyses. *Int. J. Agron.* 2018. doi:10.1155/2018/8191749.
- Marschner, P., Hawkesford, M., and Barraclough, P. (2011). The role of the rhizosphere in nutrient use efficiency in crops. *Mol. Physiol. Basis Nutr. Use Effic. Crops*, 47–63.
- Masclaux-Daubresse, C., Daniel-Vedele, F., Dechorgnat, J., Chardon, F., Gaufichon, L., and Suzuki, A. (2010). Nitrogen uptake, assimilation and remobilization in plants: challenges for sustainable and productive agriculture. *Ann. Bot.* 105, 1141–1157.
- Mashilo, J., Tshikunde, N. M., Shimelis, H., and Odindo, A. (2019). Agronomic and Physiological Traits, and Associated Quantitative Trait Loci (QTL) Affecting Yield Response in Wheat (*Triticum Aestivum* L.): A Review. *Front. Plant Sci. Wwwfrontiersinorg* 10, 1–18. doi:10.3389/fpls.2019.01428.
- May, W. E., Brandt, S., and Hutt-Taylor, K. (2020). Response of oat grain yield and quality to nitrogen fertilizer and fungicides. *Agron. J.* 112, 1021–1034.
- Maydup, M. L., Antonietta, M., Guiamet, J., Graciano, C., López, J. R., and Tambussi, E. A. (2010). The contribution of ear photosynthesis to grain filling in bread wheat (*Triticum aestivum* L.). *Field Crops Res.* 119, 48–58.
- McElrone, A. J., Choat, B., Gambetta, G. A., and Brodersen, C. R. (2013). Water uptake and transport in vascular plants. *Nat. Educ. Knowl.* 4.
- Medrano, H., Tomás, M., Martorell, S., Flexas, J., Hernández, E., Rosselló, J., et al. (2015). From leaf to whole-plant water use efficiency (WUE) in complex canopies: Limitations of leaf WUE as a selection target. *Crop J.* 3, 220–228.
- Méndez-Espinoza, A. M., Romero-Bravo, S., Estrada, F., Garriga, M., Lobos, G. A., Castillo, D., et al. (2019). Exploring agronomic and physiological traits associated with the differences in productivity between triticale and bread wheat in mediterranean environments. *Front. Plant Sci.* 10, 404.
- Michel, S., Löschenberger, F., Ametz, C., Pachler, B., Sparry, E., and Bürstmayr, H. (2019). Combining grain yield, protein content and protein quality by multi-trait genomic selection in bread wheat. *Theor. Appl. Genet.* 132, 2767–2780.
- Miezan, K., Heyne, E., and Finney, K. (1977). Genetic and Environmental Effects on the Grain Protein Content in Wheat 1. *Crop Sci.* 17, 591–593.
- Minolta, K. (2009). Chlorophyll meter SPAD-502Plus. *Konica Minolta*.
- Mitra, J. (2001). Genetics and genetic improvement of drought resistance in crop plants. *Curr. Sci.*, 758–763.

- Mittler, R., Vanderauwera, S., Gollery, M., and Van Breusegem, F. (2004). Reactive oxygen gene network of plants. *Trends Plant Sci.* 9, 490–498.
- Mohammadi, R. (2018). Breeding for increased drought tolerance in wheat: a review. *Crop Pasture Sci.* 69, 223–241.
- Mohammadi, R., Haghparast, R., Sadeghzadeh, B., Ahmadi, H., Solimani, K., and Amri, A. (2014). Adaptation patterns and yield stability of durum wheat landraces to highland cold rainfed areas of Iran. *Crop Sci.* 54, 944–954.
- Moll, R., Kamprath, E., and Jackson, W. (1982). Analysis and interpretation of factors which contribute to efficiency of nitrogen utilization 1. *Agron. J.* 74, 562–564.
- Mondal, S., Singh, R., Mason, E., Huerta-Espino, J., Autrique, E., and Joshi, A. (2016). Grain yield, adaptation and progress in breeding for early-maturing and heat-tolerant wheat lines in South Asia. *Field Crops Res.* 192, 78–85.
- Monneveux, P., Jing, R., and Misra, S. (2012). Phenotyping for drought adaptation in wheat using physiological traits. *Front. Physiol.* 3, 429.
- Morison, J., Baker, N., Mullineaux, P., and Davies, W. (2008). Improving water use in crop production. *Philos. Trans. R. Soc. B Biol. Sci.* 363, 639–658.
- Muli, J. M. (2014). The impact of irrigated agriculture in dry lands on the natural environment: a case study of chala ward in taita taveta county, Kenya.
- Munjonji, L., Ayisi, K. K., Vandewalle, B., Haesaert, G., and Boeckx, P. (2016). Combining carbon-13 and oxygen-18 to unravel triticale grain yield and physiological response to water stress. *Field Crops Res.* 195, 36–49.
- Muñoz-Huerta, R. F., Guevara-Gonzalez, R. G., Contreras-Medina, L. M., Torres-Pacheco, I., Prado-Olivarez, J., and Ocampo-Velazquez, R. V. (2013). A review of methods for sensing the nitrogen status in plants: advantages, disadvantages and recent advances. *sensors* 13, 10823–10843.
- Mwadzingeni, L., Shimelis, H., Tesfay, S., and Tsilo, T. J. (2016). Screening of bread wheat genotypes for drought tolerance using phenotypic and proline analyses. *Front. Plant Sci.* 7, 1276.
- Nakashima, K., Ito, Y., and Yamaguchi-Shinozaki, K. (2009). Transcriptional regulatory networks in response to abiotic stresses in Arabidopsis and grasses. *Plant Physiol.* 149, 88–95.
- Nehe, A., Misra, S., Murchie, E., Chinnathambi, K., and Foulkes, M. (2018). Genetic variation in N-use efficiency and associated traits in Indian wheat cultivars. *Field Crops Res.* 225, 152–162.
- Neumann, S., Paveley, N., Beed, F. D., and Sylvester-Bradley, R. (2004). Nitrogen per unit leaf area affects the upper asymptote of Puccinia striiformis f. sp. tritici epidemics in winter wheat. *Plant Pathol.* 53, 725–732.

- Nezhadahmadi, A., Prodhon, Z., and Faruq, G. (2013). Drought tolerance in wheat. *Sci World J* 2013: 610721.
- Omarova, E., Bogdanova, E., and Polimbetova, F. (1995). Regulation of water-loss by the leaves of soft winter-wheat with different organization of leaf structure. *Russ. J. Plant Physiol.* 42, 383–385.
- Osakabe, Y., Osakabe, K., Shinozaki, K., and Tran, L.-S. P. (2014). Response of plants to water stress. *Front. Plant Sci.* 5, 86.
- Ottman, M., and Thompson, T. (2006). Fertilizing small grains in Arizona.
- Oury, F.-X., and Godin, C. (2007). Yield and grain protein concentration in bread wheat: how to use the negative relationship between the two characters to identify favourable genotypes? *Euphytica* 157, 45–57.
- Oyiga, B. C. (2017). Genetic variation of traits related to salt stress response in Wheat (*Triticum aestivum* L.).
- Oyiga, B. C., Ogonnaya, F. C., Sharma, R. C., Baum, M., Léon, J., and Ballvora, A. (2019). Genetic and transcriptional variations in NRAMP-2 and OPAQUE1 genes are associated with salt stress response in wheat. *Theor. Appl. Genet.* 132, 323–346.
- Oyiga, B. C., Palczak, J., Wojciechowski, T., Lynch, J. P., Naz, A. A., Léon, J., et al. (2020). Genetic components of root architecture and anatomy adjustments to water-deficit stress in spring barley. *Plant Cell Environ.* 43, 692–711.
- Oyiga, B. C., Sharma, R. C., Shen, J., Baum, M., Ogonnaya, F. C., Léon, J., et al. (2016). Identification and Characterization of Salt Tolerance of Wheat Germplasm Using a Multivariable Screening Approach. *J. Agron. Crop Sci.* 202, 472–485. doi:10.1111/jac.12178.
- Ozturk, A., and Aydin, F. (2004). Effect of water stress at various growth stages on some quality characteristics of winter wheat. *J. Agron. Crop Sci.* 190, 93–99.
- Pacheco, Á., Vargas, M., Alvarado, G., Rodríguez, F., Crossa, J., and Burgueño, J. (2015). GEA-R (Genotype x Environment Analysis with R for Windows) Version 4.1-, hdl: 11529/10203. *CIMMYT Res. Data Softw. Repos. Netw.* 16.
- Pandey, J. K., Dash, S. K., and Biswal, B. (2017). Loss in photosynthesis during senescence is accompanied by an increase in the activity of  $\beta$ -galactosidase in leaves of *Arabidopsis thaliana*: modulation of the enzyme activity by water stress. *Protoplasma* 254, 1651–1659.
- Pandey, V., and Shukla, A. (2015). Acclimation and tolerance strategies of rice under drought stress. *Rice Sci.* 22, 147–161.
- Papatheodorou, I., Moreno, P., Manning, J., Fuentes, A. M.-P., George, N., Fexova, S., et al. (2020). Expression Atlas update: from tissues to single cells. *Nucleic Acids Res.* 48, D77–D83.

- Pasam, R. K., and Sharma, R. (2014). “Association mapping: a new paradigm for dissection of complex traits in crops,” in *Agricultural bioinformatics* (Springer), 1–20.
- Pask, A., Pietragalla, J., Mullan, D., and Reynolds, M. (2012). *Physiological breeding II: a field guide to wheat phenotyping*. CIMMYT.
- Peleg, Z., Fahima, T., Krugman, T., Abbo, S., Yakir, D., Korol, A. B., et al. (2009). Genomic dissection of drought resistance in durum wheat × wild emmer wheat recombinant inbred line population. *Plant Cell Environ.* 32, 758–779.
- Perchlik, M., and Tegeder, M. (2017). Improving plant nitrogen use efficiency through alteration of amino acid transport processes. *Plant Physiol.* 175, 235–247.
- Perkons, U., Kautz, T., and Köpke, U. (2014). Root growth response of spring wheat (*Triticum aestivum* L.) and mallow (*Malva sylvestris* L.) to biopore generating precrops. *Build. Org. Bridg.* 2, 477–480.
- Perten Instruments (Inc., USA). DA 7250 At-line NIR Instrument-PERDAB|PerkinElmer. Available at: <https://www.perkinelmer.com/product/da-7250-at-line-nir-instrument-perdab> ; [https://www.perkinelmer.com/lab-solutions/resources/docs/app\\_analysis\\_of\\_wheat\\_flour\\_da7250.pdf](https://www.perkinelmer.com/lab-solutions/resources/docs/app_analysis_of_wheat_flour_da7250.pdf) (Accessed 30 April 2021) [Accessed April 30, 2021].
- Phukan, U. J., Jeena, G. S., and Shukla, R. K. (2016). WRKY transcription factors: molecular regulation and stress responses in plants. *Front. Plant Sci.* 7, 760.
- Piepho, H.-P., and Möhring, J. (2007). Computing heritability and selection response from unbalanced plant breeding trials. *Genetics* 177, 1881–1888.
- Pimentel, D., Berger, B., Filiberto, D., Newton, M., Wolfe, B., Karabinakis, E., et al. (2004). Water resources: agricultural and environmental issues. *Bioscience* 54, 909–918.
- Pingali, P. L. (2012). Green revolution: impacts, limits, and the path ahead. *Proc. Natl. Acad. Sci.* 109, 12302–12308.
- Pinto, F., Celesti, M., Acebron, K., Alberti, G., Cogliati, S., Colombo, R., et al. (2020). Dynamics of sun-induced chlorophyll fluorescence and reflectance to detect stress-induced variations in canopy photosynthesis. *Plant Cell Environ.*
- Porter, J. R., and Semenov, M. A. (2005). Crop responses to climatic variation. *Philos. Trans. R. Soc. B Biol. Sci.* 360, 2021–2035.
- Prechamandra, G., Saneora, H., Fujita, K., and Ogata, S. (1992). Osmotic adjustment and stomatal response to water deficit in maize. *J Exp Bot* 43, 1451–1456.
- Pritchard, J. K., and Przeworski, M. (2001). Linkage disequilibrium in humans: models and data. *Am. J. Hum. Genet.* 69, 1–14.

- Pritchard, J. K., Stephens, M., and Donnelly, P. (2000). Inference of population structure using multilocus genotype data. *Genetics* 155, 945–959.
- Purcell, S. (2010). PLINK (1.07) Documentation.
- R Core Team (2020). R: a language and environment for statistical computing. Vienna: The R Foundation, 2017.
- Rakszegi, M., Darkó, É., Lovegrove, A., Molnár, I., Láng, L., Bedő, Z., et al. (2019). Drought stress affects the protein and dietary fiber content of wholemeal wheat flour in wheat/*Aegilops* addition lines. *PLoS One* 14, e0211892.
- Ramakrishnan, A. (2013). Linkage disequilibrium.
- Rasheed, A., and Xia, X. (2019). From markers to genome-based breeding in wheat. *Theor. Appl. Genet.* 132, 767–784.
- Reddy, A. R., Chaitanya, K. V., and Vivekanandan, M. (2004). Drought-induced responses of photosynthesis and antioxidant metabolism in higher plants. *J. Plant Physiol.* 161, 1189–1202.
- Reganold, J. P., and Wachter, J. M. (2016). Organic agriculture in the twenty-first century. *Nat. Plants* 2, 1–8.
- Remington, D. L., Thornsberry, J. M., Matsuoka, Y., Wilson, L. M., Whitt, S. R., Doebley, J., et al. (2001). Structure of linkage disequilibrium and phenotypic associations in the maize genome. *Proc. Natl. Acad. Sci.* 98, 11479–11484.
- Reynolds, M., Balota, M., Delgado, M., Amani, I., and Fischer, R. (1994). Physiological and morphological traits associated with spring wheat yield under hot, irrigated conditions. *Funct. Plant Biol.* 21, 717–730.
- Reynolds, M., Bonnett, D., Chapman, S. C., Furbank, R. T., Manès, Y., Mather, D. E., et al. (2011). Raising yield potential of wheat. I. Overview of a consortium approach and breeding strategies. *J. Exp. Bot.* 62, 439–452.
- Reynolds, M. P., Gutiérrez-Rodríguez, M., and Larqué-Saavedra, A. (2000). Photosynthesis of wheat in a warm, irrigated environment: I: genetic diversity and crop productivity. *Field Crops Res.* 66, 37–50.
- Reynolds, M. P., Pask, A. J., Hoppitt, W. J., Sonder, K., Sukumaran, S., Molero, G., et al. (2017). Strategic crossing of biomass and harvest index—source and sink—achieves genetic gains in wheat. *Euphytica* 213, 257.
- Richard, C. A., Hickey, L. T., Fletcher, S., Jennings, R., Chenu, K., and Christopher, J. T. (2015). High-throughput phenotyping of seminal root traits in wheat. *Plant Methods* 11, 1–11.
- Richards, R., Watt, M., and Rebetzke, G. (2007). Physiological traits and cereal germplasm for sustainable agricultural systems. *Euphytica* 154, 409–425.

- Risch, N., and Merikangas, K. (1996). The future of genetic studies of complex human diseases. *Science* 273, 1516–1517.
- Roper, M., and Gupta, V. (2016). Enhancing non-symbiotic N<sub>2</sub> fixation in agriculture. *Open Agric. J.* 10.
- Rosseel, Y. (2012). lavaan: An R package for structural equation modeling. R package version 0.5-15 <http://lavaan.org>. *J. Stat. Softw.* 48, 1–36.
- Rouse, J., Haas, R. H., Schell, J. A., and Deering, D. W. (1974). Monitoring vegetation systems in the Great Plains with ERTS. *NASA Spec. Publ.* 351, 309.
- Royo, C., Alvaro, F., Martos, V., Ramdani, A., Isidro, J., Villegas, D., et al. (2007). Genetic changes in durum wheat yield components and associated traits in Italian and Spanish varieties during the 20th century. *Euphytica* 155, 259–270.
- Ruta, N., Liedgens, M., Fracheboud, Y., Stamp, P., and Hund, A. (2010). QTLs for the elongation of axile and lateral roots of maize in response to low water potential. *Theor. Appl. Genet.* 120, 621–631.
- Saade, S., Maurer, A., Shahid, M., Oakey, H., Schmöckel, S. M., Negrão, S., et al. (2016). Yield-related salinity tolerance traits identified in a nested association mapping (NAM) population of wild barley. *Sci. Rep.* 6, 32586.
- Sallam, A., Alqudah, A. M., Dawood, M. F. A., Baenziger, P. S., and Börner, A. (2019). Drought stress tolerance in wheat and barley: Advances in physiology, breeding and genetics research. *Int. J. Mol. Sci.* 20. doi:10.3390/ijms20133137.
- Sallam, A., Arbaoui, M., El-Esawi, M., Abshire, N., and Martsch, R. (2016). Identification and verification of QTL associated with frost tolerance using linkage mapping and GWAS in winter faba bean. *Front. Plant Sci.* 7, 1098.
- Samarah, N. H. (2016). “Understanding how plants respond to drought stress at the molecular and whole plant levels,” in *Drought Stress Tolerance in Plants, Vol 2* (Springer), 1–37.
- Sánchez, J., Curt, M. D., Robert, N., and Fernández, J. (2019). “Biomass resources,” in *The Role of Bioenergy in the Bioeconomy* (Elsevier), 25–111.
- Sanchez-Bragado, R., Elazab, A., Zhou, B., Serret, M. D., Bort, J., Nieto-Taladriz, M. T., et al. (2014). Contribution of the ear and the flag leaf to grain filling in durum wheat inferred from the carbon isotope signature: genotypic and growing conditions effects. *J. Integr. Plant Biol.* 56, 444–454.
- Sanchez-Garcia, M., Alvaro, F., Peremarti, A., Trevaskis, B., Martin-Sanchez, J. A., and Royo, C. (2015). Breeding effects on dry matter accumulation and partitioning in Spanish bread wheat during the 20th century. *Euphytica* 203, 321–336.
- Sannemann, W. (2013). Marker-trait-sensor association in a multi-parent advanced generation intercross (MAGIC) population in barley (*Hordeum vulgare* ssp. *vulgare*).

- Sarieva, G., Kenzhebaeva, S., and Lichtenthaler, H. (2010). Adaptation potential of photosynthesis in wheat cultivars with a capability of leaf rolling under high temperature conditions. *Russ. J. Plant Physiol.* 57, 28–36.
- SAS Institute (2015). *Base SAS 9.4 procedures guide*. SAS Institute.
- Schlosser, C. A., Strzepek, K., Gao, X., Fant, C., Blanc, É., Paltsev, S., et al. (2014). The future of global water stress: An integrated assessment. *Earths Future* 2, 341–361.
- Schreiber, L. (2010). Transport barriers made of cutin, suberin and associated waxes. *Trends Plant Sci.* 15, 546–553.
- Searle, S. R., Casella, G., and McCulloch, C. E. (2009). *Variance components*. John Wiley & Sons.
- Semenov, M., Stratonovitch, P., Alghabari, F., and Gooding, M. (2014). Adapting wheat in Europe for climate change. *J. Cereal Sci.* 59, 245–256.
- Sharma, R., Crossa, J., Velu, G., Huerta-Espino, J., Vargas, M., Payne, T., et al. (2012). Genetic gains for grain yield in CIMMYT spring bread wheat across international environments. *Crop Sci.* 52, 1522–1533.
- Shavrukov, Y., Kurishbayev, A., Jatayev, S., Shvidchenko, V., Zotova, L., Koekemoer, F., et al. (2017). Early flowering as a drought escape mechanism in plants: How can it aid wheat production? *Front. Plant Sci.* 8, 1950.
- Sheffield, J., and Wood, E. F. (2012). *Drought: past problems and future scenarios*. Routledge.
- SHEN, L., HUANG, Y., and Ting, L. (2017). Top-grain filling characteristics at an early stage of maize (*Zea mays* L.) with different nitrogen use efficiencies. *J. Integr. Agric.* 16, 626–639.
- Sheskin, D. J. (2020). *Handbook of parametric and nonparametric statistical procedures*. crc Press.
- Shi, L.-X., and Schröder, W. P. (2004). The low molecular mass subunits of the photosynthetic supercomplex, photosystem II. *Biochim. Biophys. Acta BBA-Bioenerg.* 1608, 75–96.
- Shi, W., Hao, C., Zhang, Y., Cheng, J., Zhang, Z., Liu, J., et al. (2017). A combined association mapping and linkage analysis of kernel number per spike in common wheat (*Triticum aestivum* L.). *Front. Plant Sci.* 8, 1412.
- Shi, X., and Ling, H.-Q. (2018). Current advances in genome sequencing of common wheat and its ancestral species. *Crop J.* 6, 15–21.
- Shrestha, A. (2020). Genetic and molecular analysis of drought stress adaptation in cultivated and wild barley.
- Siddiqui, M. N., León, J., Naz, A. A., and Ballvora, A. (2020). Genetics and genomics of root system variation in adaptation to drought stress in cereal crops. *J. Exp. Bot.*
- Singer, S. D., Soolanayakanahally, R. Y., Foroud, N. A., and Kroebel, R. (2020). Biotechnological strategies for improved photosynthesis in a future of elevated atmospheric CO<sub>2</sub>. *Planta* 251, 1–28.

- Slafer, G. A., and Araus, J. L. (2007). Physiological traits for improving wheat yield under a wide range of conditions. *Frontis*, 145–154.
- Stockle, C. O. (2001). Environmental impact of irrigation: A review. *Wash. State Univ.*
- Stuber, C., Johnson, V. A., and Schmidt, J. W. (1962). Grain protein content and its relationship to other plant and seed characters in the parents and progeny of a cross of *Triticum aestivum* L. *Crop Sci.* 2, 506–508.
- Su, S., Zhou, Y., Qin, J. G., Yao, W., and Ma, Z. (2010). Optimization of the method for chlorophyll extraction in aquatic plants. *J. Freshw. Ecol.* 25, 531–538.
- Sukumaran, S., Reynolds, M. P., and Sansaloni, C. (2018). Genome-wide association analyses identify QTL hotspots for yield and component traits in durum wheat grown under yield potential, drought, and heat stress environments. *Front. Plant Sci.* 9, 81.
- Swarup, S., Cargill, E. J., Crosby, K., Flagel, L., Kniskern, J., and Glenn, K. C. (2020). Genetic diversity is indispensable for plant breeding to improve crops. *Crop Sci.*
- Sylvester-Bradley, R., Scott, R., and Wright, C. (1990). Physiology in the production and improvement of cereals. *Physiol. Prod. Improv. Cereals.*
- Tadesse, W., Morgounov, A., Braun, H., Akin, B., Keser, M., Yuksel, K., et al. (2013). Breeding progress for yield and adaptation of winter wheat targeted to irrigated environments at the International Winter Wheat Improvement Program (IWWIP). *Euphytica* 194, 177–185.
- Tardieu, F. (2013). Plant response to environmental conditions: assessing potential production, water demand, and negative effects of water deficit. *Front. Physiol.* 4, 17.
- Te Beest, D., Paveley, N., Shaw, M., and Van Den Bosch, F. (2008). Disease–weather relationships for powdery mildew and yellow rust on winter wheat. *Phytopathology* 98, 609–617.
- Thomas, H., and Howarth, C. J. (2000). Five ways to stay green. *J. Exp. Bot.* 51, 329–337.
- Thompson, R., Lassaletta, L., Patra, P., Wilson, C., Wells, K., Gressent, A., et al. (2019). Acceleration of global N<sub>2</sub>O emissions seen from two decades of atmospheric inversion. *Nat. Clim. Change* 9, 993–998.
- Tian, Z., Jing, Q., Dai, T., Jiang, D., and Cao, W. (2011). Effects of genetic improvements on grain yield and agronomic traits of winter wheat in the Yangtze River Basin of China. *Field Crops Res.* 124, 417–425.
- Trachsel, S., Kaeppler, S. M., Brown, K. M., and Lynch, J. P. (2011). Shovelomics: high throughput phenotyping of maize (*Zea mays* L.) root architecture in the field. *Plant Soil* 341, 75–87.
- Trenberth, K. E., Dai, A., Van Der Schrier, G., Jones, P. D., Barichivich, J., Briffa, K. R., et al. (2014). Global warming and changes in drought. *Nat. Clim. Change* 4, 17–22.

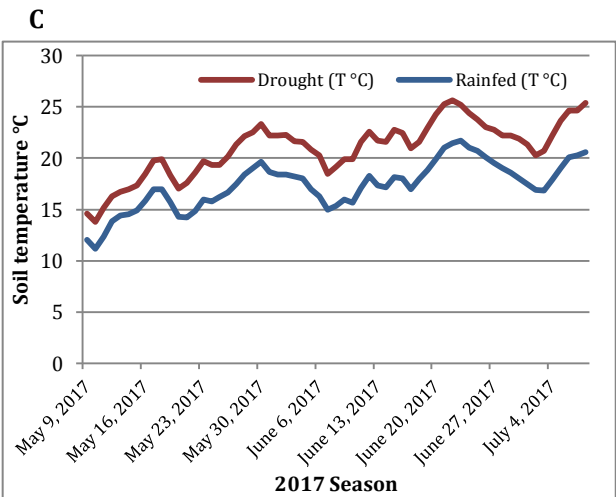
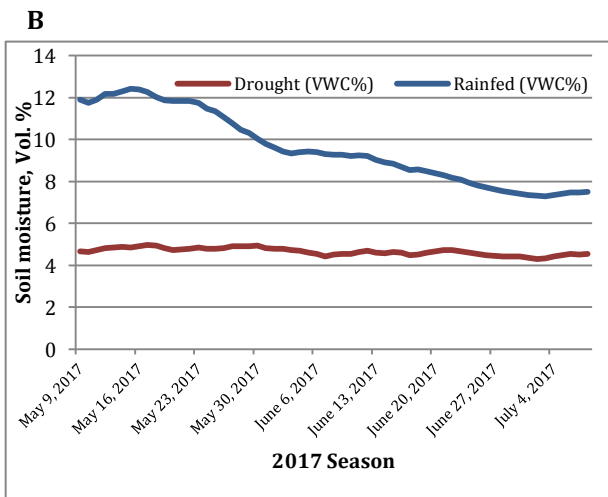
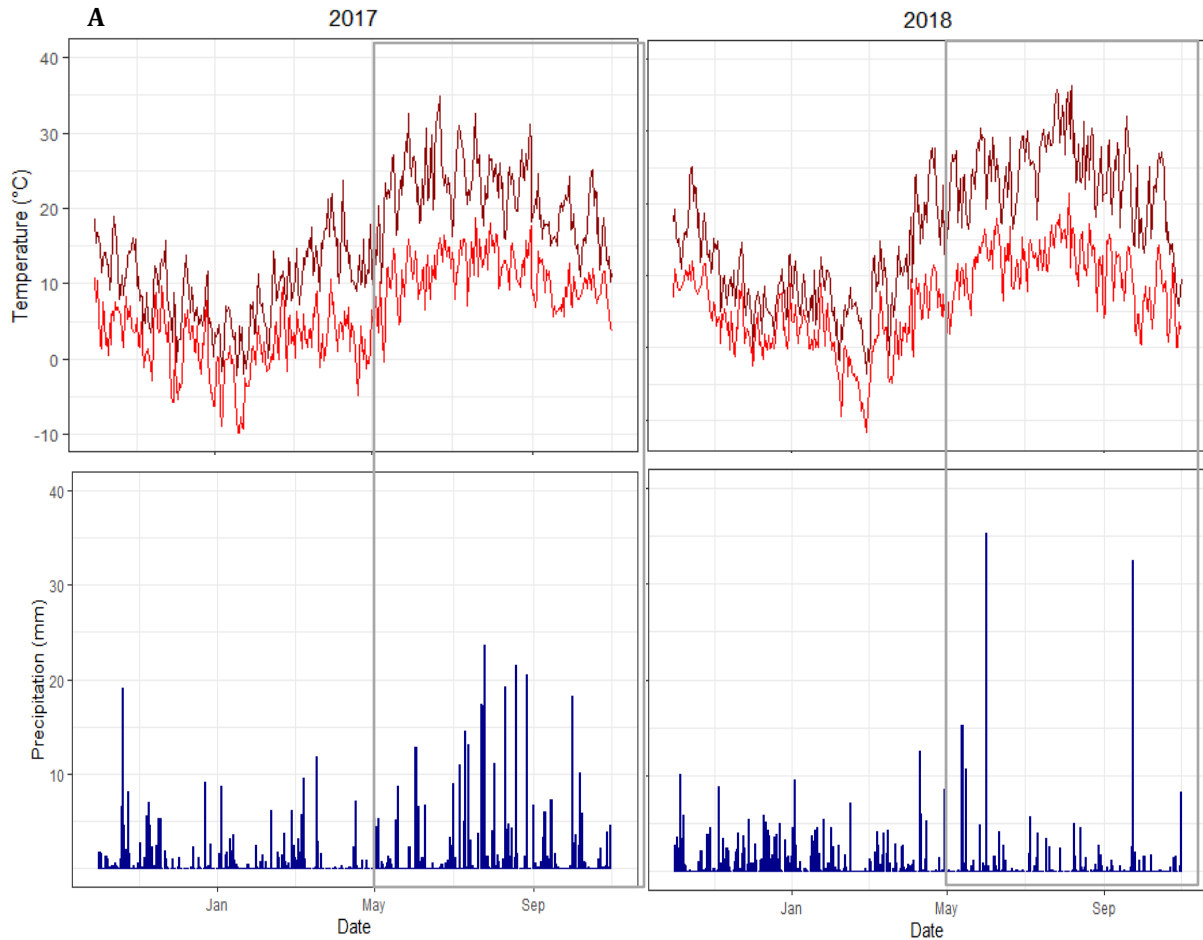
- Tripathi, S., Sayre, K., Kaul, J., and Narang, R. (2004). Lodging behavior and yield potential of spring wheat (*Triticum aestivum* L.): effects of ethephon and genotypes. *Field Crops Res.* 87, 207–220.
- Tshikunde, N. M., Mashilo, J., Shimelis, H., and Odindo, A. (2019). Agronomic and Physiological Traits, and Associated Quantitative Trait Loci (QTL) Affecting Yield Response in Wheat (*Triticum aestivum* L.): A Review. *Front. Plant Sci.* 10.
- Tucker, M. (2004). Primary nutrients and plant growth. *Essent. Plant Nutr.* 126.
- Turuspekov, Y., Baibulatova, A., Yermekbayev, K., Tokhetova, L., Chudinov, V., Sereda, G., et al. (2017). GWAS for plant growth stages and yield components in spring wheat (*Triticum aestivum* L.) harvested in three regions of Kazakhstan. *BMC Plant Biol.* 17, 1–11.
- Van Herwaarden, A., Richards, R., Farquhar, G., and Angus, J. (1998). “Haying-off”, the negative grain yield response of dryland wheat to nitrogen fertiliser III. The influence of water deficit and heat shock. *Aust. J. Agric. Res.* 49, 1095–1110.
- Varshney, R. K., Langridge, P., and Graner, A. (2007). Application of genomics to molecular breeding of wheat and barley. *Adv. Genet.* 58, 121–155.
- Vincent, D., Lapierre, C., Pollet, B., Cornic, G., Negroni, L., and Zivy, M. (2005). Water deficits affect caffeate O-methyltransferase, lignification, and related enzymes in maize leaves. A proteomic investigation. *Plant Physiol.* 137, 949–960.
- Vitousek, P. M., Naylor, R., Crews, T., David, M., Drinkwater, L., Holland, E., et al. (2009). Nutrient imbalances in agricultural development. *Science* 324, 1519–1520.
- Voss-Fels, K. P., Stahl, A., Wittkop, B., Lichthardt, C., Nagler, S., Rose, T., et al. (2019). Breeding improves wheat productivity under contrasting agrochemical input levels. *Nat. Plants* 5, 706–714.
- Walz, H. (2014). MINI-PAM-II Manual for Touch-screen Operation. *Primera*.
- Wan, Y., King, R., Mitchell, R. A., Hassani-Pak, K., and Hawkesford, M. J. (2017). Spatiotemporal expression patterns of wheat amino acid transporters reveal their putative roles in nitrogen transport and responses to abiotic stress. *Sci. Rep.* 7, 1–13.
- Wang, C., Deng, P., Chen, L., Wang, X., Ma, H., Hu, W., et al. (2013). A wheat WRKY transcription factor TaWRKY10 confers tolerance to multiple abiotic stresses in transgenic tobacco. *PLoS One* 8, e65120.
- Wang, C., Kovacs, M. I., Fowler, D., and Holley, R. (2004). Effects of protein content and composition on white noodle making quality: color. *Cereal Chem.* 81, 777–784.
- Wang, Y., Yang, L., Höller, M., Zaisheng, S., Pariasca-Tanaka, J., Wissuwa, M., et al. (2014). Pyramiding of ozone tolerance QTLs Ozt8 and Ozt9 confers improved tolerance to season-long ozone exposure in rice. *Environ. Exp. Bot.* 104, 26–33.

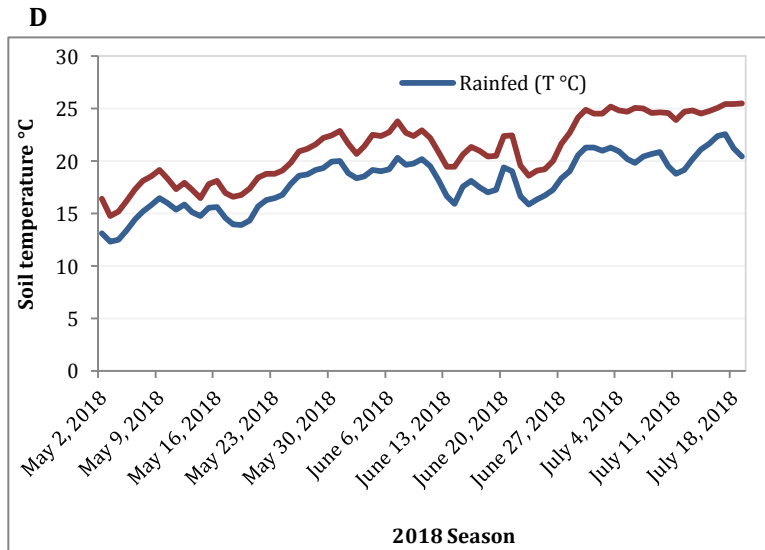
- Wei, K., and Li, Y. (2019). Functional genomics of the protein kinase superfamily from wheat. *Mol. Breed.* 39, 1–23.
- Weldearegay, D. F., Yan, F., Jiang, D., and Liu, F. (2012). Independent and combined effects of soil warming and drought stress during anthesis on seed set and grain yield in two spring wheat varieties. *J. Agron. Crop Sci.* 198, 245–253.
- Wik, M., Pingali, P., and Brocai, S. (2008). Global agricultural performance: past trends and future prospects.
- Würschum, T., Leiser, W. L., Langer, S. M., Tucker, M. R., and Longin, C. F. H. (2018). Phenotypic and genetic analysis of spike and kernel characteristics in wheat reveals long-term genetic trends of grain yield components. *Theor. Appl. Genet.* 131, 2071–2084.
- Xie, Q., Fernando, K. M., Mayes, S., and Sparkes, D. L. (2017). Identifying seedling root architectural traits associated with yield and yield components in wheat. *Ann. Bot.* 119, 1115–1129.
- Xie, Z., Nolan, T. M., Jiang, H., and Yin, Y. (2019). AP2/ERF transcription factor regulatory networks in hormone and abiotic stress responses in Arabidopsis. *Front. Plant Sci.* 10, 228.
- Xu, G., Fan, X., and Miller, A. J. (2012). Plant nitrogen assimilation and use efficiency. *Annu. Rev. Plant Biol.* 63, 153–182.
- Xu, Y.-F., Li, S.-S., Li, L.-H., Ma, F.-F., Fu, X.-Y., Shi, Z.-L., et al. (2017). QTL mapping for yield and photosynthetic related traits under different water regimes in wheat. *Mol. Breed.* 37, 34.
- Yadav, S. N., Peterson, W., and Easter, K. W. (1997). Do farmers overuse nitrogen fertilizer to the detriment of the environment? *Environ. Resour. Econ.* 9, 323–340. doi:10.1007/BF02441403.
- Yang, D., Jing, R., Chang, X., and Li, W. (2007). Quantitative trait loci mapping for chlorophyll fluorescence and associated traits in wheat (*Triticum aestivum*). *J. Integr. Plant Biol.* 49, 646–654.
- Yang, J., Zhang, J., Wang, Z., Zhu, Q., and Liu, L. (2001). Water deficit-induced senescence and its relationship to the remobilization of pre-stored carbon in wheat during grain filling. *Agron. J.* 93, 196–206.
- Yang, S., Vanderbeld, B., Wan, J., and Huang, Y. (2010). Narrowing down the targets: towards successful genetic engineering of drought-tolerant crops. *Mol. Plant* 3, 469–490.
- Yang, X., Liu, L., Yin, Z., Wang, X., Wang, S., and Ye, Z. (2020). Quantifying photosynthetic performance of phytoplankton based on photosynthesis–irradiance response models. *Environ. Sci. Eur.* 32, 1–13.
- Yu, J., and Buckler, E. S. (2006). Genetic association mapping and genome organization of maize. *Curr. Opin. Biotechnol.* 17, 155–160.

- Yu, J., Pressoir, G., Briggs, W. H., Bi, I. V., Yamasaki, M., Doebley, J. F., et al. (2005). A unified mixed-model method for association mapping that accounts for multiple levels of relatedness. *Nat. Genet.* 38, 203–208.
- Yu, T.-F., Xu, Z.-S., Guo, J.-K., Wang, Y.-X., Abernathy, B., Fu, J.-D., et al. (2017). Improved drought tolerance in wheat plants overexpressing a synthetic bacterial cold shock protein gene SeCspA. *Sci. Rep.* 7, 1–14.
- Yue, B., Xue, W., Xiong, L., Yu, X., Luo, L., Cui, K., et al. (2006). Genetic basis of drought resistance at reproductive stage in rice: separation of drought tolerance from drought avoidance. *Genetics* 172, 1213–1228.
- Zeisler-Diehl, V., Müller, Y., and Schreiber, L. (2018). Epicuticular wax on leaf cuticles does not establish the transpiration barrier, which is essentially formed by intracuticular wax. *J. Plant Physiol.* 227, 66–74.
- Zhang, J., Gizaw, S. A., Bossolini, E., Hegarty, J., Howell, T., Carter, A. H., et al. (2018). Identification and validation of QTL for grain yield and plant water status under contrasting water treatments in fall-sown spring wheats. *Theor. Appl. Genet.* 131, 1741–1759.
- Zhang, Y., Zhang, A., Li, X., and Lu, C. (2020). The role of chloroplast gene expression in plant responses to environmental stress. *Int. J. Mol. Sci.* 21, 6082.
- Zhang, Z., Ersoz, E., Lai, C.-Q., Todhunter, R. J., Tiwari, H. K., Gore, M. A., et al. (2010). Mixed linear model approach adapted for genome-wide association studies. *Nat. Genet.* 42, 355–360.
- Zhao, K., Aranzana, M. J., Kim, S., Lister, C., Shindo, C., Tang, C., et al. (2007). An Arabidopsis example of association mapping in structured samples. *PLoS Genet* 3, e4.
- Zhao, W., Liu, L., Shen, Q., Yang, J., Han, X., Tian, F., et al. (2020). Effects of water stress on photosynthesis, yield, and water use efficiency in winter wheat. *Water* 12, 2127.
- Zhao, Y., Wang, H., Chen, W., and Li, Y. (2014). Genetic structure, linkage disequilibrium and association mapping of Verticillium wilt resistance in elite cotton (*Gossypium hirsutum* L.) germplasm population. *PLoS One* 9, e86308.
- Zhe, Y., Lauer, J. G., Borges, R., and de Leon, N. (2010). Effects of genotype × environment interaction on agronomic traits in soybean. *Crop Sci.* 50, 696–702. doi:10.2135/cropsci2008.12.0742.
- Zhu, C., Gore, M., Buckler, E. S., and Yu, J. (2008). Status and prospects of association mapping in plants. *Plant Genome* 1.
- Zhu, J., Ingram, P. A., Benfey, P. N., and Elich, T. (2011). From lab to field, new approaches to phenotyping root system architecture. *Curr. Opin. Plant Biol.* 14, 310–317.
- Zou, L., Sun, X., Zhang, Z., Liu, P., Wu, J., Tian, C., et al. (2011). Leaf rolling controlled by the homeo-domain leucine zipper class IV gene Roc5 in rice. *Plant Physiol.* 156, 1589–1602.

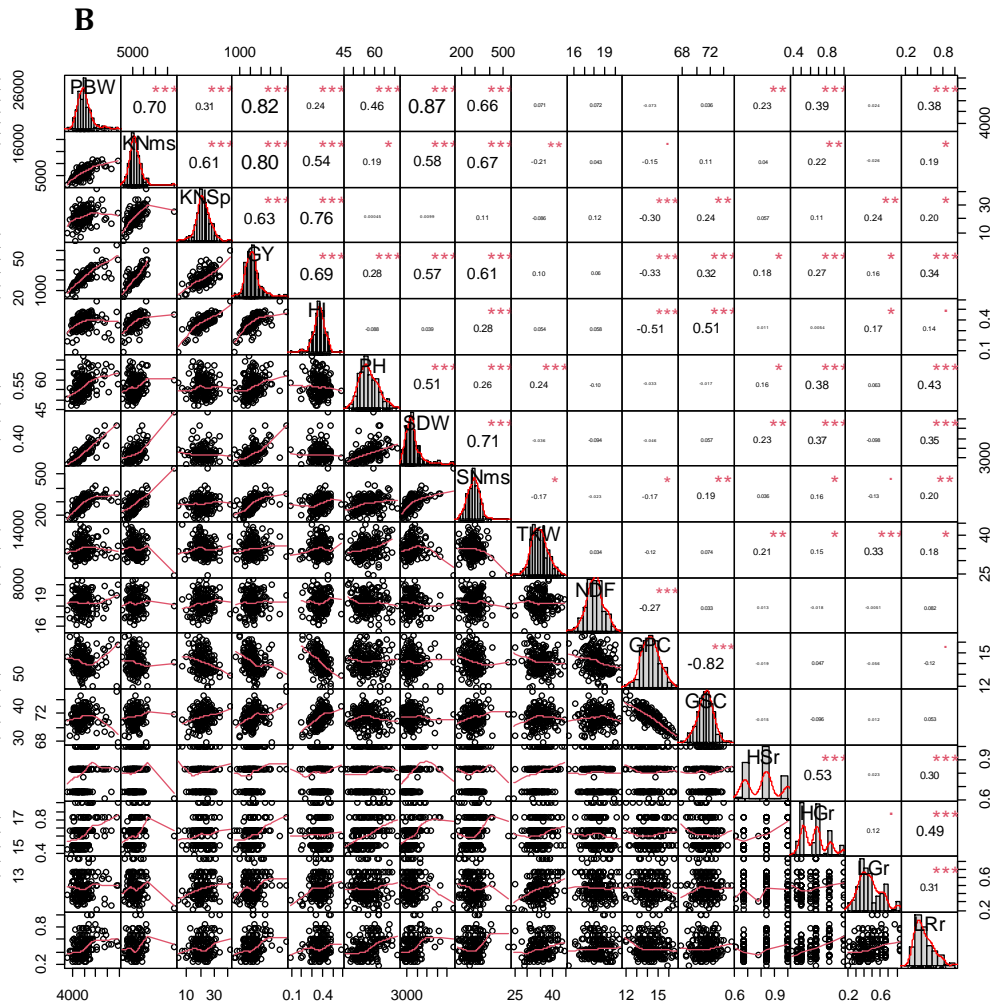
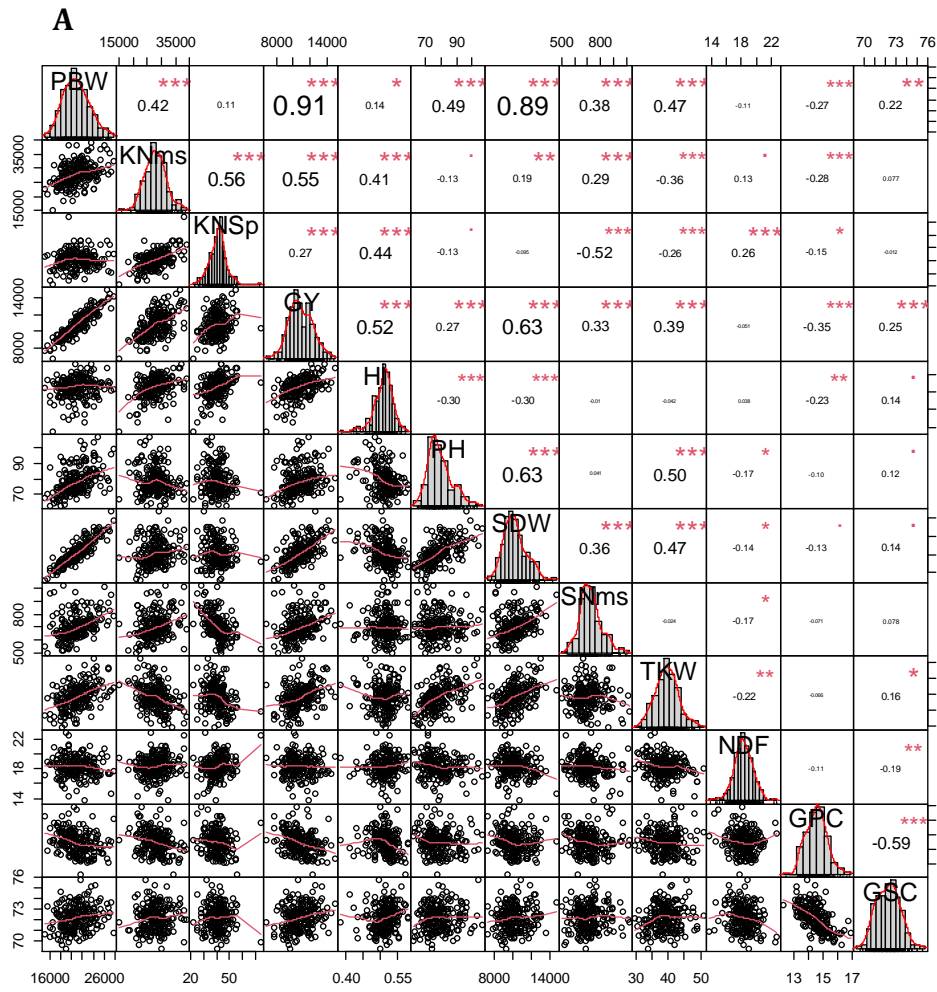
# Supplementary Files

## Supplementary Figures





**FIGURE 2.S1** | Above ground and underground weather data. (A) Graph of minimum and maximum temperature and daily precipitation sum during the experimental periods of 2017 and 2018; (BCD) Soil moisture content and soil temperature (0–30 cm depth) at latter stress time point under rainfed and drought stress of the experimental plots in the 2017 and 2018 growing seasons.



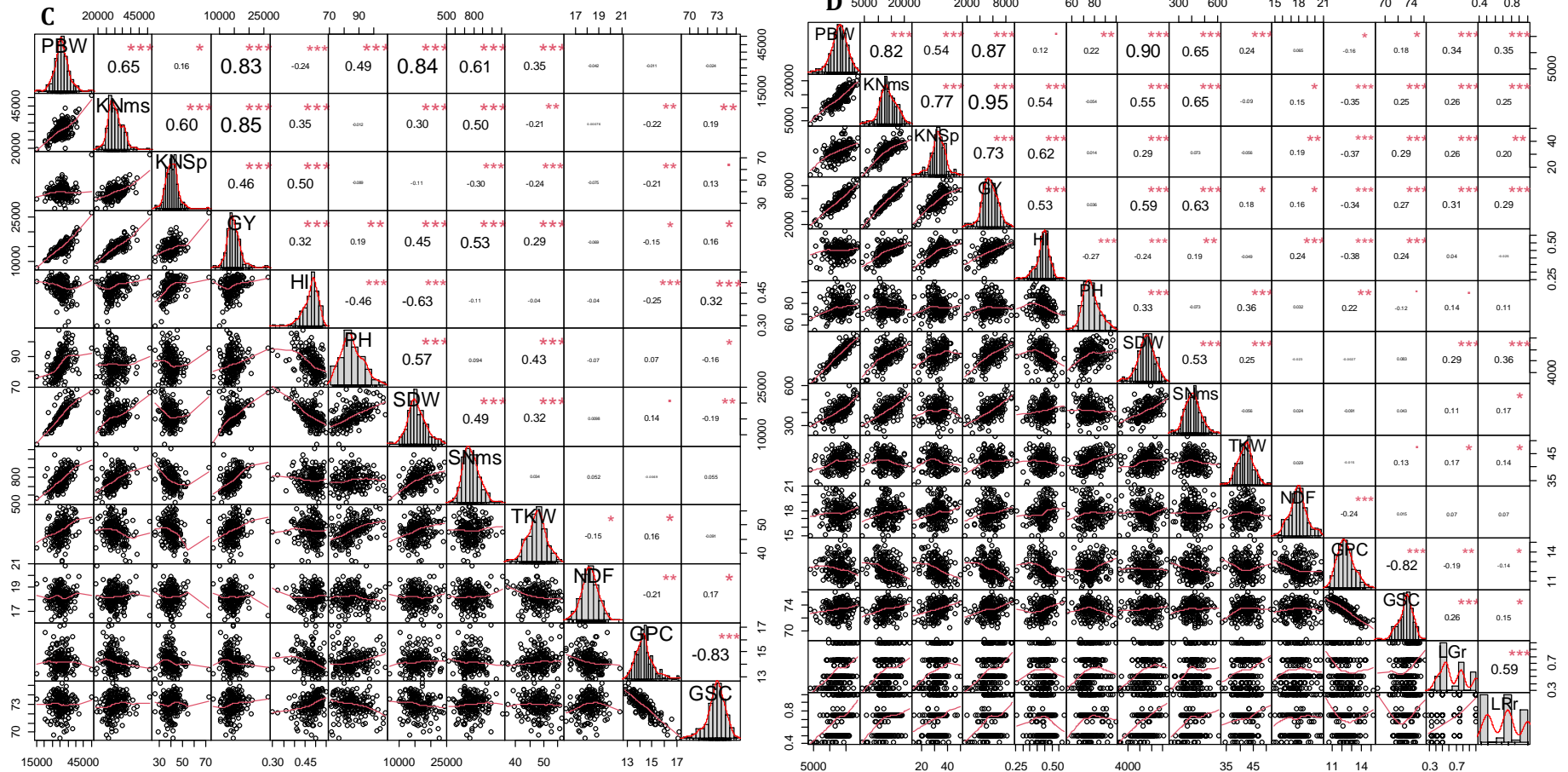


**FIGURE 2.S2** | Pearson correlation coefficients between evaluated traits in 2017 under rain fed field (Panel A) and drought stress (Panel B) and in 2018 under rain fed field (Panel C) and drought stress (Panel D) conditions. Phenotypic traits with their histograms are given in the diagonal panel. Lower diagonal panel represents the scatter plot with red line depicting the best fit. The upper panel represents the Pearson correlation coefficient value and size of the correlation coefficient is proportional to the strength of the correlation. The correlation coefficient significance level \* $P < 0.05$ , \*\* $P < 0.01$ , \*\*\* $P < 0.001$ . The abbreviations of traits names are given in Table S1.

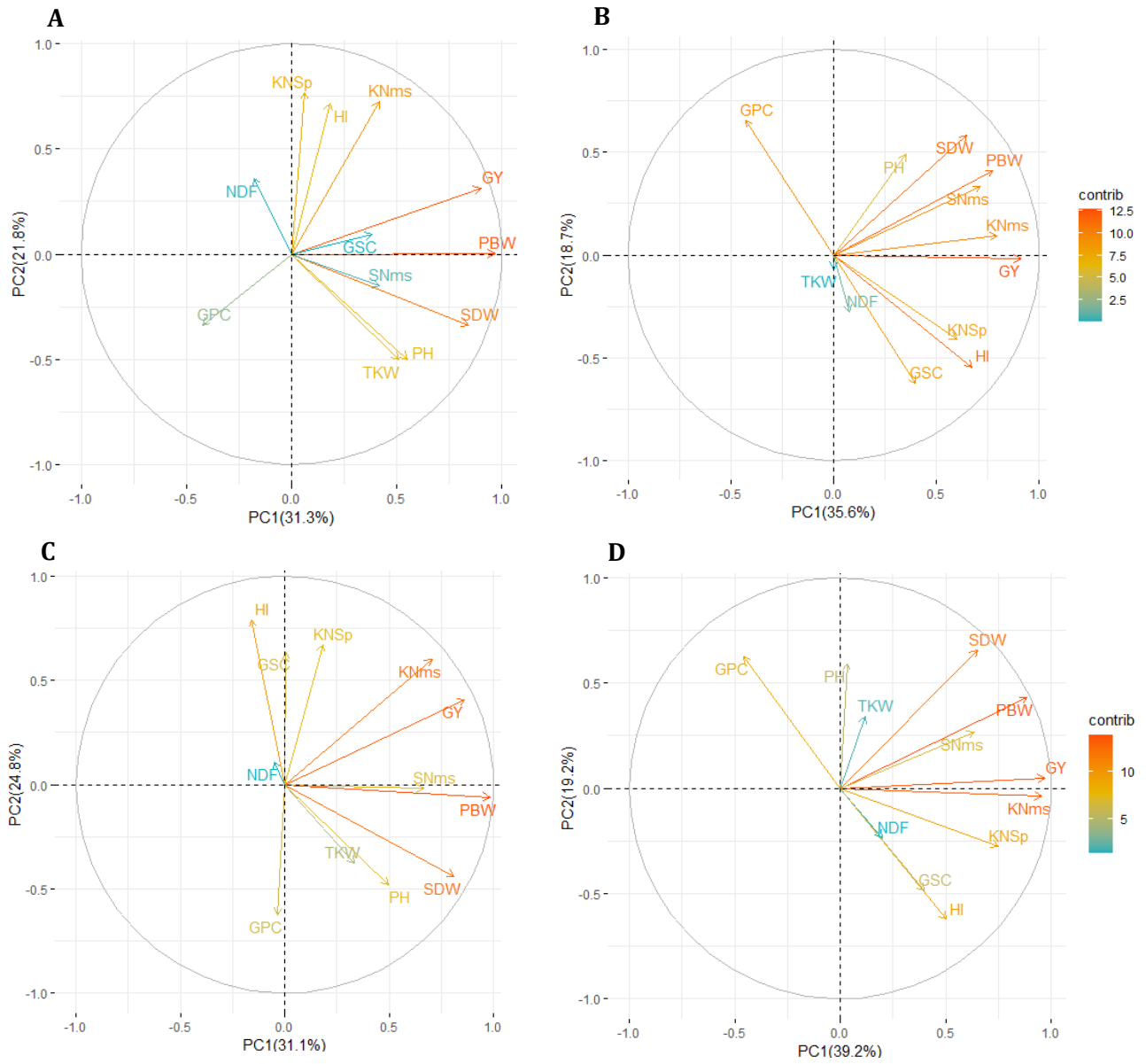


**FIGURE 2.S3** | The principal component analysis of evaluated traits with first two principal components (PC1 and PC2) under rainfed (A, C) and drought stress (B, D) during 2017 (A, B) and 2018 (C, D). The contribution of a trait to the principal components is shown by intensity of the color, ranging from the green (lower contribution) to red (higher contribution). Abbreviations: see legend of Table 1.

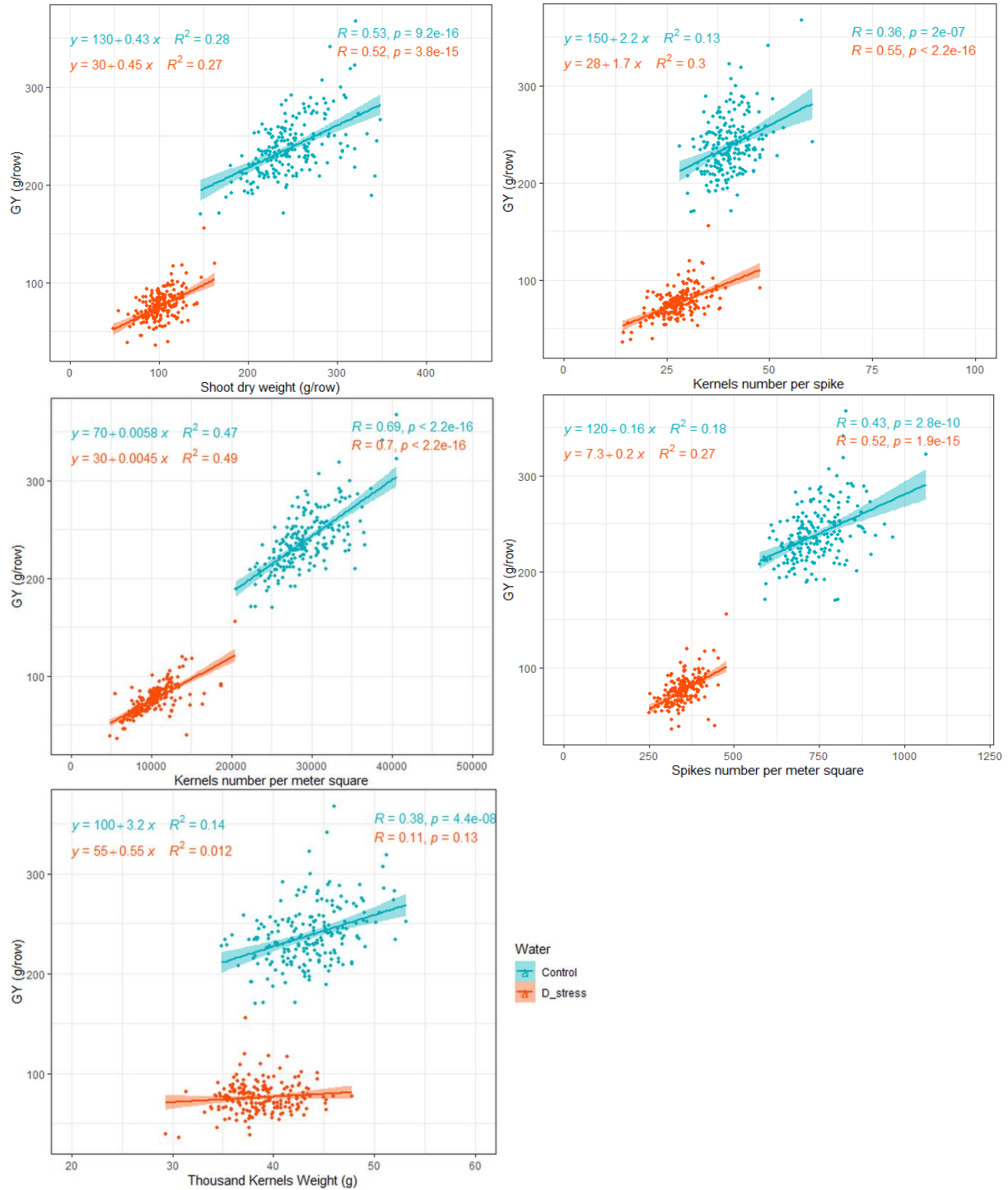


**FIGURE 2.S4** | Linear regression of GY on yield components traits showing the proportion of the variance in GY explained by the variation in each component trait ( $R^2$ ). (A) Shoot dry weight; (B) Kernels number per spike; (C) Kernels number per meter square; (D) Spike number per meter square; (E) Thousand kernels weight.

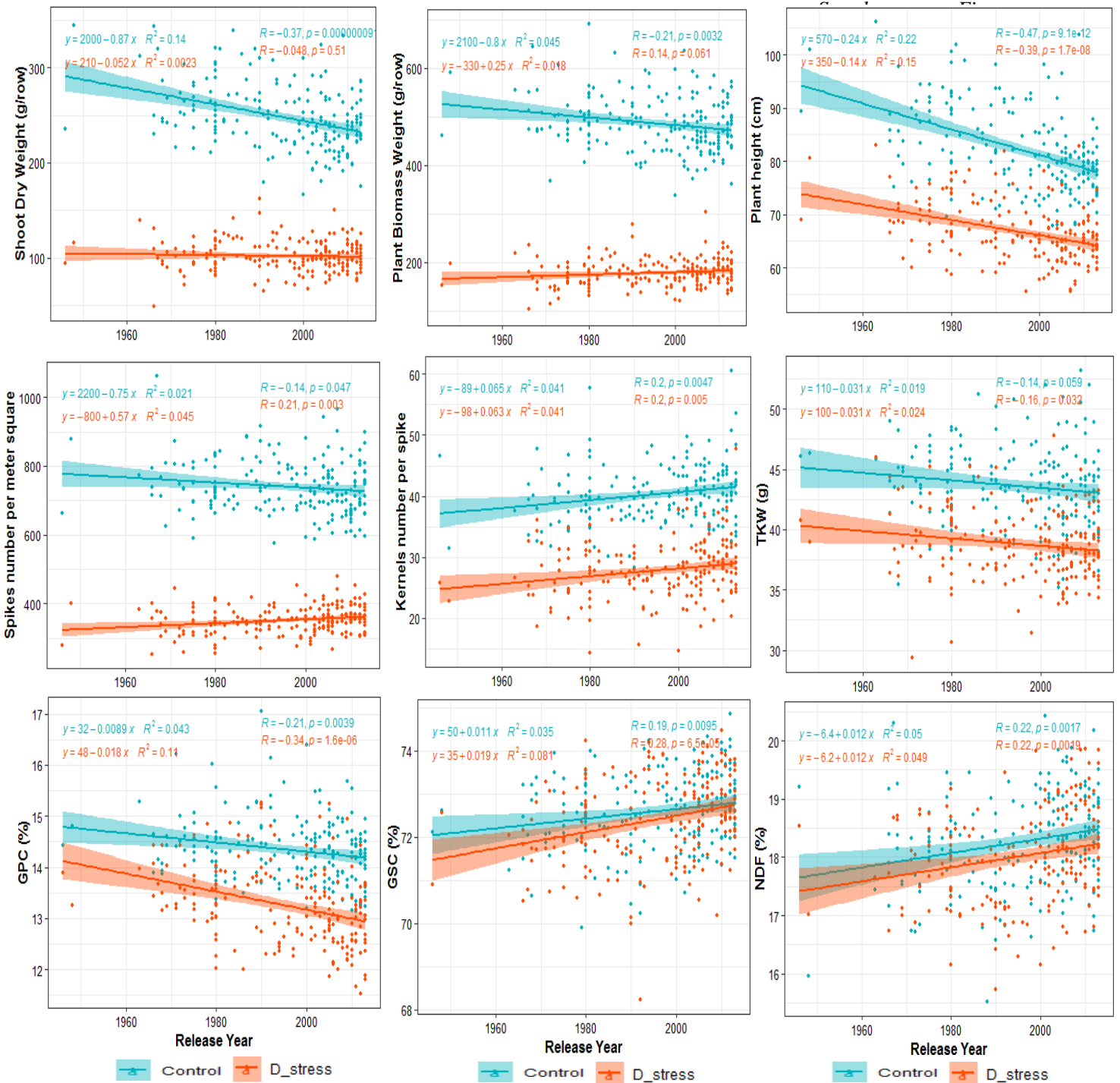


**FIGURE 2.S5** | Regression plots showing breeding progress in agronomic traits and grain quality on Blues values for two growing seasons. Each dot represents a blue value of a cultivars and the colored area represents the confidence interval of the regression line. The slopes of the linear regression lines (green lines for rainfed conditions and orange values for droughts stress field) are referred to absolute breeding progress and the relative breeding progress is the ratio between the values in 2010 and 1980 as show in Table 1.

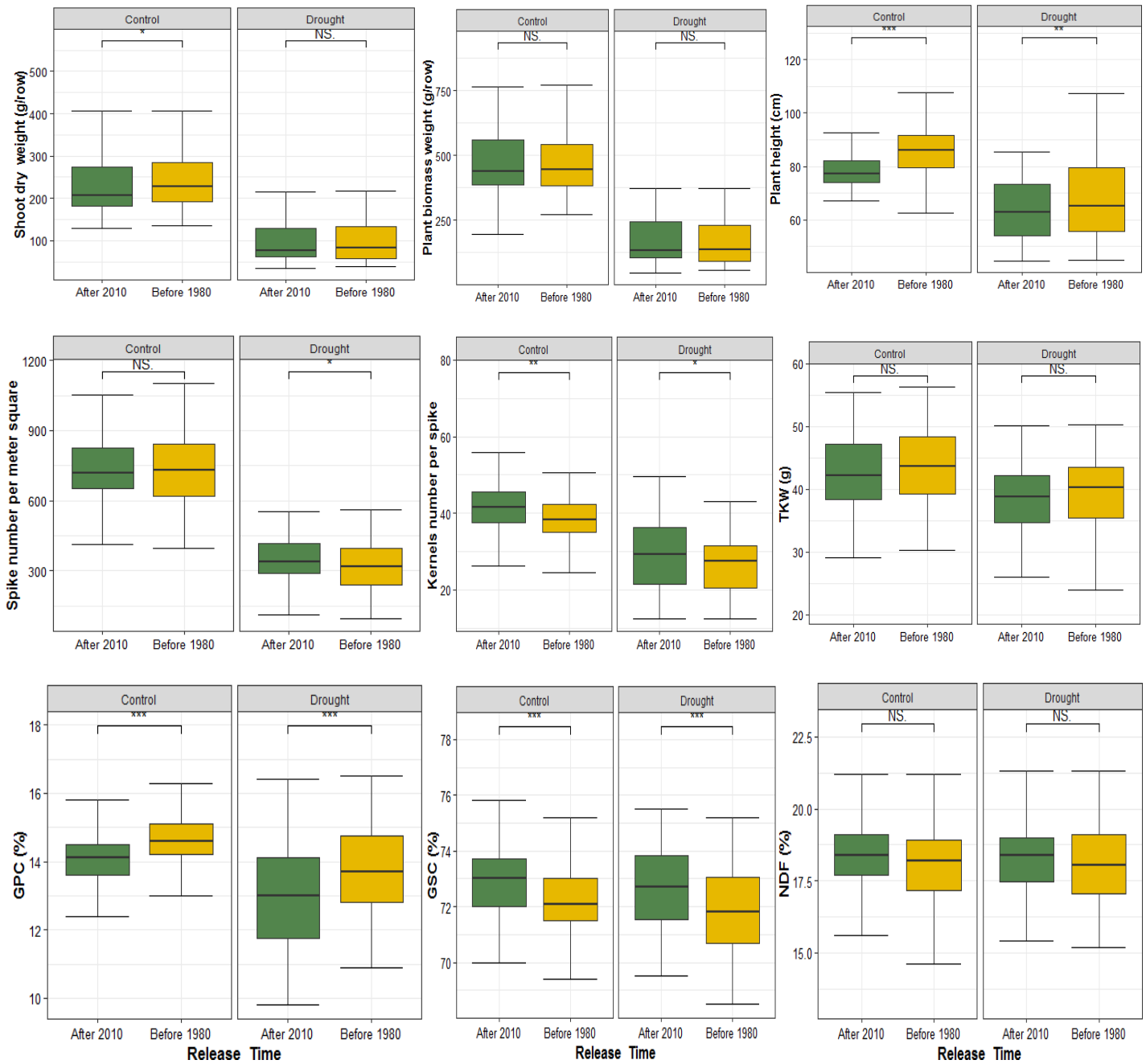


**FIGURE 2.S6** | Comparison of breeding progress in agronomic and grain quality traits between two contrasting years of release groups under control and drought stress conditions. The oldest genotypes were released before 1980 while the newest were released after 2010.

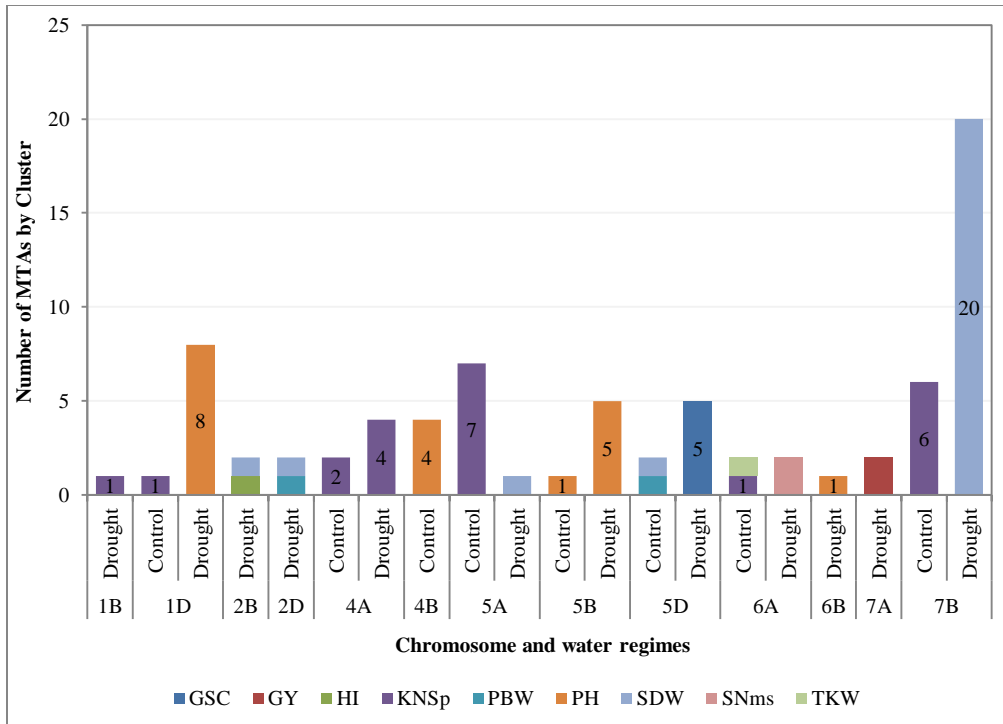


**FIGURE 2.S7** | Number of SNP-clusters with defined number of MTAs, illustrating the SNP-clusters having only one MTAs to SNP-clusters with 20MTAs.

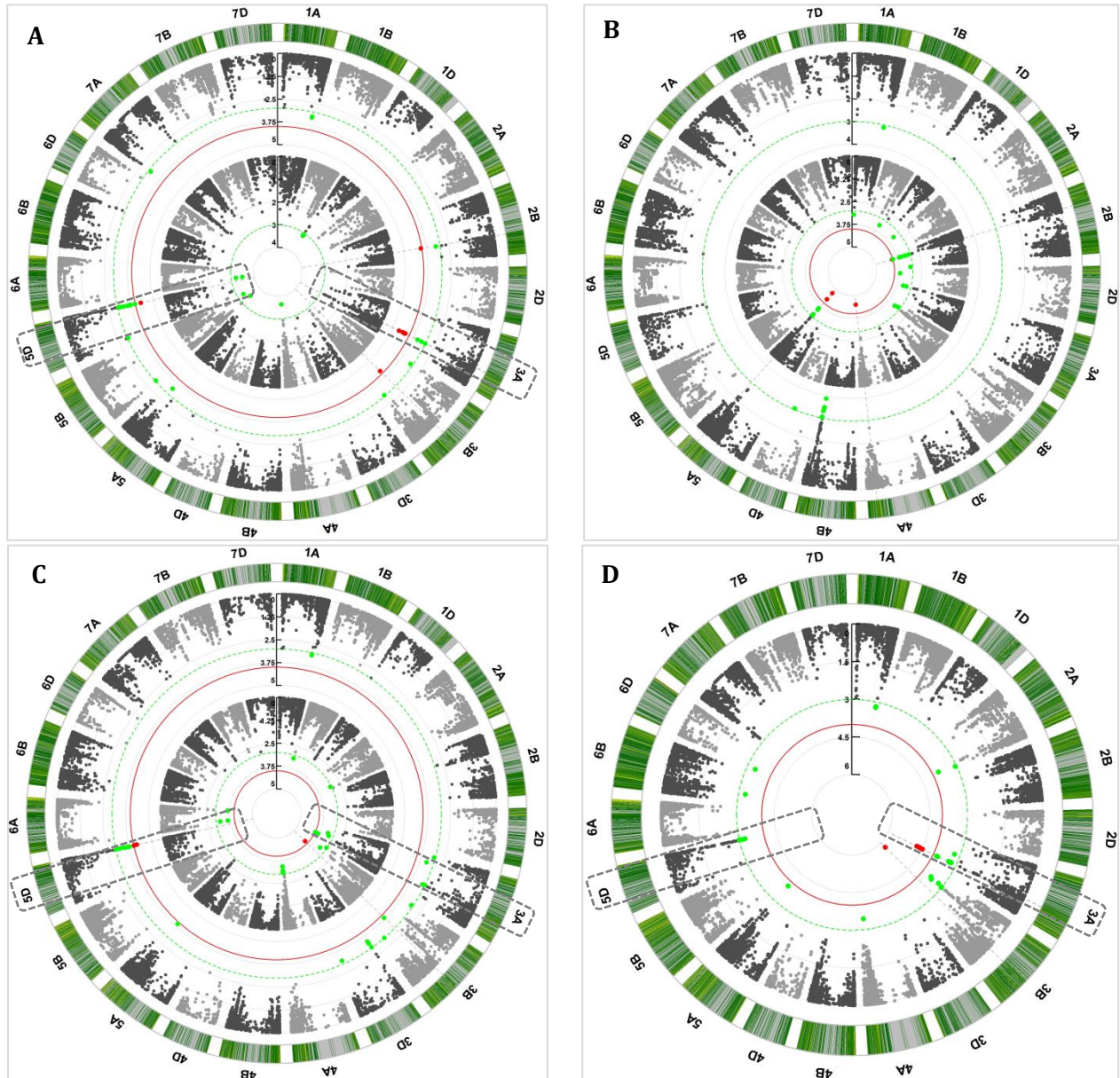


**FIGURE 2.S8** | Circular Manhattan plots displaying association mapping for GSC. (A) GSC under both conditions in 2017; (B) GSC under both conditions in 2018; (C) GSC mean under drought and rainfed; (D) GSC overall mean. The dotted square highlighted significant ( $P < 10^{-3}$  in green color and  $P < 10^{-4}$  in red color) and consistent MTAs were detected on chromosomes 3A and 5D.

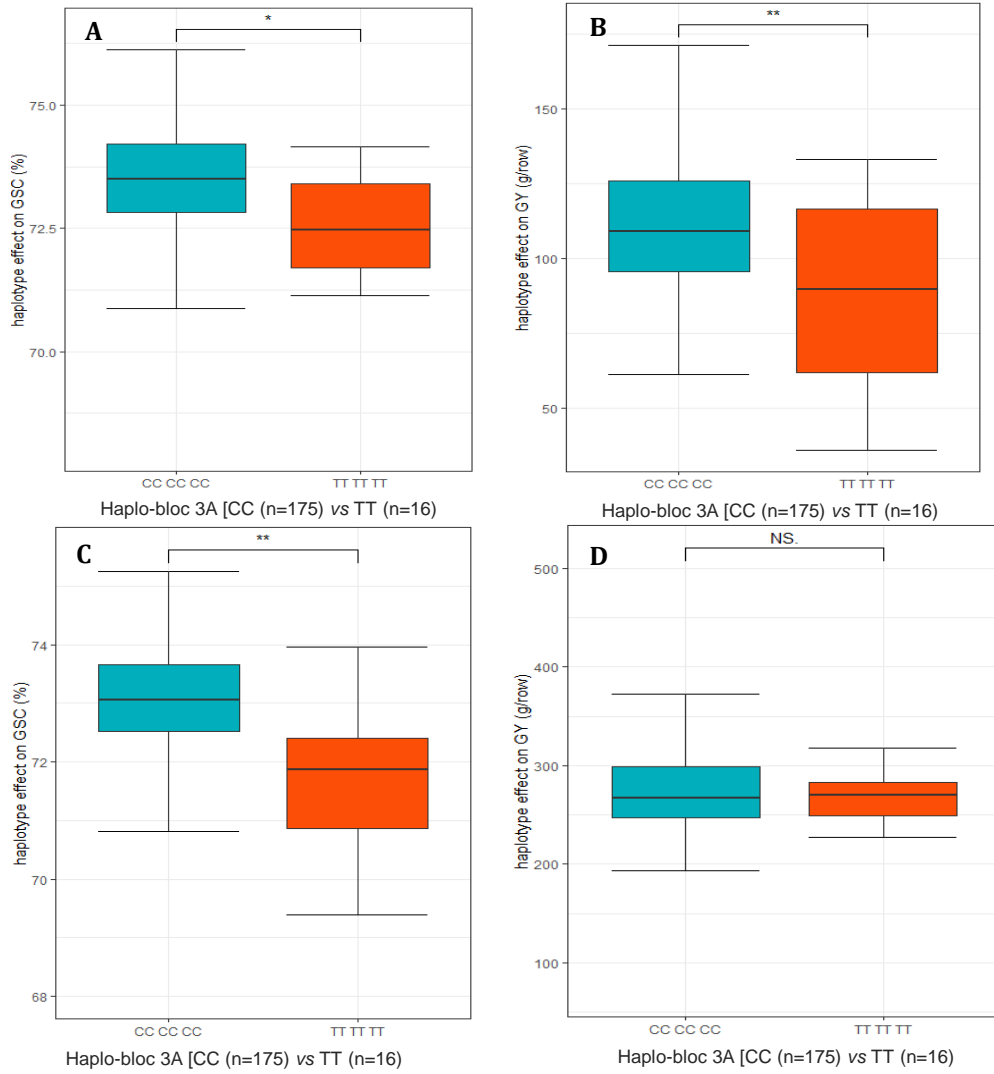


**FIGURE 2.S9** | Effect of *AX-158576764* haplotype bloc of chromosome 3A on (A) GSC and (B) GY under drought stress conditions; (C) GSC and (D) GY under control conditions.

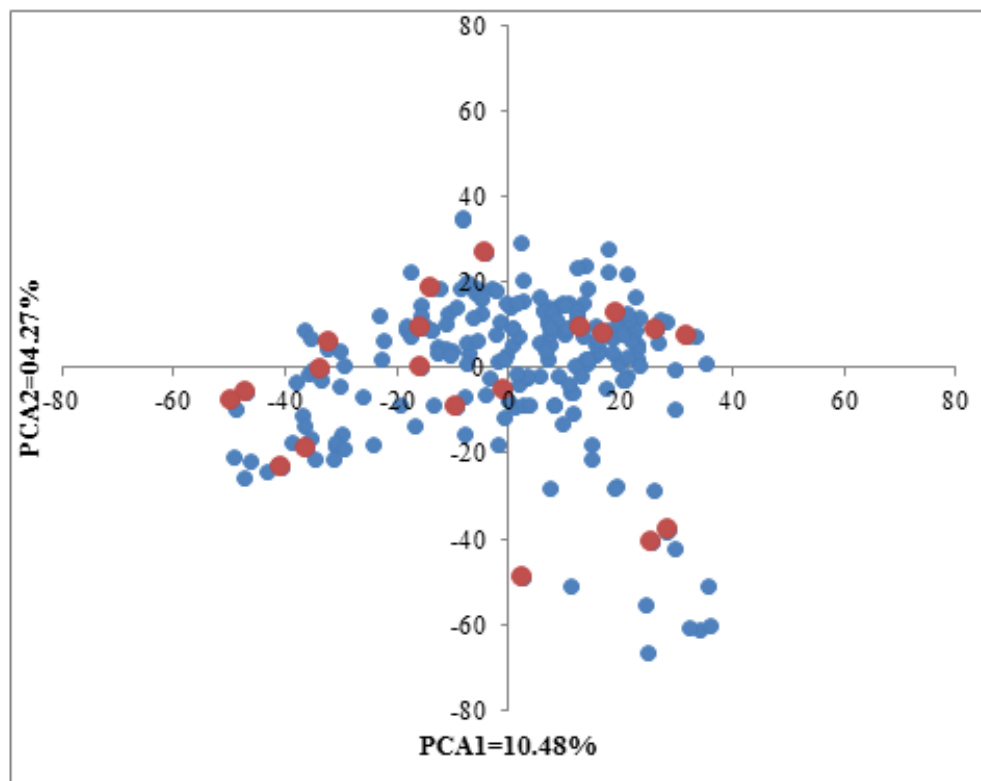


**FIGURE 3.S1** | Genetic diversity of 200 winter wheat cultivars (in blue) including the core set of 20 genotypes (in red).

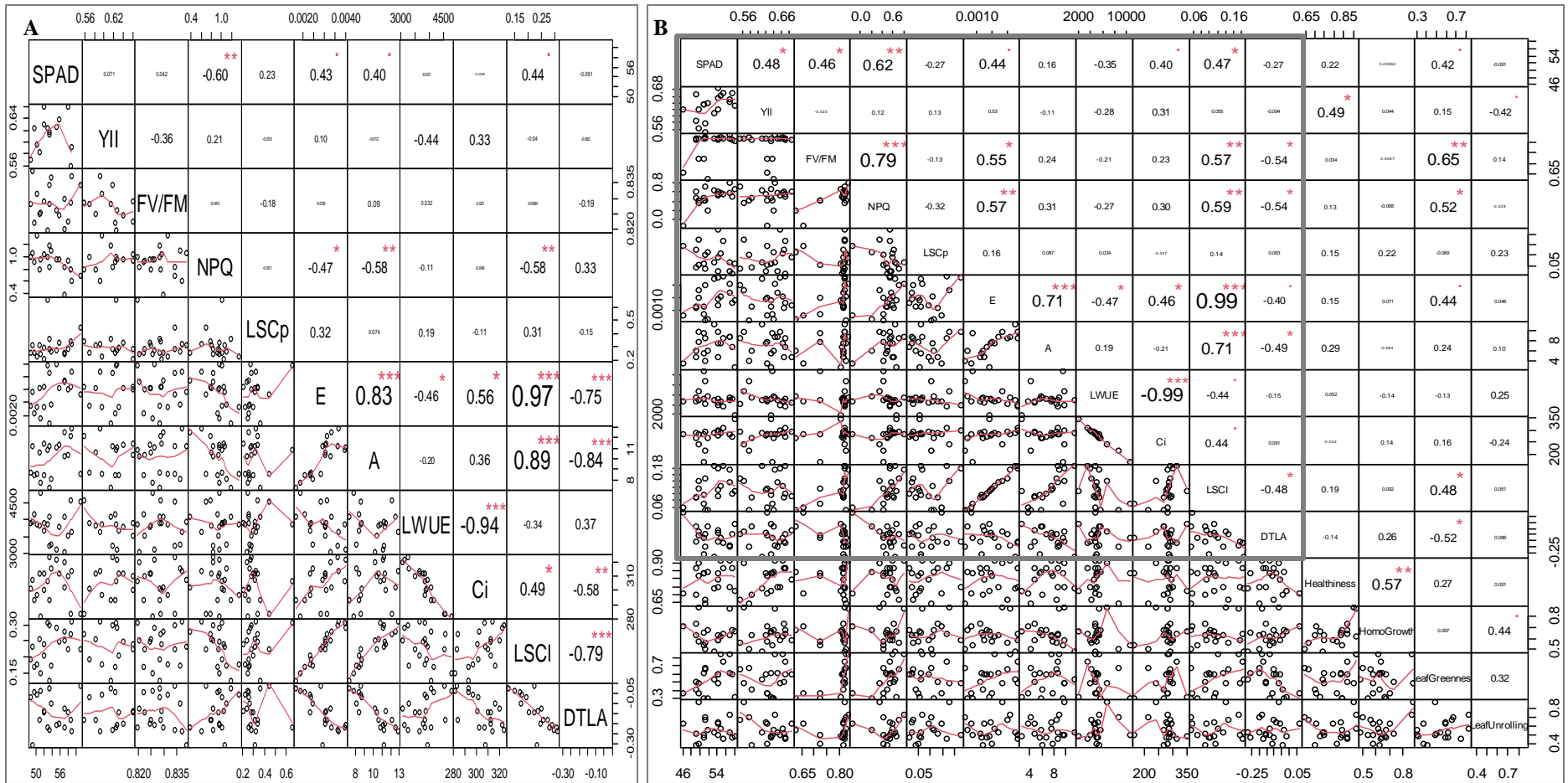


**FIGURE 3.52** | Pearson correlation coefficients between photosynthesis related under rainfed conditions (panel A). Correlation between photosynthesis related traits (grey square) and scored developmental traits under prolonged drought stress conditions (panel B). Lower diagonal panels represent the scatter plot with red line depicting the best fit. The upper panel represents the Pearson correlation coefficient value and size of the correlation coefficient is proportional to the strength of the correlation. The correlation coefficient significance level \*P<0.05, \*\*P<0.01, \*\*\*P<0.001. The abbreviations of traits names are given in Table S2.

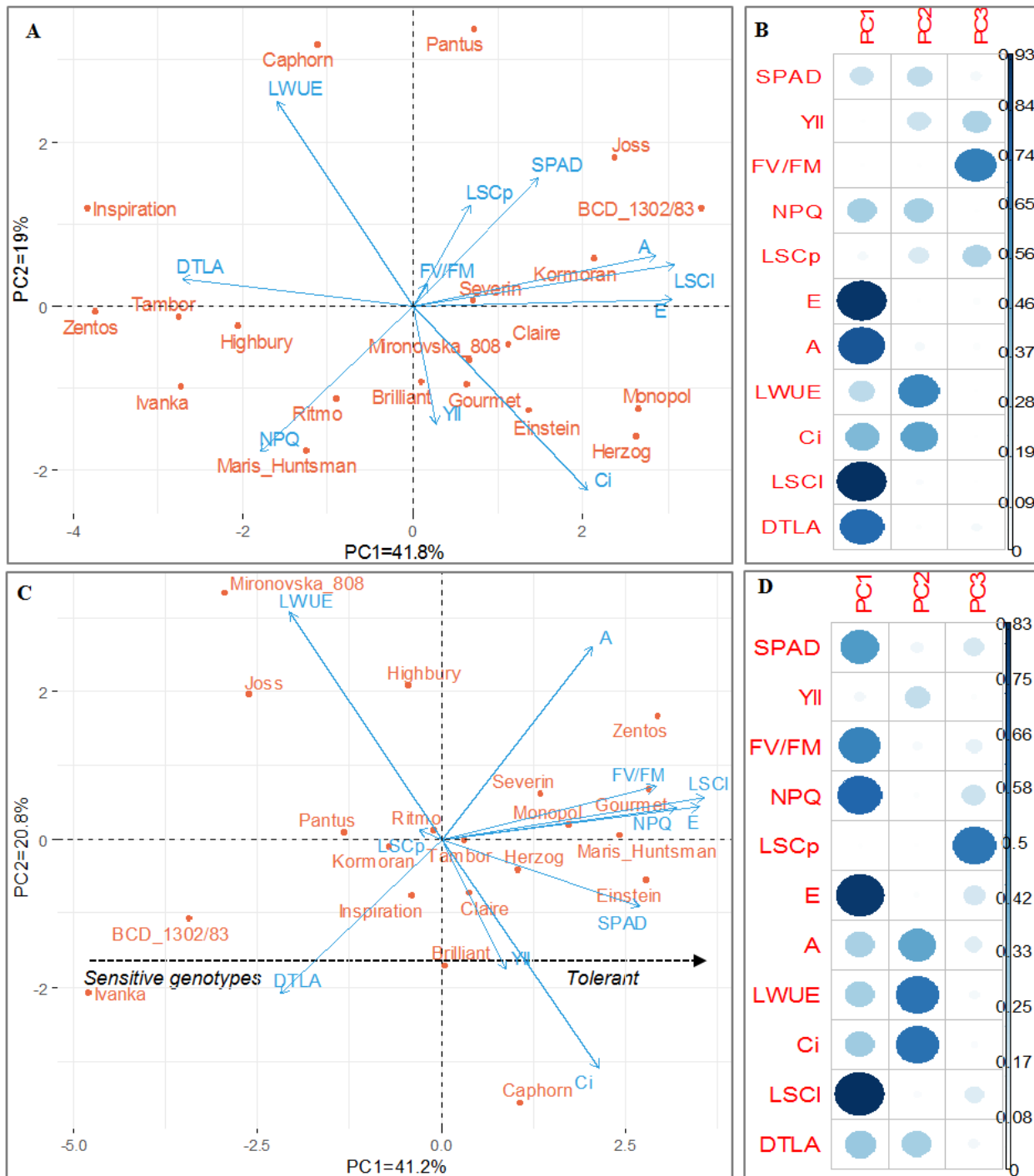


**FIGURE 3.S3** | Principal component analysis biplot using 11 photosynthesis and transpiration related variables under (A) rainfed, and (C) prolonged drought stress condition and the cosines square of the variables contributing to the newly constructed principal components under rainfed (B) and (D) prolonged drought stress conditions. The abbreviations of traits name are found in Table S2.

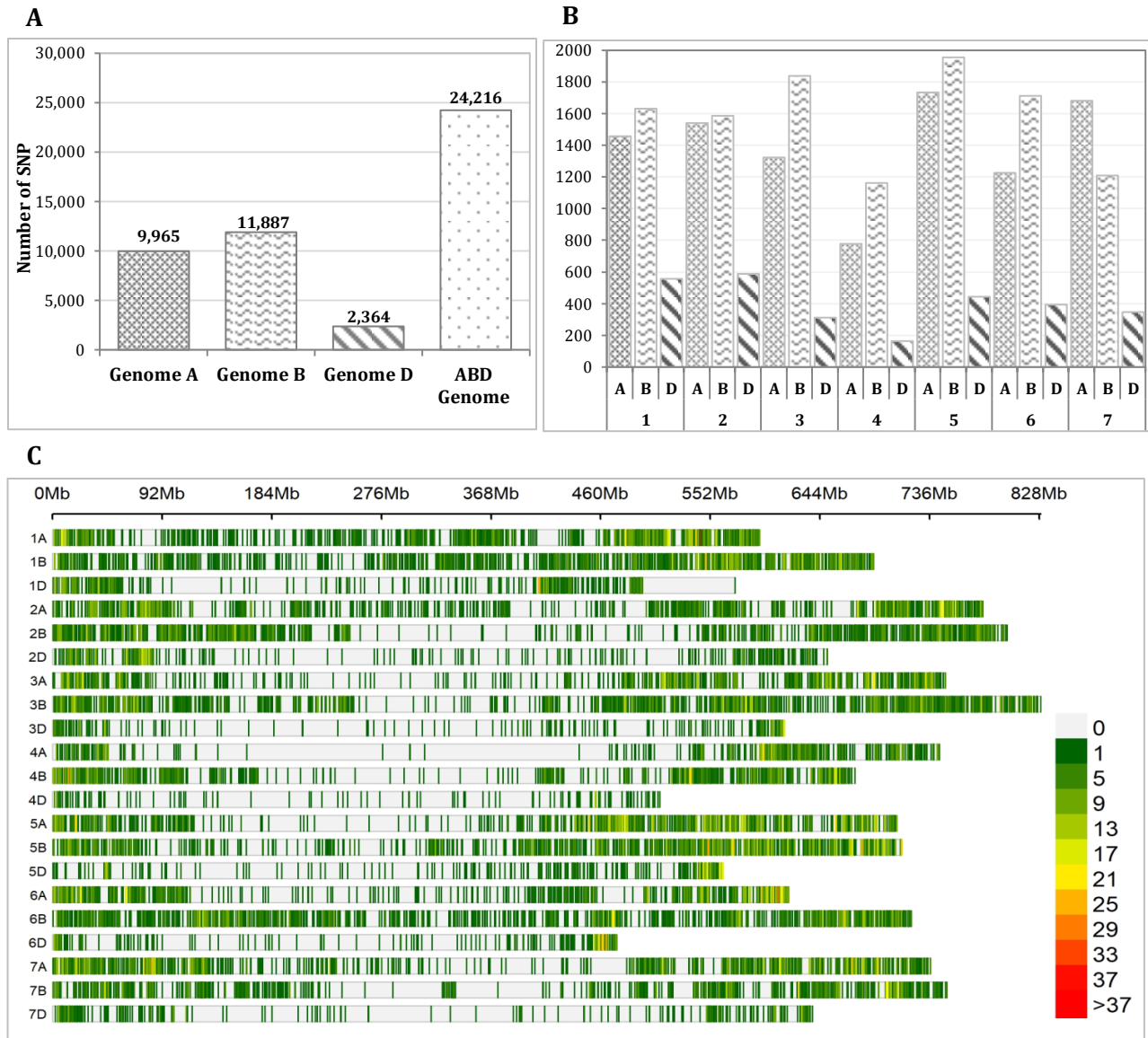


**FIGURE 3.S4** | SNP density across genomes of the studied winter wheat genotypes. (A) the number of SNP on each genome and the total number of SNP. (B) illustrates the number of SNP on each chromosome (from chromosome 1A to 7D). (C) Heatmap of the number of SNPs within 1 Mb window size per chromosome.

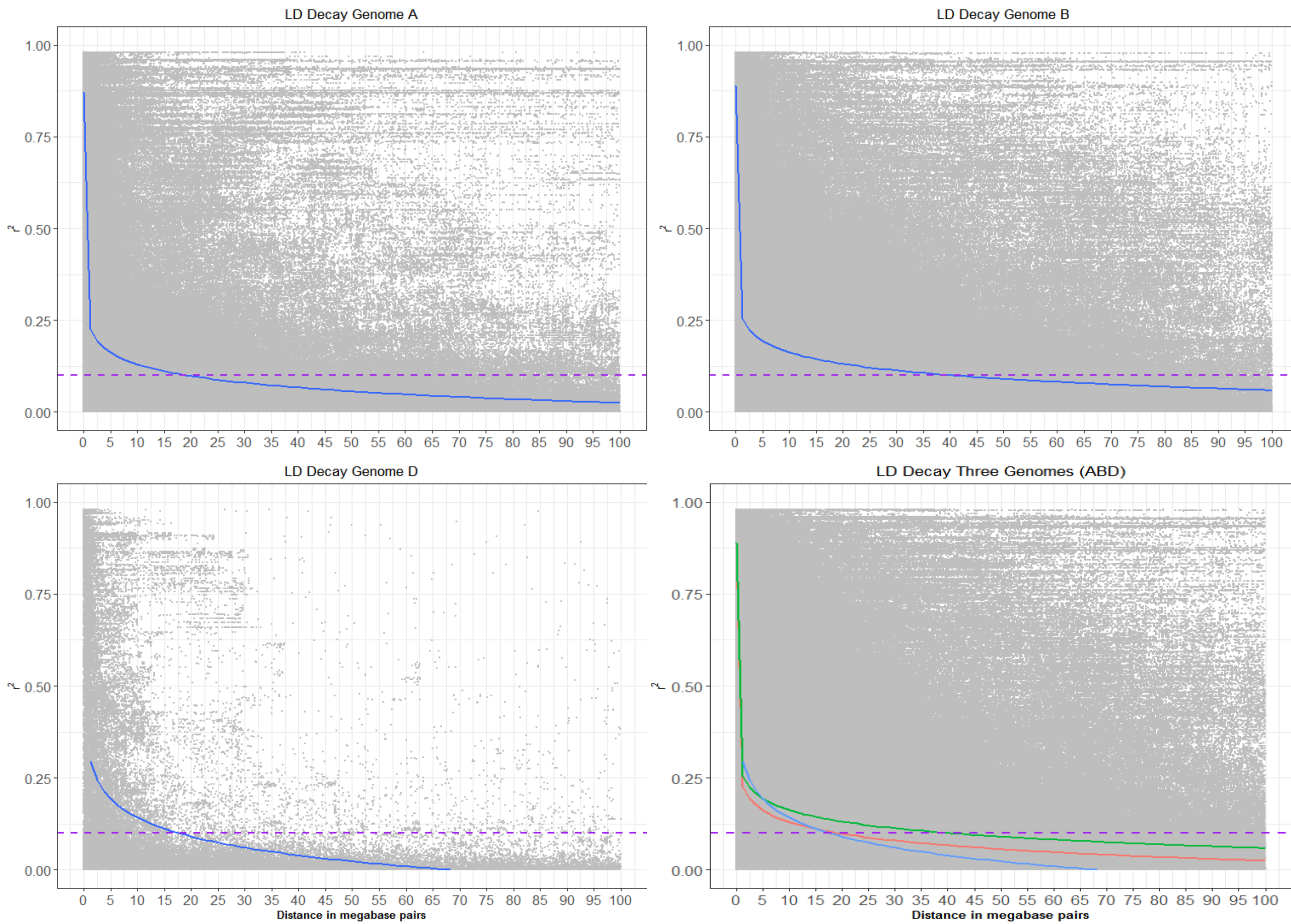
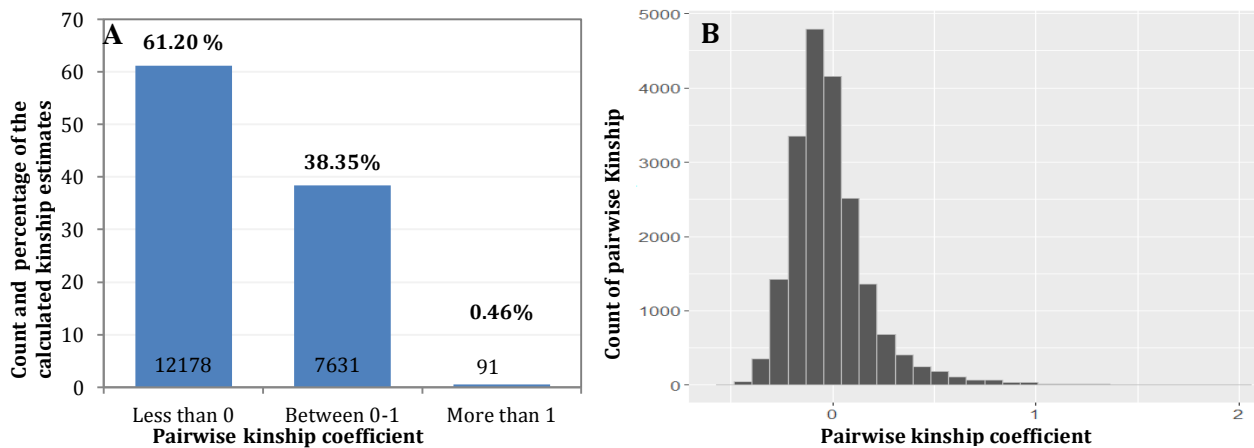


**FIGURE 3.S5** | Sliding windows showing the rate of linkage disequilibrium decay among the 200 genotypes of the diversity set across A, B, D genomes. The last window shows all three genomes in plot (non-fitting curve of genome A, B and D are colored in red, green and blue, respectively). The genetic distance corresponding to  $r^2 = 0.1$  were 19.0, 38.5 and 17.5 Mbp respectively for A, B and D genomes,



and was considered as the critical distance up to which a QTL could extend.

**FIGURE 3.S6** | (A) Classification of pairwise relative kinship into 3 classes; (B) Distribution of pairwise relative kinship estimates among 200 wheat genotypes.

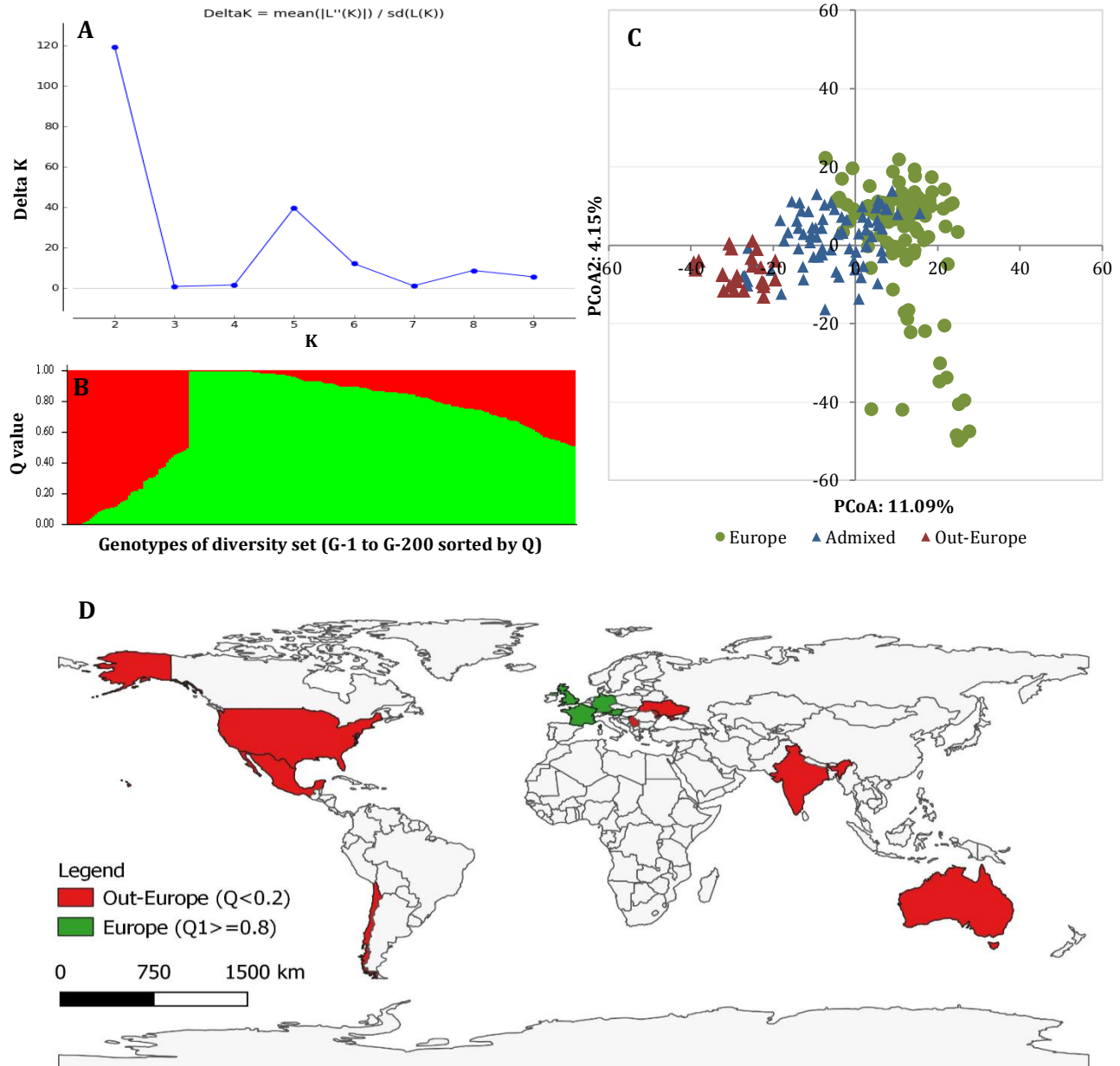


**FIGURE 3.S7** | Representation of the wheat panel population structure. (A) Inferred population structure based on the change of  $\text{LnP}(D)$  between consecutive  $K$  method developed by Evanno et al. (2005). (B) Display of ancestry coefficient  $Q$  of two subpopulations at  $K = 2$  from STRUCTURE analysis. (C) Principle components analysis (PCA) of individual cultivars of the diversity set. Legend indicates cultivars originated from Europe (green), out of Europe (red) and admixed (blue). (D) Geographical representation of ancestry coefficient  $Q_1$  at  $K=2$  showing country of origin of the two subpopulations (Europe included Germany, Great Britain, France, and Austria, while Out-Europe comprised USA, Serbia, Ukraine, Australia, Moldavia, Mexico, and Australia).

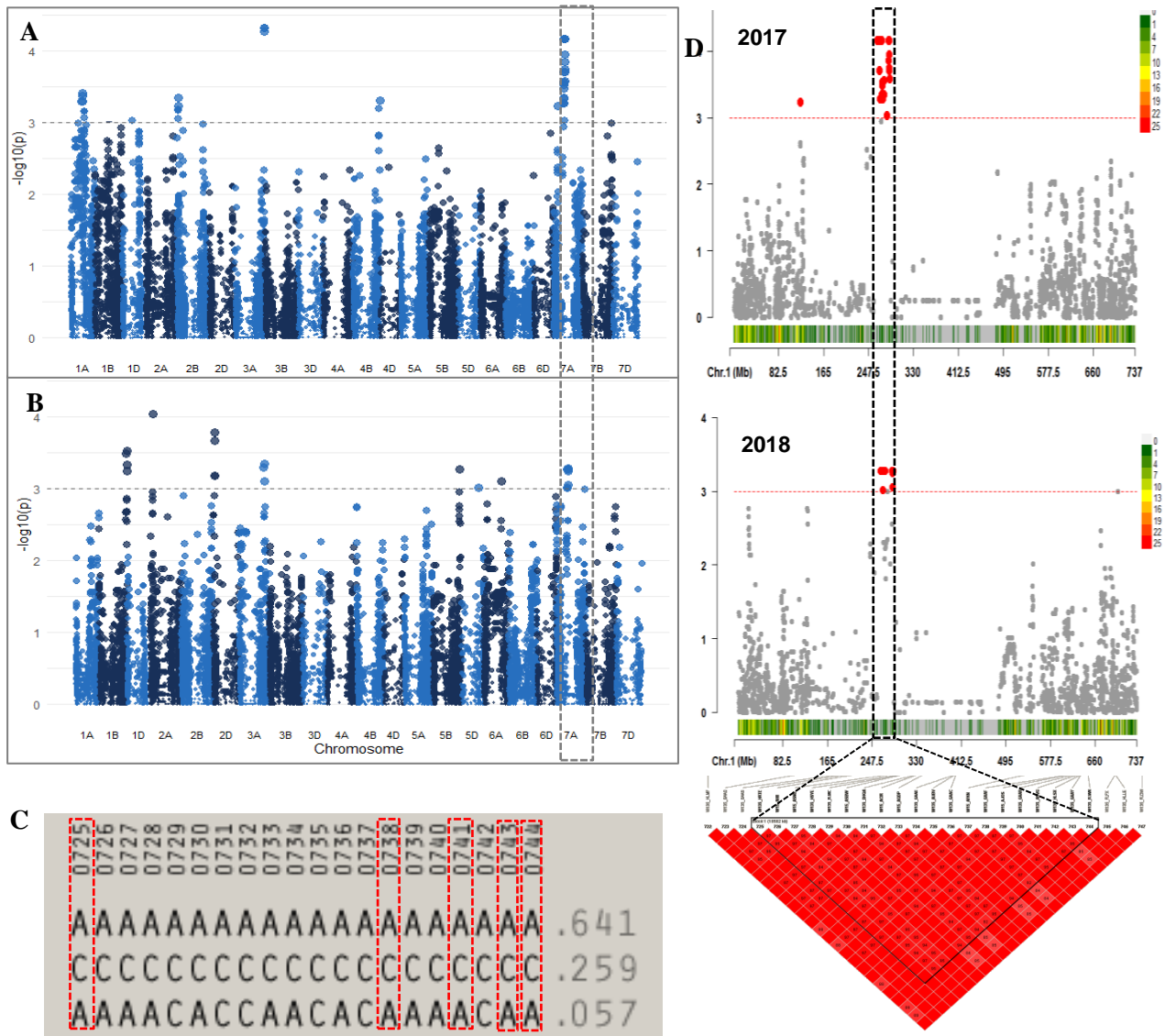


**FIGURE 3.S8** | Manhattan plot for SPAD under control including significant MTAs in (A) 2017 and (B) 2018. (C) Haplotype block on chromosome 7A comprising five SNPs [AX-94760655 (725), AX-158600987 (738), AX-108905937 (741), AX-158601006 (743), and AX-158591424 (744)] associated with SPAD in both years. (D) Manhattan plot showing a hotspot of 5 stable SNPs of CHR 7A region of 18 Mbp length delimited from AX-94760655 (267.570 Mbp) to AX-158591424 (286.152 Mbp) associated with SPAD in 2017 and 2018.

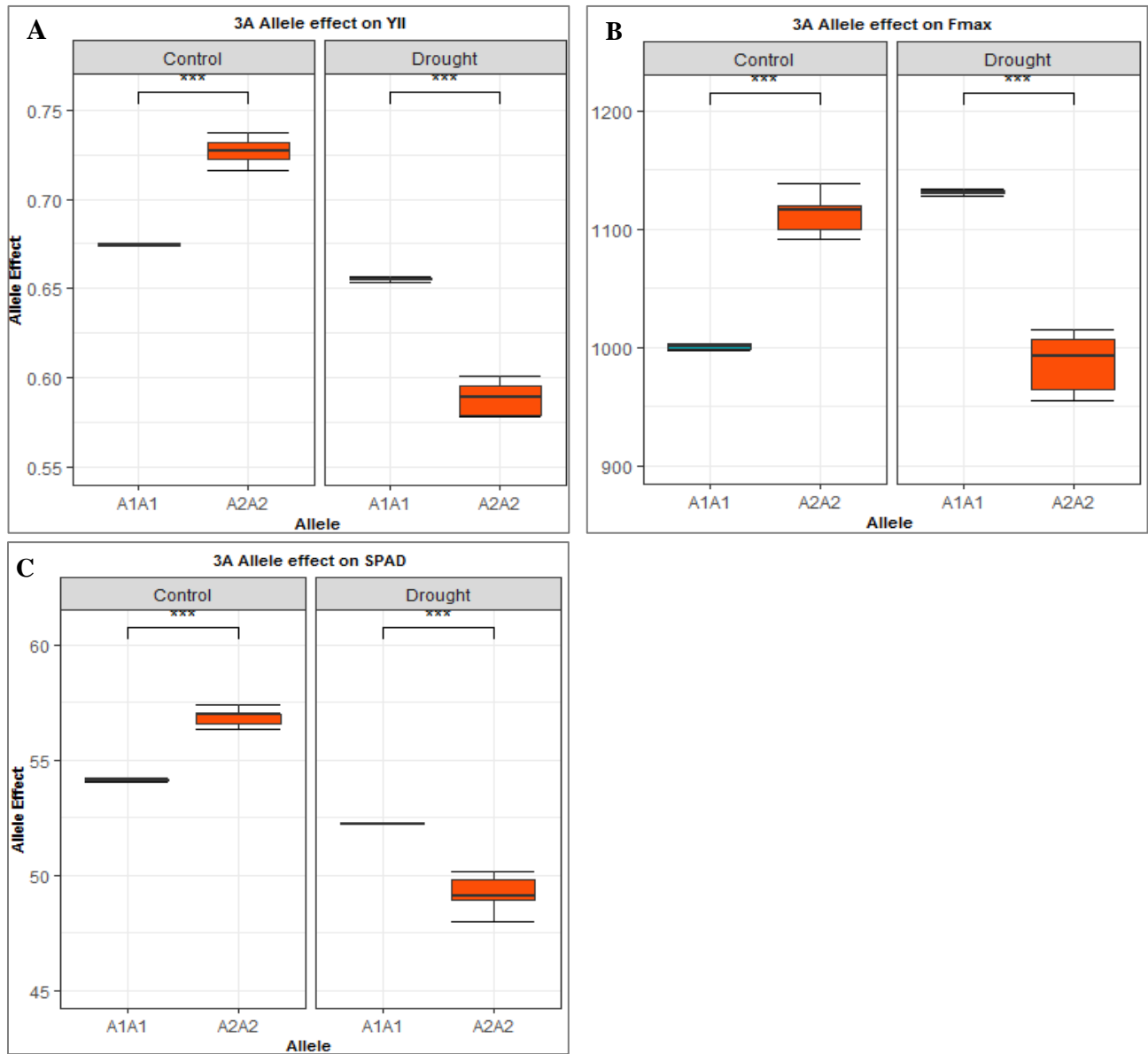


**FIGURE 3.S9** | Illustration of marker by treatment interactions on photosynthesis related traits: (A) effective quantum yield of photosystem II; (B) maximum chlorophyll fluorescence; (C) chlorophyll content. Major alleles (TT) had higher values than the minor alleles (CC) under drought conditions whereas the contrary schema was observed in control under rainfed conditions.

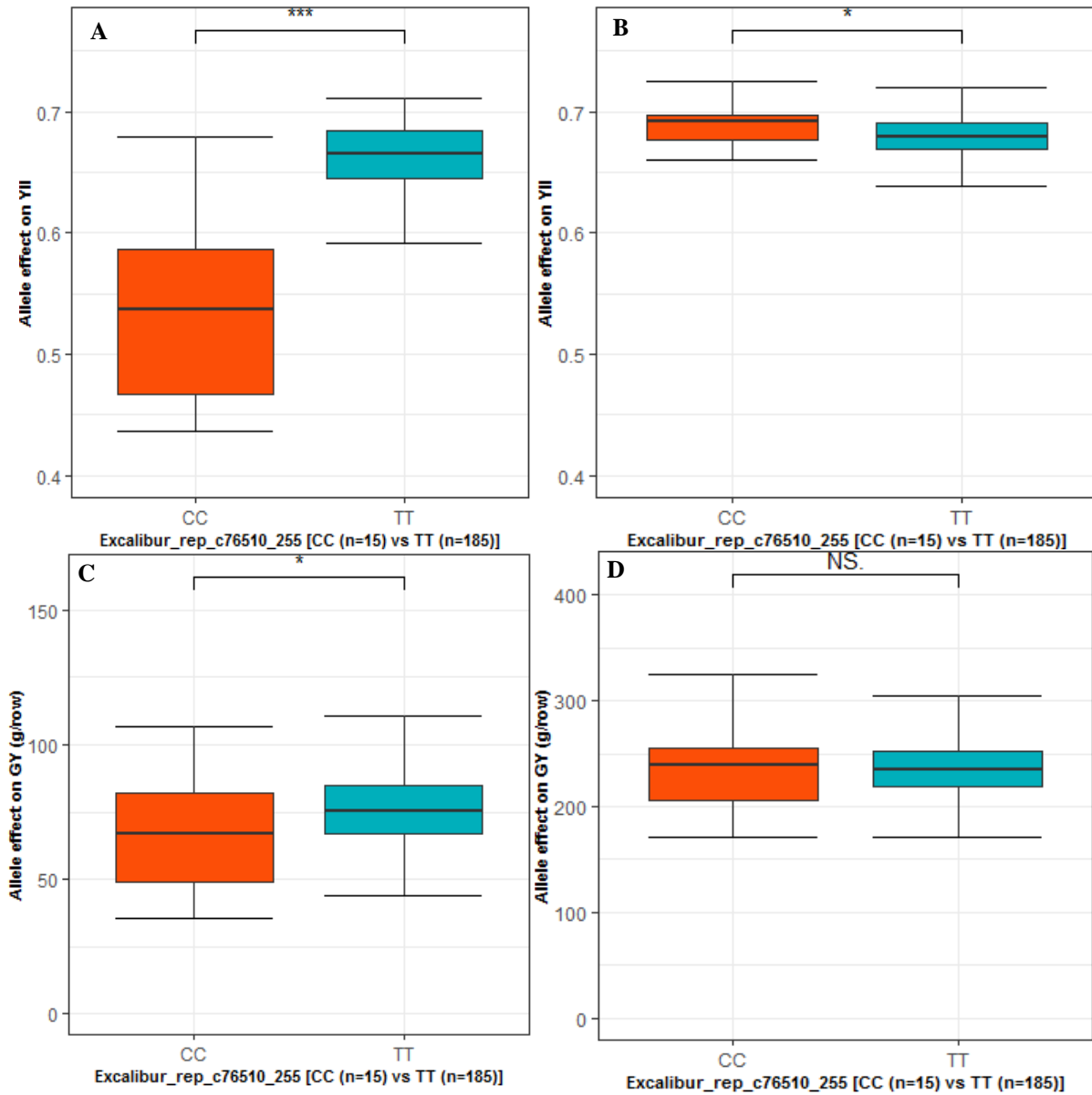


**FIGURE 3.S10** | Allelic effect of *Excalibur\_rep\_c76510\_255* on YII under drought (A) and rainfed (B); allelic effect on GY under drought (C) and rainfed (D). Two-sample *t*-test P-value shows significant allelic effect difference with reference to major and minor allele.

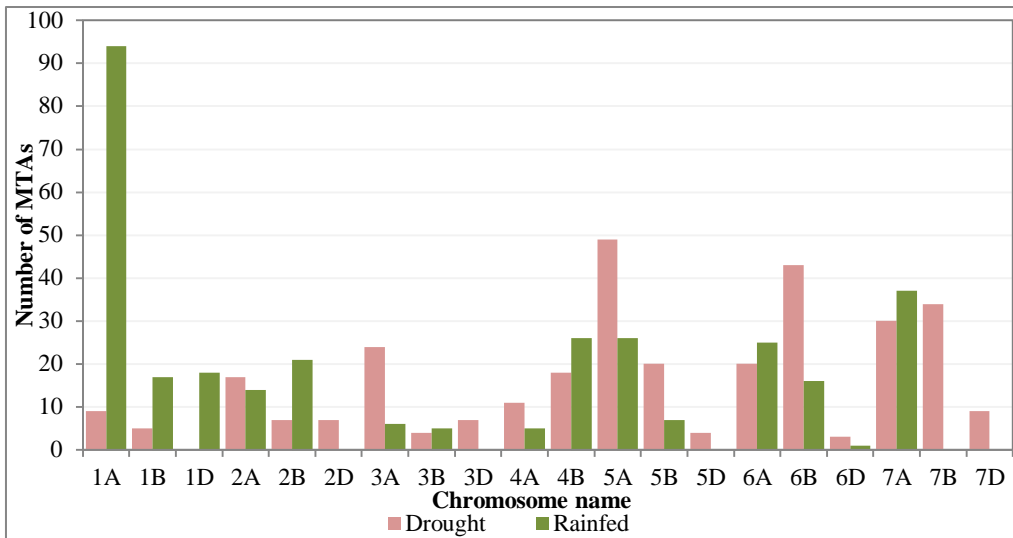


FIGURE 4.S1 | Distribution of MTAs number across chromosomes.

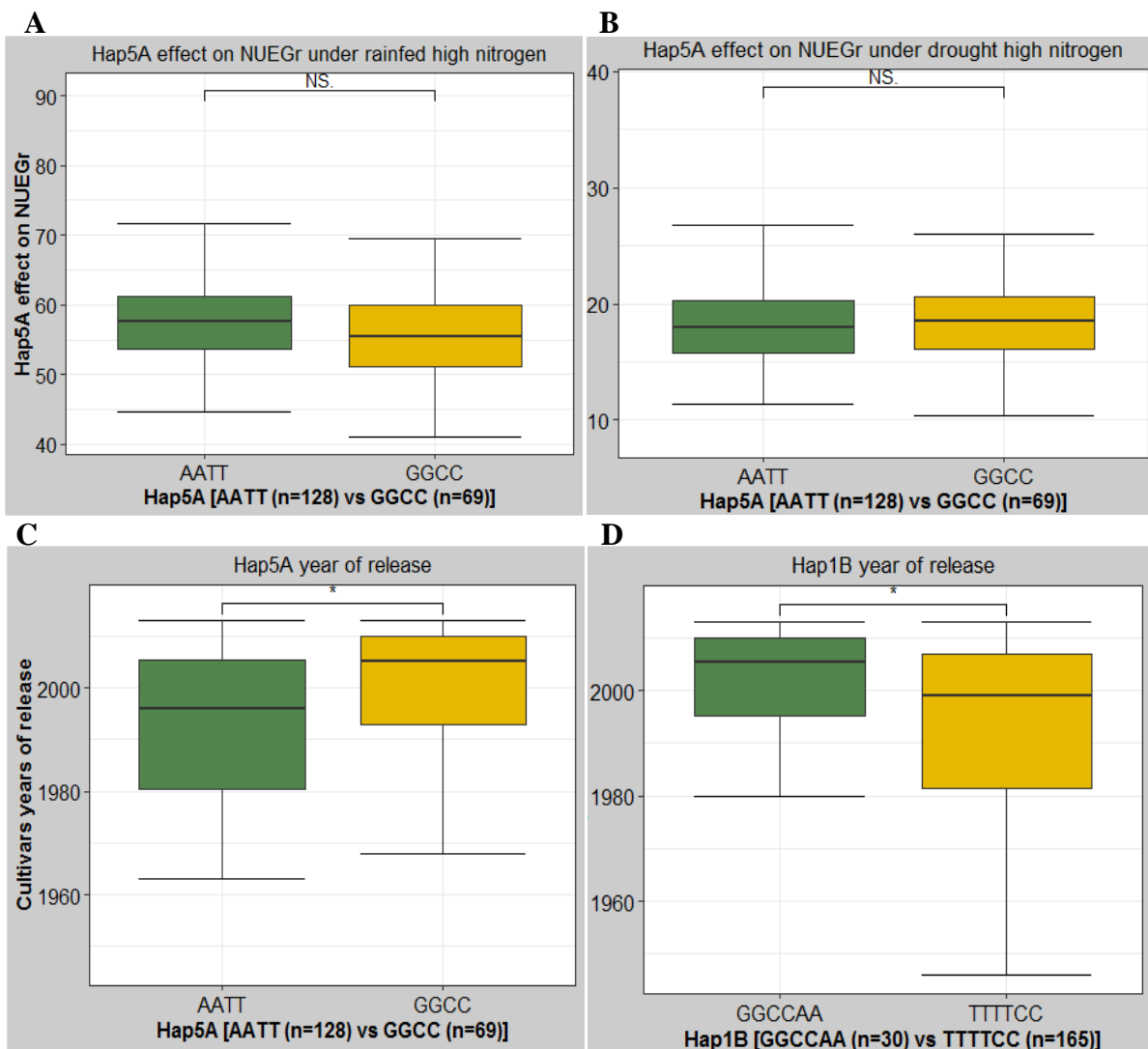
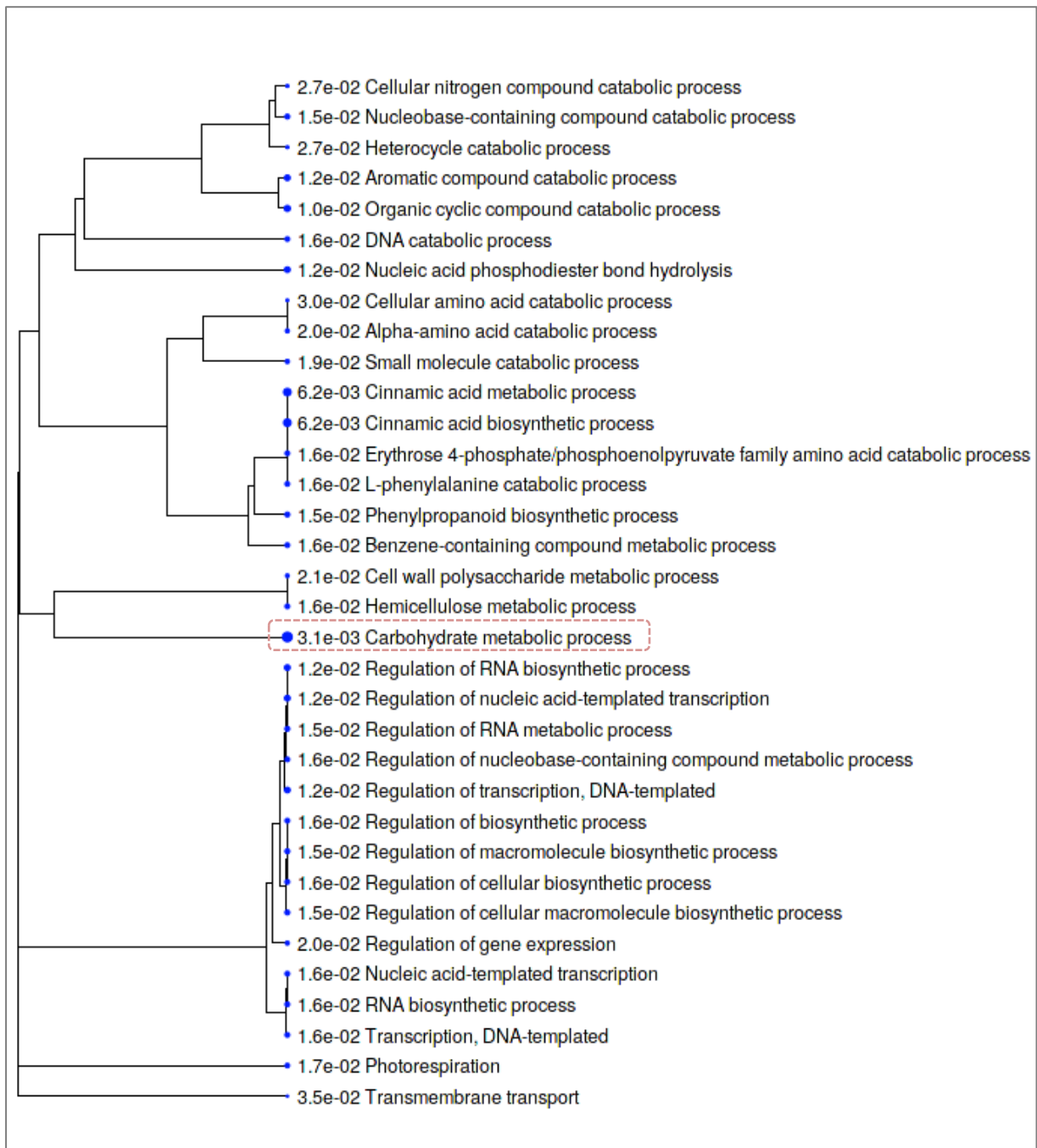
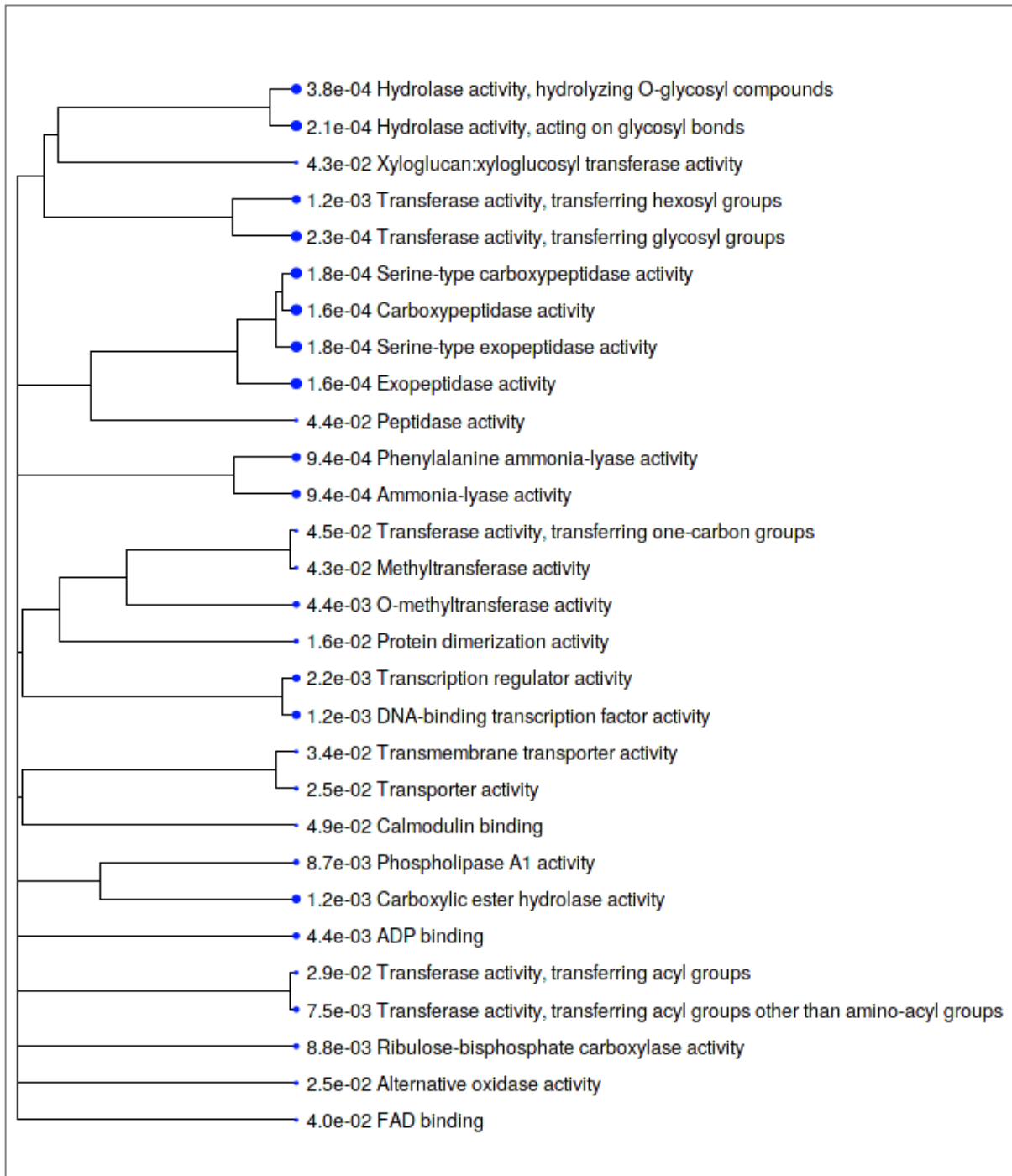


FIGURE 4.S2 | Allelic effects of the haplotype *Hap5A* on NUEGr under (A) rainfed high N and (B) drought high nitrogen. Comparison of year of release of cultivars caring the two haplotypes forms of (C) *Hap5A* and (D) *Hap1B*.



**FIGURE 4.S3** | (A) Hierarchical clustering tree summarizing the correlation among significant pathways listed in the Enrichment tab showing the biological process of 2653 genes retrieved from 27 QTL regions. Pathways with many shared genes are clustered together. Bigger dots indicate more P-values that are significant.



**FIGURE 4.S3** | (B) Hierarchical clustering tree summarizing the correlation among significant pathways listed in the Enrichment tab showing the molecular function of 2653 genes retrieved from 27 QTL regions. Pathways with many shared genes are clustered together. Bigger dots indicate more P-values that are significant.

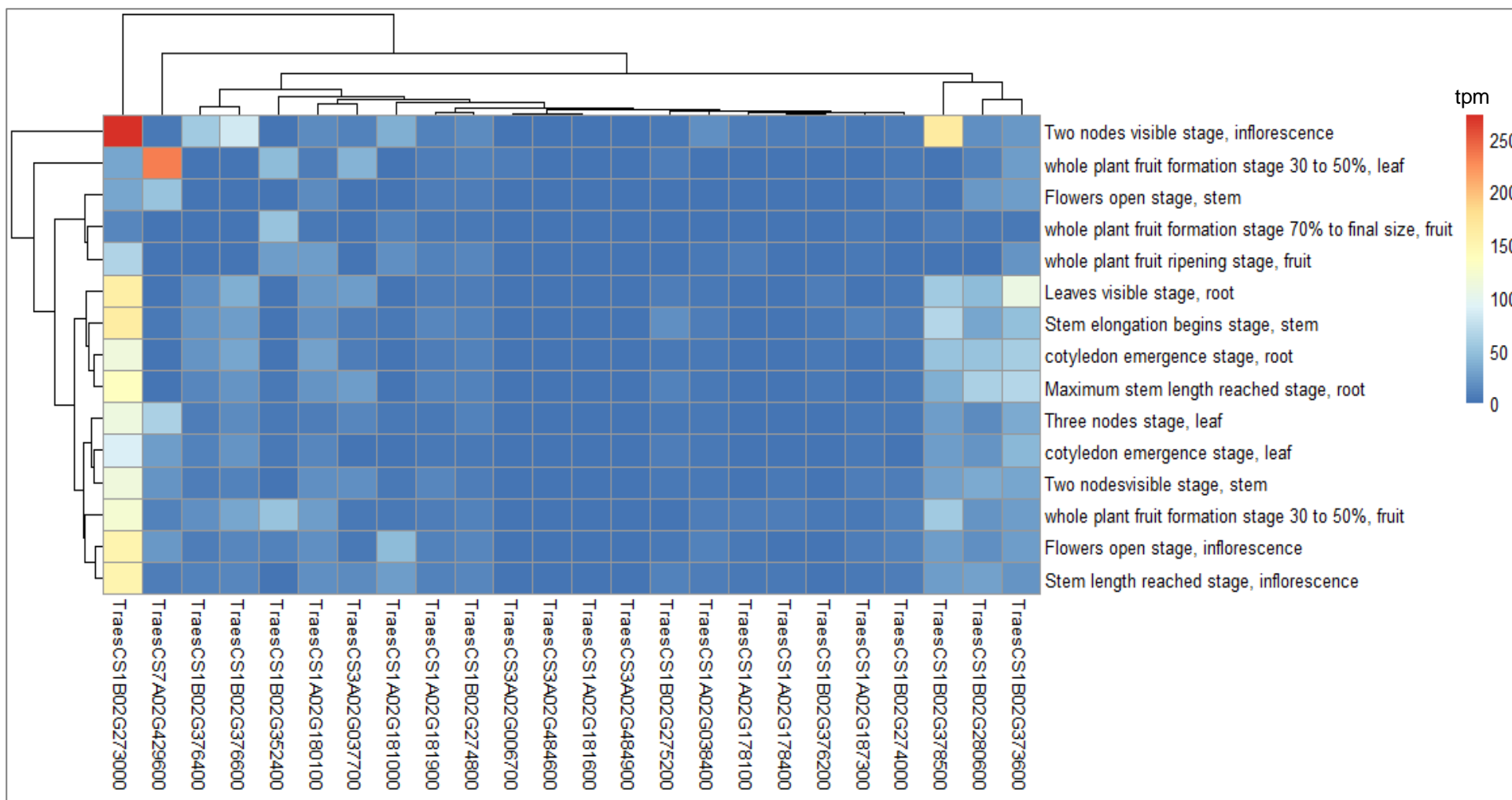
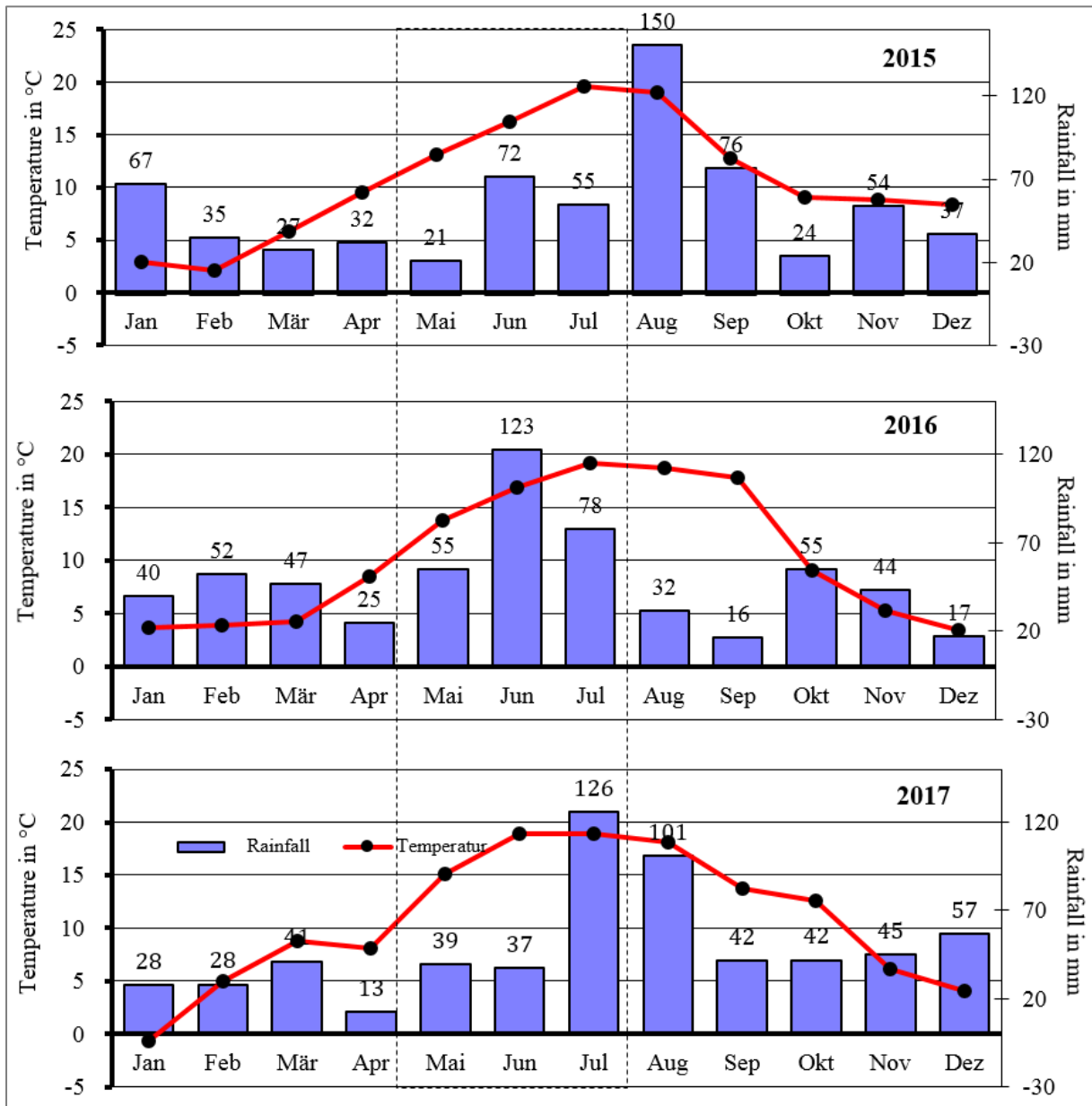
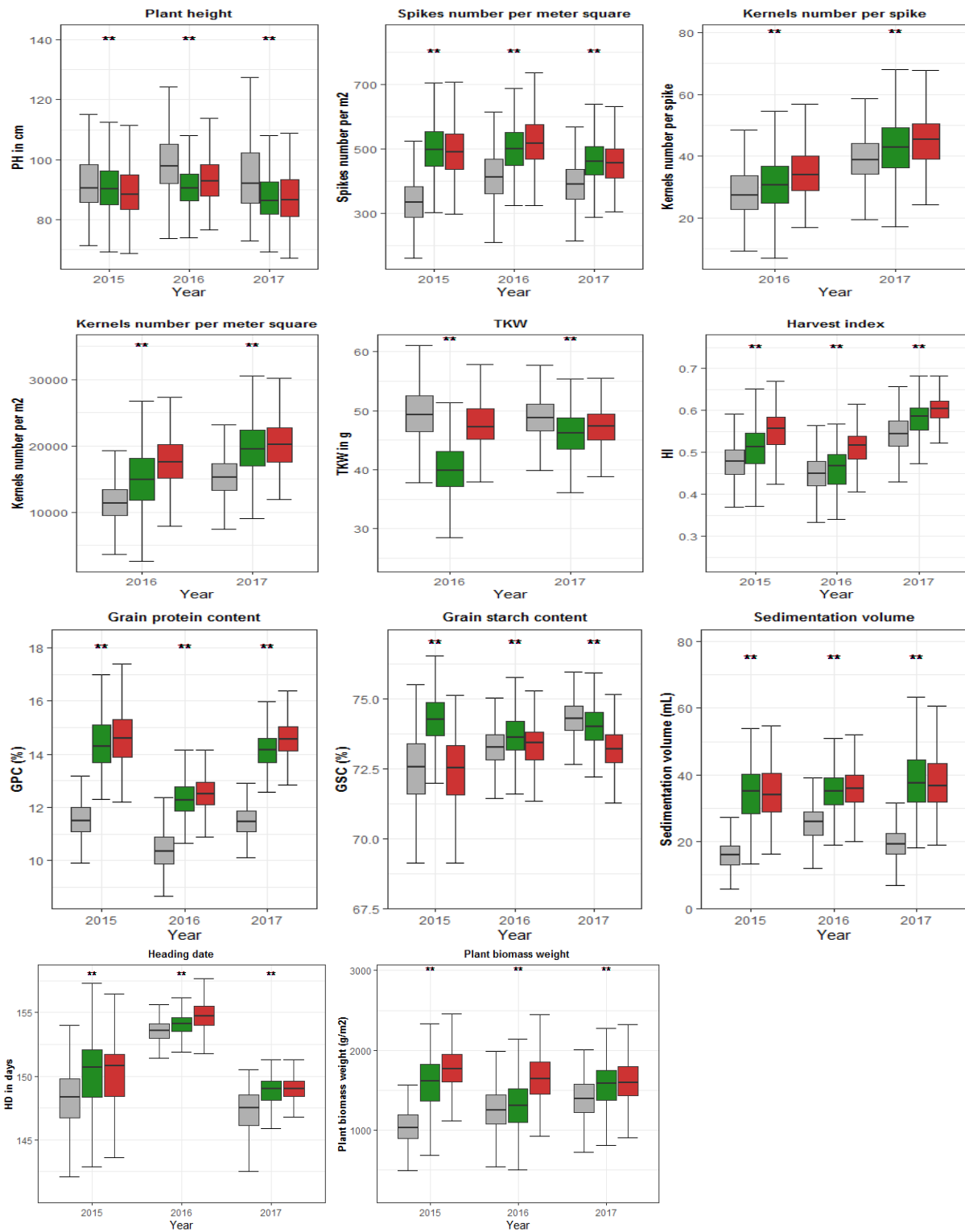


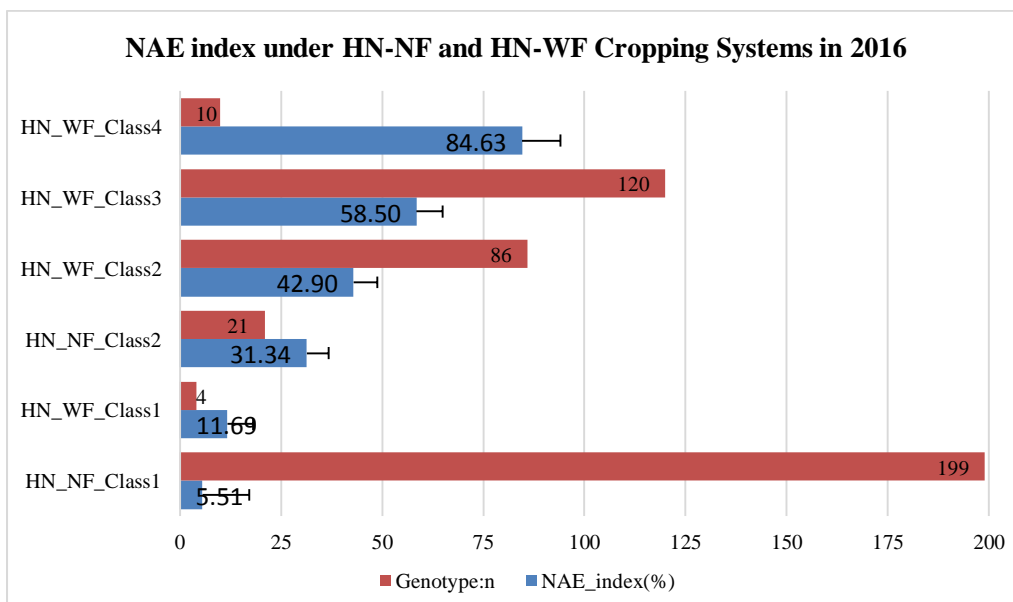
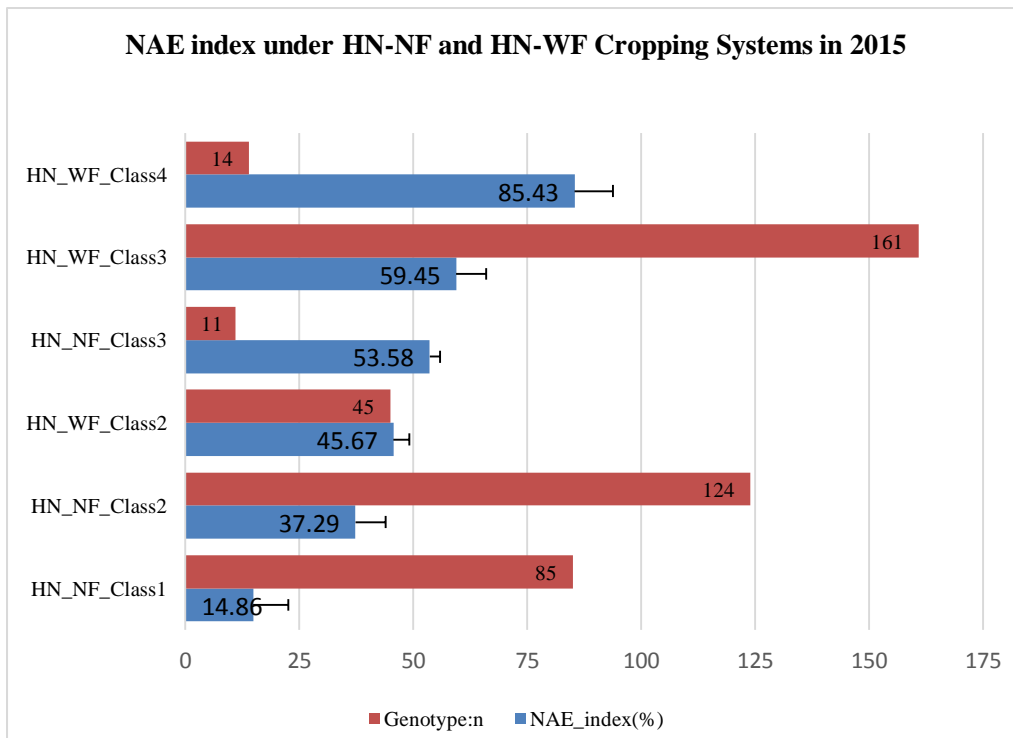
FIGURE 4.S4 | Differential genes expression (DEG) pattern estimated in TPM (transcripts per kilobase million) of 24 candidate genes.

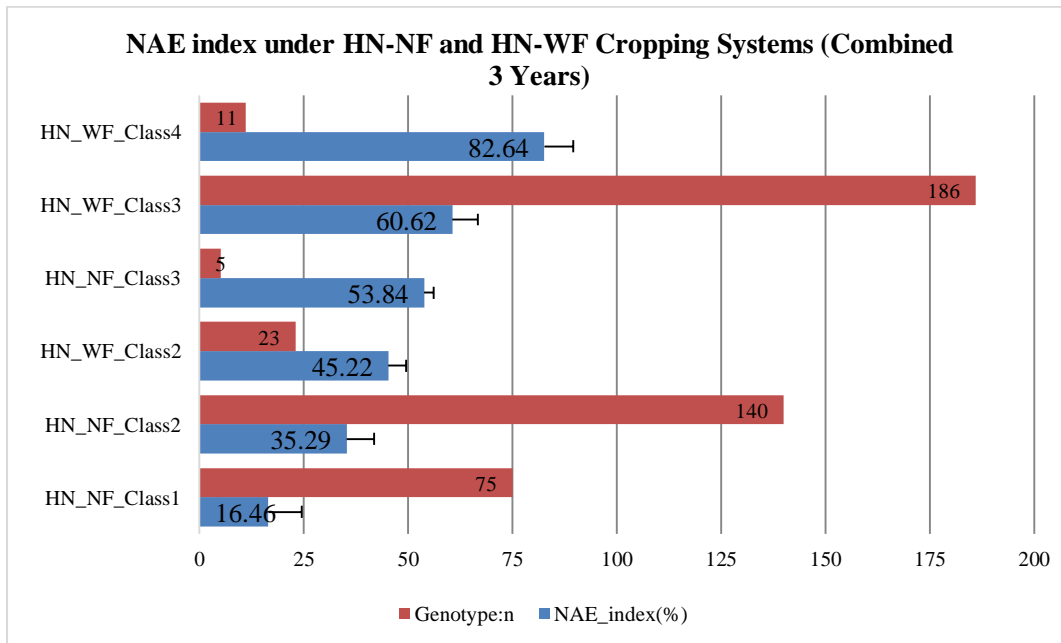
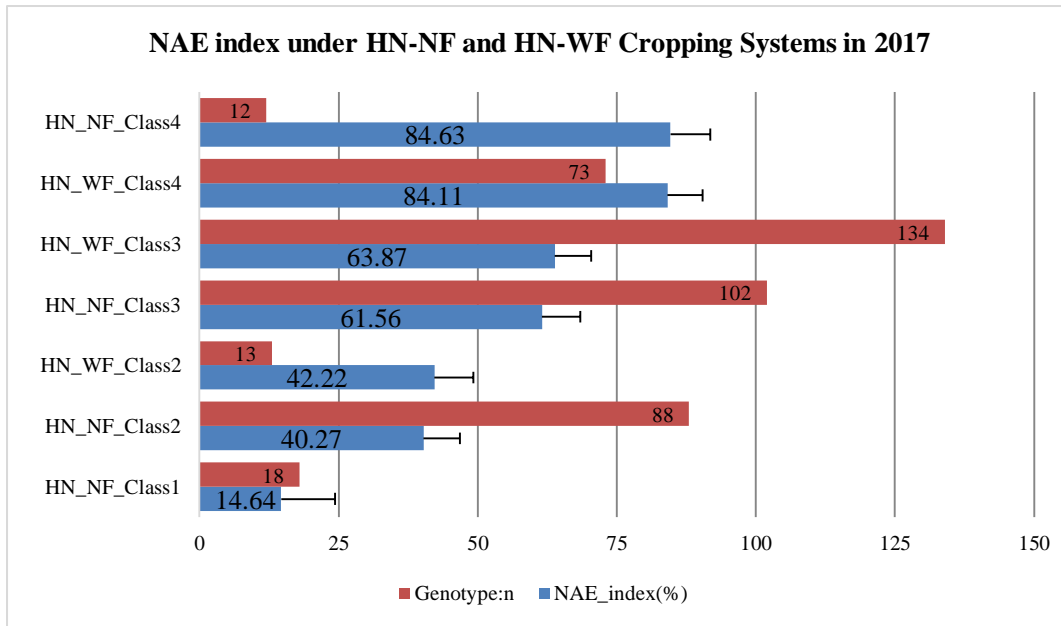


**FIGURE 5.S1** | Weather conditions data from the experimental site illustrating significant differences in rainfall (pink bars) and temperature (red curves) among growing seasons 2015, 2016, and 2017 at reproductive stage (dotted rectangle).

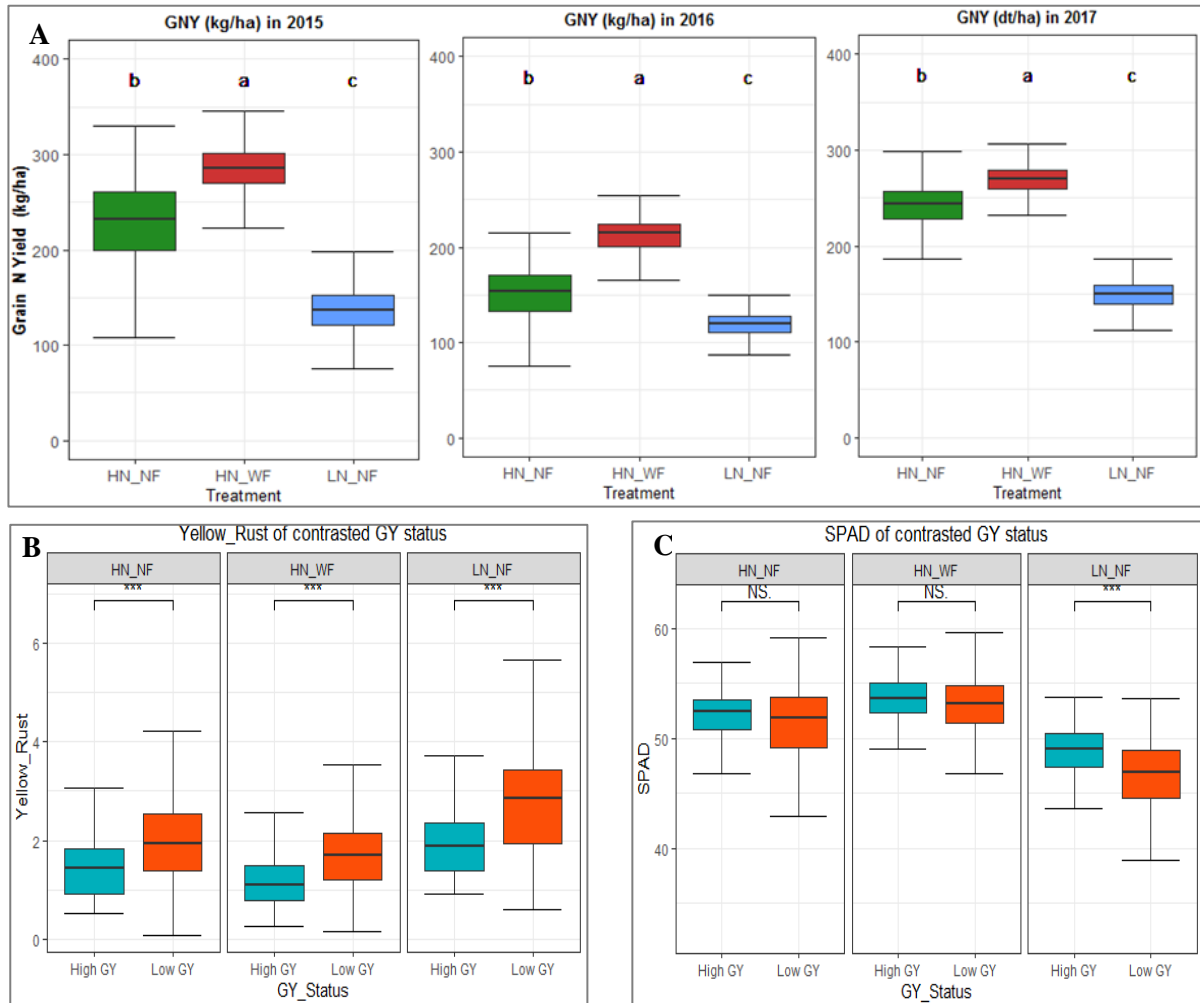


**FIGURE 5.S2** | Significant differences among the three cropping systems (CS) for evaluated traits with LN-NF in gray, HN-NF in green, and HN-WF in red color. NS means not significant at  $p=0.05$ , \*\* significant at  $p=0.01$ , and \*\*\* significant at  $p=0.001$ .

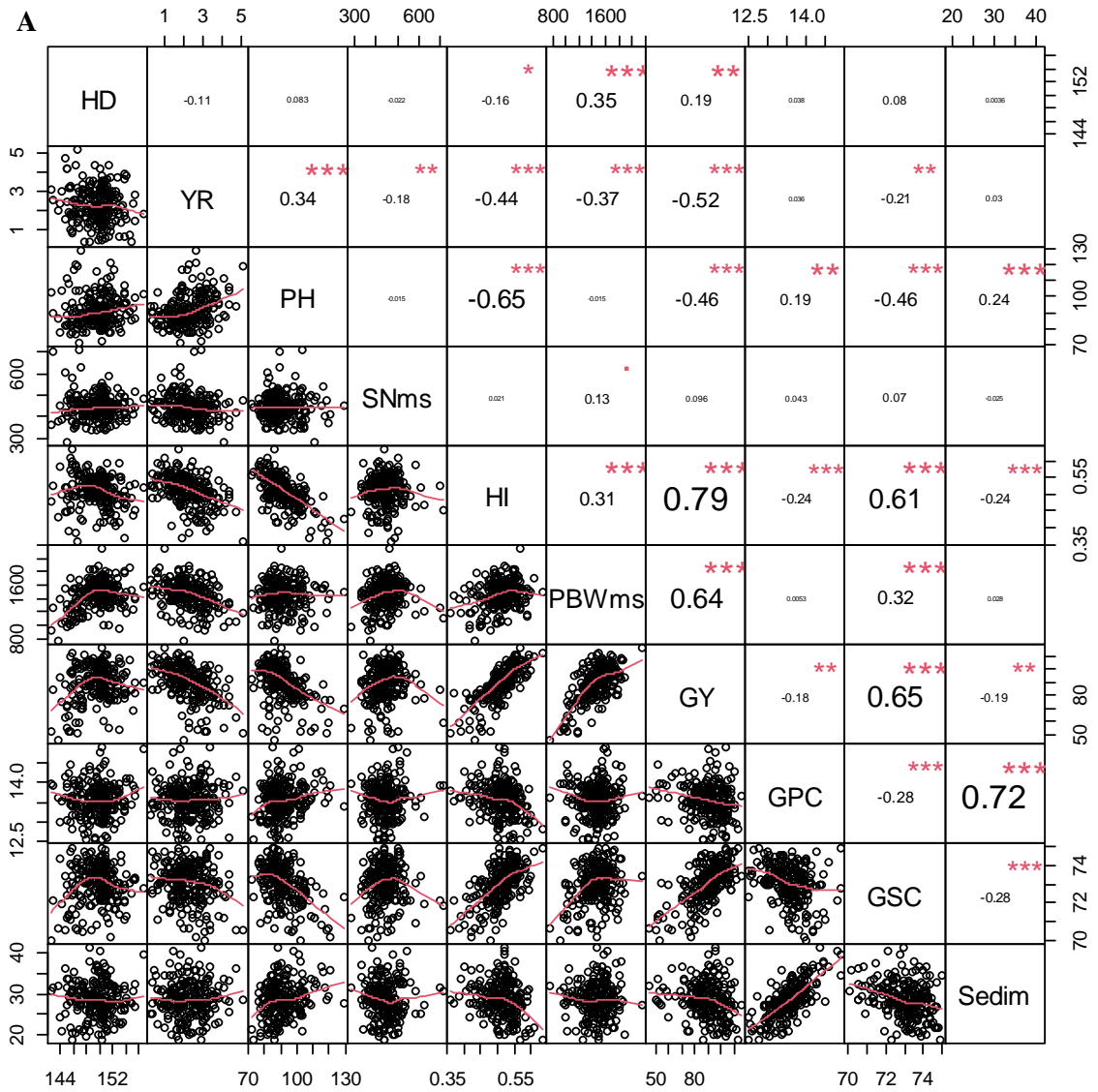


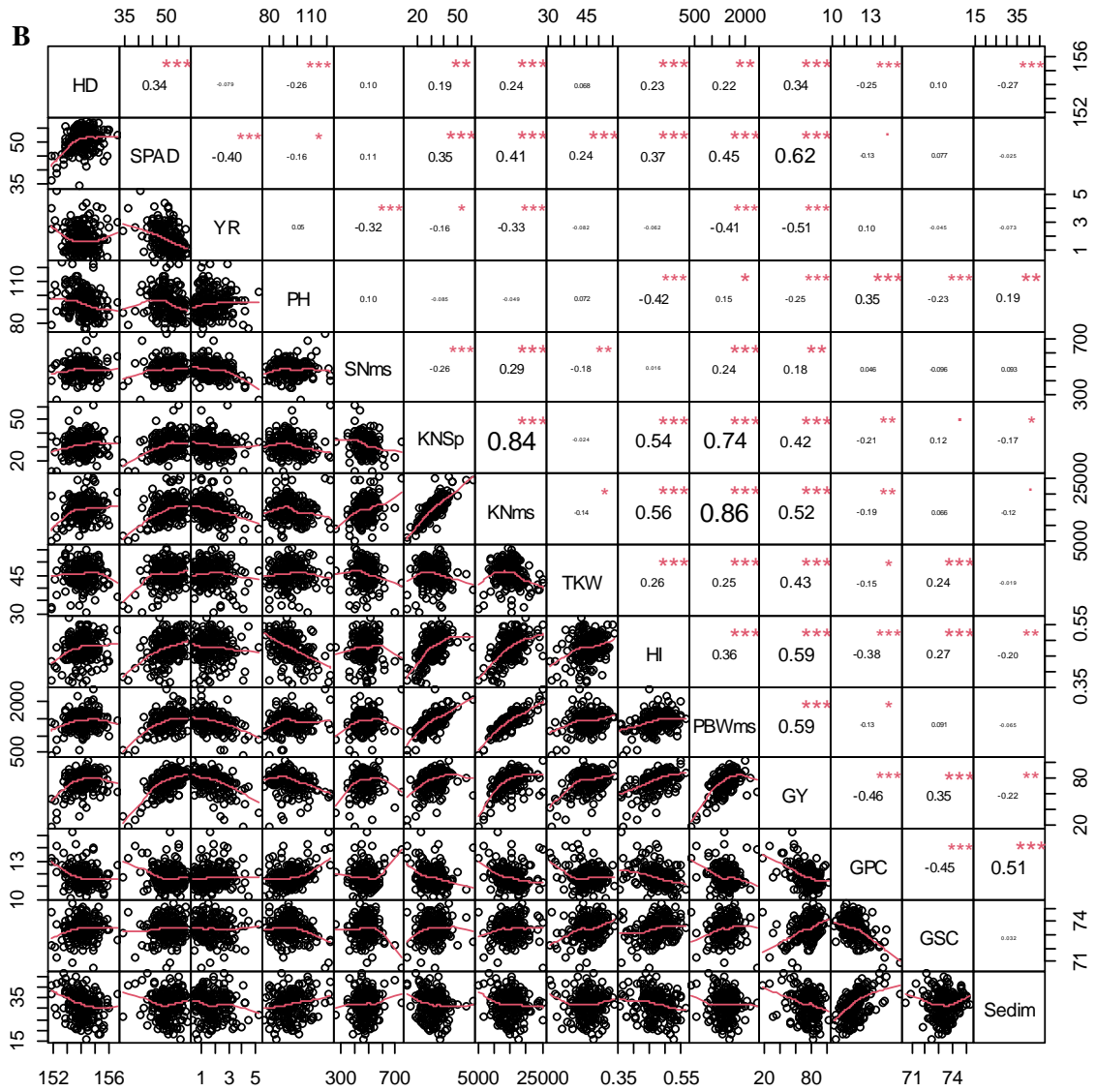


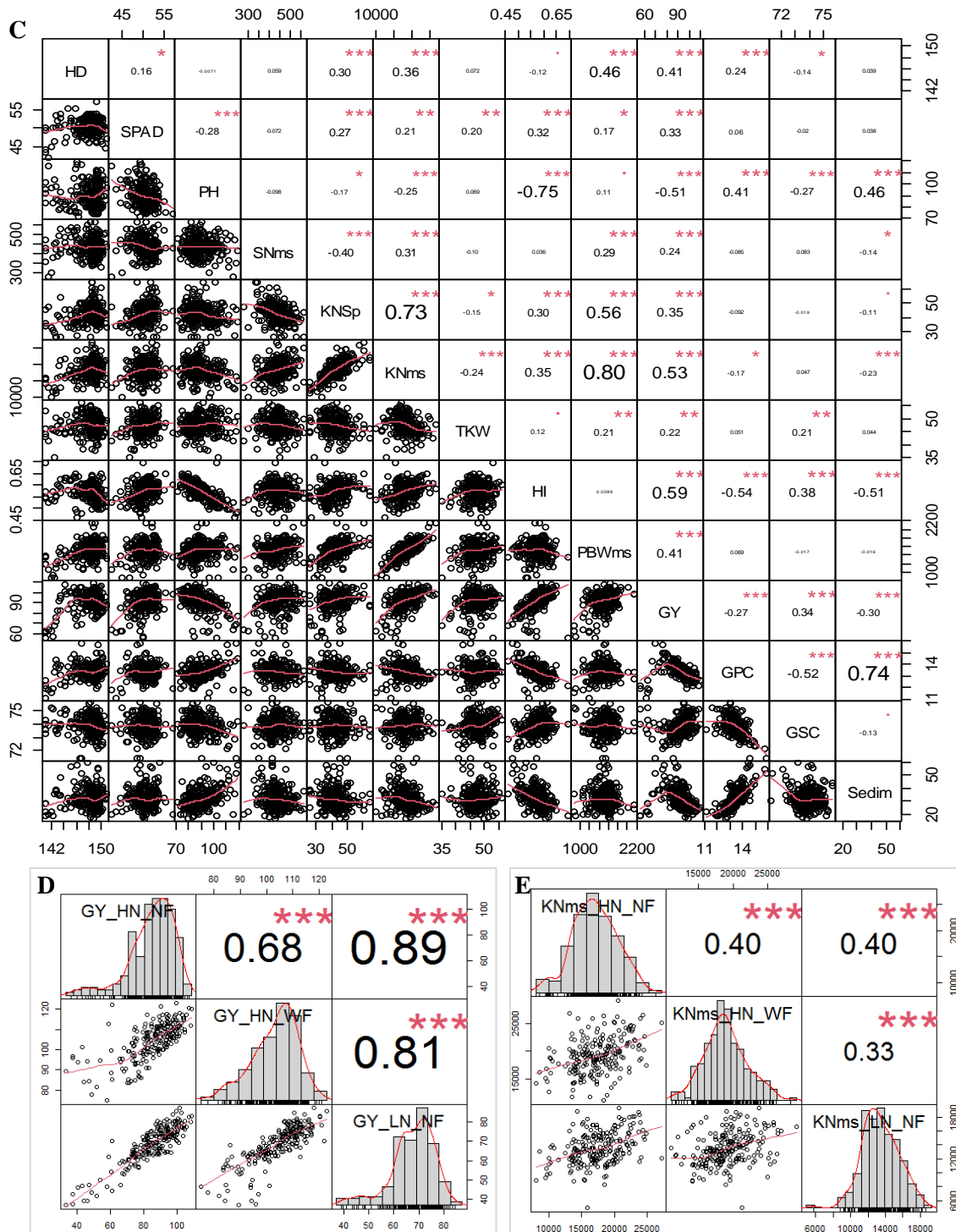
**FIGURE 5.S3** | Agronomy efficiency use of Nitrogen supplied. The red bar charts are the number of cultivars belonging to the defined class of NAE index. The blue bar charts are showing the average percentage of NAE.



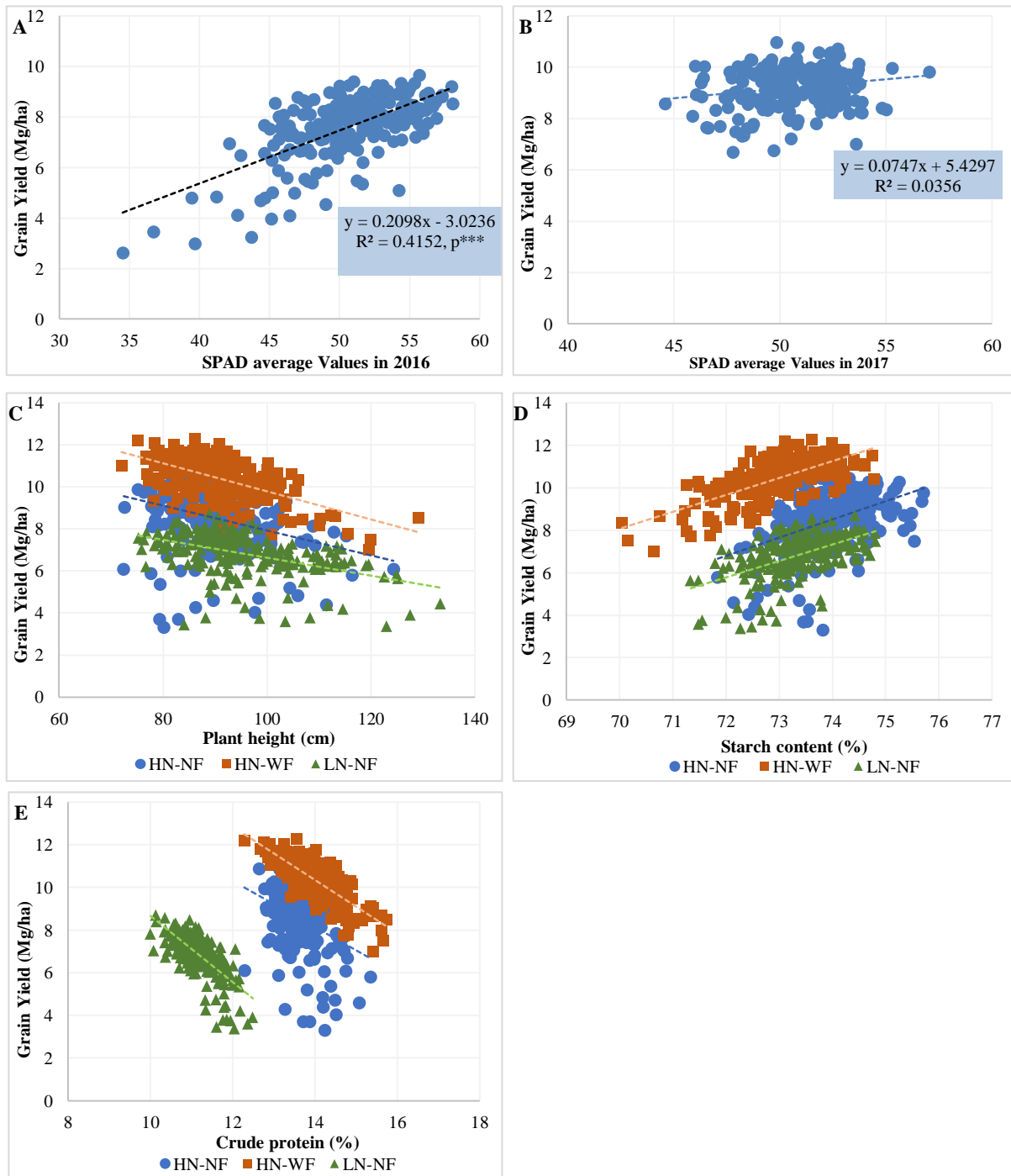
**FIGURE 5.S4** | (A) Grain N yield (GN Y) under three CS (HN-NF in green color, HN-WF in red color, LN-NF in blue color) across the three years (abc) above the boxplots denotes the groups means with a the highest and c the lowest means GNY; (B) Resilience to YR infestation of GY contrasting cultivars; (C) Chlorophyll content (SPAD) of GY contrasting cultivars. NS means not significant at  $p=0.05$  and \*\*\* significant at  $p=0.001$ .



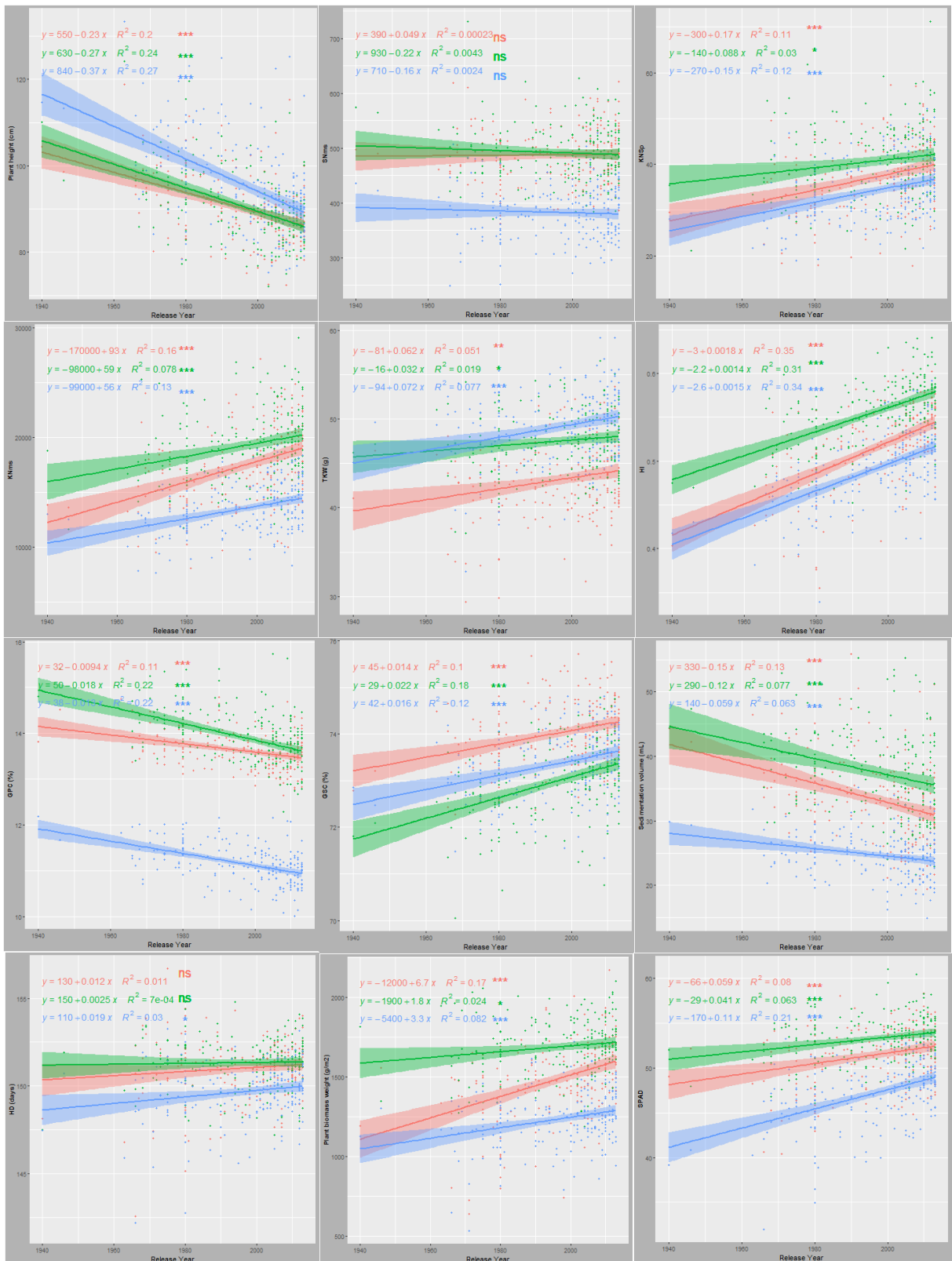


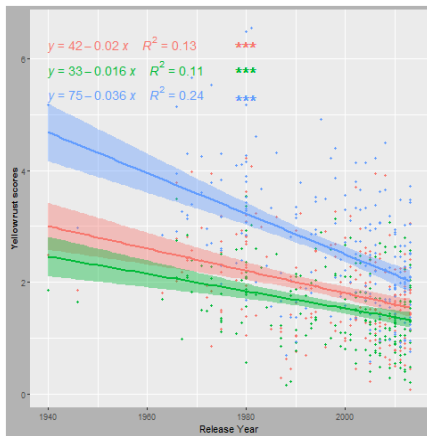


**FIGURE 5.S5** | Pearson correlation coefficients and associated probability among evaluated traits based on of the genotype mean from the three tested cropping systems in three years of trials (A)=2015; (B)=2016; (C)=2017. (DE) Correlation among the three CS for GY and KNms. All traits were measured in a wheat population containing 220 breeding lines grown in three cropping systems between 2015 and 2017. The number of stars indicates the significance level, \* $P < 0.05$ ; \*\* $P < 0.01$  and \*\*\*  $P < 0.001$ .

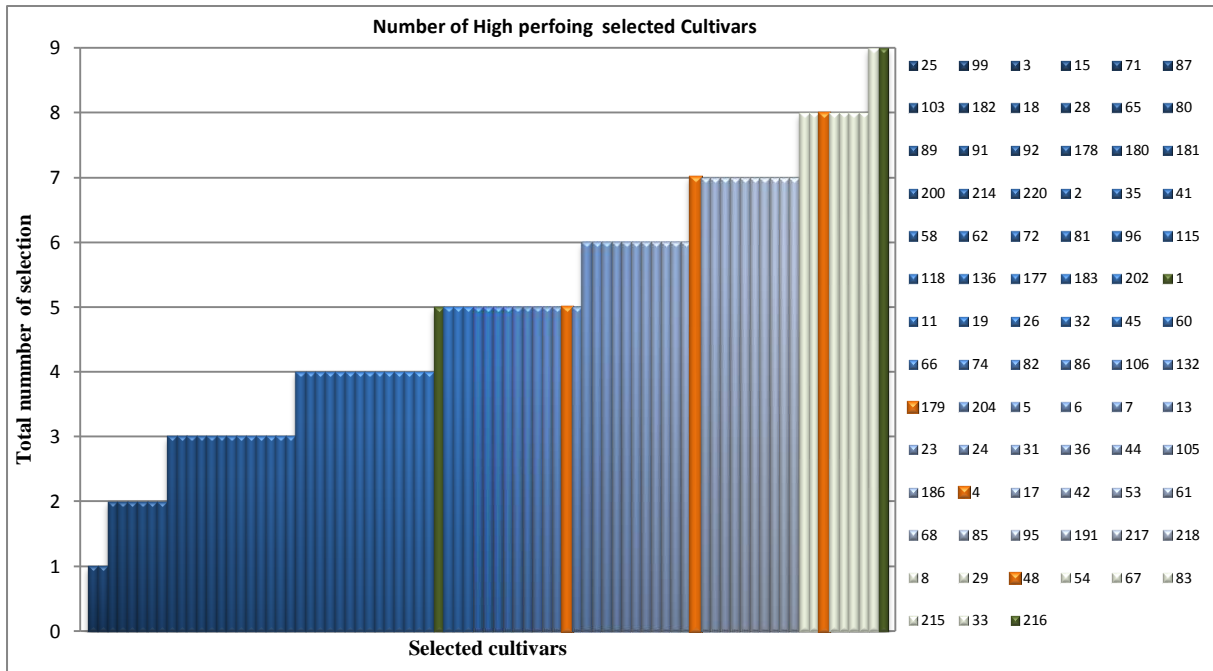


**FIGURE 5.S6** | Relationship between GY and traits of interest. (A) average SPAD in 2016; (B) average SPAD in 2017; (C) plant height (cm); (D) grain starch content (%); (E) grain crude protein content (%) under each CS. The regressions equations, the significance of the slopes and comparison among slopes of the three CS is given Table S14.





**FIGURE 5.S7** | Temporal trends observed in evaluated traits in relation to year of registration among 209 cultivars under three CS, HN-WF in green, HN-NF in red and LN- NF in blue color. The center lines represent the regression lines and the shaded regions represent the 95% confidence intervals. The signs ns stands for the slope is not significant at 0.05; \* is significant at 0.05; \*\*is significant at 0.01, \*\*\*is significant at 0.001.



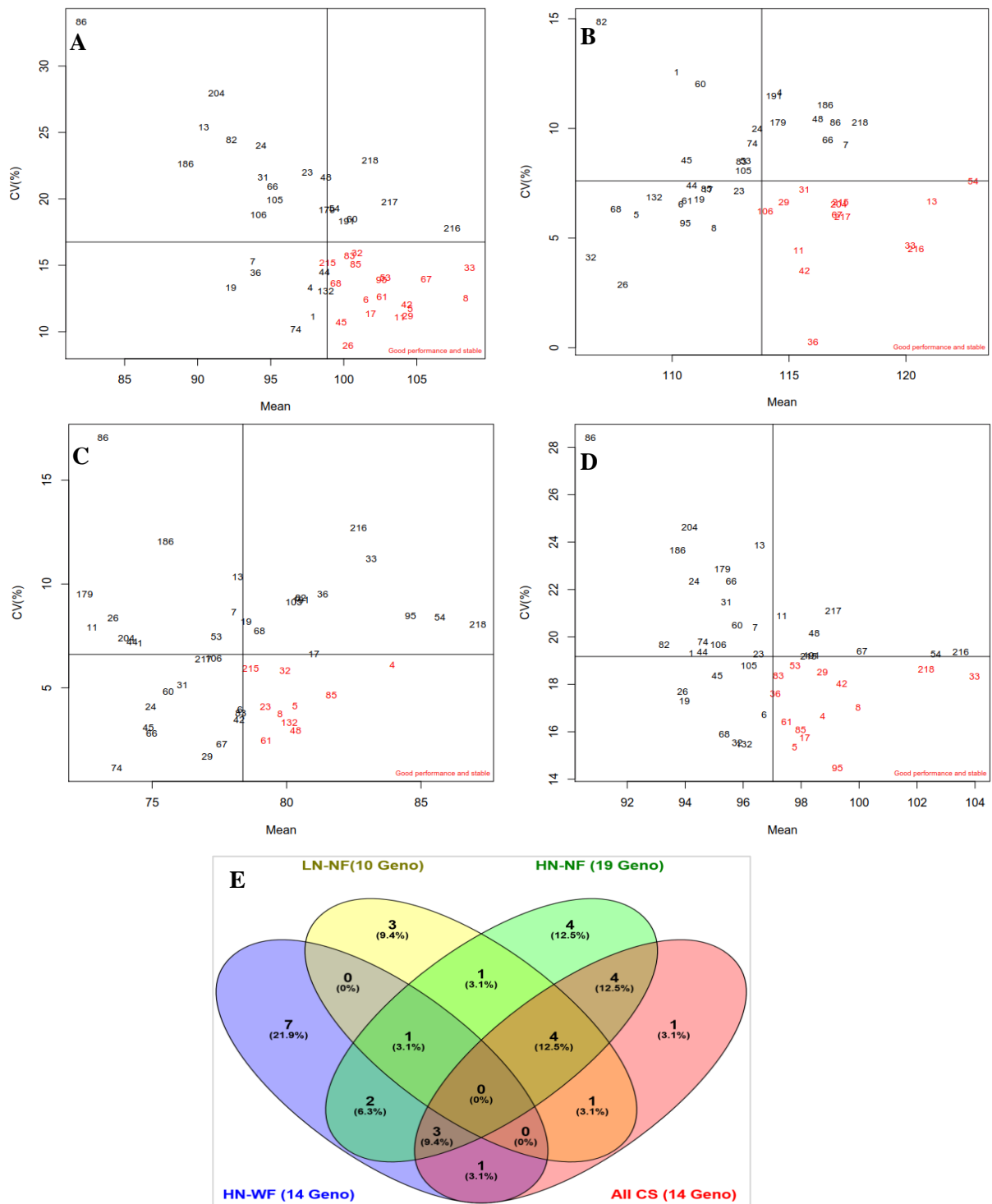


**FIGURE 5.S9** | Biplot of the Coefficient of variation (Y-axis) plotted against mean yield (X-Axis) of GY of 46 winter wheat cultivars under HN-NF (A with 19 psg), HN-WF (B 14 with psg), LN-NF (C with 10 psg) and combined 3 CS over three years (D 14 psg); psg means performant and stable cultivars. (B) Venn diagram is showing cultivars that were at least once selected (down-right quadrant) from the above biplots.

## Supplementary Tables

**TABLE 1.S1** | QTL and association mapping of drought tolerance traits in wheat. Source:(Kulkarni et al., 2017).

Drought tolerance traits	Mapping approach	Chromosomal location of QTLs	Wheat type	Stress conditions	References
Root development	QTL mapping	7AS	Emmer	Drought	Merchuk-Ovnat et al., 2017
Days to anthesis, grain filling period, 1,000 kernel weight (TKW)	QTL mapping	5A, 7A	Bread	Rainfed conditions	Gahlaut et al., 2017
Seeds per spike, number of spikes per, plant, TKW, grain yield	QTL mapping	3A, 1A, 7A	Bread	Drought	Xu et al., 2017
Plant Height, days to heading, spike length, seeds per spike, number of spikes per plant	Association mapping	5A, 5B, 6B, 2D, 2B, 6B, 7A, 1B, 4B	Bread	Drought	Mwadingeni et al., 2017
Photosynthesis, TKW, grain yield	Association mapping	5D, 6D, 7D	Bread	Drought	Saeed et al., 2017
Early ground cover	QTL mapping	6A	Bread	Rainfed conditions	Mondal et al., 2017
Plant Height, days to heading, spike length, TKW, grain yield	Association mapping	1B, 2B, 3B, 4B,5B,6B, 7B	Durum		Soriano et al., 2017
Root traits	Association mapping	2B, 5B, 7B, 6D	Bread	Not applicable	Ahmad et al., 2017
Cell wall bound phenolics	QTL mapping	4B, 6R	Triticale	Drought	Hura et al., 2017
Root length	QTL mapping	1BL, 2DS, 5AL, 6AL, 7BL, 3AL	Synthetic hexaploid/Spring wheat	Water stress	Ayalew et al., 2017
Root and shoot traits	QTL mapping	4B	Durum/ <i>T.dicoccum</i>	Not applicable	Iannucci et al., 2017
Yield, root morphology	Association mapping	1A, 1B, 4B, 6B	Durum	PEG stress	Lucas et al., 2017
Leaf water content, leaf dry weight, chlorophyll fluorescence	QTL mapping	1,2,3	<i>Brachypodium distachyon</i>	Drought	Jiang et al., 2017
Stem water soluble carbohydrates	QTL mapping	4A, 2D	Bread	Drought stress	Nadia et al., 2017
Water soluble carbohydrates	Association mapping	1A, 1B,1D, 4A	Bread	Rainfed	Ovenden et al., 2017
Seedling root traits	QTL mapping	4B, 7A, 7B	Tibetan semi-dwarf wheat	Hydroponics	Ma et al., 2017b

**TABLE 1.S2** | Identification of candidate genes for drought tolerance through transcriptome and proteome profiling, and genetic manipulation. Source:(Kulkarni et al., 2017).

<b>Transcriptome or proteome profiling or genetic manipulation studies</b>	<b>Differential expression/regulation of genes, pathways</b>	<b>Phenotypes</b>	<b>References</b>
Silicon application for drought tolerance enhancement in wheat	Upregulation of antioxidant, ascorbate—glutathione and phenylpropanoid pathway genes	Elevated drought tolerance due to increased chlorophyll content and lower H <sub>2</sub> O <sub>2</sub> , ascorbate and glutathione	<a href="#">Ma et al., 2016</a>
Succinate dehydrogenase inhibitor (SHI) fungicide spray under drought stress	Cell wall expansion, wax, and defense genes	Enhanced drought tolerance	<a href="#">Ajigboye et al., 2017</a>
Overexpression of the wheat expansin gene <i>TaEXPA2</i> for improved drought tolerance	Overexpression in tobacco	Enhanced drought tolerance, increased seed production under drought stress in tobacco	<a href="#">Chen et al., 2016</a>
Dehydration and rehydration proteomic analysis	Induction of pathways related to carbohydrate and amino acid metabolism, antioxidants and defense, and ATP synthesis	Drought tolerance	<a href="#">Chen et al., 2016</a>
Overexpression of <i>TaWRKY1</i>	Overexpression in tobacco	Slower water loss from leaves, higher biomass accumulation, enhanced osmolyte, and antioxidant accumulation leading to drought tolerance in tobacco	<a href="#">Ding et al., 2016</a>
Pre-treatment of wheat seedlings with NaHS (sodium hydrosulphide) under drought	SOD, transport, CDPK, ABA, Auxin, ribosome biogenesis	Improved drought tolerance in wheat seedlings	Li et al., 2017
Durum wheat micro-RNA targets	Target genes of micro-RNAs under drought stress: ARFs, HD-Zip, SOD, ROS, HSPs	Modulated drought response	Liu H. et al., 2017
Drought response genes in developing wheat glumes	Enhanced expression of phenylpropanoid biosynthesis pathway genes in wheat glumes	Enhanced drought tolerance	Liu C. et al., 2017
Splice variation in wheat as an effect of drought	HSFA1FD, HSFA6B, Heat Shock Protein DnaJ alternatively spliced	Drought tolerance	Liu Z. et al., 2017
Wheat transcriptome changes under drought stress	LTPL38 and alpha-Amylase3 genes	Enhanced drought tolerance at reproductive phases	Ma et al., 2017a
Response of He-Ne laser pretreated wheat seedlings to drought stress	Altered expression of genes related to photosynthesis, nutrient uptake, and transport	Enhanced drought tolerance in wheat	Qiu et al., 2017
<i>Aegilops longissima</i> substitution lines in Chinese spring	Increased expression of ascorbate peroxidase, serpin-Z2B, and alpha amylase genes under drought stress	Drought tolerance trait introduced from wild resources	Zhou et al., 2016

**TABLE 3.S3** | Examples of transcriptional activators involved in modulation of drought response. Source:(Kulkarni et al., 2017).

Gene	Identified in plant species	Functional validation	Phenotype	References
<i>DEEPER ROOTING (DRO1)</i>	Rice	Overexpression in Arabidopsis, <i>Prunus</i> species	Deeper roots	<a href="#">Uga et al., 2011, 2013</a> ; <a href="#">Guseman et al., 2017</a>
<i>MORE ROOT</i>	Wheat	Overexpression in rice and Arabidopsis	More crown roots in rice and more lateral roots in Arabidopsis	<a href="#">Li et al., 2016</a>
<i>TaER1 and TaER2</i>	Wheat	Expression pattern in wheat flag leaves	Higher transpiration efficiency	<a href="#">Zheng et al., 2015</a>
<i>ERECTA</i>	Arabidopsis	Arabidopsis mutation	Increase stomata density and reduced size, carbon isotope discrimination, photosynthesis	<a href="#">Masle et al., 2005</a>
<i>GTL2-LIKE1 (GTL1)</i>	Arabidopsis	Arabidopsis mutation	Reduced stomatal density and lowered transpiration without any effect on biomass	<a href="#">Yoo et al., 2010</a>
<i>TaERF3</i>	Wheat	Overexpression in wheat	Drought and salinity tolerance	<a href="#">Rong et al., 2014</a>
<i>TaERF1</i>	Wheat	Overexpression in Arabidopsis	Drought, salt, and low temperature tolerance	<a href="#">Xu et al., 2007</a>
<i>AtERF019</i>	Arabidopsis	Overexpression in Arabidopsis	Drought tolerance, smaller stomata aperture, and lower transpiration rate	<a href="#">Scarpeci et al., 2017</a>
<i>DREB1A</i>	Arabidopsis	Stress induced expression in wheat	Delayed water stress symptoms	<a href="#">Pellegrineschi et al., 2004</a>
<i>TAZFP34</i>	Wheat	Overexpression in wheat roots	Increased root:shoot ratio	<a href="#">Chang et al., 2016</a> ;
<i>TaWRKY10</i>	Wheat	Overexpression in tobacco	Enhanced drought tolerance	<a href="#">Wang et al., 2013</a>
<i>TaWRKY1 and TaWRKY33</i>	Wheat	Overexpression in Arabidopsis	Enhanced drought and heat tolerance	<a href="#">He G.-H. et al., 2016</a>
<i>TaWRKY1</i>	Wheat	Overexpression in tobacco	Enhanced drought tolerance and higher biomass under drought stress	<a href="#">Ding et al., 2016</a>
<i>TaWRKY93</i>	Wheat	Overexpression in Arabidopsis	Enhanced drought, salt, and low temperature tolerance	<a href="#">Qin et al., 2015</a>
<i>TaWRKY44</i>	Wheat	Overexpression in tobacco	Drought, salt, and osmotic stress tolerance	<a href="#">Wang F. et al., 2015</a>
<i>RAP2.1</i>	Arabidopsis	Mutation in the gene	Enhanced drought and frost tolerance	<a href="#">Dong and Liu, 2010</a>
<i>TaRAP2.1</i>	Wheat	Mutant overexpression in wheat	Drought tolerance	<a href="#">Amalraj et al., 2016</a>
<i>SodERF3</i>	Sugercane	Overexpression in tobacco	Drought and osmotic tolerance	<a href="#">Trujillo et al., 2009</a>
<i>OsERF4a</i>	Rice	Overexpression in rice	Enhanced drought tolerance	<a href="#">Joo et al., 2013</a>

TABLE 2.S1 A | Complete description and abbreviation of evaluated traits in the study.

Traits	Abbreviation	Descriptions
<b><i>Agronomic traits</i></b>		
Plant height	PH	Plant height was measured from three different plants of every plot at physiological maturity from the soil surface to the tip of the head, excluding awns (cm) and mean values were generated for further analysis
Grain yield	GY	The plots were harvested and the grains cleaned and weighed and the grain yield in Kg/ha was calculated.
Shoot dry weight	SDW	Dry shoot weight (g), dried shoot sample in oven set at 65°C for 3 days and the weight in Kg/ha was calculated
Aboveground plant biomass weight	PBW	After drying, plant Biomass weight (Biomass) and seed weight was recorded to estimate the HI as the ratio of seed weight to total biomass weight
Spike number per meter square	SNms	Spike numbers were counted for a genotype within 90centimeter row from all genotypes one by one before harvesting, and were used to calculated the SNms.
Kernels number per meter square	KNms	Grain number per m <sup>2</sup> , grain number per spike were calculated based on the Thousand kernel weight, Spike numbers per meter square, grain weight per meter square
Kernels number per spike	KNSp	
Harvest index	HI	Ratio =GY/ PBW
Thousand kernel weights	TKW	Weight of a thousand well developed whole grains dried sample (g)
<b><i>Developmental traits</i></b>		
Relative plant healthiness	HSr	The score of each trait was given with the customized scale from 1 to 5 equivalent to 0, 25, 50, 75 and 100% of damage, where the score 1 was 0 % of bad phenotype indicating the best performance while 100% of bad phenotype was the full expression of worst performance. For example, the leaf greenness was scored as follow 1 means 0 % leaves were yellow and 100% were green; 2 means 25% leaves were yellow, 75% leaves were green and 5 means 100% leaf are yellow. For leaf rolling and greenness, observations were done on the flag leaves and second youngest leaves. The relative value of each developmental trait was calculated as the inverse function of the visual scored value. The greater the relative value, the higher was the performance of the genotype.
Relative plants homogeneity of growth	HGr	
Relative plant leaves greenness	LGr	
Relative plant leaves rolling state	LRr	
<b><i>Grain quality</i></b>		
Grain protein content ratio	GPC	The grain quality were analyzed using NIRS instrument (Pertent, DA 7250) following the manufacturers guidelines (the values are given in %)
Grain starch content ratio	GSC	
Neutral detergent fiber ratio	NDF	

**TABLE 2.S1 B** | Duration of developmental growth stages.

Year	Sowing date	Starting of drought (in DAS)	Harvesting date (*DAS)		Duration prebooting (Start of drought) to harvesting		Growth stage	Duration (days after sowing, DAS Anova <sup>b</sup> )	
			Ds	Rf	Ds	Rf		Ds	Rf
2017	29.11.2016	15.04.2017 (137)	28.06.2017 (211)	28.07.2017 (241)	74	104	Prebooting		170
							Booting	170	175
							Heading	174	187
							Anthesis	178	191
							Fruit Development	191	
2018	02.11.2017	14.04.2018 (163)	03.07.2018 (243)	19.07.2018 (259)	80	96	Prebooting	188	191
							Booting	189	197
							Heading	192	197
							Anthesis	191	217
							Fruit Development	218	

DAS means date after sowing

\* Duration from sowing to harvesting;

<sup>b</sup> Anova of water regime on developmental traits duration

Water Regime treatment T (P<0.001)

Growth stage GS (P<0.001)

Interaction W\*GS (P<0.001)

**TABLE 2.S2** | ANOVA and descriptive statistics developmental (Dev) traits of 200 wheat genotypes evaluated in two water regimes across 2017 and 2018 growing seasons.

Developmental traits								
Statistics	Drought stress 2017				Drought stress 2018			
	HSr	HGr	LGr	LRr	HSr	HGr	LGr	LRr
Mean	0.811	0.634	0.475	0.459	-	-	0.617708	0.714052
CV (%)	30.07	37.08	45.26	55.86	-	-	42.38	35.91
Heritability	-	0.29	0.25	0.21	-	-	0.43	0.28
G effect	ns	**	**	*	-	-	***	**

The abbreviations of traits names are given in Table S1. CV means coefficient of variation. The significance level \*P<0.05, \*\*P<0.01, \*\*\*P<0.001;

**TABLE 2.S3** | Multiple linear regression of GY *vs* evaluated traits under rain fed and drought stress conditions during 2017 and 2018. Note that PBW and HI were not included in the regression because PBW is the sum of SDW and GY, and not an independent component. HI is the ratio of GY to PBW weight.

Years	Treatment	Control			Drought		
		Pvalue	Sig	Adj. R-squared (%)	Pvalue	Sig	Adj. R-squared(%)
2017	PH	0.0449	*	78.85	0.269		78.92
	SNms	<0.001	***		<0.001	***	
	KNms	<0.001	***		0.036978	*	
	KNSp	<0.001	***		<0.001	***	
	SDW	<0.001	***		<0.001	***	
	TKW	<0.001	***		<0.001	***	
	NDF	0.885			0.638		
	GPC	0.033	*		0.791		
	GSC	0.451			0.073	.	
	HSr	-			0.831		
	HGr	-			0.055	.	
	LGr	-			0.267		
	LRr	-			0.059	.	
2018	PH	0.048	*	96.17	1.000		98.08
	SNms	<0.001	***		0.436		
	KNms	<0.001	***		<0.001	***	
	KNSp	<0.001	***		0.983		
	SDW	0.165			0.692		
	TKW	<0.001	***		<0.001	***	
	NDF	0.892			0.838		
	GPC	0.221			0.110		
	GSC	0.838			0.292		
	HSr	-			-		
	HGr	-			-		
	LGr	-			0.678		
	LRr	-			0.228		

The significance level \*P<0.05, \*\*P<0.01, \*\*\*P<0.001; The abbreviations of traits names are given in Table S1.

**TABLE 2.S4** | Summary statistics of breeding progress (absolute and relative) of GY related traits and grain quality for 2017 and 2018 growing seasons together (Lsmeans) and the type of dynamic in the ABP.

Traits	Lsmeans													Pattern Types <sup>a</sup>
	Control						Drought							
	Mean	Mean	Sig (p)	ABP (slope)	R <sup>2</sup>	RBP (%)	Mean	Mean	Sig (p)	ABP (slope)	R <sup>2</sup>	RBP		
Oldest	Newest	Oldest					Newest							
PH (cm)	87.11	78.23	***	-0.24	0.22	-7.59	69.82	65.01	***	-0.14	0.15	-5.77	Types II	
GY (g/row)	226.67	238.54	ns	3.5	1E <sup>-3</sup>	0.83	65.07	76.42	***	16	0.09	12.16	Types I	
SDW (g/row)	251.06	230.76	***	-46	0.14	-9.41	96.47	96.72	ns	-2.8	2.3E <sup>-3</sup>	-1.46	Types II	
PBW (g/row)	476.62	469.30	**	-42	0.05	-4.65	162.19	173.26	ns	13	0.02	4.55	Types III	
TKW (g)	43.97	42.81	ns	-0.03	0.02	-1.91	39.22	38.19	*	-0.03	0.02	-2.41	Types II	
SNms	750.28	737.01	*	-0.75	0.02	-3.15	338.07	365.91	*	0.57	0.05	5.2	Types III	
KNms	28152.74	30184.73	ns	26	0.01	2.74	9394.34	10895.8	**	32	0.04	9.27	Types I	
KNSp	38.65	41.95	**	0.07	0.04	4.91	26	28.84	**	0.06	0.04	7.07	Types I	
HI	0.48	0.51	***	7.6E <sup>-4</sup>	0.16	4.52	0.39	0.43	***	9.3E <sup>-4</sup>	0.11	6.32	Types I	
GPC	14.58	14.05	**	-0.01	0.04	-1.86	13.67	12.89	***	-0.02	0.11	-4.37	Types II	
GSC	72.31	72.92	**	0.01	0.04	0.46	71.85	72.72	***	0.02	0.08	0.78	Types I	
NDF	18.09	18.38	**	0.01	0.05	2.07	17.97	18.31	**	0.01	0.05	2.05	Types I	

<sup>a</sup> The regression results (Figure 2, Figure S5) revealed three types of patterns in the absolute breeding progresses when comparing the slopes of control and drought treatments as indicated in Table S4. The pattern type I is when breeding has increased genotypes achievements under both water regimes. In this group were found GY (Figure 2A) and its key components, namely KNms (Figure 2B) and KNSp (Figure S5E), HI (Figure 2C), GSC and NDF (Figure S5HI); Type II means negative slopes, which indicated a decrease in trait performance brought by breeding (SDW, PH, TKW and GPC in Figure S5ACFG), while Type III indicated a positive slope under drought and a negative slope under control conditions. \* P-value tests the significance of the slope. While the third pattern included PBW SDW, and SNms (Figure S5ABD), where breeding has increased genotypes performance under drought but reduced it under control.

Means oldest and newest are the average value of genotypes released before 1980 and after 2010, respectively. Absolute (ABP) and relative (RBP) breeding progress were derived from regression models. Sig (p) gives the significance level of the slopes (\*\*\*) means significant at 0.001, \*\* at 0.01 and \* at 0.05 and ns. indicates not significant at 0.05). Relative breeding progress is expressed in percent (%).

**TABLE 2.S5** | Pairwise comparison of regressions coefficients (intercepts and slopes) of model GY vs yield components, and traits of interest vs year of release under both water regimes.

Traits	<i>Intercepts</i> <sup>+</sup>	<i>Slopes</i> <sup>+</sup>
<i>GY vs Yield components</i>		
SDW	7.9e-14 ***	0.834 ns
KNSp	2.96e-14 ***	0.324 ns
KNms	0.000381 ***	0.038531 *
SNms	2.38e-08 ***	0.433 ns
TKW	0.107211	0.000206 ***
<i>Traits vs Year of release</i>		
PBW	6.82e-05 ***	0.000497 ***
SDW	6.19e-07 ***	4.50e-06 ***
GY	0.0506	0.1485 ns
KNms	0.451 ns	0.771 ns
KNSp	0.8916 ns	0.9508 ns
HI	0.3748 ns	0.4826 ns
PH	0.0103 *	0.0173 *
SNms	0.000354 ***	0.001800 **
TKW	0.885043 ns	0.973138 ns
GPC	0.08446	0.06561
GSC	0.2141 ns	0.2196 ns
NDF	0.98461 ns	0.98461 ns

<sup>+</sup> the numbers are displaying the P values from the comparisons.

**TABLE 2.S6** | Drought-tolerant and Drought-sensitive genotypes identified based on the SWP values of agronomic, developmental and grain quality (GQ) traits.

Tolerant						Sensitive					
Entry name	Release Year	Agr o	Dev Traits	G Q	Times selected	Entry name	Release Year	Agr o	Dev Traits	G Q	Times selected
Claire	1999	1			1	Estivus	2012	1	1		2
Zappa	2009	1		1	2	Kronjuwel	1980	1			1
Meister	2010	1			1	Mulan	2006	1	1		2
KWS Santiago	2011	1	1		2	Solstice	2001	1			1
Brigand	1979	1		1	2	Arktis	2010		1	1	2
Edward	2013	1			1	Joss	1972	1			1
Jenga	2007	1		1	2	Rektor	1980	1			1
TJB 990-15	1980	1	1	1	3	Cappelle Desprez	1946	1			1
Gourmet	2013	1	1		2	Tiger	2001	1			1
Kalahari	2010	1			1	Ibis	1991	1			1
Intro	2011	1	1		2	Aszita	2005	1		1	2
Primus	2009		1	1	2	Kobold	1978	1		1	2
Inspiration	2007	1			1	Benno	1973	1	1		2
SY Ferry	2012	1	1		2	Benni multifloret	1980	1		1	2
Terrier	2001	1			1	Caphorn	2000	1		1	2
Xanthippe	2011	1		1	2	Soissons	1987		1	1	2
Knirps	1985	1			1	BCD 1302/83	NA	1		1	2
Akteur	2003	1	1		2	Sonalika	1967	1	1	1	3
Diplomat	1966	1			1	Cajeme 71	1971	1	1		2
Basalt	1980	1	1		2	Siete Cerros 66	1966	1	1	1	3
Average Release year	2000.8					Average Release year	1985.6				

**TABLE 2.S7** | Summary of SNP markers significantly associated with evaluated traits under both water regimes.

Traits	Rainfed		Drought		Both Water regimes	
	MTAs number	MTAs R <sup>2</sup> (%)	MTAs number	MTAs R <sup>2</sup> (%)	MTAs number	MTAs R <sup>2</sup> (%)
<b>PH</b>	5	8.13	14	7.68	19	7.80
<b>GY</b>			2	8.45	2	8.45
<b>PBW</b>	1	7.44	1	9.63	2	8.54
<b>SDW</b>	1	8.11	23	8.76	24	8.74
<b>HI</b>			1	7.84	1	7.84
<b>KNSp</b>	17	8.41	5	8.80	22	8.50
<b>SNms</b>			2	7.29	2	7.29
<b>TKW</b>	1	7.65			1	7.65
<b>GSC</b>			5	7.13	5	7.13
<b>Grand Total</b>	<b>25</b>	<b>8.27</b>	<b>53</b>	<b>8.26</b>	<b>78</b>	<b>8.26</b>

**TABLE 3.S1** | List of measured leaf *chlorophyll a* fluorescence parameters.

Extracted (Abbreviation)	Parameter	Formula explanation	Sample State	Description
Minimum fluorescence level (F <sub>Min</sub> or F <sub>0</sub> )			Dark	Measured by very low intensity of measuring light to keep PS II reaction centers open
Maximum fluorescence level (F <sub>Max</sub> or F <sub>M</sub> )			Dark	Measured by a pulse of saturating light (Saturation Pulse) which closes all PS II reaction centers
Minimum fluorescence level (F <sub>min</sub> or F)			Light	The F corresponds to the momentary fluorescence level (F <sub>t</sub> ) of an illuminated sample measured shortly before application of a Saturation Pulse
Maximum fluorescence level (F <sub>max</sub> or F <sub>M</sub> ')			Light	The F <sub>M</sub> ' is induced by a Saturation Pulse which temporarily closes all PS II reactions centers.
Maximum photochemical quantum yield of PS II (F <sub>v</sub> /F <sub>M</sub> )		$F_v/F_M = (F_M - F_0) / F_M$	Dark	Demonstrates the ability of PSII to perform photochemistry (QA reduction)
Effective photochemical quantum yield of PS II (YII)		$YII = (F_M' - F) / F_M'$	Light	
Non photochemical fluorescence quenching (NPQ)		$NPQ = (F_M / F_M') - 1$	Dark and Light	Estimates the non-photochemical quenching from F <sub>M</sub> to F <sub>M</sub> '. Monitors the apparent rate constant for heat loss from PSII.

**TABLE 3.S2** | Complete description and abbreviation of evaluated traits in the study.

Traits	Abbreviation	Descriptions
<i>Agronomic traits</i>		
Grain yield	GY	The plots were harvested and the grains cleaned and weighed and the grain yield in Kg/ha was calculated.
Shoot dry weight	SDW	Dry shoot weight (g), dried shoot sample in oven set at 65°C for 3 days and the weight in Kg/ha was calculated
Plant biomass weight	PBW	After drying, plant Biomass weight (Biomass) and seed weight was recorded to estimate the HI as the ratio of seed weight to total biomass weight
<i>Developmental traits</i>		
Relative plant healthiness	HSr	The score of each trait was given with the customized scale from 1 to 5 equivalent to 0, 25, 50, 75 and 100% of damage, where the score 1 was 0 % of bad phenotype indicating the best performance while 100% of bad phenotype was the full expression of worst performance. For example, the leaf greenness was scored as follow 1 means 0 % leaves were yellow and 100% were green; 2 means 25% leaves were yellow, 75% leaves were green and 5 means 100% leaf are yellow. For leaf rolling and greenness, observations were done on the flag leaves and second youngest leaves.
Relative plants homogeneity of growth	HGr	
Relative plant leaves greenness	LGr	
Relative plant leaves rolling state	LRr	

Table S2 Continues

Table S2 Continued

<i>Physiological and functional traits</i>		
Chlorophyll Content	<b><i>SPAD</i></b>	SPAD and MINI-PAM measurements were made at the mid-point of a fully expanded leaf, on three plants randomly chosen within a plot using a SPAD 502 instrument (Konica Minolta, Osaka, Japan). During the measurements, special care of leaves angle or shading was observed to avoid change of the ambient state of the leaves (Rascher et al., 2000). The average of the three SPAD measurements per genotype per repetition was calculated and used for the analysis, while the nine data points per genotype from three repetitions were used for analyses. The Chlorophyll a fluorescence parameters evaluated (Walz, 2014) are fully described in Table S1.
Effective quantum Yield of Photosystem II	<b><i>YII</i></b>	
Maximum quantum Yield of Photosystem II	<b><i>FV/FM</i></b>	
Maximum fluorescence level (of light and dark adapted samples)	<b><i>Fmax; FMax</i></b>	
Minimum fluorescence level (of light and dark adapted samples)	<b><i>Fmin; FMin</i></b>	
Nonphotochemical fluorescence quenching	<b><i>NPQ</i></b>	
Diffusion porometer based Leaf stomatal conductance	<b><i>LSCp</i></b>	Diffusion based leaf stomatal conductance (gsLSCp) was measured across four growth stages, prebooting, booting, anthesis and postanthesis by diffusion porometer (AP4-Delta-T Eijelkamp, Giesbech, The Netherlands) with limits operating of 0 to 50 °C temperature and 10 to 90% relative humidity (Devices, n.d.). Readings were done on the second youngest leaves at prebooting and booting, and on flag leaves at anthesis and post-anthesis. Three measurements within a plot of one genotype were made as mmol H <sub>2</sub> O m <sup>-2</sup> s <sup>-1</sup> exciting water vapor at full clear air conditions between 10:00 am and 16:30 pm, with about 1500 PAR light intensity and 1000 hPa pressure.
Photosynthetic rate	<b><i>A</i></b>	Net photosynthetic rate (APR, μmol CO <sub>2</sub> m <sup>-2</sup> s <sup>-1</sup> ), an IRGA based stomatal conductance (gswLSCI, mol H <sub>2</sub> O m <sup>-2</sup> s <sup>-1</sup> ), intercellular CO <sub>2</sub> concentration (CiIntCO <sub>2</sub> , μmol CO <sub>2</sub> mol <sup>-1</sup> ), transpiration rate (ETR, mmol H <sub>2</sub> O m <sup>-2</sup> s <sup>-1</sup> ) and the leaf temperature (T, °C) were investigated using LI-6800 (LI-COR, Lincoln, USA) in open system from 10:00 a.m. to 14:00 a.m. at anthesis growth stage. The photosynthetic active radiation (PAR) of LI-6800 was set as 1000 μmol m <sup>-2</sup> s <sup>-1</sup> . For each line, the flag leaves of three plants in the middle of the plot were selected and the readings were taken at the midpoint part. The difference in temperature (ΔT) was calculated with the formular ΔT=T <sub>leaf</sub> - T <sub>air</sub> . Leaf instantaneous water use efficiency (LWUE, μmol/ mmol) was calculated as follows LWUE = A/E where A is photosynthetic rate, E is transpiration rate as described by Munjonji et al. (2016).
Interceluar CO <sub>2</sub>	<b><i>Ci</i></b>	
Transpiration rate	<b><i>E</i></b>	
IRGA based Stomatal conductance	<b><i>LSCI</i></b>	
Leaf instantaneous water use efficiency	<b><i>LWUE = A/E</i></b>	
Difference temperature Leaf-Air	<b><i>DTLA</i></b>	

**TABLE 3.S3** | Chlorophyll content and fluorescence ratio parameters across growth stages in 2017 and 2018 growing seasons.

Physiological Traits	Statistic	Water regime	BBCH growth stage in 2017			BBCH growth stage in 2018					Heritability (%)	
			GS40-49	GS50-59	GS60-69	GS30-39	GS40-49	GS50-59	GS60-69	GS70-85	H <sup>2</sup>	h <sup>2</sup>
SPAD	Mean	Control	52.72	53.24	52.86	54.00					92.57	47.33
		Drought	52.12	53.24	51.03	52.78					67.07	35.22
		Reduction (%)	1.13	0.00	3.47	2.26						
	CV (%)	Control	5.95	7.06	10.19	7.83						
		Drought	7.48	6.20	14.03	8.50						
	Treatment effect	Water (W)	**	ns	*	ns						
		Genotype (G)	***	***	*	**						
		W*G	*	***	ns	ns						
	Fmin	Mean	Control	772.61	623.39	270.35	480.00	452.17	399.17	342.64	351.67	0
Drought			195.09	479.53	813.68	454.49	415.08	389.49	385.87	413.61	0	4.38
Reduction (%)			74.75	23.08	-200.97	2.43						
CV (%)		Control	52.71	67.41	25.93	22.71	27.65	22.14	23.42	43.50		
		Drought	16.27	79.87	58.52	30.27	21.52	19.23	21.67	28.18		
Treatment effect		W	***	***	***	ns	**	ns	***	***		
		G	***	***	***	**	***	***	***	***		
		W*G	***	***	***	***	ns	***	*	***		
Fmax		Mean	Control	1903.15	1584.45	1095.20	1194.82	1106.13	981.58	897.45	971.08	4.74
	Drought		500.77	1128.55	1703.27	1188.41	1117.09	1072.82	1059.79	992.52	29.66	22.70
	Reduction (%)		73.69	28.77	-55.52	-9.30						
	CV (%)	Control	39.53	41.99	31.50	18.60	23.16	26.07	18.03	34.81		
		Drought	8.48	63.11	31.97	18.40	16.91	21.00	18.00	26.91		
	Treatment effect	W	***	***	***	ns	ns	***	***	ns		
		G	***	***	***	ns	**	***	***	*		
		W*G	***	***	*	***	ns	*	*	**		

Table S3 (Continued)

Physiological Traits	Statistic	Water regime	Measured BBCH growth stage in 2017			Measured BBCH growth stage in 2018						
			GS40-49	GS50-59	GS60-69	GS30-39	GS40-49	GS50-59	GS60-69	GS70-85		
YII	Mean	Control	0.61	0.63	0.74	0.60	0.59	0.58	0.62	0.64	0	8.69
		Drought	0.61	0.59	0.54	0.62	0.63	0.63	0.63	0.56	0	6.37
		Reduction (%)	0.00	6.35	27.03	-3.33	-6.78	-8.62	-1.61	12.50		
	CV (%)	Control	20.60	21.88	8.55	9.05	10.06	11.25	9.96	12.02		
		Drought	9.35	23.05	34.75	11.26	9.40	9.66	8.56	24.53		
	Treatment effect	W	**	***	***	***	***	***	***	ns	***	
G		***	***	***	**	*	**	***	**			
W*G		*	***	***	***	***	ns	*	ns	ns		

GS30-39: Prebooting growth stage; GS40-49: Booting; GS50-59: S3\_Heading; GS60-69: Anthesis, GS70-85: Postanthesis, Fmin, Fmax are respectively the minimum and maximum fluorescence of light acclimated sample; YII is the effective photochemical, Significance levels: \*P < 0.05, \*\*P < 0.01, \*\*\*P < 0.001, ns means not significant.

**TABLE 3.S4** | Dark and light adapted chlorophyll fluorescence ratio parameters measured at anthesis stage.

Statistic	Water regime	2017				2018			
		F <sub>Min</sub>	F <sub>Max</sub>	Fv/ F <sub>Max</sub>	NPQ	F <sub>Min</sub>	F <sub>Max</sub>	Fv/F <sub>Max</sub>	NPQ
Mean	Control	245.40	946.29	0.77	0.54	286.78	1676.32	0.83	0.95
	Drought	311.60	1408.45	0.75	0.26	321.68	1667.20	0.80	0.49
	Reduction (%)	-26.97	-48.84	3.25	50.77	-12.17	0.54	3.56	47.90
CV (%)	Control	6.20	5.39	3.77	46.70	5.21	6.23	1.16	31.87
	Drought	26.76	10.78	3.61	113.51	16.05	16.65	8.38	54.61
Treatment effect	W	***	***	***	***	***	ns	***	***
	G	ns	***	ns	*	***	***	***	*
	W*G	ns	***	ns	***	**	***	**	***

F<sub>Min</sub>, F<sub>Max</sub> are respectively the minimum and maximum fluorescence of dark adapted sample; Fv/F<sub>Max</sub> is the maximum photochemical quantum yield of PSII, NPQ in the non-photochemical quenching. Significance levels: \*P < 0.05, \*\*P < 0.01, \*\*\*P < 0.001, ns means not significant.

**TABLE 3.S5** | Stomatal conductance (gsw) dynamic across growth stage in 2018.

Statistic	Water Regime	Stomatal conductance (gsw) ( $\text{mol m}^{-2} \text{s}^{-1}$ )			
		GS30-39	GS40-49	GS60-69	GS70-85
Mean	Control	0.24	0.22	0.33	0.28
	Drought	0.32	0.22	0.13	0.09
	Reduction (%)	-33.33	0.00	60.61	67.86
CV(%)	Control	85.45	203.70	36.21	25.28
	Drought	156.92	60.32	44.69	77.64
Treatment effect	T	ns	ns	***	***
	G	ns	ns	*	ns
	T*G	***	ns	ns	ns

GS30-39: Prebooting growth stage; GS40-49: Booting; GS60-69: Anthesis, GS70-85: Postanthesis,

**TABLE 3.S6** | Photosynthesis related parameters measured with the Licor 6800 at anthesis growth stage.

Water regime	A ( $\mu\text{mol m}^{-2} \text{s}^{-1}$ )	E ( $\text{mol m}^{-2} \text{s}^{-1}$ )	LWUE ( $\mu\text{mol}/\text{mol}$ )	Ci ( $\mu\text{mol}/\text{mol}$ )	LSCI ( $\text{mol m}^{-2} \text{s}^{-1}$ )
Control	10.089	0.003	3835.472	304.520	0.232
Drought	7.110	0.001	5279.863	277.275	0.115
Reduction (%)	29.53	66.67	-37.66	8.95	50.43
Drought effect (P-Value)	0.007 **	<0.001 ***	0.011*	0.034 *	<0.001 ***

A = Photosynthetic rate; E = Transpiration rate; LWUE = Leaf instantaneous water use efficiency; Ci = Intercellular CO<sub>2</sub>; LSCI = IRGA based Stomatal conductance. Significance levels: \*P < 0.05, \*\*P < 0.01, \*\*\*P < 0.001, ns means not significant.

**TABLE 4.S1** | List of the thirty winter wheat cultivars grown in pot experiment in 2019.

<b>BRISONr.</b>	<b>Cultivars names</b>	<b>Year of release</b>	<b>Origine of cultivars</b>	<b>Selection type*</b>
1	Einstein	2004	GBR	Diversity panel
4	Claire	1999	GBR	Diversity panel
8	Zappa	2009	Deutschland	Drought-tolerant
13	KWS Santiago	2011	GBR	Drought-tolerant
14	Brigand	1979	GBR	Drought-tolerant
57	Gourmet	2013	Deutschland	Diversity panel
59	Ritmo	1993	Deutschland	Diversity panel
79	Brilliant	2005	Deutschland	Diversity panel
80	Inspiration	2007	Deutschland	Diversity panel
84	Maris Huntsman	1975	Deutschland	Diversity panel
98	Severin	1980	Deutschland	Diversity panel
108	Herzog	1986	Deutschland	Diversity panel
117	Pantus	1966	Deutschland	Diversity panel
119	Joss	1972	Deutschland	Diversity panel
127	Tambor	1993	Deutschland	Diversity panel
129	Sokrates	2001	Deutschland	Drought-tolerant
135	Monopol	1975	Deutschland	Diversity panel
149	Zentos	1989	Deutschland	Diversity panel
150	Diplomat	1966	Deutschland	Drought-tolerant
153	Kormoran	1973	Deutschland	Diversity panel
170	Centurk	1971	USA	Drought-sensitive
172	Benni multifloret	1980	USA/Indiana	Drought-sensitive
176	Mironovska 808	1963	Ukraine	Diversity panel
177	Caphorn	2000	Frankreich	Diversity panel
190	BCD 1302/83	-	Moldawien	Diversity panel
194	Cajeme 71	1971	Mexico	Drought-sensitive
196	Ivanka	1998	Serbien	Diversity panel
205	Highbury	1968	GBR	Diversity panel
206	Siete Cerros 66	1966	Mexiko	Drought-sensitive
210	NS 46/90	-	Serbien	Drought-sensitive

\* The selection type column described the selection process, cultivars of Diversity panel are selected to represent the genetic diversity in the panel. Other cultivars are either drought-tolerant or drought-sensitive.

**TABLE 4.S2** | Traits description for field trials in 2017 and 2018 and pot experiment in 2019.

Traits	Abbreviations (unit)	Descriptions and units
<i>Agronomic traits</i>		
Plant biomass weight	<b>PBW</b> (g/row)	The aboveground plant part per plot was harvested at maturity (BBCH99). After drying in oven at 65°C for three days, the PBW was measured. The sample was then thrashed and the cleaned grains were weighed to determine GY. The thrashed product without grains corresponded to SDW. To determine SWaP from the pot experiment, the aboveground plant biomass was harvested at anthesis (BBCH60-69) to estimate the shoot fresh biomass weight (SFW) and then dried as described previously to measure the shoot dried biomass weight (SDW).
Grain yield	<b>GY</b> (g/row)	
Shoot dry weight	<b>SDW</b>	
Shoot water potential at anthesis	<b>SWaP</b>	
<i>Photosynthesis related traits</i>		
Chlorophyll Content	<b>SPAD</b>	SPAD and YII measurements were made at the mid-point of a fully expanded leaf using a SPAD-502 instrument (Konica Minolta, Osaka, Japan) and the MINI-PAM II fluorometer (Walz, 2014), respectively. During the measurements, special care of leaves angle or shading was observed to avoid change of the ambient state of the leaves (Rascher et al., 2000). The average of the SPAD measurements of three plants per genotype per repetition was calculated and used for the analysis, while the nine data points per genotype from three repetitions were used for YII analyses.
Effective photochemical quantum yield of PS II (YII)	<b>YII</b>	
Normalized difference vegetation index	<b>NDVI</b>	
<i>Nitrogen use related traits</i>		
Nitrogen use efficiency for Biomass production	<b>NUEBio</b>	$NUE_{Bio} = PBW / \text{available N [equivalent of medium N input (110 Kg/ha) or high N input (220 Kg/ha)]}$ .
Nitrogen use efficiency for Grain Yield production	<b>NUEGr</b>	$NUE_{Gr} = GY / \text{available N} = NUtE \times NUpE$
Nitrogen in aboveground plant biomass	<b>NAB</b>	$\text{Grain yield} \times (\text{N content in seed}/100) + \text{Shoot dry weight} \times (\text{N content in straw}/100)$
Nitrogen uptake efficiency	<b>NUpE</b>	$NAB / \text{available N}$
Nitrogen utilization efficiency	<b>NUtE</b>	$GY / NAB$
N content in grain	<b>NGr</b>	$NGr = \text{Grain protein content} / 5.7$ (Gauer et al., 1992)
N content in straw	<b>NSt</b>	Nst was measured by NIRS machine
N content in leaves at anthesis	<b>NLf</b>	The N content in leaves harvested at anthesis (BBCH60-69)
Nitrogen remobilization efficiency	<b>NRE</b>	$NRE = 1 - (NGr/NLf)$
Nitrogen harvest index	<b>NHI</b>	$NHI = \text{N content in seed} / (\text{N content in seed} + \text{N content in straw})$

<i>Root architectural traits</i>		
Fresh root weight at anthesis	<b><i>FRW</i></b>	The fresh root biomass weight (FRW) of two plants per pot after washing was weighed, then dried in oven at 65°C and the dry root weight (DRW) was measured. The root water potential corresponds to the difference between FRW and DRW.
Root dry weight at anthesis	<b><i>DRW</i></b>	
Root water potential	<b><i>RWaP</i></b>	
Root area	<b><i>RA</i></b>	The part within 5 cm from the crown down the root system of one plant was cut off and placed on the scoreboard to measure the right ( $\alpha$ ) and left ( $\beta$ ) angles ( <b>Figure 1</b> ). Thereafter, the root area was calculated using the equation 1 in the main text.

**TABLE 4.S3** | SNP loci showing multiple and interacting effects on the evaluated traits and the corresponding underlying genes.

Marker Peak code (region)	Marker name	Chr	Pos	Block	Total genes	Human readable description of genes
<i>Pleiotropic markers</i>						
W15_AOWZ	Tdurum_contig594_49_249	1B	487407563	Block (470936325-489206981)	<b>96</b>	Myb transcription factor; Protein NRT1/ PTR FAMILY 1.1; F-box family protein; Cold shock protein; Amino acid permease; Cytochrome P450; Aminotransferase; Protein NRT1/ PTR FAMILY 5.5
W135_BCLB	AX-111561744	2D	23416219	No block	<b>26</b>	Cytochrome P450 family protein; Cystathionine gamma-synthase; Short-chain dehydrogenase/reductase; transmembrane protein, putative (DUF594); F-box protein family-like
W135_EQVM	AX-158577204	3A	714294127	No block	<b>40</b>	B3 domain-containing protein; Beta-1,3-glucanase; Amino acid permease; RNA-binding protein, putative; BTB/POZ domain containing protein, expressed; GRAS family transcription factor containing protein
W135_HPIW	AX-89650364	3A	8213038	Block (8213038-8686717)	<b>26</b>	Kinase family protein; Receptor-kinase, putative; Disease resistance protein (TIR-NBS-LRR class); Disease resistance protein RPM1; Disease resistance protein (NBS-LRR class) family; NBS-LRR-like resistance protein
W135_EBWG	AX-158567084	7A	692900585	No block	<b>30</b>	Chaperone protein dnaJ; Histone-lysine N-methyltransferase; Bidirectional sugar transporter SWEET; Photosystem II reaction center PsbP family protein; Peptide transporter; Patatin
<i>Nitrogen deficiency induced markers ( under drought)</i>						
W135_ACAD	AX-108817594	1B	575723086	Block	<b>2</b>	Magnesium transporter; Cleavage stimulation factor subunit;

				(575868657-575723086)		magnesium transporter NIPA (DUF803)
W135_ALNQ (NRE)	AX-109874485	2A	747160989	Block (747088588-747611742)	<b>6</b>	Receptor-like protein kinase; Antimicrobial peptide; 3-oxoacyl-reductase; Heterogeneous nuclear ribonucleoprotein U-like protein 1
W15_AKXT (NRE)	RAC875_c2437_1 569	5B	479025051	Block (478758747-479200398)	<b>5</b>	Beta-glucosidase; CCR4-NOT transcription complex subunit 2
W15_AJKR (NAB NUptE)	Kukri_c4780_395	6B	667071383	Block (665516798-667773729)	<b>9</b>	SRF-type transcription factor; DNA topoisomerase (Pfam=GRF zinc finger); AGAMOUS-like MADS-box protein (Pfam=SRF-type transcription factor); CCR4-NOT transcription complex family protein
W135_CNBZ (NRE)	AX-158539517	7A	33187933	Block (32805151-33246377)	<b>3</b>	Receptor protein kinase; Cell cycle regulated microtubule associated protein; LOB domain-containing protein, putative
W135_EBWH	AX-158567085	7A	692019147	Block (692019147-696821540)	<b>48</b>	Bidirectional sugar transporter SWEET; Alkaline alpha-galactosidase seed imbibition protein; Patatin; Peptide transporter ; Beta-catenin-like protein 1; Photosystem II reaction center PsbP family protein; Cytochrome P450 family protein, expressed; Histone-lysine N-methyltransferase; Protein kinase; Cytochrome b561 and DOMON domain-containing protein; WRKY transcription factor
<i>Nitrogen deficiency Interaction markers (under drought)</i>						

W15_AQTM	w SNP_Ex_c23795_33033150	5A	679665943	Block (679665943-679666083)	<b>6</b>	MADS-box transcription factor; 2-oxoglutarate (2OG) and Fe(II)-dependent oxygenase superfamily protein; Basic helix-loop-helix transcription factor; Kinase family protein; Endoribonuclease Dicer-like protein 3
W15_ACLA	BS00081951_51	5A	677631836	Block (677135858-679666083)	<b>20</b>	Pectin lyase-like superfamily protein; F-box protein; Receptor-like protein kinase, putative; Beta-1,3-N-acetylglucosaminyltransferase lunatic fringe; Sugar transporter, putative; 2-oxoglutarate (2OG) and Fe(II)-dependent oxygenase superfamily protein; Basic helix-loop-helix transcription factor
W135_AJWO	AX-109506123	5D	528818863	Block (528818863-529854459)	<b>40</b>	Receptor lectin kinase; Sugar transporter family protein, putative, expressed; Protein NRT1/ PTR FAMILY 5.5; Disease resistance protein (NBS-LRR class) family; Pectin acetyltransferase; UDP-glycosyltransferase; Calmodulin-binding protein, putative, expressed; Cytochrome P450
W135_APNO	AX-110366518	6B	665737258	Block (665715744-667884690)	<b>11</b>	AGAMOUS-like MADS-box protein (Pfam= SRF-type transcription factor (DNA-binding and dimerisation domain); carboxyl-terminal peptidase (DUF239); Zinc finger protein VAR3, chloroplastic; MADS-box transcription factor family protein; Two-component response regulator; DNA topoisomerase (GRF zinc finger)
W135_AOSG	AX-110038525	7A	736688441	Block (736555653-736688441)	<b>2</b>	RNA-binding family protein (Pfam: RNA recognition motif. (a.k.a. RRM, RBD, or RNP domain); Phosphatidylinositol-4-phosphate 5-kinase, core)
<i>Nitrogen deficiency Interaction markers (under rainfed)</i>						

W15_AOFR ; W15_AORH	Tdurum_contig292 80_216; durum_contig5035 5_269	1A	33375555; 33020906	Block (33020906- 33375555)	<b>2</b>	F-box family protein; Protein aluminum sensitive 3
W135_EFVY (for NUE, Seed yield; Peak; High Sigh)	AX-158569780	1A	333880952	Block (320336587- 355344855)	<b>70</b>	Cytochrome P450 family protein, expressed; Serine carboxypeptidase S28 family protein; Serine carboxypeptidase S28 family protein; Zinc finger CCCH domain protein; Serine carboxypeptidase S28 family protein; Cytochrome b5; Pectinesterase; Glutathione S-transferase,
W15_AFBX	Excalibur_c20307_ 654	7A	621320529	Block (620533841- 641435870)	<b>35</b>	Chlororespiratory reduction 42; Phosphate import ATP-binding protein PstB (ABC transporter); 3-oxoacyl-reductase (short chain dehydrogenase); Peroxidase; carboxyl-terminal peptidase (DUF239); Zinc finger family protein (C2H2-type zinc finger)
W15_ACHH	BS00076743_51	7A	545056389	Block (544255244- 545544574)	<b>9</b>	F-box protein Phloem protein 2; Protein phosphatase 2C; Zeaxanthin epoxidase, chloroplastic; CAAX amino terminal protease family protein; CAAX amino terminal protease family protein; Auxin-responsive protein
W135_AADV	AX-108731092	3B	722362075	block(7223620 75-719443875)	<b>26</b>	Glutathione S-transferase; zinc knuckle (CCHC-type) family protein; Myb transcription factor; glycosyltransferase family exostosin protein; RING/U-box superfamily protein; Ubiquitin-conjugating enzyme E2, putative; Disease resistance protein RPM1

**TABLE 5.S1** | Year wise soil information of the experimental site.

Level (cm)	Nmin (kg/ha). 2015	Nmin (kg/ha). 2016	Nmin (kg/ha). 2017
0-30	13.6	22.2	27.1
30-60	24.3	10.8	36.1
60-90	27.0	10.1	25.1
Total	<b>64.9</b>	<b>43.1</b>	<b>88.3</b>
<b>Soil (mg)/100 g</b>			
P <sub>2</sub> O <sub>5</sub>	15	20	13
K <sub>2</sub> O	21	17	19
MgO	8	9	9
PH	6.6	6.8	7.0
Org. subs (%)	1.8	1.6	2.4

**TABLE 5.S2** | Fertilizer application, amount and the developmental stage of crop.

Date of Application	Treatments	N- Fertilizer <sup>a</sup>	BBCH <sup>b</sup>	Amount of Fertilizer(kg/ha)
12/3/2015	HN-NF, HN-WF	KAS	22	50
15/4/2015	HN-NF, HN-WF	KAS	30	45
27/5/2015	HN-NF, HN-WF	KAS	49-65	60
17/3/2016	HN-NF, HN-WF	KAS	25	50
6/4/2016	HN-NF, HN-WF	KAS	30	55
27/5/2016	HN-NF, HN-WF	KAS	51-59	60
24/3/2017	HN-NF, HN-WF	KAS	25	50
19/4/2017	HN-NF, HN-WF	KAS	31-32	25
29/5/2017	HN-NF, HN-WF	KAS	49-69	60

<sup>a</sup> The treatment LN-NF did not receive further nitrogen fertilization;

KAS means Kalkammonsalpeter (Calcium ammonium nitrate). It contains 27 kg N/100 Kg (dt) KAS fertilizer, including 13.5 kg/dt for each of NH<sub>4</sub> and NO<sub>3</sub>, and 55 kg CaO (calcium oxide) per 100 kgN and 4 kg MgO (magnesium oxide) per 100 kgN.

<sup>b</sup> BBCH means Biologische Bundesanstalt, Bundessortenamt und CHEmische Industrie.

**TABLE 5.S3** | Application of herbicide, fungicide, and growth regulators on different developmental stages of the wheat.

Year	Treatment	Plant protection/Growth regulator			
		Application round	Date (d.m.Y)	Amount	Spraying agents (active ingredients <sup>a</sup> )
2015	low nitrogen, no fungicide (LN_NF)	1st herbicide	17.03.2015	150 gr/ha + 0.7 l/ha + 1.5 l/ha	Broadway 68.3 g/kg Pyroxsulam + 22.8 g/kg Florasulam + 68.3 g/kg Cloquintocet-Mexyl (Safener) + FHS (mesosulfuron) + Arelon Top (isoproturon)
		2nd herbicide	11.05.2015	1.5 l/ha	MCPA (2-methyl-4-chlorophenoxyacetic acid)
		1st insecticide	12.06.2015	75 ml/ha	Karate Zeon (250 g/L Lambda-Cyhalothrin; Oxiran)
	high nitrogen, no fungicide (HN_NF)	1st herbicide	17.03.2015	150 gr/ha + 0.7 l/ha + 1.5 l/ha	Broadway + FHS + Arelon Top
		2nd herbicide	11.05.2015	1.5 l/ha	MCPA
		1st insecticide	12.06.2015	75 ml/ha	Karate Zeon
		1st growth regulator	07.04.2015	1.0 l/ha	CCC (Chlormequat-chloride)
		2nd growth regulator	16.04.2015	0.5 l/ha + 0.3 l/ha	CCC + Moddus (Trinexapac-ethyl)
	high nitrogen, with fungicide (HN_WF)	1st herbicide	17.03.2015	150 gr/ha + 0.7 l/ha + 1.5 l/ha	Broadway + FHS + Arelon Top
		2nd herbicide	11.05.2015	1.5 l/ha	MCPA
		1st insecticide	12.06.2015	75 ml/ha	Karate Zeon
		1st fungicide	07.04.2015	1.1 l/ha	Diamant (114 g/l Pyraclostrobin (F 500) + 43 g/l Epoxiconazol + 214 g/l Fenpropimorph)
		2nd fungicide	17.04.2015	1.75 l/ha	Capallo (75 g/litre metrafenone+ 62.5 g/litre epoxiconazole + 200 g/litre fenpropimorph)
		3rd fungicide	11.05.2015	1.25 l/ha	Input classic (160 g/l Prothioconazol 300 g/l Spiroxamine)
		4th fungicide	27.05.2015	1.0 l/ha + 1.0 l/ha	Osiris (37.5 g/l Epoxiconazol + 27.5 g/l Metconazol) + SkywayXpro (75 g/L bixafen, + 100 g/L prothioconazole + 100 g/L tebuconazole).
		1st growth regulator	07.04.2015	1.0 l/ha	CCC
		2nd growth regulator	16.04.2015	0.5 l/ha + 0.3 l/ha	CCC + Moddus
	2016	low nitrogen, no fungicide (LN_NF)	1st herbicide	16.11.2015	4.0 l/ha
2nd herbicide			08.04.2016	180 g/ha	Hoestar super (125 g/kg Amidosulfuron + 12.5 g/kg Iodosulfuron-methyl-natrium + 125 g/kg Mefenpyr-diethyl)
1st insecticide			10.06.2016	75 ml/ha	Karate Zeon
high nitrogen, no		1st herbicide	16.11.2015	4.0 l/ha	Malibu

	fungicide (HN_NF)	2nd herbicide	08.04.2016	180 g/ha	Hoestar super
		1st insecticide	10.06.2016	75 ml/ha	Karate Zeon
		1st growth regulator	12.04.2016	0.5 l/ha + 0.3 l/ha	CCC + Moddus
	high nitrogen, with fungicide (HN_WF)	1st herbicide	16.11.2015	4.0 l/ha	Malibu
		2nd herbicide	08.04.2016	180 g/ha	Hoestar super
		1st insecticide	10.06.2016	75 ml/ha	Karate Zeon
		1st fungicide	12.04.2016	2.0 l/ha	Capallo
		2nd fungicide	20.04.2016	0.2 l/ha + 1.0 l/ha	Alto (Cyproconazole ) + Bravo (500 g/l chlorothalonil)
		3rd fungicide	02.05.2016	1.2 l/ha + 1.0 l/ha	Adexar (62.5 g/l epoxiconazole+ 62.5 g/litre fluxapyroxad); Credo (100g/l picoxystrobin + 500g/l chlorothalonil)
		4th fungicide	19.05.2016	1.0 l/ha	Input classic
1st growth regulator	12.04.2016	0.5 l/ha + 0.3 l/ha	CCC + Moddus		
2017	low nitrogen, no fungicide (LN_NF)	1st herbicide	03.11.2016	4.0 l/ha	Malibu
		2nd herbicide	15.05.2017	1.5l/ha	MCPA
		1st insecticide	02.06.2017	75 ml/ha	Karate Zeon
	high nitrogen, no fungicide (HN_NF)	1st herbicide	03.11.2016	4.0 l/ha	Malibu
		2nd herbicide	15.05.2017	1.5 l/ha	MCPA
		1st insecticide	02.06.2017	75 ml/ha	Karate Zeon
		1st growth regulator	23.03.2017	1.0 l/ha	CCC
		2nd growth regulator	21.04.2017	0.5 l/ha + 0.3 l/ha	CCC + Moddus
	high nitrogen, with fungicide (HN_WF)	1st herbicide	03.11.2016	4.0 l/ha	Malibu
		2nd herbicide	15.05.2017	1.5 l/ha	MCPA
		1st insecticide	02.06.2017	75 ml/ha	Karate Zeon
		1st fungicide	24.04.2017	2.0 l/ha	Capallo
		2nd fungicide	15.05.2017	1.75 l/ha +1.0 l/ha	Adexar + Credo
		3rd fungicide	31.05.2017	1.25 l/ha + 1.0 l/ha	Osiris + Skyway Xpro
		1st growth regulator	23.03.2017	1.0 l/ha	CCC
2nd growth regulator	21.04.2017	0.5 l/ha + 0.3 l/ha	CCC + Moddus		

<sup>a</sup> the active ingredient of the chemical is given in bracket the first time it appeared in the Table.

**TABLE 5.S4** | Description of the measured variable in the experiments.

Traits Category	Traits	Symbols	Method to measure
Yield related traits	Grain yield	GY (Mg/ha)	Harvesting of central part of each plot was done at the end of the growing season and GY (in Mg. ha <sup>-1</sup> ) was recorded automatically with the help of combine harvester. Grain moisture was immediately measured after trashing at the end of maturity phase (BBCH99) and GY was corrected to standard moisture of 14%.
	Spike number per meter square	SNms	Spike numbers were counted for within one meter from all cultivars one by one before harvesting and after flowering.
	Kernels number per spike	KNSp	Kernels per spike, Kernels per m <sup>2</sup> were calculated based on the Thousand kernel weight, Spike numbers per meter square, seed weight per meter square
	Kernels number per meter square	KNms	
	Thousand kernel weight	TKW (g)	TKW was calculated in 2016 and 2017. Three replicates of five hundred seeds were counted with the help of automatic seed counter and weighed. The average of the three replicates was multiplied by two to calculate thousand kernel weight.
	Harvest index	HI, PBWms (g/m <sup>2</sup> )	Plants in one-meter row of every plot were manually harvested after maturity (BBCH 99) used by Voss-Fels et al. (2019) and dried in oven at 65°C for 3 days. After drying, plant biomass weight (shoot dry weight plus grain weight) and seed weight was recorded to estimate the HI as the ratio of seed weight to total biomass weight
	Plant biomass weight,		
	Heading date	HD (Days)	Visually recorded as number of days from 1st of January to the date when the ears from approximately 70 % of total tiller in each plot came out from flag leaf sheath at around BBCH59
Plant height	PH	The measurement was taken from soil to the top of the spike of the main tiller of the plant between BBCH 65-69 growth stage	
Physiological trait	Leaf chlorophyll contents	SPAD	SPAD were measured at BBCH 45-49 using SPAD 502 Plus Chlorophyll Meter (Konica Minolta, Japan) from 3 different plants of each plot. The SPAD values were recorded based on light absorption by chlorophyll between the wave length of 650 nm to 940 nm
Disease incidence	Yellow rust	YR	YR severity (leaf area covered by rust pustules) was visually scored using linear phenotyping scale from 1 to 9 according Pask et al. (2012), where 1 is the most resistant and 9 the most susceptible genotype. Scores for each plot (genotype) were estimated by reflection of the average leaf area covered with disease as well as the plot area covered by the yellow rust and their severity.
Grain quality traits	Grain crude protein content	GPC (%)	The grain quality were analyzed using NIRS instrument (Perten, DA 7250) following the manufacturers guidelines.
	Grain starch content	GSC(%)	
	Sedimentation	Sedimentation (%)	
	Grain N yield	GNY (kg.ha <sup>-1</sup> )	The grain N yield was calculated by dividing the grain crude protein yield by the wheat-specific protein factor of 5.7, and multiply the result by the GY

**TABLE 5.S5** | Summary of analysis of variance of agronomic and grain quality traits of 220 genotypes tested in three different environments.

Year	Traits	Wald statistic			CV (%)	H <sup>2</sup>
		G	CS	G*CS		
2015	<i>Agronomic traits</i>					
	GY	6891.7***	2396.56***	2290.12***	26.66	0.73
	SNms	619.17**	313.14**	403.97ns	24.59	0.66
	KNSp	-	-	-	-	-
	KNms	-	-	-	-	-
	TKW	-	-	-	-	-
	HD	3875.16**	131.73**	452.34ns	1.88	0.94
	PH	2853.91**	519.06**	393.14ns	10.82	0.96
	HI	5625.89**	143.5**	3065.83**	13.13	0.73
	PBWms	413.41**	365.87**	449.19 ns	29.72	0.44
	<i>Physiological trait</i>					
	SPAD	-	-	-	-	-
	<i>Disease incidence</i>					
	YR	1497.98**	91.29**	466.34ns	50.97	0.84
	<i>Grain quality traits</i>					
GPC	2083.91**	3655.31**	519.8ns	12.04	0.87	
GSC	899.82**	316.97**	431.9ns	2.12	0.76	
Sedimentation	227.99 ns	408.07**	431.09ns	38.77	0.22	
2016	<i>Agronomic traits</i>					
	GY	13408.46***	4810.61***	2557.78***	25.6	0.8
	SNms	395.81**	254.37**	488.64ns	19.13	0.39
	KNSp	32.4E4***	34.4E3***	39.2E4***	0.301	0.38
	KNms	11.3E5***	65.8E4***	98.1E4***	0.32	0.55
	TKW	9751.16**	4636.41**	2154.6**	13.49	0.87
	HD	881.68**	119.44**	504.05ns	0.71	0.69
	PH	5712.85**	369.1**	1099.83**	10.66	0.91
	HI	1619.80**	725.85**	557.05**	12.16	0.69
	PBWms	396.77**	63.09**	389ns	26.62	0.5
	<i>Physiological trait</i>					
	SPAD	216.1**	512.66**	416.66ns	10.3	0.60
	<i>Disease incidence</i>					
	YR	3848.78**	308.45**	579.39**	62.73	0.92
	<i>Grain quality traits</i>					
GPC	6861.23**	4956.56**	1532.27**	10.7	0.89	
GSC	574.71**	23.74**	399.47ns	1.41	0.66	
Sedimentation	980.55**	195.82**	595**	24.1	0.95	

Table S5 (continued)

Year	Traits	Wald statistic			CV (%)	H2
		G	CS	G*CS		
2017	<i>Agronomic traits</i>					
	GY	4001.76***	1413.27***	1103.88***	17.36	0.75
	SNms	339.53**	99.85**	343.16ns	17.79	0.48
	KNSp	13.1E4***	13651.95***	15.4E4***	0.237	0.43
	KNms	25.7E5***	15.6E4***	28.5E4***	0.24	0.46
	TKW	14852.82**	190.71**	1898.15**	8.04	0.93
	HD	4327.21**	271.57**	412.95ns	1.46	0.95
	PH	10147.78**	362.09**	888.29**	11.71	0.95
	HI	1533.21**	575.06**	539.66**	8.44	0.82
	PBWms	375.31**	25.44**	467.58ns	20.01	0.38
	<i>Physiological trait</i>					
	SPAD	901.86**	88.85**	529.39ns	9.46	0.70
	<i>Disease incidence</i>					
	YR	-	-	-	-	-
	<i>Grain quality traits</i>					
	GPC	5857.53**	9955.66**	761.25**	11.39	0.93
	GSC	2574.5**	665.49**	699.41**	1.26	0.86
Sedimentation	9302.4**	2909.79**	3171.77**	38.91	0.83	

\*\* Significant at the 0.01 probability level

\*\*\* Significant at the 0.001 probability level

† ns, nonsignificant at the 0.05 probability level

**TABLE 5.S6** | Arithmetic mean and treatments effect of agronomic and grain quality traits of 220 genotypes tested in 3 different CS over three growing seasons.

Traits	2015						2016						2017					
	Means			Treatment effect (%)			Means			Treatment effect (%)			Means			Treatment effect (%)		
	HN-NF	HN-WF	LN-NF	N	NF	F <sub>HN</sub>	HN-NF	HN-WF	LN-NF	N	NF	F <sub>HN</sub>	HN-NF	HN-WF	LN-NF	N	NF	F <sub>HN</sub>
GY(Mg/ha)	8.976b*	11.225a	6.680c	34.36	68.03	25.06	6.867b	9.583a	6.455c	6.39	48.46	39.55	9.678b	10.525a	7.410c	30.61	42.03	8.75
SNms	501.69a	493.90a	336.88b	48.92	46.61	-1.55	497.44b	525.12a	415.20c	19.81	26.48	5.57	464.65a	455.75a	391.67b	18.63	16.36	-1.92
KNSp	-	-	-	-	-	-	30.87b	34.81a	28.70c	7.54	21.25	12.76	42.94b	45.24a	39.66c	8.28	14.09	5.36
KNms	-	-	-	-	-	-	15171.13b	17847.11a	11648.78c	30.24	53.21	17.64	19562.48b	20307.22a	15290.47c	27.94	32.81	3.81
TKW (g)	-	-	-	-	-	-	39.83c	47.57b	49.14a	-18.94	-3.18	19.44	46.22c	47.36b	48.78a	-5.25	-2.91	2.46
HD (days)	150.30a	150.20a	148.27b	1.37	1.3	-0.07	154.04b	154.73a	153.54c	0.33	0.77	0.45	148.56a	148.74a	147.06b	1.02	1.15	0.12
PH (cm)	91.61a	90.01b	92.50a	-0.96	-2.69	-1.75	91.12c	93.66b	99.43a	-8.36	-5.8	2.79	87.47b	87.86b	94.48a	-7.43	-7.01	0.45
HI	0.51b	0.55a	0.48c	5.97	15.05	8.57	0.46b	0.51a	0.45c	2.01	13.43	11.19	0.58b	0.60a	0.54c	6.69	10.83	3.89
PBWms (g/m <sup>2</sup> )	1566.62b	1774.60a	1031.14c	51.93	72.1	13.28	1302.53b	1661.50a	1266.59b	2.84	31.18	27.56	1561.35a	1596.43a	1382.99b	12.9	15.43	2.25
SPAD	-	-	-	-	-	-	50.50b	55.43a	46.15c	9.41	20.09	9.77	52.40a	51.25b	47.99c	9.18	6.78	-2.2
YR	2.17b	1.73c	2.95a	-26.59	-41.29	-20.02	1.58b	1.44b	2.33a	-32.3	-38.08	-8.54	-	-	-	-	-	-
GPC (%)	14.42b	14.63a	11.61c	24.22	26.03	1.46	12.35b	12.61a	10.41c	18.71	21.18	2.08	14.20b	14.60a	11.51c	23.39	26.85	2.8
GSC (%)	74.25a	72.38b	72.44b	2.49	-0.08	-2.51	73.67a	73.32b	73.27b	0.55	0.07	-0.47	74.04b	73.17c	74.32a	-0.37	-1.54	-1.18
Sedimentation (%)	34.56a	34.71a	16.20b	113.31	114.24	0.44	34.6b	35.7a	25.3c	36.76	41.11	3.181	39.37a	38.22a	19.41b	102.82	96.87	-2.93

\* Means values within a year in the same row line with different letters indicate a significant difference at  $P < 0.05$

N means nitrogen effect, NF means nitrogen plus fungicide effect, and F<sub>HN</sub> means fungicide effect under low and high nitrogen

**TABLE 5.S7** | GY (Mg.ha<sup>-1</sup>) statistics for the applied cropping systems and the years of experiments.

Year	CS	Mean	Maximum	Minimum	Range	CV (%) <sup>*</sup>
2015	HN-NF	8.976	12.511	2.051	10.46	22.47
	HN-WF	11.225	14.073	7.916	6.157	9.54
	LN-NF	6.68	9.62	2.155	7.465	18.79
2016	HN-NF	6.867	9.645	1.239	8.406	23.03
	HN-WF	9.524	12.217	4.127	8.09	13.43
	LN-NF	6.393	8.569	1.751	6.818	19.25
2017	HN-NF	9.678	11.996	5.856	6.14	10.97
	HN-WF	10.525	12.367	7.619	4.748	7.72
	LN-NF	7.41	9.424	4.635	4.989	11.16
Average of three years	HN-NF	8.507	11.384	3.049	8.335	18.82
	HN-WF	10.425	12.886	6.554	6.332	10.23
	LN-NF	6.828	9.204	2.847	6.424	16.4

<sup>\*</sup>CV stands for coefficient of variation

**TABLE 5.S8** | Detailed analysis of variance of GY of winter wheat genotypes in cropping systems (CS) by year (Y).

Year	2015				2016			2017		
Source	DF	Anova SS	Mean Square	% Variance Explained	Anova SS	Mean Square	% Variance Explained	Anova SS	Mean Square	% Variance Explained
<b>Cropping systems (CS)</b>	2	454374.824	227187.4121***	70.9	250658.57	125329.2852***	61.36	228223	114111.6963***	77.15
<b>Genotype(G)</b>	219	221449.968	1011.1871***	19.67	208916.91	953.9585***	29.85	83031.4	379.139***	16.36
<b>CS*G</b>	438	66754.6403	152.4079***	9.44	37041.749	84.5702***	8.8	21640.8	49.4083***	6.5
<b>Error</b>	660	9913.6521	15.0207		2135.0851	3.235		3818.17	5.7851	

\*\*\* Significant at the 0.0001 probability level, DF=Degree of freedom

**TABLE 5.S9** | Three ways ANOVA of GY of winter wheat genotypes (G) in three cropping systems (CS) across three years (Y).

Source	DF	Anova SS	Mean Square	% Variance Explained	F Value
<b>Y</b>	2	198589.9929	99295.00***	10.38	12390.8
<b>CS</b>	2	855052.0568	427526.03***	54.45	53350.1
<b>G</b>	219	439141.9294	2005.21***	16.22	250.23
<b>Y*CS</b>	4	78204.7304	19551.18***	7.89	2439.75
<b>Y*G</b>	438	74256.3878	169.5351***	3.3	21.16
<b>CS*G</b>	438	80519.4934	183.83***	4.03	22.94
<b>Y*CS*G</b>	1314	44917.7155	51.2759 ***	3.74	11.32
<b>Error</b>	1980	15866.908	8.014***		

**TABLE 5.S10** | N flow related analysis of variance and statistics.

(A) Combined ANOVA of NUE, NAE, and Grain N yield of winter wheat genotypes (G) in three cropping systems (E) across three years (Y).

Anova Factors	Fvalue (NUE)	Fvalue (NAE)	Fvalue (Grain N yield)
<b>Year (Y)***</b>	156.94***	4.16E+09***	9523.02***
<b>Cropping System (CS)</b>	35649.5***	1.35E+10***	29853.64***
<b>Genotype (G)</b>	28.76***	1.27E+07***	42.78***
<b>Y*G</b>	3	7661408	6.32***
<b>Y*CS</b>	1103.28***	8.13E+08***	1030.96***
<b>CS*G</b>	6.18***	1.67E+07***	7.57***
<b>Y*CS*G</b>	1.32***	2867525***	2.18***

\*\*\* Significant at the 0.001 probability level

(B) Cultivars harvested GY (Mg.ha<sup>-1</sup>) and grain nitrogen yield (GNY in kg.ha<sup>-1</sup>) under the three CS.

Genotypes	Briweccs Number	GY <sup>a</sup> (HN-NF <sup>b</sup> )	GY(HN-WF)	GY(LN-NF)	GNY <sup>b</sup> (HN-NF)	GNY (HN-WF)	GNY (LN-NF)
Name							
Einstein	1	9.789	11.019	7.455	229.7	264.23	145.05
Oakley	2	6.093	12.2	7.033	133.1	264.43	124.74
Jafet	3	9.973	10.406	7.055	235.14	263.43	138.36
Claire	4	9.771	11.46	8.394	228.36	269.04	150.07
Rebell	5	10.455	10.847	8.031	260.26	266.48	156.5
Memory	6	10.153	10.821	7.826	238.57	245.86	151.55
Kurt	7	9.377	11.743	7.804	221.58	291.37	145.69
Zappa	8	10.836	11.179	7.976	251.64	271.29	155.82
Chevalier	9	9.334	10.335	7.242	228.16	250.84	142.95
Gordian	10	9.785	10.591	7.253	246.12	245.53	135.58
Mentor	11	10.382	11.541	7.276	247.91	279.7	134.75
Meister	12	8.488	11.161	7.511	203.72	282.75	143.09
KWS Santiago	13	9.041	12.11	7.818	205.44	272.84	138.24
Brigand	14	8.453	10.281	7.21	213.16	256.41	141.54
Profilus	15	9.134	10.778	7.418	213.35	259.19	137.59
Durin	16	8.238	9.858	7.197	201.91	248.61	137.96
KWS Pius	17	10.184	11.152	8.101	248.01	277.55	159.21
Paroli	18	8.473	11.259	7.521	199.16	271.37	142.86
Estivus	19	9.227	11.013	7.849	218.13	268.56	148.11
Kronjuwel	20	7.636	9.34	6.022	184.56	242.31	125.79
Desamo	21	9.559	10.521	7.283	232.69	258.41	141.05
Carenius	22	9.242	11.057	7.252	216.88	259.18	141.7
Mulan	23	9.751	11.286	7.922	232.07	267.58	144.09

Kredo	24	9.435	11.364	7.495	232.72	264.91	143.86
Nelson	25	9.63	10.287	6.396	239.39	263.93	127.06
Patras	26	10.03	10.789	7.355	243.5	267.27	145.41
Götz	27	8.211	10.083	6.024	200.6	256.67	120.72
Robigus	28	5.874	11.276	6.216	137.01	267.76	118.96
Anapolis	29	10.438	11.478	7.705	255.14	275.73	144.51
Solstice	30	8.194	10.76	7.256	199.13	253.68	139.82
Biscay	31	9.448	11.566	7.612	223.04	271.69	141.37
Capone	32	10.092	10.652	7.994	246.89	254.56	153.39
Tabasco	33	10.862	12.019	8.315	242.94	280.31	156.22
Kometus	34	7.485	11.117	6.699	184.25	266.67	126.81
Cubus	35	9.76	10.812	7.204	231.55	255.77	137.04
Edward	36	9.397	11.603	8.134	226.86	284.69	158.91
Famulus	37	9.155	9.979	6.749	223.1	252.75	132.06
Dekan	38	8.715	10.781	7.864	203.62	259.88	154.86
SW Topper	39	9.39	10.126	6.446	233.44	265.69	129.11
Matrix	40	8.061	11.093	7.036	194.89	271.6	136.76
Jenga	41	8.977	11.156	7.933	208.69	263.64	148.17
Linus	42	10.432	11.566	7.823	253.39	271.97	152.52
TJB 990-15	43	9.382	10.264	7.009	227.1	250.95	141.3
Forum	44	9.869	11.085	7.426	232.37	272.2	146.54
Colonia	45	9.983	11.062	7.486	240.34	268.37	148.08
Transit	46	8.76	10.684	7.533	213.66	271.93	147.13
Potenzial	47	9.463	10.85	7.337	223.98	256.72	145.92
Gaicho	48	9.878	11.623	8.034	234.99	275.68	148.99
Tarso	49	8.976	10.332	6.649	215.78	266.14	133.3
Hermann	50	8.224	10.637	7.091	195.11	266.72	137.79
Glaucus	51	9.646	10.959	7.575	245.09	269.1	147.89
Tuareg	52	9.538	11.3	7.419	225.92	278.18	134.91
Atomic	53	10.285	11.314	7.739	247.33	270.89	151.74
Tobak	54	9.937	12.288	8.571	225.36	293.89	156.24
Pionier	55	9.464	10.932	7.248	228.62	259.93	139.9
Manager	56	8.847	10.883	7.709	218.08	256.15	142.14
Gourmet	57	8.933	10.047	6.311	226.29	255.11	123.66
Limes	58	9.702	10.984	7.399	238.72	281.05	146.55
Ritmo	59	8.741	10.701	6.942	209.23	264.24	135.74
Kalahari	60	10.057	11.121	7.56	232.07	267.23	147.95
Intro	61	10.263	11.064	7.925	242.29	261.65	151.59
Oxal	62	9.868	10.893	7.632	239.2	263.68	142.6
Zobel	63	8.289	10.866	6.525	197.78	268.29	126.51
Event	64	9.46	10.615	6.469	225.46	257.36	133.76
Joker	65	9.453	10.663	7.403	222	249.04	147.51
Global	66	9.513	11.666	7.498	222.8	273.48	141.29
Elixer	67	10.566	11.706	7.759	251.89	280.35	151.9
Fedor	68	9.946	10.76	7.899	227.1	254.94	152.88
Türkis	69	9.108	11.1	7.337	210.74	255.32	140.76
Skagen	70	9.327	10.79	7.66	223.77	262.48	147.69
Greif	71	9.364	10.46	7.56	225.3	249.83	144.55
Esket	72	10.023	10.661	7.013	236.46	254.33	138.05

Primus	73	8.796	11.116	7.257	201.9	261.34	139.16
Skalmeje	74	9.672	11.343	7.368	222.88	266.47	139.98
Genius	75	9.59	10.49	6.776	237.83	263.78	135.68
Enorm	76	8.867	10.011	6.621	216.54	250.14	131.7
Florian	77	9.257	10.192	7.118	223.88	255.29	151.14
Skater	78	7.447	10.984	6.846	169.58	257.52	133.21
Brilliant	79	9.025	10.824	7.346	210.54	266.26	140.78
Inspiration	80	9.421	11.143	7.448	216.82	270.71	146.08
Apertus	81	10.026	11.025	7.634	239.07	269.44	149.45
Ellvis	82	9.231	10.698	8.053	226.04	267.53	158.47
Edgar	83	10.04	11.296	7.829	234.89	274.87	148.85
Maris Huntsman	84	8.671	10.713	6.627	208.79	265.4	130.73
SY Ferry	85	10.082	11.147	8.167	245.13	275.58	155.86
Landsknecht	86	8.204	11.698	7.317	189.48	264	136.09
Sponsor	87	8.39	10.462	7.49	200.37	245.85	144.36
Impression	88	9.792	11.123	7.707	236.81	267.68	148.76
Winnetou	89	8.59	11.504	6.932	207.06	271.48	131.56
Toronto	90	8.7	10.227	6.973	222.66	256.68	140.21
Torrild	91	9.621	10.74	7.342	230.47	265.91	141.41
Contra	92	8.81	11.107	7.797	209.69	274.9	152.94
Schamane	93	8.676	10.475	6.63	206.3	261.38	129.56
Granada	94	4.274	10.113	4.711	101.69	240.93	93.44
KWS Cobalt	95	10.259	11.057	8.461	236.1	250.43	162.71
Tommi	96	9.611	10.71	7.468	233.35	270.77	147.95
Saturn	97	8.225	10.47	6.797	194.34	246.99	131.59
Severin	98	6.576	9.556	5.862	162.41	242.07	121.32
JB Asano	99	7.571	10.881	6.558	174.03	266.89	126.96
Kerubino	100	8.77	11.145	6.879	206.99	265.84	137.03
Arktis	101	8.789	10.543	6.914	211.02	247.81	129.18
Urban	102	7.942	9.809	6.547	192.17	243.56	125.74
Orestis	103	8.687	10.718	7.355	204.72	254.26	137.71
Flair	104	7.594	10.532	6.727	177.16	252.72	122.55
Anthus	105	9.527	11.304	8.027	222	266.13	146.97
Bombus	106	9.416	11.398	7.728	224.85	272.9	143.67
Lucius	107	9.047	10.399	6.722	216.4	254.47	132.55
Herzog	108	8.263	10.673	7.014	193.2	254.6	128.94
Sorbis	109	8.278	9.903	6.471	205.3	253.02	131.41
Tabor	110	8.307	9.112	6.35	207.74	227.11	124.89
Terrier	111	8.199	10.854	7.405	189.91	255.85	137.29
Magister	112	8.007	9.959	6.11	199.81	255.2	117.74
Altos	113	9.195	9.993	6.507	219.15	254.08	130.17
Progress	114	8.558	9.796	6.667	206.3	238.67	126.72
Xanthippe	115	8.968	11.44	7.062	212.42	269.51	132.87
Avenir	116	9.64	10.631	7.35	231.44	252.47	146.83
Pantus	117	7.415	10.573	6.47	176.38	256.57	128.06

Drifter	118	8.822	11.031	8.027	212.61	263.52	151.36
Joss	119	8.555	9.596	6.305	207.68	244.45	126.49
Kranich	120	7.429	9.666	6.223	178.63	233.57	117.72
Sperber	121	9.274	10.279	6.404	227	260.71	124.43
Discus	122	8.09	10.601	7.096	195.28	263.67	138.94
Helios	123	3.709	9.675	4.265	92.02	239.49	84.71
Obelisk	124	8.588	10.956	6.872	213.13	265.53	129.52
Magnus	125	8.315	10.856	6.977	192.3	259.04	141.31
Disponent	126	8.447	10.49	6.81	203.15	269.15	135.97
Tambor	127	8.801	10.051	6.555	215.76	252.24	133.37
Boxer	128	8.936	11.161	7.215	203.03	264.25	136.74
Sokrates	129	9.194	11.199	7.042	222.95	267.57	135.82
Carisuper	130	7.854	9.295	6.231	192.03	235.43	127.07
Rektor	131	7.112	9.906	6.086	168.08	248.37	122.81
Alves	132	9.876	10.923	8.01	231.5	257.97	151.65
NaturaStar	133	7.431	9.694	6.176	176.75	243.22	124.53
Alidos	134	8.819	9.906	6.313	217.37	251.09	130.26
Monopol	135	7.485	9.272	6.189	176.5	233.55	128.64
Akratos	136	9.051	11.191	7.445	208.53	272.46	149.84
Knirps	137	7.319	9.729	6.453	180.21	241.65	126.5
Bussard	138	8.143	9.74	6.336	199.58	249.85	127.95
Oberst	139	7.541	10.419	6.251	183.5	256.65	125.91
Cappelle Desprez	140	7.73	8.66	6.209	197.59	234.27	127.77
Tiger	141	9.248	10.632	7.186	222.05	267.44	148.16
Ibis	142	9.308	10.127	7.185	231.05	244.22	147.42
Batis	143	8.74	10.593	7.29	202.28	257.78	140.55
Topfit	144	8.013	9.722	6.695	191.95	245.72	132.79
Akteur	145	8.055	10.292	6.432	196.54	268.13	131.7
Ludwig	146	8.973	10.625	7.058	218.75	260.98	140.41
Asketis	147	8.222	10.826	6.721	192.14	256.14	131.04
Aristos	148	7.983	10.524	7.077	192.5	257.09	138.42
Zentos	149	8.529	10.107	6.914	202.26	253.21	133.17
Diplomat	150	7.499	9.344	6.39	182.22	231.56	127.35
Astron	151	8.365	9.867	6.907	204.17	256.91	142.09
Basalt	152	7.318	9.462	6.465	175.01	233.51	124.87
Kormoran	153	7.815	9.845	6.477	192.28	247.67	131.09
Aron	154	8.264	10.067	6.696	203.71	255.35	137.4
KWS Milaneco	155	8.062	9.926	6.507	197.99	242.28	133.13
Aszita	156	7.499	8.503	5.72	193.23	234.97	122.42
Kobold	157	8.136	9.408	6.309	196.08	245.23	122.94
Carimulti	158	8.313	9.116	6.395	206.32	246.06	127.47
Admiral	159	7.955	9.489	6.31	188.95	237.45	124.86
Vuka	160	7.056	9.903	6.08	167.89	248.4	121.45
Benno	161	7.345	9.693	6.526	181.22	247.04	135.78
Apollo	162	8.33	10.387	6.795	198.63	250.95	132
Aquila	163	6.79	10.095	5.942	159.86	245.36	115.4
Kanzler	164	7.279	10.337	6.269	168.75	259.29	126.58
Kraka	165	7.401	10.178	6.433	178.02	245.45	125.86
Caribo	166	7.377	9.835	6.258	182.64	250.12	126.14

Butaro	167	7.674	8.671	5.637	199.24	238.01	119.78
Konsul	168	7.203	8.435	5.822	186.78	225.28	122.55
Ares	169	7.319	10.339	6.238	170.8	256.13	125.47
Centurk	170	4.704	8.449	4.75	122.13	219.48	96.95
NS 22/92	171	7.844	8.621	6.783	202.24	223.01	137.98
Benni multifloret	172	4.837	7.77	4.37	121.17	202.76	90.54
Hope	173	5.18	8.176	4.201	127.71	213.32	90.24
Vel	174	5.795	7.504	4.646	157.25	205.81	102.71
Phoenix	175	4.395	8.4	3.926	110.69	226.47	83.93
Mironovska 808	176	6.081	8.51	4.455	158.22	224.71	92.92
Caphorn	177	9.759	10.607	7.375	244.79	264.01	147.6
Cordiale	178	9.041	10.782	7.581	211.57	251.57	152.62
Apache	179	9.883	11.452	7.248	239.75	271.63	138.2
Premio	180	10.124	11.167	6.926	249.21	275.08	131.76
Isengrain	181	9.511	10.766	7.035	235.19	253.93	139.45
Alixan	182	8.099	11.274	6.667	188.09	275.59	130.8
Boregar	183	9.424	11.271	7.712	226.11	268.61	148.52
Renesansa	184	6.04	8.861	5.444	154.53	230.71	113.57
Tremie	185	8.933	11.082	7.201	214.43	264.09	140.42
KWS Ferrum	186	8.916	11.654	7.549	216.93	264.79	141.17
Triple Dirk "S"	187	6.807	8.951	5.305	170.99	223.34	106.49
Cardos	188	7.424	10.217	6.24	183.44	253.63	127.19
Soissons	189	8.858	9.973	6.384	223.88	244.81	126.82
BCD 1302/83	190	5.377	9.47	5.019	136.92	248.82	104.38
Arlequin	191	10.018	11.435	8.054	230.96	259.5	150.34
Sonalika	192	6.703	9.554	5.983	160.06	226.35	116.87
Camp Remy	193	8.608	10.06	6.379	217.92	250.74	130.42
Cajeme 71	194	3.308	8.943	3.714	83.32	239.35	76.34
Avalon	195	8.147	9.11	6.318	203.67	227.38	133.77
Ivanka	196	3.694	9.577	3.768	87.57	236.34	76.6
Pobeda	197	6.686	9.038	5.337	175.02	244.23	114.35
NS 66/92	198	7.683	8.908	5.682	199.15	230.21	118.14
Mexico 3	199	7.482	9.315	5.804	187.43	235.55	118.41
Orcas	200	7.966	10.869	7.239	189.29	269.99	143.3
Nimbus	201	6.016	9.96	5.415	147.12	241.5	113.91
Muskat	202	10.449	10.994	7.592	265.96	262.59	143.71
Florida	203	6.939	9.063	5.549	177.29	230.96	113.86
Rumor	204	9.129	11.713	7.404	219.85	267.09	143.45
Highbury	205	7.139	8.341	5.637	184.61	221.44	119.2
Siete Cerros 66	206	4.03	9.378	4.632	104.28	245.57	95.12
Kontrast	207	8.883	9.973	6.409	220.64	256.69	133.28
WW 4180	208	8.904	10.454	6.808	218.88	253.84	132.37
INTRO 615	209	7.077	8.521	6.017	182.59	215.37	124.93
NS 46/90	210	4.592	9.434	3.926	122.7	257.33	84.52
Mex. 17 bb	211	7.003	8.35	5.504	181.65	218.75	113.11
Labriego-Inia	212	6.627	9.401	4.731	163.5	237.98	96.92
Pegassos	213	8.172	10.589	6.818	195.51	254.66	135.27
Hybred	214	9.655	11.119	7.221	226.74	261.38	140.75
Hyland	215	9.89	11.721	7.866	231.32	266	154.36
Hybery	216	10.741	12.043	8.268	253.75	272.97	154.85
Hystar	217	10.314	11.729	7.691	248.35	269.3	143.87
Hylux	218	10.18	11.803	8.711	234.84	263.24	155.86

Piko	219	8.949	9.734	6.626	221.59	233.09	127.76
SUR 99820	220	9.074	11.329	7.748	207.38	261.31	144.05

(C) Summary of three years averages of grain nitrogen yield (GNY in kg.ha<sup>-1</sup>) under the three CS.

Yielding Status	GNY (HN-NF)	GNY(HN-WF)	GNY(LN-NF)
High Yielding	234.16	269.45	148.89
Low Yielding	197.56	252.10	130.04
Mean	215.86	260.775	139.465
Difference (High-Low)	36.60	17.36	18.84

(D) Summary of three years averages nitrogen flow under the three CS and correlations coefficient between GY and GNY under each CS.

Treatment	GY (Mg/ha)	GNY (kg/ha)	Nitrogen available (kg/ha)	Applied N fertilizer	<sup>a</sup> Utilized N from fertilizer (kg/ha)	Lost N from fertilizer (kg/ha)	N	<sup>b</sup> N utilized for 1 Mg grain	Corr
HN-NF	8.51	205.21	220.00	151.67	72.8	78.87		25.86	0.98
HN-WF	10.44	255.72	220.00	151.67	72.8	78.87		21.07	0.90
LN-NF	6.84	133.98	65.43	0.00	0.00	0.00		9.56	0.97

<sup>a</sup> Utilized N from fertilizer (kg/ha) to grain N yield is equal to 48% of the applied n fertilizer according to Ladha et al. [43]; <sup>b</sup>

N utilized for 1t grain calculated according to Angus [44]

Corr: Correlation coefficient between GY and GNY.

**TABLE 5.S11** | Pairwise comparison of GYs and its components correlation coefficients among cropping systems.

P-values	HN-NF	HN-WF
<i>PBWms</i>		
HN-WF	0.001***	1
LN-NF	0.001***	0.001***
<i>HI</i>		
HN-WF	0.06	1
LN-NF	0.01**	0.56
<i>TKW</i>		
HN-WF	0.001***	1
LN-NF	0.8	0.001***
<i>KNms</i>		
HN-WF	0.01**	1
LN-NF	0.36	0.01**
<i>KNSps</i>		
HN-WF	0.01**	1
LN-NF	0.45	0.08
<i>SNms</i>		
HN-WF	0.14	1
LN-NF	0.67	0.06

The table displays p-values and significance levels

**TABLE 5.S12** | Pairwise comparison of coefficients (intercepts and slopes) of regressions model GY vs traits of interest under three CS.

	Regression Equation	Rsquare ; Pvalue	HN-NF		HN-WF	
<i>Chlorophyll content (GY vs SPAD in 2016)</i>						
HN-NF	$y = 0.1518x - 0.7986$	$R^2 = 0.3042; p^{***}$	<i>intercepts</i>	<i>Slopes</i>	<i>intercepts</i>	<i>Slopes</i>
HN-WF	$y = 0.0717x + 5.5511$	$R^2 = 0.0369; p^{***}$	2.03e-05 <sup>a</sup> ***	0.00341 **		
LN-NF	$y = 0.1332x + 0.2681$	$R^2 = 0.4196; p^{***}$	0.25763	0.336	0.0001 ***	0.0154*
<i>Chlorophyll content (GY vs SPAD in 2017)</i>						
HN-NF	$y = 0.0375x + 7.4074$	$R^2 = 0.0079$	<i>intercepts</i>	<i>Slopes</i>	<i>intercepts</i>	<i>Slopes</i>
HN-WF	$y = 0.0319x + 8.6046$	$R^2 = 0.0112$	0.514	0.866		
LN-NF	$y = 0.0795x + 0.31376$	$R^2 = 0.059; p^{***}$	0.020*	0.218	0.001 ***	0.108
<i>YR (Yellow rust)</i>						
HN-NF	$y = -0.966x + 10.317$	$R^2 = 0.317, p^{***}$	<i>intercepts</i>	<i>Slopes</i>	<i>intercepts</i>	<i>Slopes</i>
HN-WF	$y = -0.451x + 11.142$	$R^2 = 0.1114, p^{***}$	0.001 ***	2.93e-05 ***	2.93e-05 ***	
LN-NF	$y = -0.533x + 8.2365$	$R^2 = 0.364, pns$	< 2e-16 ***	1.20e-05 ***	< 2e-16 ***	0.396
<i>HD (Heading Date)</i>						
HN-NF	$y = 0.257x - 30.389$	$R^2 = 0.1293, p^{***}$	<i>intercepts</i>	<i>Slopes</i>	<i>intercepts</i>	<i>Slopes</i>
HN-WF	$y = 0.150x - 12.247$	$R^2 = 0.0669, p^*$	0.035 *	0.058		
LN-NF	$y = 0.260x - 32.151$	$R^2 = 0.229, p^{***}$	0.826	0.959	0.008 **	0.027 *
<i>PH (plant height)</i>						
HN-NF	$y = -0.059x + 13.826$	$R^2 = 0.113, p^{***}$	<i>intercepts</i>	<i>Slopes</i>	<i>intercepts</i>	<i>Slopes</i>
HN-WF	$y = -0.067x + 16.489$	$R^2 = 0.376, p^{***}$	0.012 *	0.495		
LN-NF	$y = -0.043x + 10.918$	$R^2 = 0.222, p^{***}$	0.003**	0.129	8.39e-13 ***	0.003 **
<i>GPC (grain protein content)</i>						
HN-NF	$y = -1.085x + 23.33$	$R^2 = 0.127^{***}$	<i>intercepts</i>	<i>Slopes</i>	<i>intercepts</i>	<i>Slopes</i>
HN-WF	$y = -1.253x + 27.91$	$R^2 = 0.631^{***}$	0.419	0.615		
LN-NF	$y = -1.550x + 24.16$	$R^2 = 0.491^{***}$	0.626	0.545	0.723	0.846
<i>GSC (grain starch content)</i>						
HN-NF	$y = 0.857x - 54.91$	$R^2 = 0.1775^{***}$	<i>intercepts</i>	<i>Slopes</i>	<i>intercepts</i>	<i>Slopes</i>
HN-WF	$y = 0.7953x - 47.6$	$R^2 = 0.481^{***}$	0.052	0.326		
LN-NF	$y = 0.776x - 50.12$	$R^2 = 0.295^{***}$	0.733	0.017 *	0.012*	0.015*

<sup>a</sup> Pvalue of the comparison between both intercepts and slopes

\* Significant at the 0.05 probability level

\*\* Significant at the 0.01 probability level

\*\*\* Significant at the 0.001 probability level

ns, nonsignificant at the 0.05 probability level

**TABLE 5.S13** | Full regression (A) and path models (B) with direct and indirect effects of 13 independent variables on GY of 220 cultivars tested in 3 different CS over three growing seasons.**A**

Full regression model									
Variable	HN-NF			HN-WF			LN-NF		
	b <sup>a</sup>	± std Error	Prob <sup>sig</sup>	b	± std Error	Prob <sup>sig</sup>	b	± std Error	Prob <sup>sig</sup>
<i>Constant</i>	-			-			-		
	232.20	69.76	0.001 **	95.24	56.63	0.094	209.5	51.92	0 ***
HD	0.82	0.24	0.001 ***	0.81	0.22	0 ***	0.7	0.19	0 ***
SPAD	0.28	0.14	0.04 *	0.04	0.13	0.738	0.36	0.1	0 ***
YR	-2.71	0.58	0 ***	-1.66	0.42	0 ***	-2.08	0.28	0 ***
PH	-0.06	0.06	0.382	-0.07	0.05	0.176	0.04	0.04	0.332
SNms	0.00	0.01	0.837	-0.01	0.01	0.134	0.03	0.01	0.032 *
KNSp	-0.21	0.14	0.128	-0.12	0.09	0.201	0.11	0.12	0.347
KNms	0.00	0.00	0.206	0	0	0.747	0	0	0.312
TKW	0.16	0.15	0.294	0.24	0.11	0.034 *	0.13	0.11	0.206
HI	161.30	14.70	0 ***	86.37	13.16	0 ***	94.32	13.49	0 ***
PBWms	0.03	0.00	0 ***	0.01	0	0.026 *	0.01	0	0.001 ***
GPC	-1.06	1.20	0.379	-5.75	0.88	0 ***	-3.69	0.93	0 ***
GSC	1.26	0.63	0.047 *	1.51	0.53	0.004 **	1.69	0.51	0.001 **
Sedimentation	-0.13	0.08	0.137	-0.13	0.06	0.03 *	0	0.1	0.986
R square (%)	86.2			81.6			84.7		

<sup>a</sup> regression slope

\* Significant of the slope at the 0.05 probability level

\*\* Significant of the slope at the 0.01 probability level

\*\*\* Significant of the slope at the 0.001 probability level

ns, nonsignificant of the slope at the 0.05 probability level

## B

Path Analysis model												
Variable	HN-NF				HN-WF				LN-NF			
	Direct effect	Indirect effect	ri/j	Prob <sup>sig</sup>	Direct effect	Indirect effect	ri/j	Prob <sup>sig</sup>	Direct effect	Indirect effect	ri/j	Prob <sup>sig</sup>
HD	0.11	0.175	0.285	0***	0.127	-0.014	0.113	0***	0.132	0.330	0.462	0***
SPAD	0.064	0.426	0.490	0.032*	0.012	0.198	0.210	0.729	0.13	0.433	0.563	0***
YR	-0.158	-0.405	-0.563	0***	-0.128	-0.179	-0.307	0***	-0.243	-0.359	-0.602	0***
PH	-0.031	-0.304	-0.335	0.365	-0.067	-0.541	-0.608	0.16	0.042	-0.522	-0.480	0.314
SNms	0.009	0.153	0.162	0.831	-0.079	0.102	0.023	0.12	0.131	0.065	0.196	0.026*
KNSp	-0.115	0.556	0.441	0.114	-0.101	0.334	0.233	0.185	0.077	0.307	0.384	0.33
KNms	-0.112	0.666	0.554	0.19	0.029	0.329	0.358	0.738	-0.093	0.649	0.556	0.295
TKW	0.047	0.375	0.422	0.277	0.092	0.006	0.098	0.027	0.056	0.345	0.401	0.19
HI	0.51	0.275	0.785	0***	0.354	0.346	0.700	0***	0.389	0.278	0.667	0***
PBWms	0.447	0.298	0.745	0***	0.118	0.090	0.208	0.02*	0.214	0.314	0.528	0***
GPC	-0.035	-0.321	-0.356	0.362	-0.38	-0.414	-0.794	0***	-0.172	-0.532	-0.704	0***
GSC	0.062	0.359	0.421	0.039*	0.137	0.546	0.683	0.003**	0.122	0.426	0.548	0.001**
Sedimentation	-0.056	-0.287	-0.343	0.123	-0.098	-0.480	-0.578	0.024*	0.001	-0.430	-0.429	0.985
R square	86.2				81.6				84.7			

**TABLE 5.S14** | Summary of winning genotypes in the three environments and their year of release.

Genotypes (Name)	Briweccs Number	Release Year	Selected_HN-NF	Selected_HN-WF	Selected_LN-NF	all 3 CS	Score Summary
Memory	6	2013	1	0	0	0	1
KWS Santiago	13	2011	0	1	0	0	1
Mulan	23	2006	0	0	1	0	1
Patras	26	2012	1	0	0	0	1
Biscay	31	2000	0	1	0	0	1
Colonia	45	2011	1	0	0	0	1
Gaucha	48	1993	0	0	1	0	1
Tobak	54	2011	0	1	0	0	1
Fedor	68	2007	1	0	0	0	1
Bombus	106	2012	0	1	0	0	1
Alves	132	2010	0	0	1	0	1
Rumor	204	2013	0	1	0	0	1
Hybery	216	2010	0	1	0	0	1
Hystar	217	2007	0	1	0	0	1
Hylux	218	2012	0	0	0	1	1
Claire	4	1999	0	0	1	1	2
Mentor	11	2012	1	1	0	0	2
KWS Pius	17	2010	1	0	0	1	2
Capone	32	2012	1	0	1	0	2
Edward	36	2013	0	1	0	1	2
Atomic	53	2012	1	0	0	1	2
Elixer	67	2012	1	1	0	0	2
Edgar	83	2010	1	0	0	1	2
KWS Cobalt	95	2013	1	0	0	1	2
Rebell	5	2013	1	0	1	1	3
Zappa	8	2009	1	0	1	1	3
Anapolis	29	2013	1	1	0	1	3
Tabasco	33	2008	1	1	0	1	3
Linus	42	2010	1	1	0	1	3
Intro	61	2011	1	0	1	1	3
SY Ferry	85	2012	1	0	1	1	3
Hyland	215	2009	1	1	1	0	3

The digits 0, 1, 2, 3 indicate the number of selection times of a high yielding genotype under the defined CS

**TABLE 5.S15** | Pairwise comparison of coefficients (intercepts and slopes) of regressions model traits of interest vs years of release under three CS.

Traits	Treatment	HN-NF		HN-WF	
		<i>intercepts</i>	<i>Slopes</i>	<i>intercepts</i>	<i>Slopes</i>
HD	HN-WF	0.352	0.359		
	LN-NF	0.482	0.523	0.0865	0.103
SPAD	HN-WF	0.32005	0.34407		
	LN-NF	0.00763 **	0.01061 *	0.000188 ***	0.000354 ***
YR	HN-WF	0.38921	0.4043		
	LN-NF	0.00173 **	0.00218 **	9.33e-05 ***	0.000136 ***
PH	HN-WF	0.43362	0.43585		
	LN-NF	0.00488 **	0.00573 **	0.0532	0.0591
SNms	HN-WF	0.402	0.406		
	LN-NF	0.627	0.517	0.727	0.8558
KNSp	HN-WF	0.0694	0.0755		
	LN-NF	0.7736	0.7488	0.12285	0.14113
KNms	HN-WF	0.0574	0.0640		
	LN-NF	0.0609	0.0475 *	0.978	0.889
TKW	HN-WF	0.1817	0.21242		
	LN-NF	0.78471	0.69281	0.0926	0.0861
HI	HN-WF	0.0568	0.0701		
	LN-NF	0.3039	0.2786	0.356	0.443
PBWms	HN-WF	4.99e-05 ***	6.97e-05 ***		
	LN-NF	0.00795 **	0.00584 **	0.1164	0.1715
GY	HN-WF	0.000247 ***	0.000486 ***		
	LN-NF	0.000609 ***	0.000340 ***	0.761	0.904
GPC	HN-WF	0.00181 **	0.00215 **		
	LN-NF	0.32759	0.1585	0.0384 *	0.108
GSC	HN-WF	0.0587	0.0759		
	LN-NF	0.7434	0.8002	0.126	0.137
Sedimentation	HN-WF	0.5219	0.4838		
	LN-NF	0.0072 **	0.0103 *	0.0332 *	0.0522

## List of Publications

- **Koua, P. A.**, Oyiga, B. C., Léon J. & Ballvora, A. (2021) Breeding enriched genetic variants for drought tolerance of winter wheat for key yield components and grain starch content. DOI: 10.3389/fpls.2021.684205.
- **Koua, P. A.**, Baig, M. M., Oyiga, B. C., Léon J. & Ballvora, A. (2021) Fungicide application affects nitrogen utilization efficiency and grain yield and quality of winter wheat <https://doi.org/10.3390/agronomy11071295> .
- **Koua, P. A.**, Oyiga, B. C., Rasher, U., Léon J. & Ballvora, A. Chromosome 3A harbors several pleiotropic and stable droughts inducible QTLs (SNPs) selected through breeding and associated with photosynthesis activity (**Manuscript under review at Plant Direct**).
- **Koua, P. A.**, Md. Nurealam S., Heß, K., Klag, N., Caroline K., Duarte-Delgado, D., Oyiga, B. C., Léon J. & Ballvora, A. Genome wide dissection study and *in-silico* transcript analysis provides candidate loci for improved drought tolerance and nitrogen use efficiency in winter wheat (**Manuscript under internal review**),

## Conferences or Poster Presentation

- **Koua P. A.**, Baig M. M., Léon J. & Ballvora, A. (2018). Breeding innovations in wheat for resilient cropping systems: Nitrogen Use Efficiency and Drought Tolerance. Conference Gemeinschaft zur Förderung von Pflanzeninnovation e. V. (GFPi). Campus Klein-Altendorf 23rd and 24th Mai 2018 (Talk).
- **Koua P. A.**, Léon J. & Ballvora, A. (2018). Effect of drought stress and nitrogen availability on shoot-root system and function in winter wheat. Workshop visit of vietnamien student. Bonn 24. Juli 2018 (Talk).
- **Koua P. A.**, Baig M. M., Léon J. & Ballvora, A. (2018). Breeding innovations in wheat for resilient cropping systems: Nitrogen Use Efficiency and Drought Tolerance. Poster presentation at German Plant Breeding Conference (GPZ) 2018. Wernigerode, Germany (Poster).
- **Patrice Koua \***, Bahman Sadeqi, Majid Baig, Jens Léon, Agim Ballvora (2019) Breeding innovations in wheat for resilient cropping systems: Nitrogen Use Efficiency and Drought Tolerance. Status seminar Potsdam 2019, Germany (Poster).

## **Acknowledgements**

I would like to express my profound gratitude to all the people who contributed in some way to the work described in this thesis, and to the people that have been alongside with me during this journey leading to the grades of “*Doktor der Agrarwissenschaften*”.

First and foremost, I thank my academic advisor, **Prof. Jens Léon** for accepting me into his group. During my PhD, the door to Prof. Léon’s office was always open whenever I ran into a trouble spot or had a question about my research. The fruitful discussions we had, particularly on statistics, data analysis and his insightful feedback pushed me to sharpen my thinking and brought my work to a higher level. I am also thankful to **Prof. Dr. Uwe Rascher** for being my second supervisor, sharing the research ideas and providing valuable comments on my thesis. The intelligible introduction to the non-invasive phenotyping method using the Mini-Pam I had with Prof. Rascher was the starting point that inspired me to lead my research on Photosynthesis. Besides my supervisors, I would like to thank my committee members **Prof. Dr. Mathias Becker**, **Prof. Dr. Scherer** for their interest in my work. Without their passionate participation and input, the validation survey could not have been successfully conducted.

My sincere thanks also goes to my tutor, **Dr. Agim Ballvora** for his valuable guidance throughout my studies. He provided me with the tools that I needed to choose the right direction and successfully complete my dissertation. He has been there in the tough moment of the PhD from the right beginning to the end. I would express my deep gratitude to the senior researchers, **Dr. Benedict Oyiga** for the time he provided for our tough discussions that would finally help me shaping the thesis and reaching this goal. To **Dr. Bobby Mathew** for his assistance and lecture in data analysis, statistics and for the time to conduct fruitful discussions. To the senior scientist **Dr. Dadshani and Majid Baig** for they support particularly in the first year of my PhD research where we had several field work to organize.

My sincere gratitude also goes to all my colleagues and friends (**Frau Karin Voitol**, **Mischael Schneider**, **Honecker Andreas**, **Salma Benaouda**, **Hasina Begun**, **Md Nurealam Siddiqui**, **Bahman Siddiqui**, **Newton Md Kamruzzaman**, **Asis Shresta**, **Caroline Mukiri Kambona**) who helped me in the field and green house data collection, all of them have won the “Trophies”. To my mademoiselle **Salma Banaouda**, and **Diana Delgado** for the insightful contribution on my lab work and for correcting my thesis, **Frau Karin Voitol** and **Dr. Helen Behn** for correcting the summary in German language.

My sincere appreciation and standing ovation go to **Christian Brinkmann**, **Marlen Prinz**, **Koffi Mawuena Founou**, **Katrin Heß**, **Niko Klag**, and **Angela Dankwah** for their hard work and significant contribution to this research.

I would also like to thank the staff of Campus Kleinaltdorf for helping in the management of the field trials and experiment inside the rainout shelter. I would also send my sincere appreciation to the staff managing the greenhouse and climate chamber, especially **Josef Höckling, Josef Bauer, Petra Rings**, for helping to organize experiments and particularly the root phenotyping in Auf dem Hügel.

I am grateful for the funding sources that allowed me to pursue my PhD studies in Germany, the **Konrad Adenauer Stiftung** for their financial support, and to my Supervisor at the Konrad Adenauer Stiftung, **Prof. Dr. Dorothea Bartels** for the time she advocated reading my annual report and giving feedbacks. My thanks are also due to the **Deutscher Akademischer Austauschdienst (DAAD)** and **Frau Sandra Pappel** for the get-finished PhD financial support.

To my friends Rv. Fr. L'Abbé **Hirlary Aboh, Benedict Oyiga, Kingsyley Ogbu, Oyewole Ogini, Mellon, Isaac Mensa, Bonnaventure Kouassi, Loukou Kouassi, Johannes, Julia, Charleen, Angeline Wanjiku, Caroline Mukiri Kambona**, you are the best. To **Frau Kathrin Marshall** and **Herr Christian Marshall**, words are not sufficient to express my profound gratitude for your generous encouragement and assistance during my stay in Germany.

Finally, I would like to express my very profound gratitude to my parents, to my mum (**M'man**) for the sacrifice she endured and the prayers to make sure I could get to the highest educational level I want, to my late dad (**Baba**) for being proud of me as a son and for being there for me. My best gratitude goes my cousin **Adjé Clement** and his wife **Atta Judith**. To my girlfriend **Marie Josée Desteck N'guessan** for being a trustful person, and to my kids, nephews, cousin niece **Prince Koua, Bryan Koua, Ilian Koua, Hermann Ahoua, Emmanuella Koua** for your appreciation and prayers. To my brothers and sisters for being there for me whenever I needed their prayers and assistance. Thanks.